

ASSESSMENT OF WOODY BIOMASS AND SOLAR  
ENERGY RESOURCES WITH REMOTE SENSING AND GIS  
TECHNIQUES – A REGIONAL STUDY IN THE HIGH  
MOUNTAINS OF THE EASTERN PAMIRS (TAJIKISTAN)

Harald Zandler

Mag. rer. nat., born on 24 September 1984 in Feldkirch, Austria

Dissertation

Submitted to the Faculty of Biology, Chemistry and Earth Sciences of the  
University of Bayreuth, Germany

in partial fulfilment of the requirements for the academic degree of

Doctor of Natural Sciences (Dr. rer. nat.)

Bayreuth, September 2015



Die vorliegende Arbeit wurde in der Zeit von März 2012 bis Februar 2013 am Institut für Geographie und Regionalforschung der Universität Wien und von März 2013 bis September 2015 am Geographischen Institut der Universität Bayreuth unter Betreuung von Herrn Professor Dr. Cyrus Samimi angefertigt.

Vollständiger Abdruck der von der Fakultät für Biologie, Chemie und Geowissenschaften der Universität Bayreuth genehmigten Dissertation zur Erlangung des akademischen Grades eines Doktors der Naturwissenschaften (Dr. rer. nat.).

Dissertation Eingereicht am: 24.09.2015

Zulassung durch die Promotionskommission: 01.10.2015

Wissenschaftliches Kolloquium: 08.12.2015

Amtierender Dekan: Prof. Dr. Stefan Schuster

Prüfungsausschuss:

Prof. Dr. Cyrus Samimi (Erstgutachter)

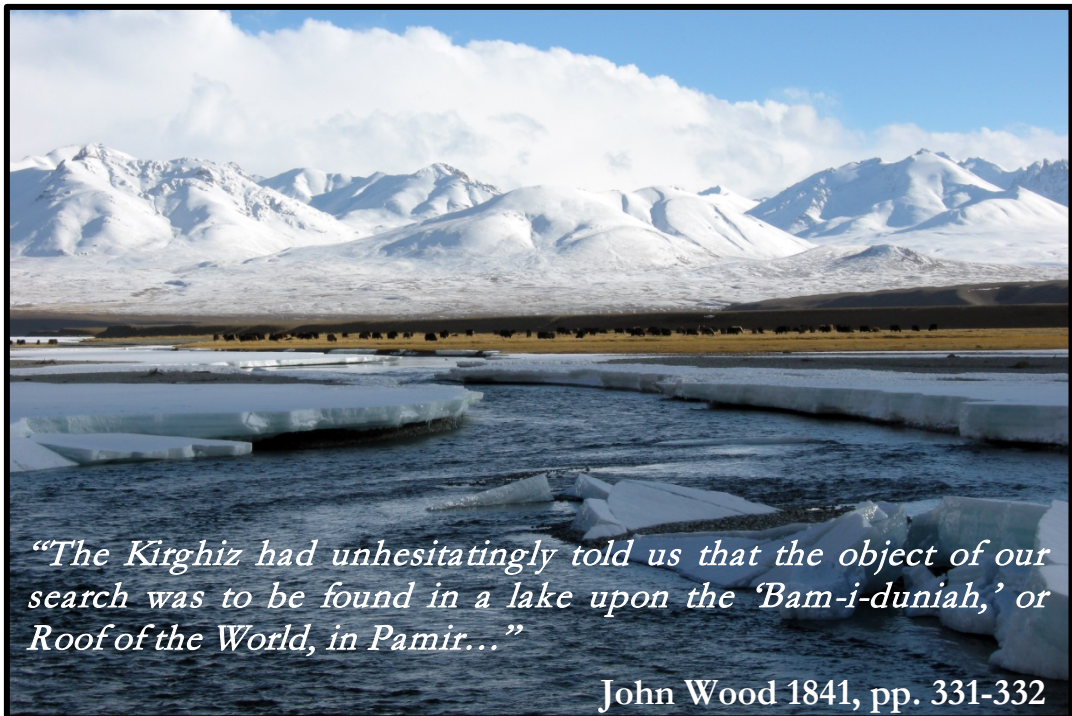
Prof. Dr. Thomas Köllner (Zweitgutachter)

Prof. Dr. Anke Jentsch (Vorsitz)

Prof. John Tenhunen, Ph.D.







*“The Kirghiz had unhesitatingly told us that the object of our search was to be found in a lake upon the ‘Bam-i-duniah,’ or Roof of the World, in Pamir...”*

John Wood 1841, pp. 331-332



# Acknowledgements

---

First, I would like to express my gratitude to **Cyrus Samimi** for giving me the possibility of working in a fascinating research field and in one of the most intriguing regions of the world. As my supervisor, he supported me in a variety of ways and settings, from the field to the university, and continually encouraged my ideas throughout this dissertation. Thank you! My thanks also go to the **Volkswagen Foundation** with **Matthias Nöllenburg** as a helpful consultant. Without their financing of the scientific research project, this study would have been impossible. Special thanks also go to **Alexander Brenning** for his remarkable help and for teaching me a lot about statistics, the power of R and academic publishing.

I am also very grateful to all the people involved in the Pamir II project. In particular, I want to thank **Tobias Kraudzun** for his assistance with innumerable regional and practical issues. Thank you that you always picked up the phone when certain problems arose. Furthermore, I want to thank **Fanny Kreczi** and **Georg Hohberg** for their valuable collaboration and their company during memorable research trips. I wish to thank especially **Rustam, Behruz, Michael**, and the team of the **GIZ Khorog** for their help in establishing the climate stations. Furthermore, I am very grateful for all the support, friendliness and openness of the **people of the Pamirs** whom I met. More than once, and even in the most remote locations, your unexpected help saved the day. I also want to thank **Jamilla Madailewa** for her frequent assistance in translation or administrative issues. Thanks also go to **Thomas Morche** for joining me in the field and supporting the project with an extensive graduate thesis.

Many other people contributed to this thesis in different ways. I want to thank **Kim André Vanselow** for discussing various regional and methodological subjects and for fostering the dissemination of my results. The efforts of **Jussi Griebinger** and his laboratory team to find solutions for regional dwarf shrub dating are highly appreciated. I also wish to thank **Raphael Spiekermann** for proofreading my manuscripts. Very special thanks also go to my **colleagues and friends from the University of Bayreuth** for many discussions, interesting coffee breaks and nice meetings during as well as outside of working hours. Furthermore, I want to thank **Martin Brandt** for always providing advice and a good example in accomplishing a PhD. I am also grateful to **Bunafsha Mislimshoeva** for her important up-to-date information and other contributions to better understanding Tajikistan. Sincere thanks to all institutions making earth observation products freely available for the scientific community, in particular **NASA**, the **USGS**, and **DLR** in the case of this thesis. Such data is invaluable for global research.

I would also like to thank all the people that supported me besides the university. Among them, special thanks go to **my parents** for always doing their best to make me have a good time when visiting home. Finally, I want to thank you, **Angela**, for your limitless support beyond all borders. You have been wonderful!

# Abstract

---

Energy issues have been a main concern of geographical research in the Eastern Pamirs of Tajikistan. Dwarf shrubs (*Krascheninnikovia ceratoides*, *Artemisia* spp.), as the only woody vegetation, are of central importance in this context by representing a key thermal energy resource. But despite their relevance for sustainable development, neither an assessment of woody biomass quantities nor an evaluation of potential alternatives has been conducted. Remote sensing and GIS techniques are considered as appropriate tools to study these objectives. However, common space-borne remote sensing methods reach their limits in such arid environments characterized by scarce vegetation cover. Therefore, the main research goals of this dissertation are to evaluate and extend existing remote sensing approaches and test different sensors for woody biomass quantification in drylands to contribute to the clarification of global earth observation problems. Furthermore, related empirical results are intended to shed light on the ongoing regional degradation debate. Finally, the feasibility of photovoltaic energy as an alternative local energy resource for sustainable development should be assessed.

Field data represented the basis for the study by providing spatially allocated biomass amounts using an allometric model, climate measurements, and complementary information. A large number of remote sensing variables, potentially relevant for woody biomass prediction, according to the literature, were derived from the Landsat OLI, RapidEye, EO-1 Hyperion and ASTER sensors. Several spectral variables were experimentally adapted to account for interfering background signals. Various techniques and models were applied to compare their performance in spatial biomass prediction. An interdisciplinary analysis including external survey data was used to contrast dwarf shrub availability, accessibility, and demand. An integrative study of field measurements, a spatial solar radiation model, framework scenarios, and literature based cost calculations provided the mean for an evaluation of the local photovoltaic energy potential and anticipated environmental effects.

The results show that remote sensing based biomass quantification is possible even under the difficult arid conditions of the research area, but relatively high modeling errors have to be taken into account (RMSE  $\sim$ 1000 kg/ha). Statistical models with adequate selection procedures and shrinkage techniques proved to be important in this high dimensional setting. A performance assessment demonstrated that common vegetation indices are not successful and variables adjusting for soil effects are necessary in this region. The comparison of sensors indicated that a large spectral range, comprising plant as well as background information, is advantageous in dryland vegetation modeling. The hyperspectral sensor revealed an increased potential for woody biomass prediction, with the ability to reduce the relative RMSE by a maximum of 20 percentage points compared to multispectral data. Narrowband indices, calculated from the short wave infra-red spectral domain, showed to be particularly suitable for dwarf shrub detection. A conservative biomass model enabled the comparison of available dwarf shrub stocks with harvesting amounts in a case study

village by taking prediction errors and harvesting practices into account. Associated results suggest that locally, biomass quantities are sufficient to meet thermal energy demand on the medium term. However, restricted accessibility may limit future energy supply, and long-term sustainability is questionable due to the low regeneration rate of regional dwarf shrubs. The implemented spatial radiation model performed well in deriving solar energy amounts. The assessment of photovoltaic energy resources as substitutes for woody biomass showed that the generation of thermal energy is feasible within reasonable cost limits when restricted to certain basic applications. The estimations of the environmental effects of potentially increased photovoltaic infrastructure showed that it would result in a considerable mitigation of degraded areas and an amplification of carbon sequestration. This demonstrated the benefits of solar photovoltaic energy as an alternative renewable energy resource in peripheral arid high mountains.

This dissertation provided contributions to the utilization of remote sensing and GIS techniques in drylands and high mountain regions. It was thereby shown that they offer valuable tools to resolve environmental research issues, but are also subject to major restrictions that require field based method adaptations. This study indicates that upcoming satellite sensors, earth observation products, and sophisticated statistical models will have much potential for regional and global research on natural resources in arid environments.

# Zusammenfassung

---

Energiefragen stellten im tadschikischen Ostpamir stets ein Schwerpunkt geographischer Forschung dar. In diesem Zusammenhang sind Zwergsträucher (*Krascheninnikovia ceratoides*, *Artemisia* spp.), die einzige verholzte Vegetation in der Region, von zentraler Bedeutung als thermische Energieressource. Jedoch wurde, trotz deren Wichtigkeit für eine nachhaltige Entwicklung, bisher weder eine Abschätzung der verholzten Biomassemengen noch eine Untersuchung potentieller Alternativen durchgeführt. Fernerkundung und GIS-Techniken werden als geeignete Werkzeuge für eine Analyse dieser Bereiche angesehen. Allerdings stoßen gebräuchliche weltraumbasierte Fernerkundungsmethoden in einer solch ariden Umwelt mit spärlicher Vegetationsdecke an ihre Grenzen. Daher sind die wichtigsten Forschungsziele dieser Dissertation die Evaluierung und die Erweiterung existierender Fernerkundungsansätze, sowie das Testen verschiedener Sensoren für eine Biomassenquantifizierung in Trockengebieten, um zu globalen Problemstellungen der Erdbeobachtung beizutragen. Des Weiteren sollen die damit verbundenen empirischen Ergebnisse zur Klärung der gegenwärtigen regionalen Degradationsdebatte beitragen. Schließlich soll die Umsetzbarkeit von Photovoltaikenergie als alternative lokale Energieressource für eine nachhaltige Entwicklung abgeschätzt werden.

Durch die Bereitstellung räumlich verorteter Biomassemengen unter Nutzung eines allometrischen Modells, von Klimadaten und von zusätzlichen Informationen repräsentierten Felddaten die Basis dieser Studie. Eine große Zahl von fernerkundlichen Variablen, welche laut Literaturangaben wichtig für eine Modellierung verholzter Biomasse sein könnten, wurden von den Sensoren Landsat OLI, RapidEye, EO-1 Hyperion und ASTER abgeleitet. Eine Reihe spektraler Variablen wurde experimentell angepasst, um beeinflussende Hintergrundsignale zu berücksichtigen. Der Einsatz verschiedener Modelle und Techniken diente dem Eignungsvergleich für die räumliche Biomassemodellierung. Eine interdisziplinäre Betrachtung unter Einbeziehung externer Umfragedaten wurde herangezogen um Zwergstrauchverfügbarkeit, Zugänglichkeit und Bedarf gegenüberzustellen. Eine integrative Analyse, welche feldbasierte Messungen, ein räumliches Solarstrahlungsmodell, verschiedene Szenarien zu allgemeinen Rahmenbedingungen und literaturbasierte Kostenberechnungen vereint, wurde durchgeführt um das lokale Photovoltaikenergiepotential und erwartete Umwelteffekte zu evaluieren.

Die Ergebnisse zeigen, dass fernerkundungsbasierte Biomassenquantifizierung auch unter den schwierigen ariden Bedingungen des Untersuchungsgebietes möglich ist, aber auch ein relativ hoher Modellierungsfehler berücksichtigt werden muss (RMSE  $\sim$ 1000 kg/ha). Statistische Modelle mit angemessenen Auswahlprozessen und Verkleinerungstechniken zeigten sich als wichtig in dieser hochdimensionalen Situation. Eine Leistungsabschätzung demonstrierte, dass herkömmliche Vegetationsindizes in diesen Regionen nicht erfolgreich sind und Variablen, welche Anpassungen an den Boden beinhalten, benötigt werden. Der Vergleich der Sensoren deutete darauf hin, dass eine große spektrale Abdeckung, welche

sowohl Pflanzen- als auch Hintergrundinformationen einschließt, vorteilhaft in der Vegetationsmodellierung von Trockengebieten ist. Für den hyperspektralen Sensor konnte ein erhöhtes Potential zur Vorhersage verholzter Biomasse festgestellt werden. Dieser ermöglichte eine Verringerung des relativen RMSE um bis zu maximal 20 Prozentpunkte im Vergleich zu multispektralen Daten. Schmalbandindizes, welche aus Bändern der kurzwelligen Infrarotregion errechnet wurden, zeigten eine spezielle Eignung in der Erfassung von Zwergsträuchern. Durch die Berücksichtigung des Vorhersagefehlers und der Erntemethoden in einem konservativen Biomassemodell konnte der verfügbare Zwergstrauchbestand mit entsprechenden Erntemengen in einem Fallstudiendorf verglichen werden. Die Ergebnisse legen nahe, dass lokale Biomassemengen mittelfristig ausreichen, um den thermischen Energiebedarf zu decken. Eingeschränkte Zugänglichkeit könnte die zukünftige Energieversorgung jedoch beeinträchtigen und die langfristige Nachhaltigkeit ist auf Grund der langsamen Regenerationsrate der Zwergsträucher fragwürdig. Das implementierte räumliche Strahlungsmodell zeigte eine gute Leistung in der Ableitung verfügbarer Solarenergie. Die Bewertung von Photovoltaikenergieressourcen als Ersatz für verholzte Biomasse demonstrierte, dass die Erzeugung thermischer Energie innerhalb eines realistischen Kostenrahmens umsetzbar ist, wenn deren Einsatz auf bestimmte Basisanwendungen beschränkt wird. Die Abschätzung der Umwelteffekte in Folge des potentiellen Ausbaus der Photovoltaikinfrastruktur resultierte in der Erwartung einer deutlichen Verminderung degradierter Flächen und einer erhöhten Kohlenstofffixierung. Die Vorteile von solarer Photovoltaikenergie als alternative Energieressource in peripheren ariden Hochgebirgen wurden hierdurch dargelegt.

Diese Dissertation lieferte Beiträge zur Nutzung von Fernerkundungs- und GIS-Techniken in Trockengebieten und Hochgebirgsregionen. Dabei wurde gezeigt, dass diese wertvolle Werkzeuge zur Lösung umweltbezogener Forschungsfragen bieten, aber auch bedeutenden Einschränkungen unterliegen welche eine feldbasierte Methoden Anpassung erfordern. Diese Studie legt nahe, dass zukünftige Satellitensensoren, Erdbeobachtungsprodukte und ausgereifte statistische Modelle ein hohes Potential für die regionale und globale Erforschung natürlicher Ressourcen in ariden Ökosystemen haben werden.

# Резюме

---

Энергетические вопросы были основной проблемой географических исследований на Восточном Памире Таджикистана. Карликовые кустарники (*Krascheninnikovia ceratoides*, *Artemisia* spp.), будучи единственной древесной растительностью, имеют центральное значение в этом контексте, являясь ключевым ресурсом для выработки тепловой энергии. Но, несмотря на их актуальность для устойчивого развития, ни количественная оценка древесной биомассы, ни оценка возможных альтернатив проведены не были. Методы дистанционного зондирования и технологии ГИС рассматриваются как соответствующие инструменты для этих целей. Тем не менее, общие методы дистанционного зондирования космического происхождения достигают предела своих возможностей в засушливых условиях, характеризующимися скудным растительным покровом. Таким образом, основными научными целями данной диссертации являются оценка и распространение существующих подходов дистанционного зондирования и тестирования различных датчиков для определения количества древесной биомассы в засушливых районах, чтобы внести свой вклад в разъяснение глобальных проблем наблюдения Земли. Кроме того, соответствующие эмпирические результаты предназначены для, чтобы пролить свет на текущие региональные дебаты по деградации. Наконец, возможность фотоэлектрической энергии в качестве альтернативного местного энергетического ресурса для устойчивого развития должна быть оценена.

Полевые данные послужили основой для исследования, посредством пространственно распределенной биомассы, используя аллометрическую модель, климатические измерения и дополнительную информацию. Большое количество переменных, основанных на отдаленном зондировании и имеющих потенциальное отношение к прогнозу древесной биомассы, согласно источникам, были получены с помощью датчиков Landsat Оли, RapidEye, EO-1 Гипериона (Hyperion) и АСТЕР (ASTER). Несколько спектральных переменных экспериментально приспособлены для учета влияния на фоновые сигналы. Различные методы и модели были применены, чтобы сравнить их производительность для прогноза пространственной биомассы. Междисциплинарный анализ, включая внешние данные обследования позволил сопоставить наличие карликовых кустарников, доступность и спрос. Интеграционное изучение полевых данных, пространственной модели излучения, рамочных сценариев и расчеты расходов, сделанных на основе изучения литературы, позволили провести оценку местного потенциала фотоэлектрической энергии и связанных с этим экологических последствий.

Результаты показали, что количественное дистанционного зондирования на основе биомассы возможно даже в трудных, засушливых условиях области исследования, но относительно высокие ошибки моделирования должны быть приняты во внимание (RMSE/СКО ~ 1000 кг / га). Статистические модели с надлежащими процедурами



отбора и методов усадки являются важными в этой высокой размерной настройке. Оценка эффективности показала, что общие показатели растительности не были успешными, и регулирование переменных для эффектов почвы необходимы в этом регионе. Сравнение датчиков показали целесообразность большого спектрального диапазона в моделировании растительного покрова в засушливых областях, включающего растения, а также вводную информацию. Гиперспектральный датчик выявил повышенный потенциал для прогнозирования древесной биомассы с возможностью снижения относительного RMSE/СКО, максимум на 20 процентных пунктов по сравнению с мультиспектральными данными. Узкополосные индексы, рассчитанные на основе коротковолнового инфракрасного спектрального участка, в особенности подходят для обнаружения карликовых кустарников. Консервативная модель биомассы позволила провести сравнение имеющихся запасов карликовых кустарников с объёмом лесозаготовок на пилотном участке, принимая во внимание ошибки прогнозирования и практику лесозаготовок. Соответствующие результаты позволяют предположить, что на местном уровне, количество биомассы достаточно, чтобы удовлетворить спрос на тепловую энергию в среднесрочной перспективе. Тем не менее, ограниченный доступ может ограничить будущие поставки энергии, и долгосрочная устойчивость находится под вопросом из-за медленного восстановления региональных карликовых кустарников. Внедренная пространственная модель излучения продемонстрировала эффективность в процессе получения солнечной энергии. Оценка фотоэлектрических энергетических ресурсов, как заменителей древесной биомассы показали, что выработка тепловой энергии является возможной в приемлемых пределах стоимости при ограничении на некоторые основные приложения. Оценка экологических последствий от потенциально увеличенной фотоэлектрической инфраструктуры привели к значительному смягчению в пострадавших районах и усилению поглощения углерода. Это демонстрирует преимущество солнечной фотоэлектрической энергии в качестве альтернативного ресурса возобновляемой энергии в периферийных высокогорных областях.

Данная диссертация внесла вклад в использование методов дистанционного зондирования и ГИС технологий в засушливых и высокогорных районах. Таким образом, было продемонстрировано, что они представляют собой ценные инструменты для решения проблем окружающей среды, но при условии наличия методов адаптации, основанных на полевых данных. Это исследование показывает, что предстоящие спутниковые датчики, результаты наблюдения Земли и сложные статистические модели имеют высокий потенциал для регионального и глобального исследования природных ресурсов засушливых условиях.

# Preface

---

This dissertation was prepared within the interdisciplinary research project “Transformation Processes in the Eastern Pamirs of Tajikistan. The presence and future of energy resources in the framework of sustainable development,” which started in March 2012 and is funded by the Volkswagen Foundation<sup>1</sup>. The project aims to understand the utilization of energetic resources at the upper altitude limits of human habitation from a social sciences perspective, and their availability and accessibility using a natural scientific approach. The achieved results are subsequently integrated into an energetic model providing scenarios to develop sustainable management strategies in this peripheral high mountain region.

In this context, the research team of the University of Bayreuth, headed by Prof. Cyrus Samimi, concentrates on the natural-scientific basis of the project. The main research topic of presented thesis focuses on the detection of woody biomass with remote sensing methods in an arid environment. Furthermore, the potential of solar energy as a ubiquitous resource should be evaluated to assess the feasibility of local alternatives for thermal energy generation.

---

<sup>1</sup> For more information please refer to [http://www.klimatologie.uni-bayreuth.de/homepage\\_samimi/samimi\\_research/index.html](http://www.klimatologie.uni-bayreuth.de/homepage_samimi/samimi_research/index.html); accessed on 13 July 2015

# Contents

---

|  |      |
|--|------|
| Acknowledgements.....  | v    |
| Abstract .....   | vi   |
| Zusammenfassung .....  | viii |
| Резюме.....  | x    |
| Preface .....  | xii  |
| Contents .....   | xiii |
| List of figures.....   | xvi  |
| Acronyms .....   | xvii |
| PART I - Research framework .....                                  | 1    |
| 1 Objectives and research questions .....                          | 3    |
| 1.1 Introduction and research area.....                            | 4    |
| 1.2 State of the art research and research gaps.....               | 6    |
| 1.2.1 Regional mapping of woody vegetation .....                   | 6    |
| 1.2.2 Global remote sensing approaches on dryland vegetation ..... | 7    |
| 1.2.3 Assessment of solar energy resources.....                    | 9    |
| 1.3 Research questions and hypotheses.....                         | 10   |
| 2 Materials and Methods .....                                      | 12   |
| 2.1 Field methods and derivative data .....                        | 12   |
| 2.1.1 Allometric model.....  | 13   |
| 2.1.2 Climate data .....   | 13   |
| 2.2 Satellite data.....  | 14   |
| 2.2.1 RapidEye data.....   | 15   |
| 2.2.2 Landsat 8 OLI data.....                                      | 16   |
| 2.2.3 Hyperspectral EO-1 Hyperion data .....                       | 16   |

|                              |  |    |
|------------------------------|--|----|
| 2.2.4                        | ASTER data.....  | 16 |
| 2.3                          | Processing of satellite data and derived variables.....  | 16 |
| 2.3.1                        | Preclassification.....   | 17 |
| 2.3.2                        | Individual bands and band ratios.....  | 18 |
| 2.3.3                        | Vegetation indices.....  | 18 |
| 2.3.4                        | Soil adjusted vegetation indices .....   | 19 |
| 2.3.5                        | Color adjusted vegetation indices.....   | 19 |
| 2.3.6                        | First derivatives of reflectance and ratios.....   | 20 |
| 2.3.7                        | Principal components and ratios .....  | 20 |
| 2.3.8                        | Texture variables .....  | 20 |
| 2.3.9                        | Spectral angle based variables .....   | 20 |
| 2.3.10                       | Topographic variables.....   | 21 |
| 2.4                          | Statistical methods .....  | 21 |
| 2.4.1                        | Linear regression.....   | 21 |
| 2.4.2                        | Partial Least Squares linear regression .....  | 22 |
| 2.4.3                        | Ridge regression .....   | 22 |
| 2.4.4                        | Lasso regression .....   | 22 |
| 2.4.5                        | Random forest regression.....  | 22 |
| 2.4.6                        | Cross validation.....  | 23 |
| 2.4.7                        | Variable importance.....   | 23 |
| 2.4.8                        | Multiple test procedures.....  | 23 |
| 2.5                          | Observation based scenarios and cost assessment.....   | 24 |
| 2.6                          | GIS based solar radiation model.....   | 24 |
| 2.7                          | External data for interdisciplinary analysis.....  | 24 |
| 2.8                          | Software.....  | 25 |
| PART II - Publications ..... |  | 27 |
| 3                            | List of manuscripts and declaration of individual contributions.....   | 29 |
| 4                            | Quantifying dwarf shrub biomass in an arid environment: comparing empirical methods in a high dimensional setting..... | 31 |

|   |  |     |
|---|--|-----|
| 5 | Potential of space-borne hyperspectral data for biomass quantification in an arid environment: advantages and limitations .....  | 49  |
| 6 | High mountain societies and limited local resources - livelihoods and energy utilization in the Eastern Pamirs, Tajikistan ..... | 67  |
| 7 | Scenarios of solar energy utilization on the ‘Roof of the World’: potentials and environmental benefits.....                     | 85  |
|   | PART III - Synthesis and Outlook.....  | 105 |
| 8 | Synthesis.....   | 107 |
| 9 | Outlook .....  | 112 |
|   | Literature .....   | 115 |
|   | PART IV - Appendix .....   | 127 |
|   | Publications, presentations, posters and review activity of the author .....   | 129 |
|   | Declaration / eidesstattliche Erklärung.....   | 131 |

# List of figures

---

Figure 1: Map of the Eastern Pamirs of Tajikistan. Areal extent is approximately identical to the *rajon* (district) Murghab.....5

Figure 2: Photographs of (a) *Krascheninnikovia ceratoides* dwarf shrub formation in the front with azonal riparian grass vegetation in the background, (b) Yaks feeding on dwarf shrubs penetrating the snow, and (c) dwarf shrub harvesting. ....5

Figure 3: Illustrations of (a) differences between cover estimates performed by an experienced first observer and cover measurements using the dwarf shrub circle area formula performed by a second observer in 4 m x 4 m plots with superimposed 1:1 line, (b) typical dwarf shrub growth shape with red circle overlay for comparison, and (c) excavated dwarf shrubs for heating purposes. .... 13

Figure 4: Exemplary spectral curves of field plots with different land cover derived from the applied sensors (left) and schematic representations of individual bands with a superimposed color infrared image (right)..... 15

Figure 5: Illustrations of (a) spectral angle between a reference spectrum and a raster pixel using a hypothetical two band image according to Kruse et al. (1993), and (b) boxplots of dwarf shrub SAV values with thresholds (grey horizontal lines) of the dwarf shrub reference spectrum (left) and riparian grass vegetation spectrum (right)..... 18

Figure 6: Scatterplot of nine bare soil sites (black) and nine dwarf shrub sites (red) in the Landsat red-NIR spectral domain. The Black regression line is used for the derivation of soil line parameters. Presented vegetation plots most closely resemble the theoretical concept of the perpendicular vegetation index (cf. Jackson et al. 1980) ..... 19

# Acronyms

---

|               |  |
|---------------|--|
| AIC .....     | Akaike Information Criterion                                   |
| ASTER.....    | Advanced Spaceborne Thermal Emission and Reflection Radiometer |
| AUROC.....    | Area Under the ROC   |
| CI.....       | Correction Index   |
| DEM.....      | Digital Elevation Model  |
| DLR .....     | Deutsches Zentrum für Luft- und Raumfahrt                      |
| EnMAP.....    | Environmental Mapping and Analysis Program                     |
| EO-1 .....    | Earth Observing 1  |
| FDR .....     | First Derivatives of Reflectance                               |
| GIS.....      | Geographic Information System                                  |
| GIZ .....     | Deutsche Gesellschaft für Internationale Zusammenarbeit        |
| GPS .....     | Global Positioning System                                      |
| HypIRI.....   | Hyperspectral Infrared Imager                                  |
| LCOE.....     | Levelized Cost Of Electricity                                  |
| m.a.s.l. .... | Meters Above Sea Level   |
| MIR .....     | Mid Infra-Red  |
| NASA.....     | National Aeronautics and Space Administration                  |
| NDVI.....     | Normalized Difference Vegetation Index                         |
| NIR .....     | Near Infra-Red   |
| OLI .....     | Operational Land Imager  |
| PLS .....     | Partial Least Squares  |

|               |   |
|---------------|---|
| PC.....       | Principal Component                                 |
| RF.....       | Random Forest regression                            |
| RMSE .....    | Root Mean Square Error                              |
| RR .....      | Ridge Regression                                    |
| SAV.....      | Spectral Angle Values                               |
| SAVI.....     | Soil Adjusted Vegetation Index                      |
| SMA.....      | Spectral Mixture Analysis                           |
| SWIR.....     | Short Wave Infra-Red                                |
| TanDEM-X..... | TerraSAR-X add-on for Digital Elevation Measurement |
| UAV.....      | Unmanned Aerial Vehicle                             |
| UNEP.....     | United Nations Environment Programme                |
| USGS.....     | United States Geological Survey                     |
| VI(s).....    | Vegetation Index (Indices)                          |



# PART I

## RESEARCH FRAMEWORK



# 1 Objectives and research questions

---

Sustainable development against the background of limited resources is one of the most urgent issues worldwide. The generation of quantitative information on the availability and distribution of respective resources is a prerequisite for an adapted management. This is most obvious in developing peripheral regions that are characterized by restricted economic exchange structures. The Eastern Pamirs of Tajikistan, an arid high mountain plateau, are an illustrative example of this situation, with strong dependencies on locally available resources for the people's livelihoods. Despite the relevance of perennial woody vegetation as fuel and forage source and the associated need for quantitative plant biomass information, a sophisticated assessment of this resource is missing. Therefore, a regional objective of this study is to generate information on spatially resolved woody biomass amounts in order to analyze its availability in relation to local accessibility and demand. Remote sensing appears as a suitable method to achieve this goal. However, existing remote sensing approaches reached their limits in the study area. This leads to a research field which is of importance to remote sensing science in general: the derivation of vegetation biomass amounts in drylands. Arid lands cover major parts of the planet's land surface, and woody perennial vegetation plays a significant role, as it provides central ecosystem services in respective regions. Excessive exploitation of plant biomass, especially overgrazing and fuelwood consumption, may lead to degradation and desertification, which is considered a global concern. As the extensive arid environments cannot be surveyed and monitored by field observations alone, remote sensing is a suitable and necessary method of studying standing biomass and its alteration in arid environments. However, most remote sensing based analyses have had limited success in regions with scarce areal vegetation cover. This thesis therefore intends to contribute to general remote sensing applications and solutions in arid environments. Due to the high local and global relevance of this research topic, woody biomass mapping using remote sensing techniques constitutes the central part of the presented dissertation.

Apart from the demand on some constrained local resources, others are ubiquitously available. In particular solar power has much potential as an alternative energy resource in peripheral mountain regions. The Pamir Plateau is considered to be an ideal setting for the development of solar energy to alleviate energy poverty and pressure on the local ecosystem. However, studies on the potential of solar power systems, especially for generating thermal energy, have not been conducted. This thesis aims to fill this regional research gap and evaluate the feasibility and effects of solar power utilization as an alternative to woody biomass. Such an assessment has to be adapted to the respective local context. Therefore, an integrative approach which is straightforwardly transferable to other mountain environments, incorporating geographic information system (GIS) modeling, climate data, and field observations, should be conducted. Wind energy is not considered in this dissertation as preliminary climate data analysis showed, that even at favorable sites, this resource has a much lower potential and positive synergy effects are minimal.

## SYNOPSIS

**Part I** of this dissertation introduces the characteristics and regional challenges of the Eastern Pamirs of Tajikistan and summarizes relevant geographical research. An outline of state of the art research findings as well as gaps provides the starting point for forming research questions and hypotheses of regional as well as general relevance. Subsequently, materials and methods that are intended to contribute to these objectives are presented. In **Part II**, four peer-reviewed articles exemplify the central research activities of the dissertation in detail. **Part III** finally integrates the achieved results into a conclusion and gives an outlook of related additional research.

### 1.1 Introduction and research area

The global relevance of mountain regions and drylands is highlighted by the United Nations environment programme (UNEP) and the Millennium Ecosystem Assessment, which consider them to be key environmental systems with high vulnerability to disturbances (Hassan et al. 2005; UNEP 2012). Clearance of plant biomass and domestic livestock grazing with intensities above regeneration rates are some of the most important drivers of degradation in respective areas. The Eastern Pamirs of Tajikistan, entitled the ‘roof of the world’ by some of the first western explorers (Wood 1841), is a region where all of these criteria apply. With altitudes mostly between 3,500 and 5,500 meters above sea-level (m.a.s.l., Figure 1), a cold and arid climate showing annual mean temperatures of -1 °C, and an annual average precipitation of 94 mm (Murghab 1998-2012, Tajik Hydrometeorological Service 2013), the region can be characterized as a high mountain desert. All permanent settlements are located in the sub-alpine belt (3,500 - 4,300 m.a.s.l.) where the climatic conditions have led to the dominance of scarce dwarf shrub vegetation (*Krascheninnikovia ceratoides*, *Artemisia* spp.) with an areal cover seldom exceeding ten percent (Walter and Breckle 1986). Denser, azonal meadow vegetation (e.g. *Carex* spp., *Kobresia* spp.) exists in riparian ecosystems because of the increased water supply (Figure 2a). In the alpine belt (4,300 – 4,800 m.a.s.l.), with its higher rainfall rates, grasses, and cushions (e.g. *Acantholimon* spp.), are the most prevalent plants (Vanselow 2011). The already mentioned dwarf shrubs, common woody species in arid environments regionally known as *teresken* (McArthur et al. 2004; Heklau and von Wehrden 2011; Kraudzun et al. 2014), are of major importance to the research area. Animal husbandry is the basis of most people’s livelihood, and the shrubs are a main winter forage source due to the seasonal scarcity of other plants (Figure 2b). Another central ecosystem function of the perennial vegetation is the protection of soils from erosion (Breckle and Wucherer 2006). With the absence of trees, dwarf shrubs are the only plants that provide woody biomass and are the only locally available thermal energy carrier besides animal manure (Breu et al. 2005). Therefore, grazing and widespread harvesting of shrubs occurs simultaneously (Figure 2c). This situation made local energy resources, in the context of environmental degradation and sustainable development, a central topic of geographical research in the Eastern Pamirs.

## SYNOPSIS

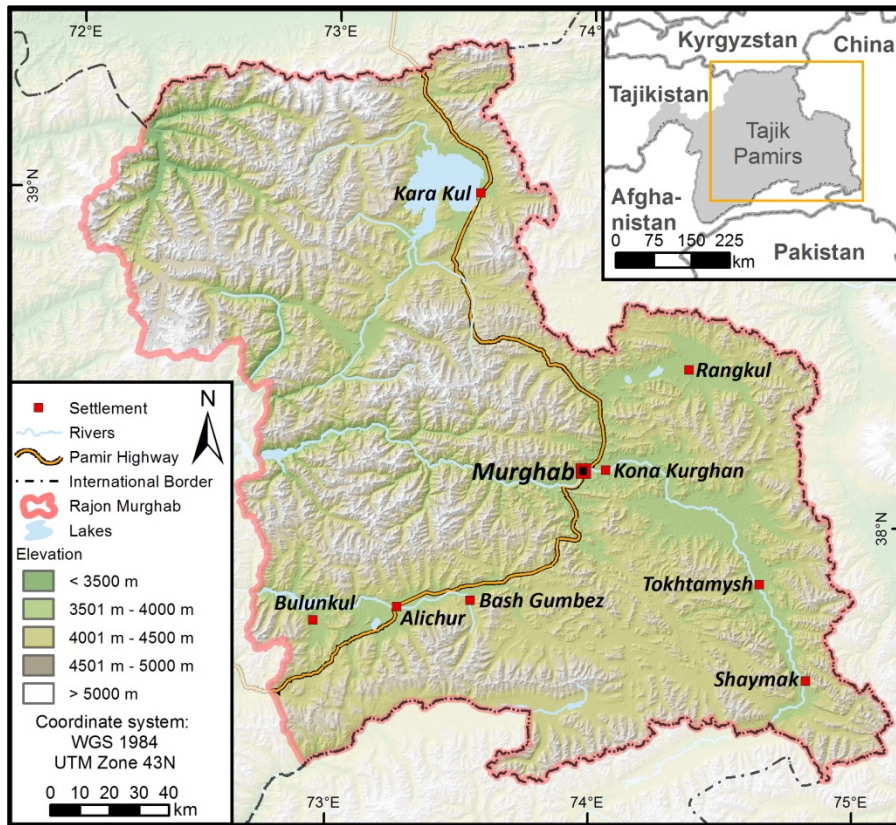


**Figure 1:** Map of the Eastern Pamirs of Tajikistan. Areal extent is approximately identical to the *rajon* (district) Murghab.

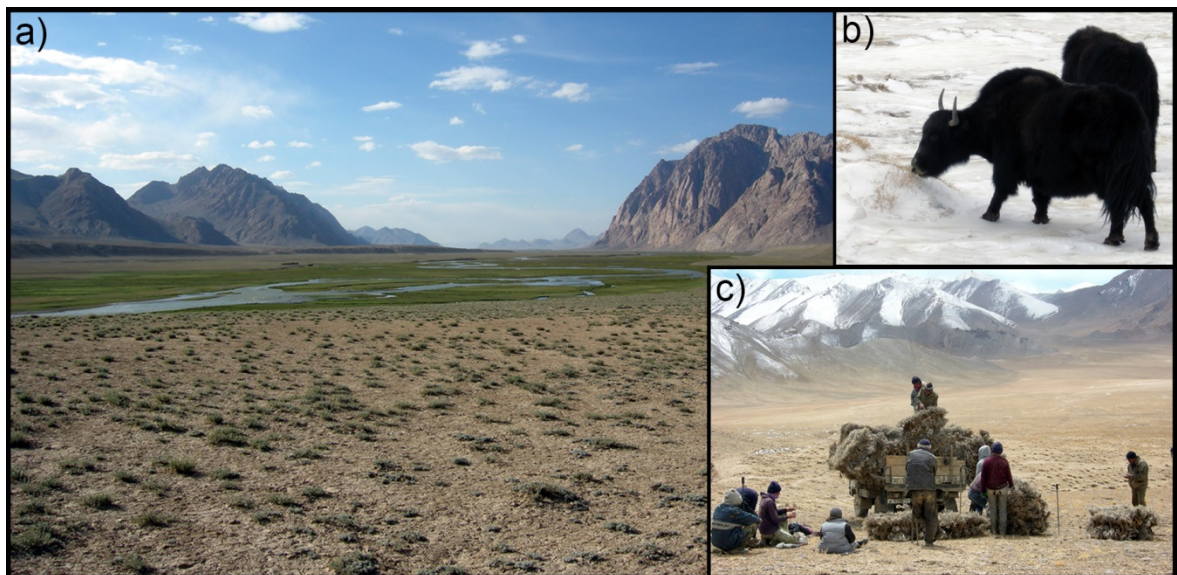


**Figure 2:** Photographs of (a) *Krascheninnikovia ceratoides* dwarf shrub formation in the front with azonal riparian grass vegetation in the background, (b) Yaks feeding on dwarf shrubs penetrating the snow, and (c) dwarf shrub harvesting.

Starting with the Czarist Empire and increasingly enforced under the Soviet rule in the 20<sup>th</sup> century, nomadism with pasture use during the summer months was replaced by permanent settlements, continuous utilization and a planned economy (Kreutzmann 2002).



## SYNOPSIS

The increased demand for thermal energy and the related excessive dwarf shrub extraction led to the ban on biomass harvesting in 1961, as the emerging degradation was recognized (Kraudzun et al. 2014). Provision was maintained with energy resources (e.g. coal) and fodder subsidies from neighboring regions. With the collapse of the Soviet Union, these subsidies ceased, and the recurring local resource exploitation, especially dwarf shrub harvesting for fuel, resulted in considerable environmental pressure (Breu et al. 2005). Geographical research after the civil war (1992-1997) focused on this issue, and a “severe energy crisis” (Droux and Hoeck 2004, p. 4), or a “*teresken* syndrome” (Breckle and Wucherer 2006), were anticipated. This culminated in the assumption that respective dwarf shrubs were totally cleared within a radius of 80 km from the district capital Murghab (Breu 2006, p. 15). However, still today dwarf shrubs can be found in walking distance from this village, and harvesting activities were observed as close as 12 km (own observations). Accordingly, more recent research on dwarf shrubs suggests a rather differentiated picture, with degraded regions appearing alongside intact vegetation, and an increased use of other energy carriers such as animal manure besides dwarf shrub biomass (Kraudzun 2014; Kraudzun et al. 2014; Vanselow and Samimi 2014). Yet, to summarize, none of these studies give quantitative figures on biomass distribution or an assessment of alternatives, but all agree that an increased utilization of renewable energies is inevitable for sustainable development (Hoeck et al. 2007; Förster et al. 2011; Wiedemann et al. 2012; Kraudzun 2014; Kraudzun et al. 2014).

## 1.2 State of the art research and research gaps

### 1.2.1 Regional mapping of woody vegetation

The first remote sensing based analyses on vegetation in the Eastern Pamirs were two diploma theses by Budka (2003) and Hergarten (2004). Budka (2003) performed an ISODATA classification (ERDAS 1999) based on Landsat 7 ETM+ images with 30 m resolution, but only distinguishes dense green vegetation from other vegetation types and does not contribute information on sparsely vegetated dwarf shrub habitats. Similarly, Hergarten (2004) used Landsat 7 ETM+ satellite data, ancillary data, a digital elevation model (DEM) and a limited set of ground observations to perform a regional land cover classification. As a part of this analysis, an ‘expert classification’, which is a rule based approach (ERDAS 1999), was conducted to separate general vegetation formations. However, the mapping of dwarf shrub vegetation was not successful with this approach due to sparse vegetation cover. Therefore, additional variables were used to extract dwarf shrub habitats but neither a validation nor performance assessments of respective results were implemented. Vanselow (2011) presented a more sophisticated vegetation classification using a large set of ground observations, 5 m RapidEye satellite images and DEM data. In doing so, an ordination method was used to preselect important predictor variables for mapping seven vegetation formations with a random forest model (Breiman 2001). The approach resulted in the first validated map considering general dwarf shrub occurrence, but information on dwarf shrub quantities was not generated. However, Vanselow (2011)

## SYNOPSIS

showed that topographic variables from the Advanced Spaceborne Thermal Emission and Reflection Radiometer (ASTER) DEM, texture variables, and vegetation indices (VIs) based on the red-edge to infrared spectral regions were important in analyzing dwarf shrub vegetation. The respective approach was subsequently adjusted to increase information on degraded and intact dwarf shrub areas and showed that the latter still cover extensive areas (Kraudzun et al. 2014). Finally, Vanselow and Samimi (2014) extended the study by using a broader spectral region, adapted topographic predictors, additional texture variables, and a VI that is intended to cope with soil noise. This increased classification accuracy and an additional random forest regression model provided information on total vegetative cover, but the prediction of dwarf shrub cover was not successful. These results indicate that remote sensing based techniques reach their limits in the Eastern Pamirs of Tajikistan, particularly regarding dwarf shrub habitats. Therefore, specialized techniques may be necessary for biomass prediction with remote sensing data.

Apart from remote sensing approaches, research on total biomass amounts of dwarf shrub communities were conducted in several studies during Soviet times which are described in detail by Vanselow (2011). However, the stated figures are inconsistent, ranging from 600 kg/ha to more than 20 t/ha according to different site conditions, and thus, an application of averaged values is not practicable to assess available biomass. Despite this absence of data on spatial availability and a large disparity of figures on local household's dwarf shrub use, varying from 1.2 t (Wiedemann et al. 2012) to 7.9 t (Droux and Hoeck 2004), an estimation of vegetation loss due to harvesting activities has been conducted, producing alarming figures (Droux and Hoeck 2004). As such an approach is not sufficient to perform a sophisticated assessment of the current situation because of the lack of empirical evidence; there is a need for research that combines reliable data on energy consumption and supply.

### 1.2.2 Global remote sensing approaches on dryland vegetation

The awareness that remote sensing and GIS are both important tools to analyze arid environments, but are also subject to major obstacles, is not new to the research community. Tueller (1987) emphasizes that in regions with a vegetation cover below 25 to 35 percent, soil is the dominant feature of a pixel's spectral signal and the detection of vegetation properties is aggravated. Moreover, the spectral variability of the vegetation itself, which consists of living green as well as of senescent or woody parts to a large extent, introduces further difficulties in the analysis of vegetation in respective regions. Eisfelder et al. (2012), in a recent review on the use of remote sensing data for plant biomass derivation in semi-arid regions, still stress the importance of additional research to address these challenges. Furthermore, the transferability of methods in time and space are considered to be an additional, central problem. Until now, a number of different techniques and sensors have been applied and tested in drylands.

Empirical models, connecting optical remote sensing indices and field measurements, are the most frequently used methods (Eisfelder et al. 2012). Therefore, a multitude of

## SYNOPSIS

potentially useful and complementary VIs have been developed since the 1970s (Huete 2014). However, the utility of most common VIs is limited in drylands (Asner and Heidebrecht 2002; Montandon and Small 2008; Yang et al. 2012), and specific methods to reduce soil background and improve the sensitivity of existing VIs are suggested (Bannari et al. 1995). Some studies showed increased performance due to such measures (Veraverbeke et al. 2012), while others report no benefits for their models (Van Der Meer et al. 2001; Calvão and Palmeirim 2011). Another promising approach in drylands is spectral mixture analysis (SMA), which uses spectra of different materials, referred to as endmembers, to model different vegetation fractions separately (Asner and Heidebrecht 2002; Yang et al. 2012). Some sources conclude that the results of SMA are superior to the VI models (Yang et al. 2012), although others acquire better results with VIs using regression models in desert environments compared to SMA (Buyantuyev et al. 2007). Additionally, as shown by Shoshany and Svoray (2002), a multi-temporal methodology based on phenological differences may be a solution to the problem of separately mapping different vegetation units such as shrubs and grasses in drylands and improving woody biomass detection. However, as this approach requires a specific variation in phenology of the species concerned, and can be inaccurate when vegetation cover is too low (Shoshany and Svoray 2002), this method is not universally applicable. Object based derivation of woody biomass, as shown by Spiekermann et al. (2015), may be a suitable alternative in semi-arid regions when the sensor resolution is sufficient to detect respective plants individually. In desert environments with small shrub vegetation, such an approach may have great potential using an unmanned aerial vehicle (UAV) that acquires very high resolution imagery (Laliberte and Rango 2011). Besides optical remote sensing approaches, radar or laser based methods are important alternatives. However, as this data is not available for the research area, or at least not in sufficient resolution, and partly involves similar limitations in regions with low vegetation cover (Eisfelder et al. 2012), related research is not discussed in the presented thesis.

Regarding spectral resolution, bands from the red and near-infrared (NIR) spectral regions, e.g. as implemented in the normalized difference VI (NDVI), were among the first used for dryland biomass analysis (Tucker et al. 1985) and are still widely applied to detect photosynthetic vegetation fractions (Eisfelder et al. 2012). Similarly, the red-edge spectral domain, which forms the transition from red to infrared wavelengths, improved the modeling of green vegetation in arid environments in some studies (Ren et al. 2011; Li et al. 2012; Ramoelo et al. 2012). Mid-infrared (MIR) or short-wave infrared (SWIR) spectral bands may contribute to biomass mapping by also capturing spectral features of senescent vegetation (Eisfelder et al. 2012). Different multispectral sensors which are used by the majority of remote sensing biomass studies in drylands (cf. Eisfelder et al. 2012) cover these wavelengths with a limited number of relatively broad spectral bands. Hyperspectral sensors, generally extending over a larger spectral domain and delivering hundreds of narrow bands, may improve vegetation analysis in arid environments as they are less susceptible to background effects and are better suited to capture spectral features of photosynthetic and non-photosynthetic plant tissue (Asner and Green 2001; Oldeland et al. 2010; Swatantran et al. 2011; Schwieder et al. 2014). However, other sources conclude that the utility of hyperspectral data is also very restricted in areas with low vegetation cover (Asner et al. 2000; Okin et al. 2001; Serrano et al. 2002).



## SYNOPSIS

In summary, research on remote sensing based vegetation and biomass analysis in arid environments is scarce due to the various methodological challenges. In particular in areas with a vegetative cover below about 30 percent, satellite based analyses have shown limited success (Eisfelder et al. 2012). Existing studies do not give clear recommendations on the suitability of specific remote sensing variables, although a large number of potentially useful predictors exist; yet these may not be adapted to arid regions. Furthermore, the applicability of different VIs may vary due to regional effects (Huete 2014) which restrict their transferability. Additionally, a comparison of different sensors in their ability to detect biomass in respective areas is missing. To address this dilemma of methodological research problems and the simultaneous need for biomass information in arid environments, enhanced research on appropriate variables, associated wavelengths, sensors, and methods is necessary to test the utility and the limits of optical remote sensing in the world's drylands.

### 1.2.3 Assessment of solar energy resources

Besides a very vague estimation by Kraudzun (2014) who sees potential in solar power to generate basic, non-thermal energy, there is no study on solar resources in the research area. Globally, many mountain areas are considered to have a high natural potential for solar power, but are also often characterized by inadequate energy infrastructure, heavy utilization of local biomass, and corresponding pressure on the environment. Therefore, a number of solar energy research approaches in high altitudes exist which either focus on the assessment of available resources (Gilman et al. 2009; Poudyal et al. 2012), the analysis of the current utilization (Wang and Qiu 2009; Bhandari and Stadler 2011), or the environmental effects of installed energy systems (Limao et al. 2012). When referring to the potentials of energy resources in general, different definitions exist, ranging from the geographical and technological to the economical or implementation potential (Painuly 2001; de Vries et al. 2007). The calculation of such potentials varies strongly as they are based on a number of context-based assumptions (de Vries et al. 2007), and hence no generally applicable approach exists. The assessment of spatial solar radiation amounts, which is the basis for deriving other potentials, is mostly conducted using GIS based solar radiation models that consider topographic effects (Tovar-Pescador et al. 2006; Pons and Ninyerola 2008; Hofierka and Kaňuk 2009; Kumar 2012) or satellite based analyses (Huld et al. 2012; Amillo et al. 2014), whereby both approaches produced reasonable results. In mountain regions, however, greater uncertainties are expected for remote sensing based radiation methods (Dürr and Zelenka 2009; Huld et al. 2012; Amillo et al. 2014) whereas GIS techniques are considered to be an adequate approach (Tovar-Pescador et al. 2006; Pons and Ninyerola 2008). Maps of the natural potential of solar radiation may be used to select suitable solar power sites (Arán Carrión et al. 2008), which in turn represent the geographical potential. The technical implementation and cost is usually calculated based on the available radiation amounts, required energy, and selected solar energy components with their respective technical specifications (Chandel et al. 2014). The evaluation of the economic feasibility is increasingly complex and often based on economic indicators like the levelized cost of electricity (LCOE, Mainali and Silveira 2013), but associated results are highly variable due to the underlying assumptions (Branker et al. 2011). Alternatively, some studies suggest that economic

## SYNOPSIS

considerations should not be solely decisive in the implementation of solar energy projects given the lack of alternative options, and social factors ought to be taken into account (Bhandari and Stadler 2011). Finally, the appraisal of the environmental effects of solar energy utilization may be based on an evaluation of existing data on ecosystem variables and solar energy development (Limao et al. 2012) or on a scenario- centered analysis (Shrestha et al. 2007).

As outlined above, a number of studies focus on solar energy resource analysis in mountainous terrain; but usually existing approaches are restricted to a certain delimited research field. A combined assessment of the feasibility and the potential effects of photovoltaic power utilization in developing mountain regions, integrating different steps of calculating renewable energy potentials, is missing. Therefore, a simple low-cost methodology is required which is adjusted to the local context, considers realistic limiting factors, and is also easily adaptable to analyze comparable developing areas.

### 1.3 Research questions and hypotheses

Dwarf shrubs play a central role for the local people and the regional ecosystem, as does perennial woody vegetation for the planet's drylands in general. Remote sensing is a tool that enables one to gain information on spatial vegetation properties over large areas; but a number of open methodological issues exist in arid environments. Therefore, the main research question of this thesis reads as follows:

#### **Is remote sensing based woody biomass quantification possible in an arid environment using space-borne data?**

Existing regional remote sensing approaches showed that a classification of general vegetation units is possible even under the challenging local settings, and that additional spectral and topographic variables may improve respective analyses. Global remote sensing studies, besides stating several difficulties, offer a wide range of variables and a number of methods to adapt existing predictors to conditions of scarce areal vegetation cover. This multitude of potentially useful predictors has not been sufficiently analyzed. Different spectral variables may be required to detect features of woody vegetation or correct for soil noise. This leads to the first general hypothesis:

**Hypothesis 1:** A combination of a large set of specifically adapted satellite based variables together with adequate selection and modeling techniques enables spatial biomass prediction even under difficult arid conditions.

Different sensors with various spatial, temporal, and spectral resolutions exist. However, existing research does not present conclusive recommendations on their suitability in arid environments. Perennial vegetation in arid environments consists of green photosynthetic, senescent and wooden parts that are characterized by different spectral properties detectable in variable wavelengths. Therefore, a broad spectral range may be advantageous in an

## SYNOPSIS

associated analysis leading to general hypothesis number two:

**Hypothesis 2:** The coverage of a broad spectral range and a high spectral resolution increase modeling performance. Hence, hyperspectral data is especially suitable for detecting woody vegetation in drylands.

Regionally, geographical research shows a contrasting picture regarding available dwarf shrubs in relation to their utilization as thermal energy carriers. On the one hand, results state a severe energy crisis with generally dwindling dwarf shrub resources; and on the other hand, a spatially differentiated situation is suggested by the existence of both degraded and non-degraded areas simultaneously. However, the existing estimations are not based on empirically derived numbers of dwarf shrub amounts or dwarf shrub demand. This leads to the second research question of this thesis, which refers to the regional scale:

**What is the spatial distribution of dwarf shrub biomass amounts in relation to their accessibility and demand?**

Remote sensing based generation of spatially resolved biomass maps allows for an interdisciplinary comparison of available dwarf shrub quantities, with survey results regarding dwarf shrub utilization and demand shedding light on the ongoing degradation debate in the Eastern Pamirs. This enables the addressing of hypothesis number three:

**Hypothesis 3:** Despite some rather pessimistic assessments regarding dwarf shrub resources in existing research, there are still regions with large stocks of dwarf shrub biomass to meet local thermal energy demands.

Finally, this thesis intends to analyze possible alternatives to currently utilized energy carriers, as existing studies consider renewable energies a prerequisite for sustainable development. To that end, solar energy, as an infinite resource, is suggested to be of major importance in mountain regions, but its potential in the Eastern Pamirs remains unknown. The introduction of thermal energy as a substitute for local dwarf shrub use is a central issue in this context. Solar thermal techniques are not considered due to the frequent recurrence of freezing temperatures even in summer months. Accordingly, the third research question is:

**Is the generation of alternative thermal energy feasible with solar photovoltaic systems?**

The assessment of renewable energy potentials or associated definitions varies widely according to underlying assumptions and the research context. A number of potentially useful methods exist, but they have to be integrated and adapted to the respective local conditions. From this knowledge, the fourth hypothesis is derived:

**Hypothesis 4:** An integrative approach, combining climatic measurements, GIS based radiation modeling, and additional survey data, enables an assessment of the feasibility and effects of increased solar photovoltaic energy utilization.

## 2 Materials and Methods

---

In this section, data, materials and methods to test the hypotheses are briefly presented. A detailed description is given in the respective manuscripts ([Part II](#)). Regionally collected field data or ground truth data present the basis of the study. Satellite data and associated processing techniques are required to address objectives on remote sensing subjects, as are statistical methods (Hypotheses 1 and 2). Observation based scenarios are used to define framework conditions regarding human or economic influences (Hypotheses 3 and 4). The GIS based radiation model, utilized for solar resource assessment, is addressed (Hypothesis 4) and external data for interdisciplinary analyses is summarized (Hypotheses 3 and 4). Finally, applied software is listed.

### 2.1 Field methods and derivative data

Ground truth data on vegetation is necessary to separate dwarf shrub habitats from other land cover (please refer to [chapter 2.3.1](#)) and for the derivation of spatially allocated biomass quantities to train and validate remote sensing based models. The basic units providing this information were field plots registered with a global positioning system (GPS) device. An associated sampling design of these plots has to meet different, partly contradictory, requirements. On the one hand, sampling design should correspond to statistical principles, whereby probability sampling is considered as ideal ([Stehman and Czaplewski 1998](#)). On the other hand, non-probability sampling may be better suited to ensuring ecological representativeness ([Roleček et al. 2007](#)). Finally, research objectives, practical considerations, and general limitations may make deviations from probability sampling inevitable ([Stehman and Czaplewski 1998](#)). Remote sensing involves a plot size that is adapted to the sensor resolution ([Justice and Townshend 1981](#)), and so a certain minimum extent is required. Furthermore, relatively homogenous vegetation is necessary ([Vanselow 2011](#)). Finally, a broad range of dwarf shrub coverage had to be mapped with the sampling design and the consideration of accessibility was central in this extensive and rugged terrain. Therefore, a three-step sampling design was implemented. First, dwarf shrub stands that meet the aforementioned criteria were preferentially selected to cover the whole research area. Within the stands, dwarf shrub quantities were recorded in sub-plots meeting size recommendations given in [Mueller-Dombois and Ellenberg \(1974\)](#). These sub-plots were randomly placed and defined the locations of the field plots. The field plots then served for the extraction of spectral properties for remote sensing analysis using different approaches and the allocation of vegetation quantities. Several methods to quantify vegetation are given in literature ([Mueller-Dombois and Ellenberg 1974](#)). Existing remote sensing approaches in the research area used estimates to derive areal vegetative cover classes ([Vanselow 2011](#); [Kraudzun et al. 2014](#); [Vanselow and Samimi 2014](#)). However, such estimates may introduce additional uncertainties ([Wilson 2011](#)), which was confirmed by testing this approach with a small pre-test sample ([Figure 3a](#)). For this reason, as well as to establish an empirical relationship to total dwarf shrub biomass, a regionally adapted measurement technique was implemented

## SYNOPSIS

which is similar to a crown diameter method (Mueller-Dombois and Ellenberg 1974). The shape of local dwarf shrub growth most closely resembles a circle (Figure 3b), and the measured plant circumference was thus used to calculate the circle area of dwarf shrubs in the sub-plots. However, as the major part of the dwarf shrub mass is located within the root zone (Figure 3c), a conversion method is necessary to derive the total biomass.

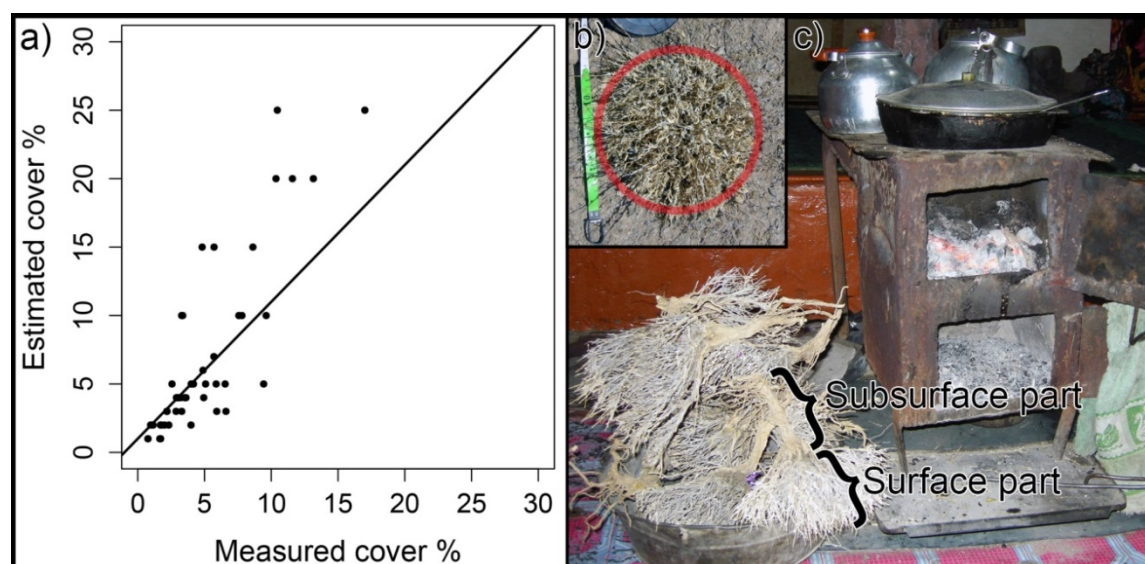


**Figure 3:** Illustrations of (a) differences between cover estimates performed by an experienced first observer and cover measurements using the dwarf shrub circle area formula performed by a second observer in 4 m x 4 m plots with superimposed 1:1 line, (b) typical dwarf shrub growth shape with red circle overlay for comparison, and (c) excavated dwarf shrubs for heating purposes.

### 2.1.1 Allometric model

Allometric models are empirical functions that permit the calculation of biomass from easily measurable morphological parameters, and are frequently used in arid environments (Perez-Quezada et al. 2011) and remote sensing studies (Eisfelder et al. 2012). The suitability of several dwarf shrub surface parameters as proxies for total biomass was examined with a small pre-test sample. Dwarf shrub circle area derived from the measured circumference proved to be the best indicator. Regression modeling of logarithmically transformed variables with subsequent 10-fold cross validation (Brenning 2012) and logarithm bias correction (Baskerville 1972) was applied using a larger sample comprising all regional dwarf shrub species to derive total biomass from dwarf shrub circle areas. The model served for the calculation of individual dwarf shrub biomass within the sub-plots. The results were aggregated to represent the total dwarf shrub biomass per ha for every field plot.

### 2.1.2 Climate data

Officially available climate data was not suitable for this study as solar radiation is not recorded. Global solar radiation measurements, at a one minute sampling and a half hourly logging interval, were performed using four automatic weather stations. The climate stations



## SYNOPSIS

are located in the villages Murghab (3,650 m.a.s.l.), Alichur (3,900 m.a.s.l.), Shaymak (3,900 m.a.s.l.), and on the summit of Pik Pionerka (4,740 m.a.s.l.). This setting was intended to simultaneously cover the main villages and different climatological conditions, such as the different valley configurations, altitudes, and compass directions. Subsequent analysis and quality control of the data led to an available time period, from October 2012 until November 2013 for the Pik Pionerka station and from October 2012 until February 2015 for the three other stations, which was then averaged to monthly values for the analysis.

## 2.2 Satellite data

Due to budgetary reasons, this dissertation is based on freely available remote sensing data. Besides, the rationale of selecting adequate satellite data depends on a number of factors. The timing of the acquisition should fall within the period from mid-summer to the beginning of fall to ensure minimum snow cover and data from the peak of the vegetation period. As the vegetation related signal is relatively low in this arid environment in general, this was necessary to achieve a maximum spectral plant response in the images. Multi-temporal approaches such as phenological decomposition (Shoshany and Svoray 2002) were not considered, as the phenology of local vegetation is concurrently timed due to the cold and arid environment with snow, low temperatures, and short vegetation periods, according to our observations and information in literature (Walter and Breckle 1986; Vanselow 2011). Furthermore, regional plants are not characterized by an immediate response to precipitation, such as short term greening after rainfall. Because of the prevailing aridity, overcast conditions are relatively rare. Therefore, a moderate temporal resolution with a monthly revisit time to allow for the acquisition of images with low cloud cover is sufficient for this analysis. Spatial resolution is also a central issue in remote sensing based analysis (Khorram et al. 2012). In the research area, dwarf shrub stands frequently cover relatively large areas with a side length above 100 m, and so a medium resolution sensor (e.g. 30 m) would be sufficient for the analysis. However, dwarf shrubs also form patches within these stands and a high to moderate resolution sensor (around 5 m, c.f. Eisfelder et al. 2012) would be required to resolve respective patterns. Sensors with both moderate and moderately high resolutions deliver a mixed signal incorporating vegetation as well as soil spectral signals. Individual dwarf shrub plants can only be detected using very high resolution imagery, well below 50 cm. At present, costly panchromatic sensors, airborne sensors, or sensors on UAVs are able to deliver data in this resolution. However, UAV or airborne operations are currently not possible in the research area because of legal restrictions. Furthermore, very high resolution sensors also involve significantly higher computational and processing costs when analyzing large areas (Matese et al. 2015). Finally, the selection of the spectral resolution is also critical for remote sensing- based analysis (Khorram et al. 2012). As noted earlier, a higher spectral resolution is hypothesized to increase performance of dwarf shrub detection and so a number of sensors with a broad spectral range and a large number of spectral divisions that meet aforementioned criteria are considered ideal for this thesis (Figure 4).

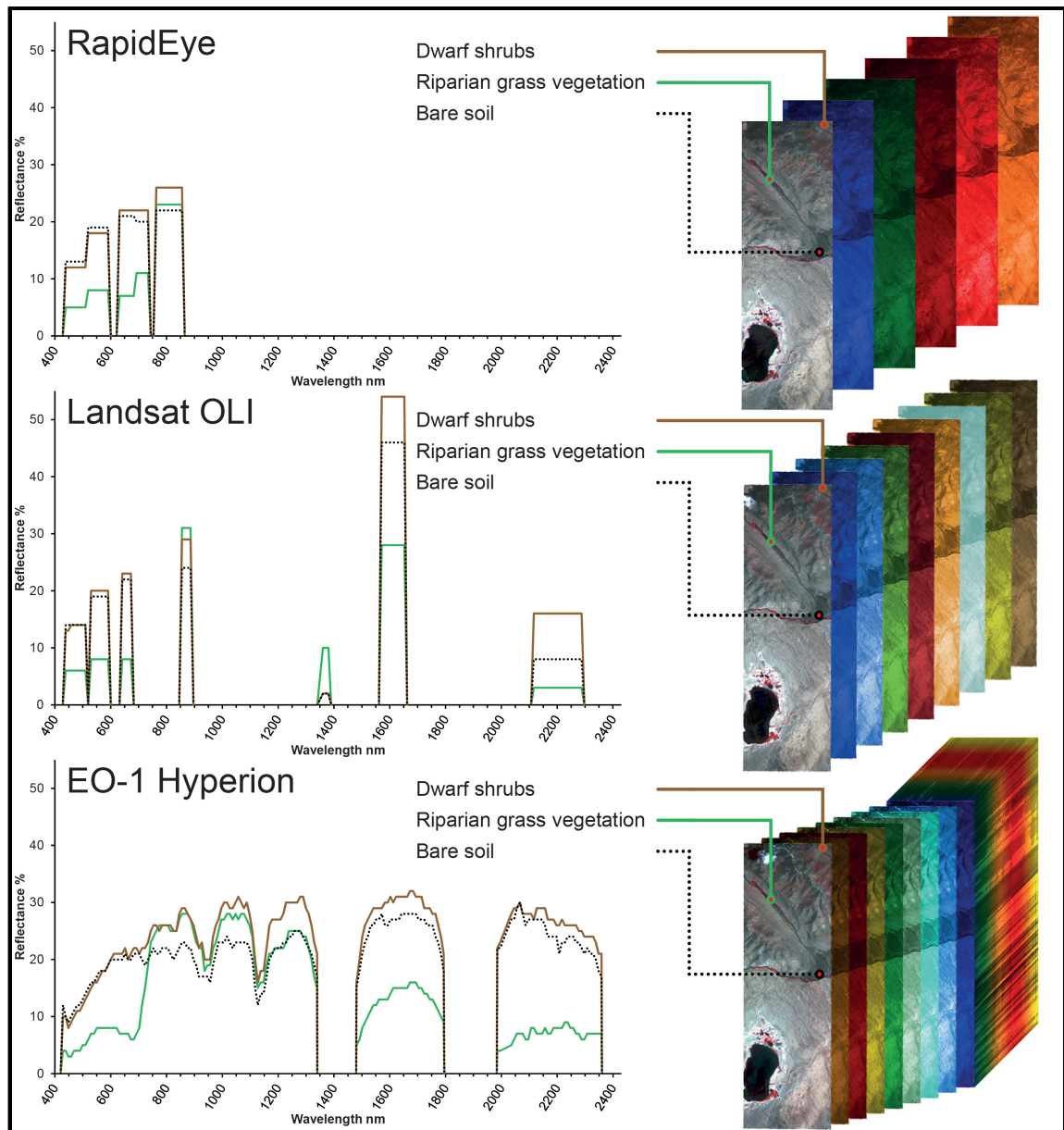


**Figure 4:** Exemplary spectral curves of field plots with different land cover derived from the applied sensors (left) and schematic representations of individual bands with a superimposed color infrared image (right).

### 2.2.1 RapidEye data

The RapidEye sensor has a spatial resolution of 5 m (resampled from 6.5 m nominal ground resolution), a revisit time of about six days, and five spectral bands from the blue to the NIR regions (RapidEye AG 2011). A special feature of this sensor is that it offers a band covering the red-edge domain and there are indications that this band may be more effective in dryland vegetation studies (Eisfelder et al. 2012; Li et al. 2012; Ramoelo et al. 2012). In addition, with the relatively high spatial resolution, this sensor may be able to detect patch features of dwarf shrub vegetation using texture variables.

### 2.2.2 Landsat 8 OLI data

The Operational Land Imager (OLI) sensor onboard the Landsat 8 satellite has a multispectral resolution of 30 m, covers the whole globe in a 16-days cycle and offers eight spectral bands (USGS 2015). The spatial resolution of this sensor is very useful for the regional scale (Eisfelder et al. 2012). Besides several bands ranging from the blue to NIR regions, two SWIR bands may make this sensor particularly suitable for the analysis. The 15 m panchromatic band was not used in this study.

### 2.2.3 Hyperspectral EO-1 Hyperion data

The National Aeronautics and Space Administration's (NASA) Hyperion sensor onboard the Earth Observing 1 (EO-1) satellite was the first (Khorram et al. 2012) and is presently the only space-borne hyperspectral sensor providing data for the research area. This sensor has a spatial resolution of 30 m, a temporal resolution of 200 days, a very high spectral resolution with 242 bands ranging from 356–2577 nm, and a bandwidth of about 10 nm (Beck 2003). This spectral resolution may offer new possibilities in analyzing woody vegetation in drylands by capturing various plant features, but processing constitutes an additional challenge in respective research (Khorram et al. 2012). The narrow swath width, low temporal resolution, and limitations on collectable images per day require tasking of the satellite (Beck 2003). Therefore, only a small number of 7.5 km broad images are available for analysis with this experimental sensor.

### 2.2.4 ASTER data

The ASTER global DEM provides ground elevation data from processed stereo pairs of nadir and non-nadir-looking NIR cameras with a resolution of one arc second (METI and NASA 2009). These images served the derivation of additional topographic variables after resampling to a pixel size of 30 m.

## 2.3 Processing of satellite data and derived variables

A modeling approach that connects field data to a multitude of potentially useful spectral variables by simultaneously using different modeling techniques was selected to quantify biomass in this thesis. A SMA approach, as a potential remote sensing based alternative in semi-arid environments, was not considered. The main reason for this is that a complex spectral unmixing methodology would be required that resolves non-linear mixing issues whereby single plant components may not be detectable in this sparsely-covered region (Asner et al. 2000; Okin et al. 2001). Besides field spectra, such an approach would also be based on the separate mapping of photosynthetic and non-photosynthetic vegetation, which



## SYNOPSIS

is an unresolved issue and one of the largest error sources in existing research (Meyer and Okin 2015). In contrast, the applied method aims to utilize remote sensing- based variables indicative of a mixed biomass signal comprising spectral properties of soil, photosynthetic, and non-photosynthetic materials in a multi-variable model. Therefore, different processing steps are required. These include the preparation of raw remote sensing data, the limitation of the study region to the relevant area of interest, and the derivation of remote sensing variables that are subsequently integrated in the actual modeling (please refer to chapter 2.4).

All optical satellite products are available in preprocessed formats subject to terrain correction as well as geometric and radiometric calibrations. Digital numbers were recalculated to at-sensor radiance. Atmospheric effects influence the data recorded by a satellite sensor, and different atmospheric correction methods exist to minimize these influences (Khorram et al. 2012). For this thesis, ENVI's MODTRAN® based FLAASH® algorithm was utilized as a state of the art radiative transfer model (Guanter et al. 2009; Jiménez-Muñoz et al. 2010) by applying daily atmospheric water vapor amounts from the Aqua AIRS Level 3 Daily Standard Physical Retrieval product (AIRS science team and Teixeira 2013). The algorithm results in surface reflectance values. Products delivered in tiles were mosaicked to spatially coherent images using a feathering algorithm. Additionally, RapidEye images had to be normalized using color balancing (cf. Luedeling and Buerkert 2008) as some images contained visible illumination differences. A spatial error was still present in the RapidEye and Hyperion images despite preprocessing algorithms. Therefore, respective images were georeferenced using GPS registered ground control points and Landsat images.

### 2.3.1 Preclassification

To separate the area of interest (dwarf shrub habitats) from other regions (grass vegetation, water bodies, snow, and ice) a preclassification was performed. Existing studies suggest good spectral separability of dwarf shrub vegetation formations from other land cover types (Vanselow 2011; Vanselow and Samimi 2014). Spectral angle values (SAV, Figure 5a), which are numerical measures of the spectral resemblance of two spectra for the rapid mapping of spectrally similar areas (Kruse et al. 1993), were used to create raster maps for the subsequent implementation of the dwarf shrub biomass model. A dense dwarf shrub reference spectrum on the one hand and a closed azonal grass vegetation spectrum on the other hand were derived from Landsat data to achieve a uniform classification. From the reference spectra, SAV were calculated for the whole raster image and averaged for the vegetation plots. The ability of these variables to separate dwarf shrub habitats from grass vegetation was tested using the area under the ROC (AUROC) value, as it is considered a favorable performance measure of classifiers (Bradley 1997; Hand and Till 2001). The classification thresholds were determined using corresponding boxplot whisker values of dwarf shrub plot SAV with both reference spectra to exclude spectrally different areas (Figure 5b). Outlying areas were not considered for quantitative modeling.

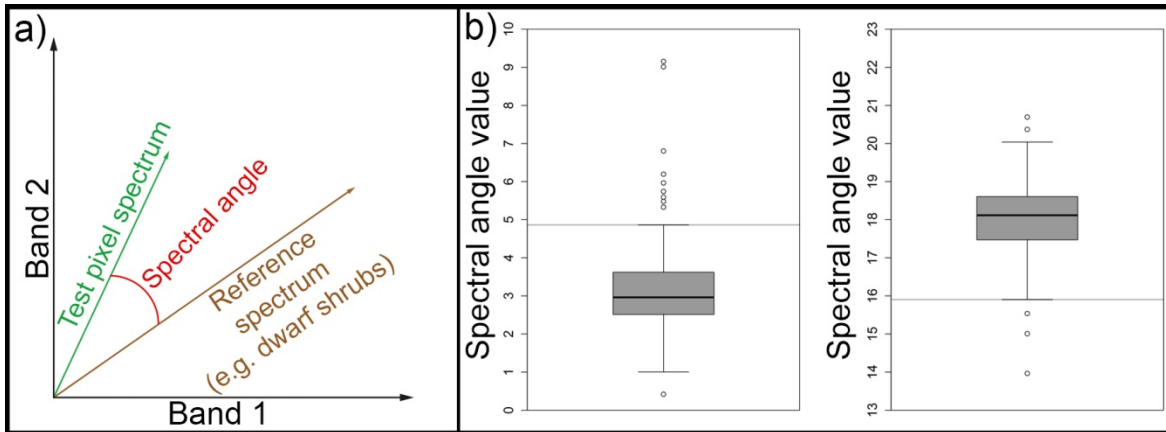


**Figure 5:** Illustrations of (a) spectral angle between a reference spectrum and a raster pixel using a hypothetical two band image according to Kruse et al. (1993), and (b) boxplots of dwarf shrub SAV values with thresholds (grey horizontal lines) of the dwarf shrub reference spectrum (left) and riparian grass vegetation spectrum (right).

### 2.3.2 Individual bands and band ratios

The application of single spectral bands for vegetation modeling is the simplest form of using remote sensing data, but they may be important indicators of vegetation biomass in drylands (Mutanga and Rugege 2006). To enhance the contrast between different materials, simple band ratios may be calculated by dividing one band by another which was successful in analyzing grass biomass in semi-arid regions (Samimi and Kraus 2004). Therefore, individual bands and band ratios were included in the present thesis.

### 2.3.3 Vegetation indices

VIs are the most frequently applied remote sensing based variables which represent normalized ratios of spectral bands to reduce noise (Huete 2014). These indices are used by the majority of dryland remote sensing studies and a number of these reported high correlations with plant biomass (Eisfelder et al. 2012). Respective indices are usually calculated as:

$$VI_{a,b} = \frac{Ra - Rb}{Ra + Rb} \quad (1)$$

Where  $R$  is reflectance;  $a$  is the first wavelength and  $b$  is the second wavelength. Respective indices using all available spectral bands and other versions suggested in literature (Gelder et al. 2009; Ramoelo et al. 2012) were derived for this study.

### 2.3.4 Soil adjusted vegetation indices

Simple VIs are subject to a number of disturbances, especially in regions with low vegetation cover, and additional indices have been developed to account for variations in soil brightness (Bannari et al. 1995). Generally, various forms of respective indices exist: Indices that are based on fixed, empirically derived constant coefficients to adjust for background influences such as the soil adjusted VI (SAVI, Huete 1988), indices using self-adjustable correction factors (Qi et al. 1994), and indices that are based on the calculation of soil line parameters by applying regional soil plots (Figure 6, Bannari et al. 1995). Spectral variables based on these principles are considered to improve dryland vegetation analysis in the study area (Kraudzun et al. 2014; Vanselow and Samimi 2014) and other regions (Bannari et al. 1995; Veraverbeke et al. 2012). In this thesis, various forms of respective indices are used and referred to as soil adjusted VIs.

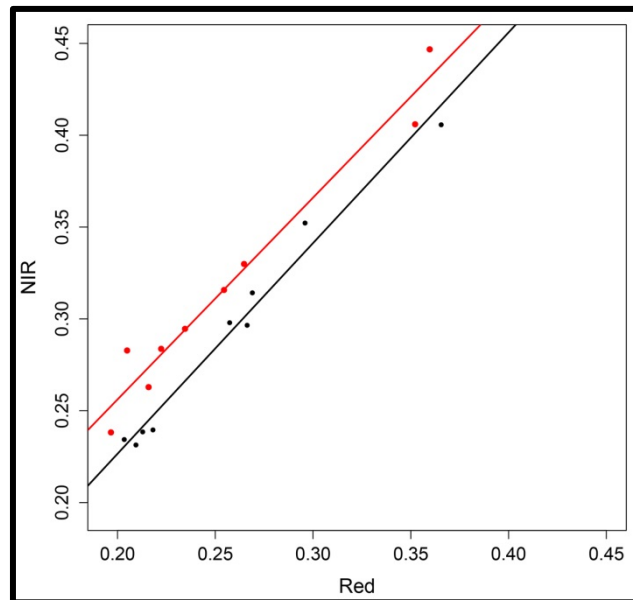


**Figure 6:** Scatterplot of nine bare soil sites (black) and nine dwarf shrub sites (red) in the Landsat red-NIR spectral domain. The Black regression line is used for the derivation of soil line parameters. Presented vegetation plots most closely resemble the theoretical concept of the perpendicular vegetation index (cf. Jackson et al. 1980)

### 2.3.5 Color adjusted vegetation indices

Besides influences of soil brightness, VIs are also subject to soil color variations. To account for such dissimilarities, specific indices were developed by correlating an additional correction index (*CI*, e.g. a redness index using red and green bands, Escadafal and Huete 1991) to existing common *VIs* such as the NDVI, and correcting for soil color using following formula:

$$VI_{corrected} = VI - (k * CI) \quad (2)$$

## SYNOPSIS

,where  $k$  is the slope of the linear correlation between  $VI$  and  $CI$ . This is considered to increase the sensitivity of VIs in arid regions (Escadafal and Huete 1991; Bannari et al. 1995). As such indices may be especially suitable for the research area with its highly variable soil colors; this approach was adopted for aforementioned variables and extended with additional CIs to derive a number of color adjusted VIs.

### 2.3.6 First derivatives of reflectance and ratios

First derivatives of reflectance (FDR) are indices that are based on the changes of the slope along the spectrum (Elvidge and Chen 1995). They may be less susceptible to soil and illumination noise (Wang et al. 2011). Therefore, FDR indices and FDR ratios were calculated for this study.

### 2.3.7 Principal components and ratios

Principal components (PCs) are low dimensional representations of data containing as much variation as possible (James et al. 2013). PCs are reported to correlate with vegetation in dryland regions (Mutanga and Rugege 2006). In this thesis, PCs and respective PC ratios were derived as they may be related to dwarf shrub features or correct for background influences.

### 2.3.8 Texture variables

Texture measures are characterizations of spatial grey-level distributions, edge quantifications of image segments, or are based on gray level co-occurrence values between a pixel and its neighbors (Irons and Petersen 1981). These variables showed to improve biomass detection in general (Fuchs et al. 2009; Sarker and Nichol 2011) as well as vegetation analysis in the research area (Kraudzun et al. 2014; Vanselow and Samimi 2014). As dwarf shrubs sometimes grow in patches with a side length of several meters, texture attributes using high-resolution data could add valuable information to model dwarf shrub biomass. Therefore, texture measures were calculated by applying grey-level co-occurrence and range filters based on RapidEye data.

### 2.3.9 Spectral angle based variables

SAV and ratios of SAV were included in this thesis as a substitute for real endmembers used in SMA approaches that performed well in other semi-arid regions (Yang et al. 2012). As pure image based endmembers cannot be mapped due to the scarce vegetation cover of the study area, this approach is intended to exploit some advantages of the method by integrating SAV of soil, dwarf shrub, and grass vegetation plots. These variables are considered as pseudo endmembers in this study.

### 2.3.10 Topographic variables

Since topography influences solar radiation, evapotranspiration, and temperature, it may be an important factor regarding biomass quantities in arid environments (Sternberg and Shoshany 2001). Correspondingly, topographic variables are considered to be major components in modeling regional vegetation (Vanselow 2011; Kraudzun et al. 2014; Vanselow and Samimi 2014). To include this information in our study, we derived elevation, the cosine of slope aspect, the sine of slope aspect, and slope as topographic predictors from the ASTER DEM.

## 2.4 Statistical methods

Preliminary plots and existing literature on semi-arid shrublands suggest that biomass shows an approximately linear relationship to spectral variables (Holm et al. 2003; Calvão and Palmeirim 2004). Therefore, this thesis mainly focuses on linear methods of biomass modeling. The high number of available spectral predictors caused by the multitude of proposed variables in literature, and the tremendous number of bands provided by hyperspectral sensors, introduce some challenges to respective modeling. Generally, time and cost constraints limit the total number of samples. This may result in a data set that contains more potential predictor variables than observations, which is a frequent research problem referred to as high dimensional (James et al. 2013). The situation leads to model overfitting with some traditional approaches, and a number of alternative methods for efficient variable selection or weighting were designed (Brenning 2009; James et al. 2013).

### 2.4.1 Linear regression

The comparatively straightforward linear regression model is a widely used method and the basis of many newer, sophisticated modeling techniques (James et al. 2013). In this thesis, stepwise forward variable selection is applied as this procedure is computationally efficient and can be used in a high-dimensional setting (James et al. 2013). The method starts with a no-predictor model (null model) and adds predictors stepwise as long as an improvement criterion is increased. The linear regression model was used in various implementations in this thesis: Simple linear regression restricted to one predictor was applied using the Pearson correlation coefficient as the selection criterion. Further, linear multiple regression models, one version restricted to a maximum of four predictors to assess the utility of sparse models and one version without predictor limitations, were applied. In these implementations, Akaike Information Criterion (AIC) was used as a selection criterion which adjusts for model size and is well-founded in statistical theory (James et al. 2013).

## 2.4.2 Partial Least Squares linear regression

Partial least square (PLS) linear regression is a supervised dimension reduction method. By means of it, all available original predictor variables are transformed to linear combinations that are related to the response variable (biomass) and so fewer feature sets for modeling are generated (James et al. 2013). Residual data is used to create new feature sets in each step. An internal cross validation procedure of the root mean square error (RMSE) is applied to choose the ideal number of steps (Mevik et al. 2015). Some remote sensing studies recommend PLS as a tool that enables high dimensional data handling (Peerbhay et al. 2013).

## 2.4.3 Ridge regression

As with least squares regression, ridge regression (RR) aims to generate coefficients leading to a small residual sum of squares; but it introduces a factor that shrinks less important coefficients towards zero using a tuning parameter  $\lambda$  (James et al. 2013). The determination of an ideal value for  $\lambda$  is critical with this approach and is determined using cross validation. Although RR penalizes the coefficients and certain variables are not very influential in the final model, the technique uses all predictors for modeling. Lazaridis et al. (2011) report good performance of RR in their study with a large number of remote sensing based predictors.

## 2.4.4 Lasso regression

The lasso regression is very similar to RR, but instead of shrinking the coefficients towards zero, lasso actually shrinks very small coefficients down to zero (James et al. 2013). In that way, not all predictors are used in the final model and lasso performs feature selection, thus leading to simpler models. *A priori*, it is usually unclear whether RR or lasso is more suitable for an analysis as this depends on the relationship of the number of predictors to the response (James et al. 2013). However, some remote sensing studies showed good performance of the lasso regression in quantifying vegetation (Gaughan et al. 2013; Takayama et al. 2013).

## 2.4.5 Random forest regression

Random forest regression (RF) is a non-linear, non-parametric tree based method that is considered an appropriate approach when handling high dimensional data (Pal 2005). In this thesis, it is used to test the advantages of non-linear models for the prediction. The technique uses a number of trees, where each tree is based on a randomly selected subset of predictors which is suggested as robust to overfitting (Breiman 2001). Selection of split variables is based on the greatest reduction of the residual sum of squares, and the number of predictors used for the subsets usually corresponds to the square root of total predictors (James et al. 2013). The RF model is considered a valuable approach for remote sensing based analysis in

the research area (Vanselow and Samimi 2014) and biomass mapping in other regions (Powell et al. 2010).

### 2.4.6 Cross validation

Knowledge regarding the test error, which is a performance measure for a method applied on new data not included in model building, is necessary for the evaluation of a statistical approach (James et al. 2013). The easiest method of calculating such a test error is using an additional test dataset not included in training the model. However, such a large test data set is often unavailable. Another approach is splitting the data randomly into two parts, training the model on the one sample, and using the resulting model to predict values for the excluded set. Error measures from this validation set allow for an estimate of the test error (James et al. 2013). However, the derived test error may be highly variable depending on included or excluded samples, and fewer training observations may reduce model performance. These effects are reduced when using leave-one-out cross validation or k-fold cross validation. The latter has a lower computational cost and is considered to give more accurate estimates of the test error (James et al. 2013). In this thesis, 10-fold cross validation is performed where the data is partitioned into ten subsets, and each subset is excluded for testing the model and the nine remaining samples are used for model fitting. The procedure is repeated until every subset has been used as a test set once. To generate results that are independent of a particular segmentation, the whole process is repeated 100 times (James et al. 2013). As spatial autocorrelation may be present in geospatial data, k-means clustering of coordinates was applied as outlined in Brenning (2012).

### 2.4.7 Variable importance

The importance of the predictors was determined using a permutation based approach in which every predictor is randomly altered and the associated change of prediction accuracy is used as a measure of the importance of the variable (Strobl et al. 2007). Several studies applied this technique for importance assessment in a spatial context (Ruß and Brenning 2010; Brenning et al. 2012).

### 2.4.8 Multiple test procedures

Hypothesis testing in correlation analysis introduces a multiple testing problem when a large number of variables are investigated. When 100 independent hypothesis tests at the 5 % significance level are conducted, five false rejections are anticipated if all the null hypotheses of zero correlation are true. With 10,000 tests, this number should increase to 500 false rejections. With more than 12,000 hyperspectral indices available, this problem has to be taken into account. Therefore, the Benjamini-Hochberg procedure (Benjamini and Hochberg 1995) was applied. The suitability of this method was suggested by Peña et al. (2012) when analyzing hyperspectral data.



## 2.5 Observation based scenarios and cost assessment

Evaluating aspects that depend on human behavior under specific circumstances are often complex and highly variable. Therefore, assumptions on certain framework conditions are required. Scenarios provide tools for scientific assessment and describe plausible situations or developments. Scenarios are not forecasts and inevitably require subjective factors (Nakićenović and Intergovernmental Panel on Climate Change 2000). Studies on sustainable development, energy resources, or the evolution of ecosystem services frequently use scenario based analyses (Hassan et al. 2005; Lund 2007; Shrestha et al. 2007; UNEP 2012). In this thesis, descriptive scenarios are applied to determine harvesting behavior, potential electric energy use, energy requirements, and economic framework conditions. The scenarios are derived using field based qualitative information such as participatory observations of local harvesting activities. Additionally, data from the literature (e.g. Kraudzun 2014) and project partners is deployed. Cost assessment for energetic infrastructure is implemented using current market prices and the adaption of literature-derived formula (Chandel et al. 2014).

## 2.6 GIS based solar radiation model

Several GIS based solar radiation models exist with different advantages and limitations (Erdélyi et al. 2014). The DEM based ArcGIS solar analyst was selected for this study as existing research showed reasonable performance of this algorithm in complex terrain (Tovar-Pescador et al. 2006), it is a relatively simple approach, and the software is widely available and frequently used (ESRI 2015). The solar analyst calculates a hemispheric viewshed for every point on the raster and overlays this viewsheds with sunmaps representing direct solar radiation and skymaps that provide diffuse solar radiation amounts (Fu and Rich 1999). The integration of the sun position allows for the calculation of every time period. The main parameters controlling the model are topographic effects and atmospheric parameters. The latter are represented by transmittivity, which is an indicator of the permeability of solar radiation through the atmosphere, and the diffuse proportion as a measure of the quantity of global radiation that reaches the surface after scattering (Fu and Rich 1999). A calibration station served the derivation of ideal corresponding parameters in this thesis.

## 2.7 External data for interdisciplinary analysis

To integratively analyze dwarf shrub quantities against the background of accessibility and demand, additional data is necessary. Respective data was generated by an extensive survey on energy consumption implemented by Hohberg and Kreczi (2013). An empirical field based model of accessibility was provided by Hohberg (submitted).



## 2.8 Software

This thesis considers a broad range of geospatial analysis software as every product provides specific tools and offers certain advantages (and disadvantages). Applied software includes ArcGIS, ENVI, QGIS, SAGA GIS and TNTmips. Statistical analysis and spatial modeling was performed using R.



PART II

PUBLICATIONS



### 3 List of manuscripts and declaration of individual contributions

---

#### **Manuscript 1** ([Chapter 4](#))

*Title:* Quantifying dwarf shrub biomass in an arid environment: comparing empirical methods in a high dimensional setting

*Authors:* Harald Zandler, Alexander Brenning, Cyrus Samimi

*Journal:* Remote Sensing of Environment 2015, 158, pages 140-155

*Status:* published

*Individual contributions*

|                           |   |
|---------------------------|---|
| <b>H. Zandler (major)</b> | concept (70 %), data acquisition (90 %), data analysis (50 %), discussion (80 %), manuscript preparation and editing (80 %) |
| A. Brenning (minor)       | concept, data analysis, discussion, manuscript preparation and editing  |
| C. Samimi (minor)         | concept, data acquisition, manuscript editing   |

#### **Manuscript 2** ([Chapter 5](#))

*Title:* Potential of space-borne hyperspectral data for biomass quantification in an arid environment: advantages and limitations

*Authors:* Harald Zandler, Alexander Brenning, Cyrus Samimi

*Journal:* Remote Sensing 2015, 7(4), pages 4565-4580

*Status:* published

*Individual contributions*

|                           |   |
|---------------------------|---|
| <b>H. Zandler (major)</b> | concept (95 %), data acquisition (100 %), data analysis (80 %), discussion (100 %), manuscript preparation and editing (90 %) |
| A. Brenning (minor)       | data analysis, manuscript preparation and editing   |
| C. Samimi (minor)         | concept, manuscript editing   |

#### **Manuscript 3** ([Chapter 6](#))

*Title:* High mountain societies and limited local resources - livelihoods and energy utilization in the Eastern Pamirs, Tajikistan

*Authors:* Georg Hohberg, Fanny Kreczi, Harald Zandler

*Journal:* Erdkunde

*Status:* accepted

## MANUSCRIPTS

### *Individual contributions*

|                           |   |
|---------------------------|---|
| <b>H. Zandler (equal)</b> | concept (33 %), data acquisition (33 %), data analysis (33 %), discussion (33 %), manuscript preparation and editing (33 %) |
| G. Hohberg (equal)        | concept, data acquisition, data analysis, discussion, manuscript preparation and editing                                    |
| F.Kreczi (equal)          | concept, data acquisition, data analysis, discussion, manuscript preparation and editing                                    |

### **Manuscript 4 (Chapter 7)**

*Title:* Scenarios of solar energy utilization on the ‘Roof of the World’: potentials and environmental benefits

*Authors:* Harald Zandler, Bunafsha Mislimshoeva, Cyrus Samimi

*Journal:* Mountain research and development

*Status:* submitted

### *Individual contributions*

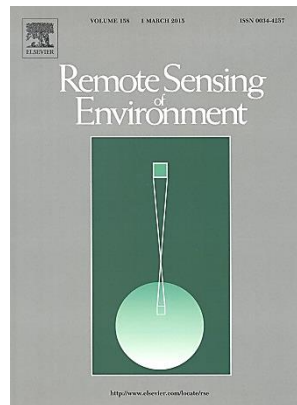
|                           |  |
|---------------------------|--|
| <b>H. Zandler (major)</b> | concept (85 %), data acquisition (80 %), data analysis (100 %), discussion (95 %), manuscript preparation and editing (90 %) |
| B. Mislimshoeva (minor)   | concept, discussion, manuscript preparation and editing  |
| C. Samimi (minor)         | concept, data acquisition, manuscript editing  |

# 4 Quantifying dwarf shrub biomass in an arid environment: comparing empirical methods in a high dimensional setting

---

Harald Zandler, Alexander Brenning & Cyrus Samimi

*Remote Sensing of Environment* 2015, 158, pages 140-155



This publication constitutes the basis of the submitted dissertation. By testing a large number of remote sensing based variables, two commonly used multispectral sensors, and various models for woody biomass quantification, the manuscript addresses **hypothesis 1** and parts of **hypothesis 2**. Furthermore, it is the methodological foundation for model-building in manuscript 3 ([chapter 6](#)) which in turn contributes to **hypothesis 3**. Finally, derived knowledge on spatial biomass amounts also contributes to assessing average dwarf shrub stocks in manuscript 4 ([chapter 7](#)). The layout of the published original is maintained.







Contents lists available at ScienceDirect

## Remote Sensing of Environment

journal homepage: [www.elsevier.com/locate/rse](http://www.elsevier.com/locate/rse)

# Quantifying dwarf shrub biomass in an arid environment: comparing empirical methods in a high dimensional setting



H. Zandler<sup>a,\*</sup>, A. Brenning<sup>b,c,d</sup>, C. Samimi<sup>a,e</sup>

<sup>a</sup> University of Bayreuth, Department of Geography, 95440 Bayreuth, Germany

<sup>b</sup> University of Waterloo, Department of Geography and Environmental Management, 200 University Avenue West, Waterloo, Ontario, Canada N2L 3G1

<sup>c</sup> University of Heidelberg, Department of Geography, 69120 Heidelberg, Germany

<sup>d</sup> Friedrich Schiller University, Department of Geography, Löbdergraben 32, 07743 Jena, Germany

<sup>e</sup> University of Bayreuth, BayCEER, 95440 Bayreuth, Germany

## ARTICLE INFO

## Article history:

Received 26 May 2014

Received in revised form 3 November 2014

Accepted 7 November 2014

Available online 2 December 2014

## Keywords:

Biomass

Arid Environment

Multispectral remote sensing

Empirical modeling

Landsat OLI

RapidEye

## ABSTRACT

Remote sensing based biomass estimation in arid environments is essential for monitoring degradation and carbon dynamics. However, due to the low vegetation cover in these regions, satellite-based research is challenging. Numerous potentially useful remotely-sensed predictor variables have been proposed, and several statistical and machine-learning techniques are available for empirical spatial modeling, but their predictive performance is yet unknown in this context. We therefore modeled total biomass in the Eastern Pamirs of Tajikistan, a region with extremely low vegetation cover, with a large set of satellite based predictors derived from two commonly used sensors (Landsat OLI, RapidEye), and assessed their utility in this environment using several suitable modeling approaches (stepwise, lasso, partial least squares and ridge regression, random forest). The best performing model (lasso regression) resulted in a RMSE of 992 kg ha<sup>-1</sup> in spatial cross-validation, indicating that biomass quantification in this arid setting is feasible but subject to large uncertainties. Furthermore, pronounced over-fitting in some commonly used models (e.g. stepwise regression, random forest) underlined the importance of adequate variable selection and shrinkage techniques in spatial modeling of high dimensional data. The applied sensors showed very similar performance and a combination of both only slightly improved results of better performing models. A permutation-based assessment of variable importance showed that some of the most frequently used vegetation indices are not suitable for dwarf shrub biomass prediction in this environment. We suggest that predictor variables based on several bands accounting for vegetation as well as background information are required in this arid setting.

© 2014 Elsevier Inc. All rights reserved.

## 1. Introduction

Drylands cover extensive parts of the planet with about one fifth of the land surface classified as arid or drier (Lal, 2004; UNEP, 2012). Although biomass per unit area is normally low in those regions, the vast extent of the earth's arid lands gives them a significant role as a carbon pool and for the supply of essential ecosystem services (Perez-Quezada, Delpiano, Snyder, Johnson, & Franck, 2011; Trumper, Ravilious, & Dickson, 2008; Safriel & Adeel, 2005). Woody perennial vegetation has a most prominent position in drylands as it stabilizes the soil, is a year round forage source, and can be used as firewood. However, over-exploitation may lead to degradation with a loss of productivity, stored carbon, and ecosystem resilience (Eisfelder, Kuenzer, & Dech, 2012; Breckle & Wucherer, 2006; Lal, 2004). Even though desertification occurs on a local scale, it can be considered as a major global problem because of the large area affected (FAO, 2004; UNEP, 2012). Therefore, comprehensive research of desertification requires remote sensing as a

tool for mapping biomass in arid environments (Eisfelder et al., 2012; Trumper et al., 2008; Yang, Weisberg, & Bristow, 2012).

In spite of these needs, remote sensing studies of vegetation in arid regions are scarce, and additional methodological research is needed to address the specific challenges faced by remote sensing techniques in these environments (Eisfelder et al., 2012). In particular, sparse and senescent vegetation may lead to a weak or ambiguous spectral response that is strongly influenced by soil background (Eisfelder et al., 2012). This also limits the utility of common vegetation indices (Asner & Heidebrecht, 2002; Montandon & Small, 2008; Yang et al., 2012). Therefore, remotely-sensed vegetation analysis in areas with plant cover under 30% has had limited success or was considered impossible (Escadafal & Chehbouni, 2008; Okin, Roberts, Murray, & Okin, 2001).

To address this methodological issue and provide biomass information in arid environments, different techniques and sensors have been applied and tested. However, existing research does not provide clear recommendations on the suitability of specific sensors for arid environments, although some studies indicate that sensors in the spectral region of the red edge such as RapidEye may be more effective than conventional sensors such as Landsat OLI (Eisfelder et al., 2012; Li, Gao, Bai, & Huang,

\* Corresponding author. Tel.: +49921554636.

E-mail address: [harald.zandler@uni-bayreuth.de](mailto:harald.zandler@uni-bayreuth.de) (H. Zandler).

2012; Ren, Zhou, & Zhang, 2011). It is therefore our goal to assess the suitability of existing spectral indices derived from two different sensors, Landsat OLI and RapidEye in mapping biomass in a dryland environment.

An additional challenge in this context and in environmental remote sensing as a whole lies in the use of large numbers of potentially useful predictor variables to model and map a biophysical variable that is observed at a limited number of reference sites. While numerous exploratory as well as predictive tools from computational statistics and machine learning have been introduced into remote sensing in recent years, best results are achieved using varying techniques adapted to the given context (e.g., Brenning, Long, & Fieguth, 2012; Xu, Li, & Brenning, 2014).

The main intention of this study is to map dwarf shrub total biomass (TB) in an environment with extremely low vegetation cover (dwarf shrubs <20%) using a large number of predictor variables consisting of individual bands, indices, topographic attributes and texture variables derived from multi-spectral Landsat OLI, RapidEye and ASTER GDEM satellite data. Embedded in this primary objective are two key challenges: (1) to apply and evaluate different empirical models to derive dwarf shrub biomass (stepwise, lasso, partial least squares and ridge regression as well as random forest); (2) and to compare two different commonly used relatively new sensors (Landsat OLI and RapidEye) for their suitability for vegetation detection in extremely arid environments.

2. Study area

Research was carried out in a high mountain desert landscape located in the Eastern Pamirs of Tajikistan (Fig. 1). The plateau-like region with elevations between 3500 and 5500 m above sea level is characterized by broad valleys with moderate slopes. A harsh climate with cold

temperatures (Murghab annual mean 1998–2012:  $-1\text{ }^{\circ}\text{C}$ , Tajik Met Service, 2013) and low precipitation (Murghab annual mean 1998–2012: 94 mm, Tajik Met Service, 2013) only allows scarce vegetation with the exception of azonal vegetation with increased water supply from orographically induced higher rainfall rates at high altitudes, surface water or groundwater (Fig. 2a & b). The majority of the non-riparian vegetation is dominated by dwarf shrubs, locally referred to as “Teresken” (Kraudzun, Vanselow, & Samimi, 2014; Vanselow, 2011). The regional dwarf shrubs are widespread woody species typical for steppe or semi-desert/desert habitats (Heklau & Röser, 2008; Heklau & von Wehrden, 2011; McArthur & Stevens, 2004).

Animal husbandry is the main economic activity and provides a livelihood for the local population. Dwarf shrubs, as the only woody plants, therefore play an important role as both forage and fuel source. For the latter purpose, the entire plant is dug up as the majority of the plant mass is located underground in the root zone (Fig. 2c). The current use has led to concerns regarding overexploitation, degradation and desertification (Breckle & Wucherer, 2006). Although much work on dwarf shrubs was done from the 1950s until the 1980s as reviewed by Walter and Breckle (1986), and generalized classifications on the occurrence of dwarf shrubs have been carried out (Kraudzun et al., 2014; Vanselow, 2011, Vanselow & Samimi, 2014), the actual occurrence and density of dwarf shrub biomass distribution remains a large research gap. The most recent remote sensing approach to quantify dwarf shrub cover by Vanselow and Samimi (2014) was abandoned due to unsatisfactory results. Besides aforementioned work, only two unpublished diploma theses exist that use satellite data and those led to very limited information regarding vegetation cover (Vanselow, 2011).

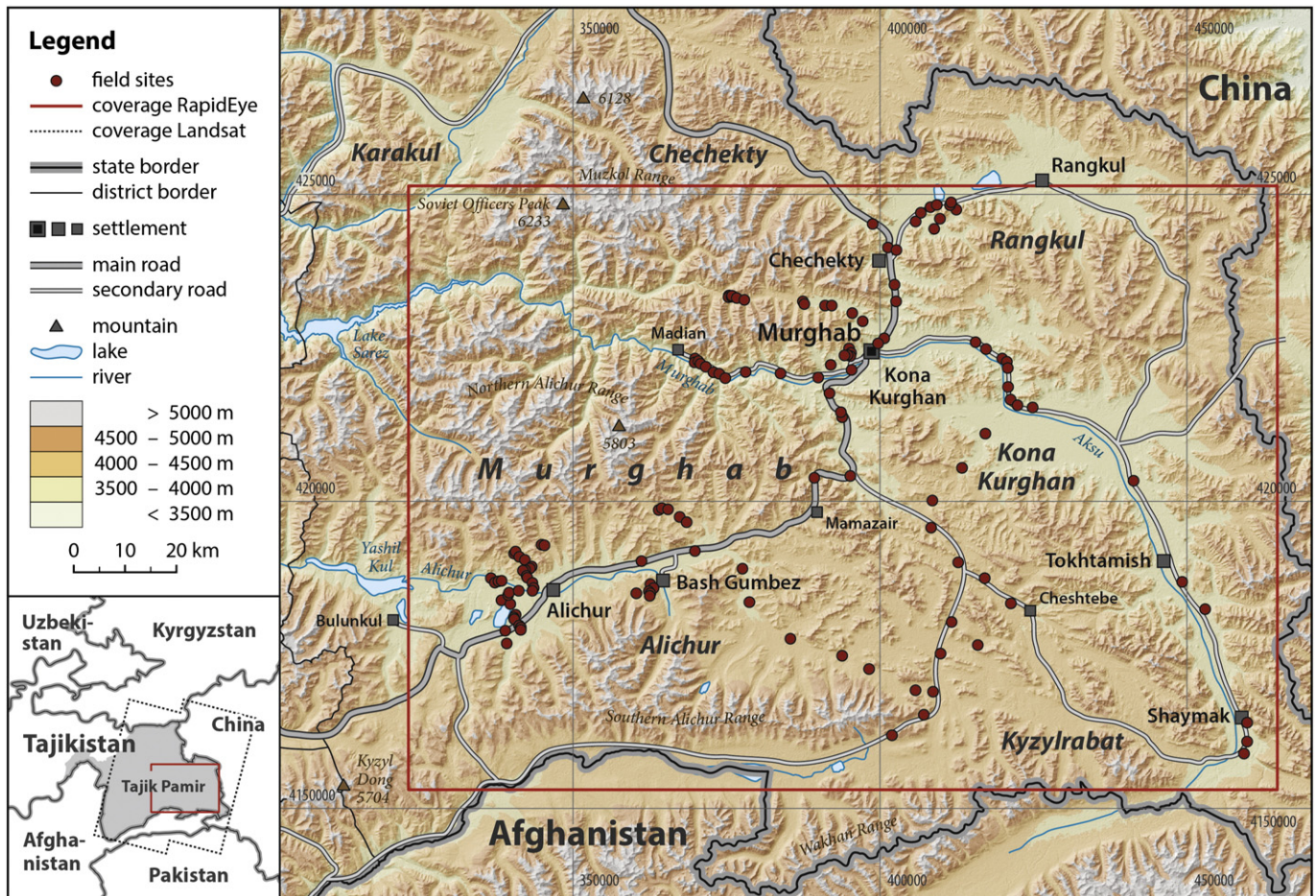


Fig. 1. Map of the study area. Research is restricted to the region covered by RapidEye images.



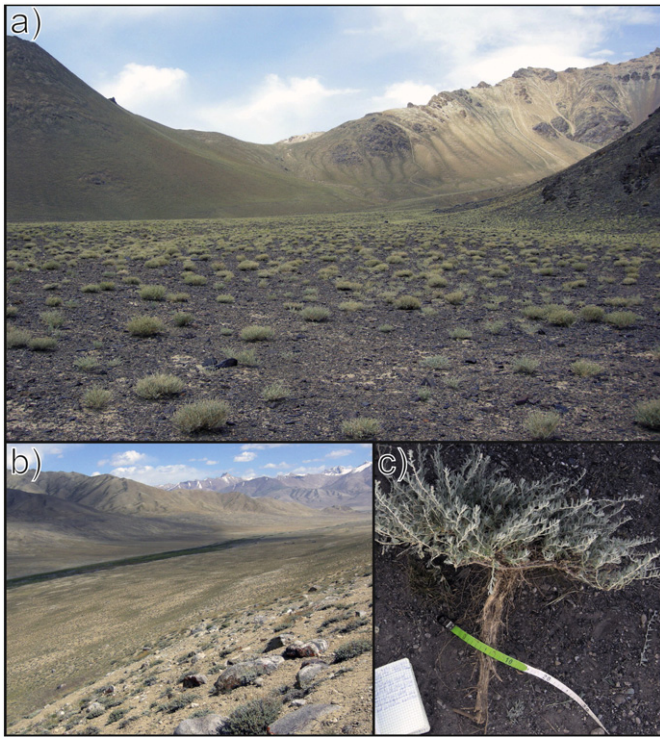


Fig. 2. Photographs of (a) a *Krascheninnikovia ceratoides* dwarf shrub site, (b) a *Krascheninnikovia ceratoides* and *Artemisia spec.* formation with azonal riparian vegetation in the background, and (c) extracted young dwarf shrub individual.

### 3. Methods

To date there is no mapping methodology to predict TB in the research area. Therefore, the methodology (Fig. 3) incorporates three separate parts: 1) the development of an allometric model to derive field biomass, 2) the processing of satellite images and 3) the combination of both data sources in the spatial prediction of dwarf shrub biomass.

#### 3.1. Allometric functions

To infer TB from surface parameters, allometric functions were used (Eisfelder et al., 2012). These functions permit derivation of biomass from simple, non-destructive measurements of morphological parameters (Perez-Quezada et al., 2011). The desired allometric model involves all regional dwarf shrub species comprising *Krascheninnikovia ceratoides* and *Artemisia spec.* (Kraudzun et al., 2014).

In a first step, several variables (e.g. dwarf shrub maximum transverse/minimum conjugate diameters, stem diameter, maximum dwarf shrub circumference in cm) were measured for a small pre-test sample preferentially derived from a small area in the central research area ( $n = 34$ ) for exploratory analysis of applicable measures. These variables were used to calculate dwarf shrub areas assuming elliptical or circular plant shapes to derive suitable morphological indicators for TB in an initial analysis.

In a second step, complete dwarf shrub individuals were extracted from the soil and weighed immediately after harvesting (1 g precision). As this study analyzes undried biomass, dry biomass can be expected to decrease, although moisture content is expected to be low in this arid setting and a major part of dwarf shrub biomass is composed of dry dead plant material as the inner old parts die off over time, while growth continues on the outer parts (Walter & Breckle, 1986). Regression analysis showed that dwarf shrub circle area calculated from circumference ( $CA_{ds}$ ) is the best proxy for dwarf shrub TB which is in agreement with the observation that circular shape is the most common growth habit of

undisturbed dwarf shrubs in the research area. Hence, further field surveys only considered this variable to reduce survey efforts.

Harvesting locations were placed according to a design that covers the whole research area stratified by geographical distribution and accessibility. At the sites, all dwarf shrubs were excavated in 3 predefined areas with a 10 m × 10 m side length. Dwarf shrub numbers in those areas ranged from 44 to 111 individuals.

In a third phase, linear regression was conducted with  $CA_{ds}$  as predictor and undried dwarf shrub TB as the response variable ( $n = 243$ ; 132 *Krascheninnikovia ceratoides*, 111 *Artemisia spec.*). Both response and predictor variables were transformed using natural logarithm in order to accommodate the shape of the empirical relationship, non-negativity of the response and model requirements. As logarithmic transformation introduces a bias in the back transformation calculation, the predicted values were multiplied with an empirical correction factor CF (Baskerville, 1972):

$$CF = e^{\left(\frac{MSE}{2}\right)} \quad (1)$$

MSE mean square error of regression

The final allometric model was then used to calculate TB for every dwarf shrub individual. The model's prediction error was estimated using 10-fold cross-validation, which reduces bias in performance measures (Brenning, 2012). For the evaluation, absolute and relative root mean square error (RMSE,  $RMSE_{rel}$ ) and BIAS of the back transformed variables were calculated:

$$RMSE = \sqrt{\frac{\sum_{i=1}^n (Y_i - \hat{Y}_i)^2}{n}} \quad (2)$$

$$RMSE_{rel} = \frac{RMSE}{\bar{Y}} \times 100\% \quad (3)$$

$$BIAS = \frac{1}{n} \sum_{i=1}^n (\hat{Y}_i - Y_i) \quad (4)$$

where  $n$  is the number of observations,  $\bar{Y}$  is the observed mean value,  $Y_i$  is the measured value and  $\hat{Y}_i$  the predicted value of case  $i$ . The same equations were applied to the assessment of empirical remote sensing models (Section 3.6).

#### 3.2. Field data

Overall, 137 field plots with homogenous vegetation cover were mapped with a GPS device in summer 2013 to serve as field sites for pre-classification and empirical model development. Of these, 122 field sites are dwarf shrub areas. Besides dwarf shrub habitats, 15 riparian green and dense grass vegetation sites (meadow vegetation) were mapped for the pre-classification. Plot size was calculated (Eq. 5) according to Justice and Townshend (1981), applying the resolution of the coarsest used sensor,

$$S = P(1 + 2L). \quad (5)$$

where  $S$  is the side length of the field plot,  $P$  is the pixel size in meters and  $L$  is the geometric accuracy of the sensor in pixels. The Landsat OLI sensor has a pixel size of 30 m and an accuracy of 12 m (0.4 pixels; USGS, 2013) resulting in a calculated minimum size of 54 m. To provide for GPS deviations of usually around 5 m (horizontal RMSE), the minimum plot size was increased to 60 m side length. Additionally, a 10 m buffer distance was maintained to environmentally different areas to minimize side effects. Preferential sampling was the favored method

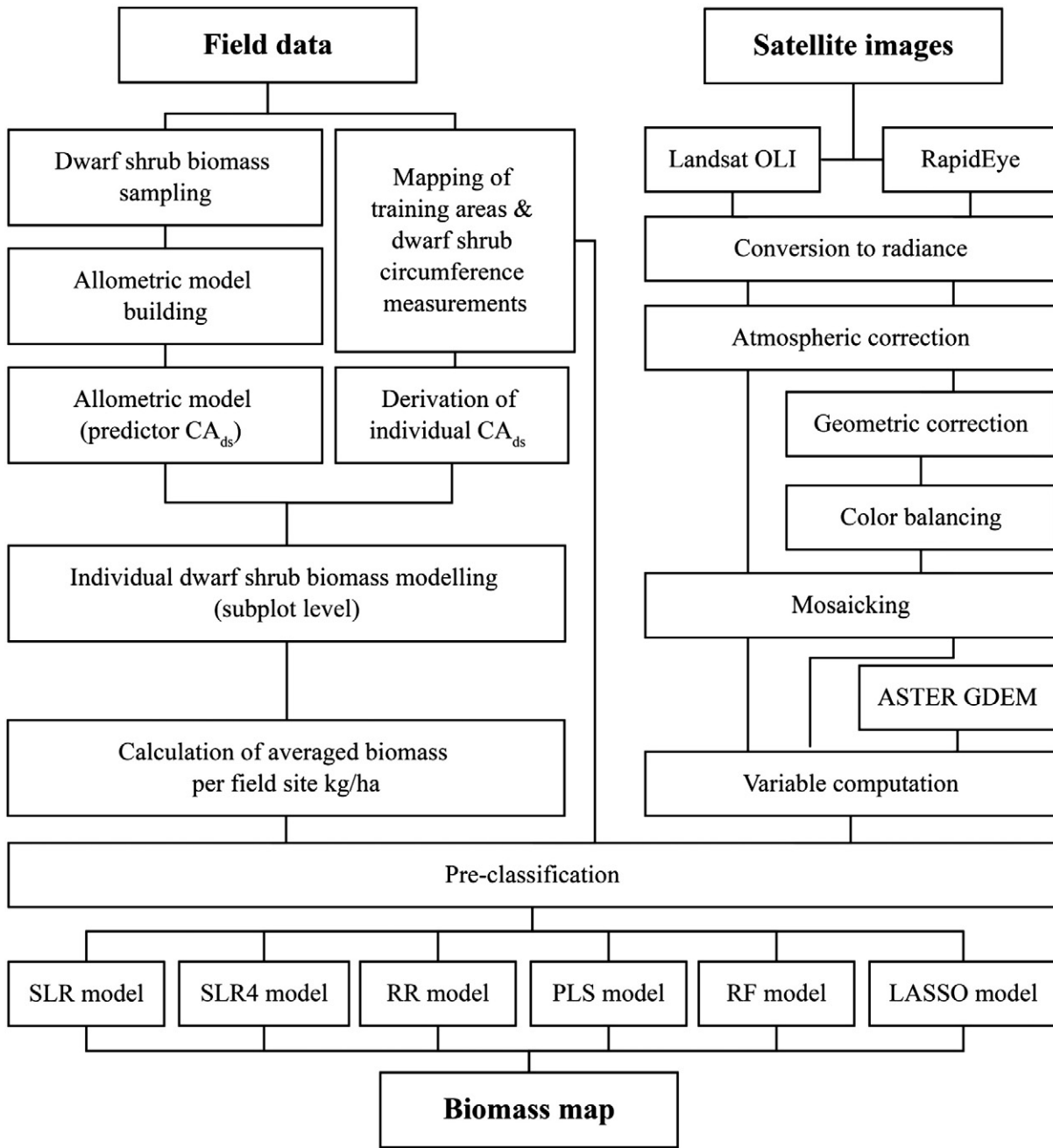


Fig. 3. Methodological workflow.

for the selection of dwarf shrub stands in this study, whereby ecologically and spectrally homogeneous sections covering the whole research area should be defined. Such a sampling design is connected to methodological concerns as it violates some assumptions of statistical analysis. On the other hand, preferential sampling may be superior from an ecological point of view in reaching ecological representativeness, so consequently no particular sampling strategy is entirely suitable (Roleček, Chytrý, Hájek, Lvončík, & Tichý, 2007). Furthermore, given the environmental conditions and plot requirements (e.g. minimum size, homogeneity), preferential sampling in the research area is far more feasible due to inaccessibility, extensive bare rock and desert areas without plants and the aim to cover the whole range of biomass densities. In order to consider statistical standards, dwarf shrub density and biomass were determined on the subplot level, which were established inside dwarf shrub stands using an adapted random walk technique (Rudnick & Gaspari, 2004).

Two 4 m × 4 m subplots according to size recommendations for woody vegetation (Mueller-Dombois & Ellenberg, 1974) were recorded at each field site. TB was derived in a two-step approach using CA<sub>ds</sub> by measurement of all circumferences in the subplot. Biomass was then derived from areal cover of the plants by using the developed allometric function described in Section 3.1., summed and averaged to mean TB kg ha<sup>-1</sup> for each field site.

Regarding site homogeneity, subsequent analysis of variance of areal dwarf shrub cover showed a standard deviation of 1.56 percentage points within the field sites which allows an approximate precision of 1.1 percentage points with the aforementioned study design. These figures were considered sufficiently homogeneous for satellite based vegetation analysis, although small scale heterogeneity and uncertainties originating from sampling design have to be considered when evaluating modeling results.

### 3.3. Satellite image acquisition and preprocessing

The study utilizes both Landsat 8 OLI and RapidEye satellite images. Landsat provides a consistent series of remotely sensed data over a long time period with global coverage (USGS, 2013), and RapidEye offers a red edge band which may be particularly suitable for vegetation detection in arid environments (Li et al., 2012). To include topographic information, ASTER Global Digital Elevation Model V002 (ASTER GDEM, METI & NASA, 2009) was resampled to 30 m × 30 m resolution. Landsat L1T images (paths 150–151, rows 33–34) with 12 m circular error (with 90% confidence) were acquired with minimal cloud and snow cover (scenes from 19 and 28 July 2013). The L1T product is radiometrically and geometrically calibrated, terrain-corrected and has a resolution of 30 m × 30 m for the non-panchromatic OLI bands (USGS, 2013). Level 3A ortho products have a resampled resolution of 5 m × 5 m (ground sampling distance 6.5 m) and a geometric accuracy below 30.34 m (circular error at the 90% confidence level; RapidEye AG, 2009). 47 RapidEye tiles were acquired from 31 July to 24 September 2013. The timing of image acquisition coincided with the peak of the vegetation period of shrubs when highest spectral plant signals may be expected (Walter & Breckle, 1986).

All scenes were converted to at-sensor radiance. For atmospheric correction, the MODTRAN® based FLAASH® approach provided by ENVI software was applied as it is considered a state-of-the-art radiative transfer model (Guanter, Richter, & Kaufmann, 2009; Jiménez-Muñoz, Sobrino, Mattar, & Franch, 2010), while alternative approaches like the 6S algorithm have been reported to perform poorly in arid environments (Maiersperger et al., 2013). The appropriate atmospheric model for each scene was chosen according to water vapor amounts given by the Aqua AIRS Level 3 Daily Standard Physical Retrieval product (AIRS Science Team & Texeira, 2013).

Prior to the analysis, all images were scrutinized for accurate geo-referencing using field-based GPS reference points (e.g., road intersections, bridges, rock formations). Further correction of Landsat images was not necessary. RapidEye images showed various deviations from GPS points. Therefore all tiles ( $n = 47$ ) were adjusted, mosaicked and finally georeferenced to GPS measurements using 9 control points covering the whole research area ( $RMSE_{XY} = 5.42$  m). Mosaicking of all satellite images was performed using a feathering algorithm. During mosaicking of RapidEye images, color balancing using statistics of cloud-free overlapping areas was necessary for some images, as they still showed sensible differences due to atmospheric and illumination effects. Color balancing is a function of the ENVI software to adjust for small differences in the image's light intensity using gain and offset values (Luedeling & Buerkert, 2008).

### 3.4. Pre-classification

A pre-classification to separate potential dwarf shrub areas from different land cover (meadow vegetation, water bodies, snow and glaciers) was performed to limit the study to the relevant area of interest. The pre-classification was based on an allocation of image pixels according to spectral similarity to dense dwarf shrub areas and spectral difference to meadow vegetation areas. Spectral information is known to be a good tool to distinguish these classes in this study region (Vanselow, 2011). The discrimination is performed using spectral angle values (SAV) which express spectral similarities to reference spectra and show little influence by illumination differences (Kruse et al., 1993). Reference spectra were extracted from field sites with the densest dwarf shrub formation on the one hand, and sites with closed meadow vegetation on the other. SAV were then calculated for the entire images and averaged for both types of reference sites.

Considerable differences in SAV between dwarf shrub and meadow vegetation were visible. Areas under the ROC (AUROC) values for group discrimination ranged between 0.96 (dwarf shrub reference spectrum) and 0.93 (meadow vegetation reference spectrum). The

pre-classification thresholds were determined using boxplots of both measures. This was done by assuming that, on the one hand, all SAVs above the upper whisker (i.e., median plus 1.5 times the interquartile range) of the dwarf shrub reference boxplot correspond to non-dwarf shrub areas and on the other hand, SAVs below the lower whisker of the meadow vegetation reference boxplot are green, grass vegetation areas. Thus, only spectrally coherent dwarf shrub regions were used as our area of interest, while other land cover types were disregarded. This also led to the elimination of eleven outlying dwarf shrub field sites from further analysis. The pre-classification was performed using Landsat bands only. After pre-classification, 111 field sites were left for further analysis.

### 3.5. Remote sensing variables and vegetation indices

To better exploit the available spectral information, derived spectral features were included in the analysis (selected important variables summarized in Tables 1 and 2). The majority of studies apply vegetation indices for remote sensing-based biomass estimation and so a variety of indices exist (Eisfelder et al., 2012). These and all other applied variables are grouped in following categories:

#### 3.5.1. Unadjusted vegetation indices

These comprise simple band reflectance, band ratios and common vegetation indices from literature that are used frequently in remote sensing studies (Bannari, Morin, Bonn, & Huete, 1995; Eitel, Long, Gessler, Hunt, & Brown, 2009; Haboudane, Miller, Pattey, Zarco-Tejada, & Strachan, 2004; Homer, Aldridge, Meyer, & Schell, 2012; Ramoelo et al., 2012; Rouse, Haas, Schell, Deering, & Harlan, 1974).

#### 3.5.2. Soil adjusted vegetation indices

As vegetation indices suffer from various soil effects, especially when vegetation cover is low (Bannari et al., 1995), additional soil adjusted vegetation indices were derived to account for soil brightness variations (e.g. SAVI, TSAVI, MSAVI). These indices are either based on empirically derived, fixed adjustment coefficients or by construction of a soil line using red and infrared spectral bands (Qi, Chehbouni, Huete, Kerr, & Sorooshian, 1994).

#### 3.5.3. Color adjusted vegetation indices

Vegetation indices do not only differ due to vegetation and brightness variations, but also because of soil color differences when cover is low (Bannari et al., 1995). Therefore, additional indices were developed to adjust for the noise arising from soil color. The method correlates an additional index that represents soil color to existing indices (e.g. NDVI, SAVI) and may thereby double the sensitivity of the vegetation index under arid conditions (Bannari et al., 1995, Escadafal & Huete, 1991). As we expect these indices to be particularly suitable for the research area with its extremely low cover and large variety of soil colors, this technique was applied to a number of variables mentioned above with different color adjustment indices.

#### 3.5.4. First derivatives of reflectance (FDR) and ratios

FDR were calculated as they may be able to reduce scatter due to illumination or soil compared to simple reflectance based indices (Wang, Qu, Hao, & Hunt, 2011). To consider different spectral regions that may be able to capture vegetation properties, FDR ratios were calculated as well.

#### 3.5.5. Principal components (PC) and ratios

To maximize the variance of the satellite data and identify combinations of features that discriminate dwarf shrub from other land cover, principal components (PCs) were derived. Furthermore, as certain PC may be related to background and others to dwarf shrub features, additional PC ratios were calculated applying the same method used for simple band ratio calculations to enhance possible differences.



**Table 1**

Overview of the most important indices, principal components, FDR and respective ratios used in this study. Variables are only an excerpt. Additional predictors are listed the Appendix (Table A1) and are based on the following studies: Bannari et al. (1995), Elvidge and Chen (1995), Gelder, Kaleita, and Cruse (2009), Homer et al. (2012), Ren et al. (2012), Rondeaux, Steven, and Baret (1996). (S = sensor; B<sub>blue2</sub> = LS Band2/RE Band1; B<sub>green</sub> = LS Band3/RE Band2; B<sub>red</sub> = LS Band4/RE Band3; B<sub>rededge</sub> = RE Band4; B<sub>nir</sub> = LS & RE Band5; a = slope of the soil line; b = intercept of the soil line; k = slope of linear correlation between index and color adjustment index; nine bare soil field sites were used for construction of soil related parameters).

| Variable   | S     | Formula   | Reference                         |
|--|-------|---|-----------------------------------|
| <i>Unadjusted vegetation indices</i>                     |       |   |                                   |
| NDVI   | LS/RE | $(B_{nir} - B_{red}) / (B_{nir} + B_{red})$   | Rouse et al. (1974)               |
| MCARI  | RE    | $((B_{rededge} - B_{red}) - 0.2 * (B_{rededge} - B_{green})) * (B_{rededge} / B_{red})$   | Ramoelo et al. (2012)             |
| <i>Soil adjusted vegetation indices</i>                  |       |   |                                   |
| SAVI1  | LS/RE | $((B_{nir} - B_{red}) / (B_{ni} + B_{red} + 1.5)) * (1 + 0.5)$  | Huete (1988)                      |
| SAVI2  | LS/RE | $((B_{ni} - B_{red}) / (B_{ni} + B_{red} + 0.5)) * (1 + 0.5)$   | Huete (1988)                      |
| MNDVI  | LS/RE | $(NDVI / (1 + ((0.55 * B_{red} - B_{blue2} + 0.12)) / (B_{nir}^2 - B_{red}^2)))) * (1 + 0.001 * (1 / (0.55 * B_{red} - B_{blue2} + 0.12)))$                 | Liu and Huete (1994)              |
| MTVI2  | LS/RE | $(1.5 * 1.2 * (B_{nir} - B_{green}) - 2.5 * (B_{red} - B_{green})) / \text{SQRT}((2 * B_{nir} + 1; 2)^2) - (6 * B_{nir} - \text{SQRT}(5 * B_{red})) - 0.5)$ | Haboudane et al. (2004)           |
| MCARI/MTVI2  | RE    | MCARI/MTVI2   | Eitel et al. (2009)               |
| WDVI   | LS/RE | $B_{nir} - (a * B_{red})$   | Qi et al. (1994)                  |
| <i>Color adjusted vegetation indices</i>                 |       |   |                                   |
| RI (color adjustment index)                              | LS/RE | $(B_{red} - B_{green}) / (B_{red} + B_{green})$   | Escadafal and Huete (1991)        |
| REI (color adjustment index)                             | RE    | $(B_{rededge} - B_{green}) / (B_{rededge} + B_{green})$   | Escadafal and Huete (1991)        |
| NDVI SA  | LS/RE | $NDVI - (k * RI)$   | Escadafal and Huete (1991)        |
| SAVI2 SA   | LS/RE | $SAVI2 - (k * RI)$  | Escadafal and Huete (1991)        |
| WDVI SA  | LS/RE | $WDVI - (k * RI)$   | acc.to Escadafal and Huete (1991) |
| NDVI REI   | RE    | $NDVI - (k * REI)$  | Escadafal and Huete (1991)        |
| <i>First derivatives of reflectance (FDR) and ratios</i> |       |   |                                   |
| FDR LS = 6, RE = 4                                       | LS/RE | First derivative of reflectance   | Entcheva-Campbell et al. (2004)   |
| FDR Band ratios, all FDR                                 | LS/RE | e.g. FDR Bandratio 54/32 = FDR54/FDR32, etc.  |                                   |
| <i>Principal components (PC) and ratios</i>              |       |   |                                   |
| PC #1-7/1-5  | LS/RE | Derived principal components  |                                   |
| PC Band ratios, all PC                                   | LS/RE | e.g. PC Bandratio 7/6 = PC#7/PC#6, etc.   |                                   |

3.5.6. Texture variables

Texture measures proved to be very useful variables in existing biomass related studies (Fuchs, Magdon, Kleinn, & Flessa, 2009; Sarker &

Nichol, 2011). In the research area they were successfully used for vegetation classification (Kraudzun et al., 2014). Therefore, we calculated grey level co-occurrence based and grey level range texture filters on a 3 × 3 processing window. The calculation of these variables was restricted to the RapidEye sensor as the resolution of the Landsat satellite of 30 m × 30 m was unsuitable to capture small-scale dwarf shrub patterns.

**Table 2**

Overview of the most important constructed SAV values, derived ratios and texture variables used in this study. Variables are only an excerpt. A complete list is given in the Appendix (Table A2).

| Variable  | Sensor | Description   |
|---|--------|---|
| <i>Texture parameters</i>                       |        |   |
| B05 TEXTURE SM                                  | RE     | Texture of Band 5 calculated by ENVI angular second moment equation   |
| <i>SAV based variables</i>                      |        |   |
| SAV 0.475–0.805 µm Shrub2                       | RE     | Calculated using field site with 2nd highest TB   |
| SAV 0.475–0.805 µm Soil1                        | RE     | Calculated using no vegetation field site 1   |
| SAV 0.475–0.805 µm Soil                         | RE     | Calculated using all non-vegetated field site   |
| SAV 0.475–0.805 µm Shrub                        | RE     | Calculated using non soil field sites   |
| SAV 0.655–0.865 µm Shrub1                       | LS     | Calculated using field site with highest TB   |
| SAV 0.655–0.865 µm Shrub >10%                   | LS     | Calculated using field site with cover > 10%  |
| SAV 0.655–0.865 µm Soil                         | LS     | Calculated using all non-vegetated field sites  |
| SAV 0.657–0.805 µm Soil1                        | RE     | Calculated using no vegetation field site 1   |
| SAV 0.655–2.2 µm Shrub1                         | LS     | Calculated using field site with highest TB   |
| SAV 0.655–2.2 µm Shrub2                         | LS     | Calculated using field site with 2nd highest TB   |
| SAV 0.655–2.2 µm Soil1                          | LS     | Calculated using no vegetation field site 1   |
| SAV 0.655–2.2 µm Soil2                          | LS     | Calculated using no vegetation field site 2   |
| SAV-Ratio 0.655–0.865 µm Soil/ Shrub >10%       | LS     | SAV 0.655–0.865 µm Soil/ SAV 0.655–0.865 µm Shrub >10%  |
| SAV-Ratio 0.475–0.805 µm Soil/Shrub             | RE     | SAV 0.475–0.805 µm Soil/ SAV 0.475–0.805 µm Shrub   |
| SA-Index 0.655–2.2 µm (Soil 1 + 2)/(Shrub1 + 2) | LS     | $(SAV 0.655-2.2 \mu m Soil1 + SAV 0.655-2.2 \mu m Soil2) / (SAV 0.655-2.2 \mu m Shrub1 + SAV 0.655-2.2 \mu m Shrub2)$ |

3.5.7. SAV based variables

Due to the absence of real endmember sites in the research area, this approach was included as a substitution to full spectral mixture analysis (SAM) that performed well in other regions to quantify vegetation fractions (Yang et al., 2012). We included SAV based on different reference sites with soil, dwarf shrub and meadow vegetation, which we refer to as pseudo-endmembers. Similar to ratio indices, SAV ratios were computed from different SAV as well.

3.5.8. Topographic variables

Topography is an important factor for biomass distribution in arid environments (Sternberg & Shoshany, 2001). To include topographic attributes as possible proxies for site suitability and background soil conditions, the sine and cosine of slope aspect, slope angle and elevation were calculated from the ASTER GDEM and used as predictors.

Thus, in total 169 predictors were available for Landsat-based biomass estimation (RapidEye: 144), including 7 (5) spectral bands, 148 (140) derived spectral features, and four topographic attributes in both predictor sets.

3.6. Statistical analysis

Numerous statistical and machine-learning techniques that have become available in recent years for remote-sensing applications could be used to address the particular challenges of this study (Brenning, 2009). In particular, the large number of available, plausible

spectral features compared to a relatively modest number of ground-truth observations creates a high-dimensional problem, in which there are more potential predictors than available observations (James, Witten, Hastie, & Tibshirani, 2013). This issue, which may lead to overfitting of models to the training data, is not uncommon in remote sensing. Several methods have been proposed to make efficient use of the available predictors in this situation, ranging from penalization or shrinkage approaches for statistical models to tree-based ensemble techniques (Brenning, 2009; James et al., 2013). In this study, prior knowledge furthermore supports the expectation that spectrally-derived predictors are nearly linearly related to the response variable, biomass (Calvão & Palmeirim, 2004; Holm, Cridland, & Roderick, 2003). We therefore focus our comparison of candidate prediction methods on linear regression methods with five different shrinkage heuristics (referred to as SLR, SLR4, LASSO, RR and PLS). We refer to James et al. (2013) for mathematical details on the prediction methods.

The random forest (RF) technique has furthermore become popular in remote sensing as a nonlinear and non-parametric alternative with promising predictive capabilities on noisy and high-dimensional data sets (Pal, 2005). RF has, in particular, become known as a tool for variable selection based on variable importance assessments (Díaz-Uriarte & Alvarez de Andrés, 2006). We therefore furthermore include this technique in order to assess whether the presumed linearity of the problem outweighs the advantages of the RF techniques.

Firstly, we applied linear regression with stepwise forward variable selection as a tool for subset selection. In this method, predictors are added to the model starting with the null model until a goodness-of-fit criterion does not improve any further (Hastie & Pregibon, 1992). We use the Akaike Information Criterion (AIC), which penalizes for model size, and apply stepwise linear regression (SLR) in two different implementations, one variant without restrictions regarding the permitted number of predictors, and one variant with a maximum of four variable selection steps, limiting model size to no more than four predictors (SLR4). This 'hard' model size limit was included to assess the utility of easily applicable simple criteria that require limited data preparation.

We further used partial least squares (PLS) linear regression, which constructs a set of predictors that are linear combinations of selected original predictors (James et al., 2013). Unlike SLR, in each step only orthogonalized (residual) features are used in each subsequent step, and the optimal number of steps is determined by an internal, speed-optimized cross-validation of the RMSE (Mevik, Wehrens, & Liland, 2013). The PLS method effectively uses all available features, although these are re-combined into a smaller number of features. This is related to principal components (PC) linear regression, but it has the advantage that the linear combinations are directed toward the response, whereas PC are calculated in an unsupervised way (James et al., 2013).

Ridge regression (RR) and the lasso (LASSO) are two additional, relatively recent approaches that use mathematically similar shrinkage penalties. Roughly speaking, these penalties push less important coefficients closer to zero in the case of ridge regression, or effectively set them to zero when the lasso technique is used (James et al., 2013). Thus, while the lasso performs variable subset selection and therefore produces sparse models that can be applied more easily in a predictive context, ridge regression effectively uses all predictors, which may produce more stable models. Optimal shrinkage parameters are obtained using an internal cross-validation.

Finally, the random forest (RF) technique is based on an ensemble of binary regression trees that are fitted to randomly selected subsets of the training data (Breiman, 2001). Variables and binary splits are selected based on the greatest reduction in the residual sum of squares. In addition to resampling the observations to obtain multiple trees, the random forest technique also selects a random subset of predictors in tree construction, which is particularly useful when large numbers of possibly redundant predictors are available. We used the random forest technique based on individual 500 trees and the square root of the available predictors as the number of randomly selected predictors

(Liaw & Wiener, 2002). The random forest technique has previously been applied in biomass mapping (Powell et al., 2010) and other remote sensing applications (Pal, 2005).

Predictive model performances were estimated 100-repeated using 10-fold spatial cross-validation. In 10-fold cross-validation, the available data is partitioned into 10 disjoint subsets, each subset being used as a test set while the remaining nine subsets form a training set for a predictive model. This is repeated until each subset has been used once as the test set, and the whole procedure is repeated 100 times to ensure that the results are independent of a particular partitioning (James et al., 2013). Since observations close to each other may be spatially autocorrelated, we chose a spatial partitioning mechanism based on 10-means clustering of the coordinates of field sites (Brenning, 2012). Bias, standard deviation and RMSE of prediction errors were estimated in this way. Predictive models were furthermore fitted to obtain spatial prediction maps of biomass for visual comparison, replacing any negative predicted values with 0.

In order to assess the utility of data derived from different satellite sensors for TB mapping, we estimated predictive model performances for each of the six models using three different sets of predictor variables: Landsat-derived predictors (LS), RapidEye-derived predictors (RE), and both sets combined (LSRE). The relative predictive importance of each predictor was furthermore measured using a permutation-based approach. Here, each predictor was randomly permuted in order to determine the resulting increase in RMSE that is associated with this loss of information (Strobl, Boulesteix, Zeileis, & Hothorn, 2007; Brenning, 2012). This calculation was embedded in a spatial cross-validation, using a total of 10000–50000 permutations per predictor, depending on each model's computational cost.

All statistical calculations were performed using R (R Core Team, 2013) with its packages 'stats' for SLR, 'pls' for PLS (Mevik et al., 2013), 'glmnet' for RR and LASSO (Friedman, Hastie, & Tibshirani, 2010), 'randomForest' for RF (Liaw & Wiener, 2002), 'sperrorst' for spatial cross-validation and variable importance (Brenning, 2012), and 'RSAGA' for spatial prediction on raster stacks (Brenning, 2008).

## 4. Results

### 4.1. Allometric model

The constructed model showed a cross-validated  $R^2$  of 0.87. Back transformed, cross-validated RMSE,  $RMSE_{rel}$  and BIAS were 71 g, 30% and 1.95 g, respectively. The model shows similarly good performance compared to dwarf shrub related allometric models elsewhere (Elzein, Blarquez, Gauthier, & Carcaillet, 2011, Shoshany, 2012), although an assessment that refers to other study designs must be interpreted with caution. This indicates the suitability of the constructed model to calculate dwarf shrub TB in the research area.

### 4.2. Empirical biomass models

Mean cross-validation performances of all prediction methods and sensors ranged from RMSE values of 992 kg ha<sup>-1</sup> (LASSO LSRE) to 1742 kg ha<sup>-1</sup> (SLR LSRE), or 75–130% of the standard deviation of biomass, with a generally small bias  $\leq 104$  kg ha<sup>-1</sup> (Table 3). Overall, LASSO, RR and SLR4 performed better than PLS, SLR and RF (relative RMSE 58–64% versus 64–103%), with PLS LSRE and SLR LSRE performing the poorest with 70 and 103%, respectively. Thus, overall, two of the three methods that perform variable subset selection (LASSO, SLR4, SLR) were among the better-performing methods, while the less sparse SLR suffered from the strongest overfitting among all linear models examined (difference between cross-validation test and training set RMSE 1080 kg ha<sup>-1</sup> for SLR LSRE compared to 123–346 kg ha<sup>-1</sup> for all other linear models). Only RF overfitted similarly strong to the training set (RMSE differences 693–701 kg ha<sup>-1</sup>).

**Table 3**  
Summary statistics of cross validated modeling results.

|            | Bias<br>(kg ha <sup>-1</sup> ) | Standard deviation<br>(kg ha <sup>-1</sup> ) | RMSE<br>(kg ha <sup>-1</sup> ) | RMSErel<br>(%) |
|------------|--------------------------------|--|--------------------------------|----------------|
| LASSO LS   | -52                            | 1038   | 1034                           | 61             |
| LASSO RE   | 31                             | 1088   | 1085                           | 64             |
| LASSO LSRE | 5                              | 996  | 992                            | 58             |
| RR LS      | -39                            | 1043   | 1039                           | 61             |
| RR RE      | 38                             | 1040   | 1038                           | 61             |
| RR LSRE    | -15                            | 1010   | 1006                           | 59             |
| SLR4 LS    | -63                            | 1067   | 1065                           | 63             |
| SLR4 RE    | 104                            | 1076   | 1077                           | 63             |
| SLR4 LSRE  | 54                             | 1076   | 1075                           | 63             |
| PLS LS     | -45                            | 1110   | 1108                           | 65             |
| PLS RE     | 20                             | 1093   | 1092                           | 64             |
| PLS LSRE   | -62                            | 1184   | 1181                           | 70             |
| RF LS      | -76                            | 1135   | 1132                           | 67             |
| RF RE      | -18                            | 1125   | 1121                           | 66             |
| RF LSRE    | -65                            | 1105   | 1103                           | 65             |
| SLR LS     | -67                            | 1134   | 1131                           | 67             |
| SLR RE     | 100                            | 1117   | 1117                           | 66             |
| SLR LSRE   | 22                             | 1741   | 1742                           | 103            |

The larger combined predictor set LSRE tended to produce equal or better mean RMSEs compared to the predictor sets LS and RE in the better-performing methods, while PLS and SLR achieved better results with smaller predictor sets. There was no appreciable performance difference between Landsat (LS) and RapidEye (RE) predictor sets. Scatterplots of predicted versus observed values of the better-performing models reveal a rather linear pattern, a consistent distribution with different models of the LS predictor set and slight differences to the combined predictor set LSRE (Fig. 4).

Biomass maps obtained with three of the best performing models (LSRE LASSO, LS LASSO, LS RR Fig. 5) generally showed similar results, although LSRE LASSO predicted slightly lower TB. Highest predicted TB was found on the slopes of side valleys at higher altitudes and lowest amounts were predicted for large plains at lower altitudes. Predicted TB tended to increase towards southwest. Furthermore, many areas with low predicted TB were situated near villages or major roads. This distribution reflects visual observations made during field work.

4.3. Variable importance

Variables derived from ASTER GDEM were among the 10 most important predictors in all of the 4 best performing single sensor set models (Fig. 6). Furthermore, variables built from SAVs, both as raw SAV or as index and covering different spectral regions, were important predictors in all models, especially in the LS LASSO and both RR models. *Color adjusted vegetation* indices ranked highly in the LASSO models but were not important in the RR models and only one *soil adjusted vegetation index* was among the important predictors in both of the RE models. Another set of predictors that played an important role in all models except the RE LASSO model were PC and derived ratios. Texture variables ranked among the 10 best predictors in the RE models. FDR variables and derived ratios showed also some importance in half of the models. Finally, the combined index MCARI/MTVI2 was very important for both RE models.

Neither the most common indices (e.g. NDVI) nor raw bands or band ratios were among the most important predictors of the 4 best performing single sensor set models.

5. Discussion

5.1. Overall performance of the biomass model

To our knowledge, this is the first study to quantify and map shrub TB in such an arid climate using optical sensors, addressing a major challenge in dryland remote sensing. We showed that predictive modeling of TB in this kind of landscape is possible with different sensors and

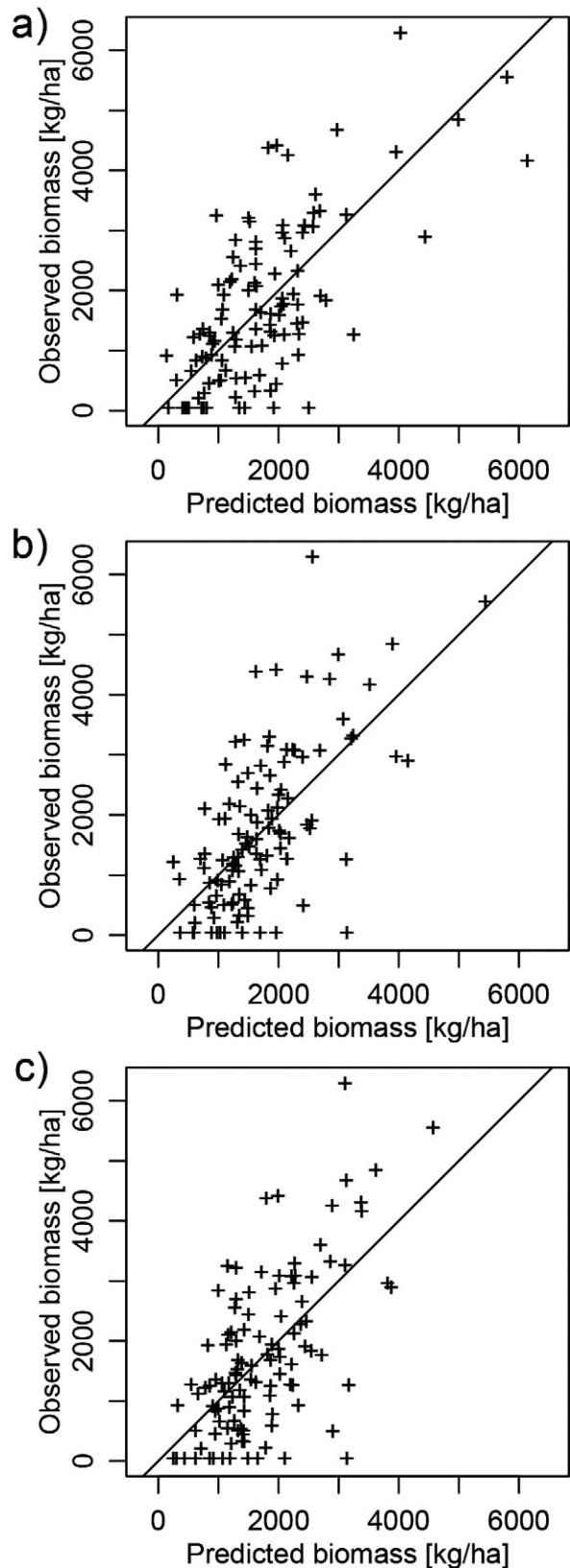


**Fig. 4.** Scatterplots of observed and predicted biomass in kg ha<sup>-1</sup>, a) LSRE LASSO, b) LS LASSO, c) LS RR. Predictions correspond to cross-validation test sets for a repetition with RMSE close to cross-validation mean RMSE (LSRE LASSO: 991 kg ha<sup>-1</sup>, LS LASSO: 1021 kg ha<sup>-1</sup>, LS RR: 1036); all scatterplots correspond to the same cross-validation partitioning.



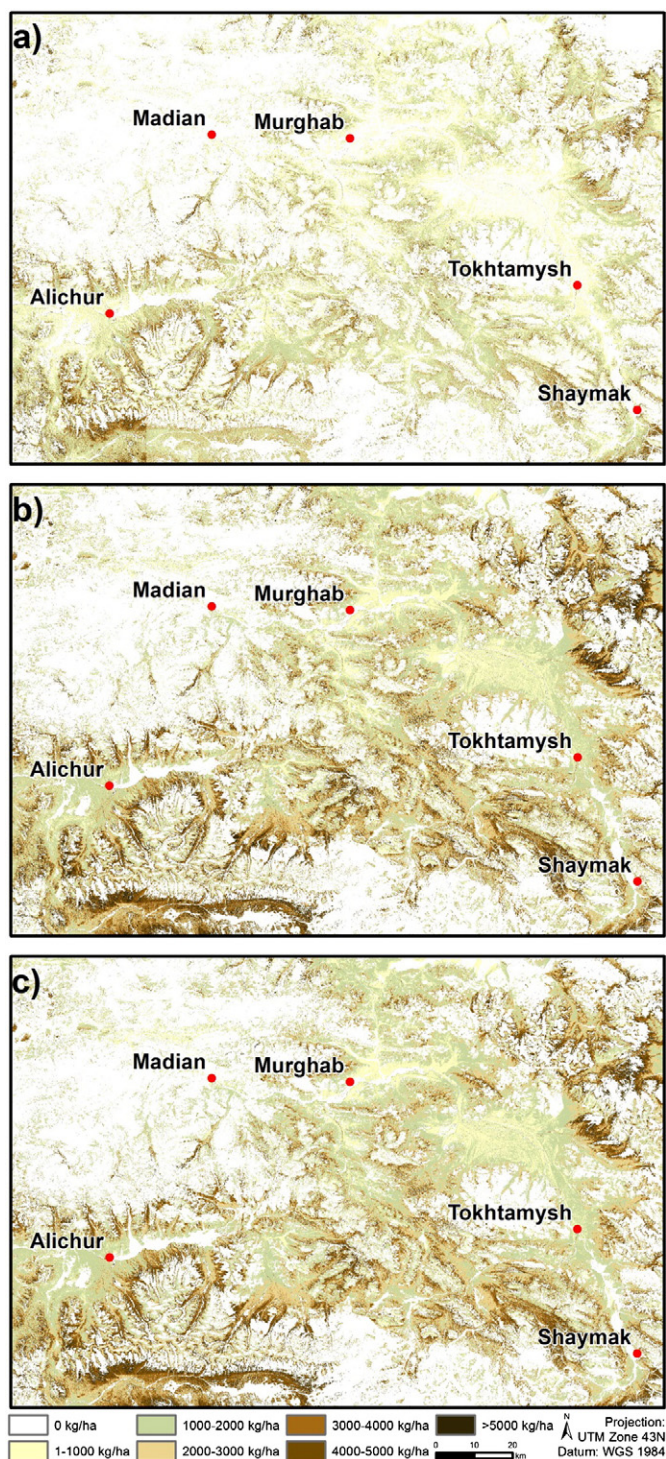


Fig. 5. Maps of predicted biomass in  $\text{kg ha}^{-1}$ . a) LSRE LASSO, b) LS LASSO and c) LS RR.

techniques, although cross-validated, relative RMSE were high with the better values ranging around 60%. These values are similar to other studies that analyze above ground biomass (AGB) or above ground carbon using spectral data (Fuchs et al., 2009; Powell et al., 2010), although direct numerical comparisons of performance measures between studies with different sampling and measurement procedures are problematic. RapidEye or the combined predictor set showed no appreciable performance improvement over Landsat-derived features, and models that utilize all predictors (RR, PLS, RF) did not outperform sparse methods, in particular LASSO and SLR4.

The observed prediction errors underline the limitations and uncertainties of dwarf shrub TB mapping from optical remote-sensing data. A general problem in the spectral derivation of dwarf shrub TB is the fact that a large part of the plant consists of non-photosynthetic, woody matter and the photosynthetic signal, captured by most spectral bands and indices, may be low in relation to the biomass amount. Furthermore, grasses, either associated with shrubs or growing in cushions within shrubs, may constitute a certain amount of the spectral signal of an area without contributing to TB. This may lead to model bias in areas with higher or lower than average amounts of grass cover. This problem was also mentioned by other authors, and a multi-temporal approach may be adequate to identify the spectral influence of grass vegetation (Duncan, Stow, Franklin, & Hope, 1993; Holm et al., 2003). Shoshany and Svoray (2002), for example, successfully mapped soil, herb, shrub and dwarf shrub cover in a semi-arid to arid environment using a multi-temporal approach based on seasonal phenological differences. However, such techniques require certain environmental conditions, e.g. that woody vegetation has a stable phenology year round (Roderick, Noble, & Cridland, 1999) or that germination and growth of vegetation is closely related to rainfall distributions (Shoshany & Svoray, 2002). In contrast to that, the short vegetation period in the Eastern Pamirs, classified as cold and arid, is increasingly determined by temperature and shrub leaves are dropped with the onset of cold conditions during fall (Walter & Breckle, 1986). At the same time, wilting of grasses takes place. Therefore, phenological conditions of different plants are more concurrently timed in the Eastern Pamirs compared to warmer arid regions. Furthermore, Shoshany and Svoray (2002) showed that phenologically derived cover estimates led to reduced accuracies with low vegetation cover which reduces the applicability of such an approach in the research area. Therefore, fine scale differences in phenology between dwarf shrub vegetation and grasses, accurately detectable by vegetation indices, have to be studied to apply this method in the research area.

Predictive uncertainties can also partly be attributed to the use of an allometric model to obtain plot-scale biomass estimates as the response variable. Our allometric model achieved a relative RMSE error of approximately 30% (absolute RMSE: 70 g) at the plant level. With on average 34 plants per  $4 \text{ m} \times 4 \text{ m}$  plot and two plots per field site, this would be expected to result in a RMSE of about  $180 \text{ kg ha}^{-1}$  for TB at the field site level. Finally, a certain amount of prediction error can be attributed to the within-site variability since only a small fraction of a pixel's area (3.6% of Landsat pixels, or 0.9% of  $60 \text{ m} \times 60 \text{ m}$  field sites) and of its dwarf shrub population were measured. An analysis of variance of plot-level TB observations suggests that plot-scale ( $4 \text{ m} \times 4 \text{ m}$ ) TB estimates varied, on average, with a standard deviation of  $732 \text{ kg ha}^{-1}$  within the  $60 \text{ m} \times 60 \text{ m}$  field sites. This results in an approximate precision of  $518 \text{ kg ha}^{-1}$  for field site TB estimation from two plots in this study, which corresponds to about one-quarter of the cross-validated prediction variance of our models. To reduce these sampling-related uncertainties substantially, much larger field efforts and environmental impacts would be required. Roughly speaking, four times the field data would be needed to improve sampling-related components of precision by 50%. On the other hand, this implies that the "net" RMSE of our models after accounting for sampling-related uncertainties is more likely in the order of  $850 \text{ kg ha}^{-1}$  for our best-performing model.

## 5.2. Relevance of predictors

One of the main limitations for dwarf shrub TB remote-sensing arises due to the extreme aridity and the associated strong influence of soil background. This problem may be enhanced in areas with highly variable geology as found in our study region (Vanselow, 2011). To approach this problem, we applied several alternative techniques that have been proposed in the literature to relieve this issue. Given the large number of predictors that have been proposed and the differences in mathematical assumptions of the available models, our variable importance assessment provides a general overview of promising

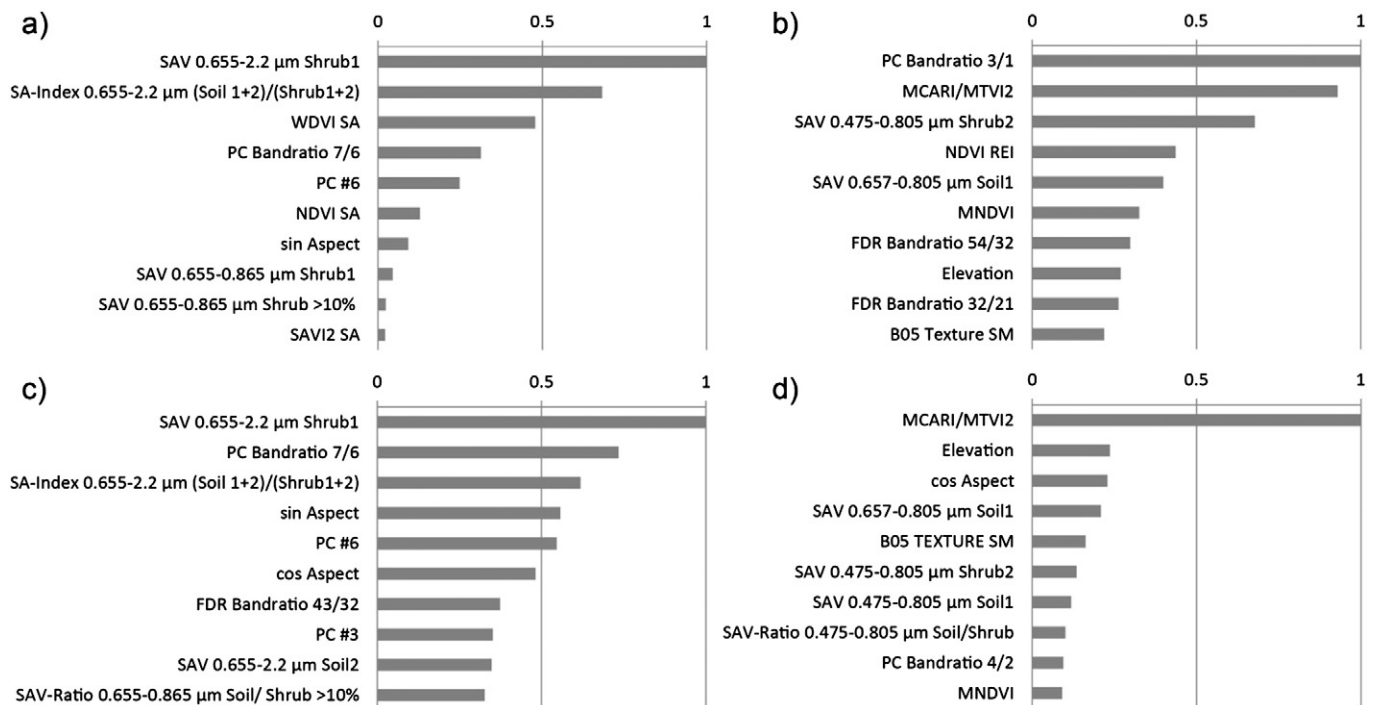


Fig. 6. Results of variable importance measures showing the 10 best predictors of a) LS LASSO, b) RE LASSO, c) LS RR and d) RE RR. Values between 0 and 1 represent relative variable importance.

predictors that warrant further research with more focused study designs. In our study none of the *unadjusted vegetation indices* made a substantial contribution in predicting TB in this environment. Also *soil adjusted vegetation indices* that incorporated slope or intercept of soil line alone (e.g. TSAVI, PVI, WDVI) were not among the most important variable sets in any models. This is consistent with the findings of Calvão and Palmeirim (2011), who found no benefits in soil-adjusted indices in Mediterranean shrubland due to the complexity of constructing a generally valid soil line. Similarly, Van Der Meer et al. (2001) state that soil-adjusted indices did not improve their AGB estimates and may have introduced additional scatter. In our study, however, the statistical uncertainty associated with soil line estimation (e.g. LS NIR-red bands: slope 1.15, standard error 0.06, intercept  $-0.003$ , standard error 0.016) implies only minor uncertainty in the resulting TSAVI and WDVI values (spearman correlations of 0.98/0.99 and 0.95/0.95 under a  $\pm$  one standard error change in the adjustment parameter/s). However, Veraverbeke et al. (2012) state that soil-adjusted vegetation indices outperformed others in environments with variable substrates and a single vegetation type, conditions that also apply to our study region after the pre-classification step. In contrast to these indices with adjustment coefficients derived from a soil line, two *soil adjusted vegetation indices* with fixed adjustment coefficients were among the most important predictors in the RE models. Especially the more complex of these, the combination index MCARI/MTVI2 ranked at 1st and 2nd position, which may be explained by its low sensitivity to soil background variation compared to single indices (Eitel et al., 2009). Among the vegetation indices, *color adjusted vegetation indices* that contain additional separate indices to correct for soil effects were frequently listed as important predictors. This is in agreement with Escadafal and Huete (1991) whose color adjusted indices performed considerably better compared to NDVI or SAVI in detecting sparse vegetation amounts.

SAV based variables were among another group of important predictors, showing that this is a valuable approach even when real endmember spectra are not available. SAV may be less susceptible to background noise due to their insensitivity to brightness variations (Kruse et al., 1993) and may better account for soil variation by encompassing a greater spectral range than most single indices. Additionally some of them account for the soil signal already by including

bare soil pseudo-endmembers. Our variable importances furthermore support the utility of SAV covering a restricted spectral region, in particular the red to SWIR region. This agrees with results obtained by Asner, Wessman, Bateson, and Privette (2000), who state that this spectral region may be able to differentiate between bare soil, green and non-green vegetation even under arid conditions.

The fact that PC and ratios played such an important role in a number of models may be due to the large share of information included in one single variable. PC variables may therefore also be able to reproduce shrub and soil characteristics better than vegetation indices. Finally, FDR and FDR ratios did show some importance in predicting TB. This could be because derivative based ratios are able to capture pairs of gradients in the spectrum (Peña, Brenning, & Sagredo, 2012), e.g. a characteristic curve pattern from the green to infrared spectral regions, which may be an important capability to detect TB in the research area.

Besides spectral data, *topographic variables* were also ranked among the best 10 predictors in all of the 4 best performing single sensor models, which is consistent with results of Powell et al. (2010) who state that biophysical variables (e.g. elevation, slope) were the second most important predictors for AGB in parts of their research area. This may be attributed to the fact that water availability, and hence plant growth, may be controlled by topography. In particular, the assumed relationships between slope orientation and evapotranspiration and between elevation and (orographic) precipitation may have contributed to the importance of topographic predictors. This is in agreement with results obtained by Sternberg and Shoshany (2001) who state that slope aspect significantly influenced shrub biomass in a region with limited water availability. Furthermore, as shown by Shoshany and Karnibad (2011), also direct use of precipitation data in biomass modeling can significantly enhance mapping of shrub vegetation on a larger scale.

One texture variable did rank among the most important predictor variables in both RE models. In other studies, texture measures outperformed other variables in biomass or carbon prediction (Fuchs et al., 2009; Sarker & Nichol, 2011), which was not the case in this study. As these authors analyze forest environments, texture related to biomass variations may be simpler to detect in satellite images compared to a finer resolution that would be required to detect variations in dwarf shrub vegetation that could be linked to biomass amounts



(Vanselow, 2011). In addition to the applied texture variables, texture measures of soil adjusted indices could be incorporated in the study which showed improved performance in other studies (Vanselow & Samimi, 2014). Also different window sizes and texture filters could be utilized (Blanco, Metternicht, & Del Valle, 2009; Dobrowski, Safford, Cheng, & Ustin, 2008). However, we did not fully utilize the whole range of possible texture variables because the abundance of existing methods and an associated evaluation goes beyond the scope of this study. Besides, as dwarf shrub patterns are expressed on the sub meter scale, texture variables derived from a 5 m × 5 m resolution also contain illumination, rock, soil and other signals beside plant information (Shoshany, 2000). Hence, further comprehensive research and mapping would be necessary to assess the relative contribution of different sources to texture variations with the applied resolution.

### 5.3. Performance of statistical models

The availability of a large number of remote sensing variables to predict a biophysical variable creates new challenges, but also provides the opportunity to extract the relevant information and filter important predictors. Two models using shrinkage techniques (LASSO, RR) outperformed the other models, which is in agreement with existing studies in a high dimensional remote sensing setting. Lazaridis, Verbesselt, and Robinson (2011) state that both techniques showed better performance in comparison to others and Gaughan, Holdo, and Anderson (2013) successfully quantified tree cover using LASSO. The restricted SLR4 that uses variable subset selection also performed well but the unrestricted SLR was among the poorest performing modeling techniques. This is contrary to results obtained by Fuchs et al. (2009) who successfully applied unrestricted SLR to select suitable predictors among image bands, indices and texture measures for above ground carbon modeling. Likewise, Sarker and Nichol (2011) evaluated SLR as a suitable approach in modeling forest AGB.

In this study, the tree based RF model performed poorer than most other models, which is different to results obtained by Powell et al. (2010), where RF resulted in the lowest RMSE in comparison to other models in predicting forest biomass. Furthermore, PLS resulted in serious over-fitting which is in contrast to findings of Mitchell, Glenn, Sankey, Derryberry, and Germino (2012), where it is shown that PLS provides a good approach when modeling with large predictor sets.

### 5.4. Sensor performance

An additional objective of this study was to assess the ability of the two applied sensors, RapidEye and Landsat OLI, for biomass modeling in arid environments. As the Landsat 8 satellite has only been in orbit since beginning of 2013, this is, to our knowledge, the first study to compare the performance of both sensors in biomass remote sensing. Our results suggest that none of the sensors performs considerably better than the other. Furthermore, a combination of the sensors did not significantly improve modeling results. Surprisingly, the RapidEye sensor with higher spatial resolution and an additional red edge band designed for vegetation analysis, showing good performance in arid regions in other studies (Li et al., 2012; Ramoelo et al., 2012; Ren et al., 2011), did not improve model performance. According to our variable assessment, the red edge band was important in those indices that account for background information. However, the red edge band did not lead to a superiority of RE over LS models. A reason for equal performance of the OLI sensor may be the coverage of the SWIR spectral region which is regarded as important in detecting shrubs (Asner et al., 2000) or non-photosynthetic vegetation (Ren, Zhou, Zhang, & Zhang, 2012). This suggests that improved dwarf shrub TB predictions may be possible by using hyperspectral sensors.

Spatially, RapidEye with its five meter pixel size, is still too coarse to recognize dwarf shrubs as distinctive delimitable entities, therefore, object based approaches which were successfully applied with large woody vegetation in other arid environments (Spiekermann, Brandt,

& Samimi, 2015) or methodologies that incorporate the influence of patch patterns on shrub biomass (Shoshany, 2012), could not be utilized in our study. Furthermore, Frank and Tweddale (2006) showed that only very high resolution imagery of below one meter was able to significantly increase detection of dwarf shrubs compared to high resolution data in an arid environment. Hence and because most vegetation formations in the Eastern Pamirs generally cover larger patches sufficiently detectable by the Landsat OLI sensor as well, the higher resolution of RapidEye data may not have led to a better performance in biomass mapping in the research area.

Regarding temporal resolution, RapidEye is highly resolved with a revisiting period between one to five and a half days (RapidEye AG, 2009) compared to 16 days with Landsat OLI. Such a high temporal frequency may be important to analyze phenological changes in remote sensing studies with a multi-temporal approach or to better capture cloud free images in regions where overcast conditions prevail (Maselli, Gilabert, & Conese, 1998). However, these circumstances do not apply to the Eastern Pamirs and the temporal resolution of Landsat may be regarded as sufficient even for multi-temporal decomposition in arid environments (Shoshany & Svoray, 2002).

As discussed above, TB prediction is complex and connected to a number of limitations. However, this is the first study that generates spectrally resolved dwarf shrub biomass information in the research area. Furthermore, when compared to existing work of dwarf shrub formation classification (Kraudzun et al., 2014; Vanselow & Samimi, 2014), there is some consistency in results. Besides, results are ecologically plausible since higher TB was predicted at higher elevations and in the Southwest, which may reflect the main precipitation gradient with rainfall rates increasing from Northeast to Southwest (Vanselow, 2011). Moreover, the smallest amounts of TB were predicted for regions that are near larger settlements or in the vicinity of major roads, which may reflect the increased anthropogenic use of dwarf shrub biomass in those areas. These rather qualitative reasons show that the presented modeling results represent valuable information in remote sensing based desertification assessment in spite of relatively large quantitative prediction errors.

## 6. Conclusions

This study showed that remote sensing based mapping of dwarf shrub TB is possible even under conditions with extremely low vegetation cover, although the predictions are subject to substantial uncertainties. The lasso technique for linear regression is a particularly appealing, sparse model that performed very well in this study. While some of the models used, in particular random forest and stepwise linear regression, suffered from strong over-fitting to the training data, the better performing prediction methods achieved cross-validation performances that were closer to their training-set errors. This study indicates that variables that incorporate the information of several bands, covering vegetation as well as background information, may be especially suitable for this arid setting. Both sensors, Landsat OLI and RapidEye, as well as their combination performed equally well. Future research may therefore benefit from a reduced set of predictors from a single sensor based on the variables identified as important in this study.

## Acknowledgements

We would like to express our gratitude to the Volkswagen Foundation for enabling research by funding the research project Pamir II (awarded to C. Samimi), and to the Alexander von Humboldt Foundation for funding A. Brenning's research at the University of Heidelberg. We further thank the DLR for the data provision from RESA and the USGS for providing additional remote sensing products. The use of facilities of the Shared Hierarchical Academic Research Computing Network (SHARCNET: [www.sharcnet.ca](http://www.sharcnet.ca)) and Compute/Calcul Canada is acknowledged. Finally, the authors thank the reviewers for their constructive comments to improve the manuscript.

Appendix A

Table A1

Derived indices, principal components, FDR and respective ratios used in this study. (S = sensor; B<sub>blue2</sub> = LS Band2/RE Band1; B<sub>green</sub> = LS Band3/RE Band2; B<sub>red</sub> = LS Band4/RE Band3; B<sub>reedge</sub> = RE Band4; B<sub>nir</sub> = LS & RE Bands5; B<sub>swir1</sub> = LS Band6; B<sub>swir2</sub> = LS Band7; a = slope of the soil line; b = intercept of the soil line; k - slope of linear correlation between Index and adjustment index; nine bare soil field sites were used for construction of soil related parameters).

| Variable                                 | S     | Formula   | Reference                      |
|--|-------|---|--------------------------------|
| <i>Unadjusted vegetation indices</i>     |       |   |                                |
| NDVI                                     | LS/RE | $(B_{nir} - B_{red}) / (B_{nir} + B_{red})$   | Rouse et al. (1974)            |
| Band ratios (BR); all bands              | LS/RE | e.g. $B_{swir2} / B_{swir1}$ ; $B_{swir2} / B_{nir}$ ; etc.   | Bannari et al. (1995)          |
| NDRE                                     | RE    | $(B_{nir} - B_{reedge}) / (B_{nir} + B_{reedge})$   | Eitel et al. (2009)            |
| NDTI                                     | LS    | $(B_{swir1} - B_{swir2}) / (B_{swir1} + B_{swir2})$   | Gelder et al. (2009)           |
| RDVI                                     | LS/RE | $(B_{nir} - B_{red}) / \text{SQRT}(B_{nir} + B_{red})$  | Ramoelo et al. (2012)          |
| RDVI2                                    | RE    | $(B_{nir} - B_{reedge}) / \text{SQRT}(B_{nir} + B_{reedge})$  | Ramoelo et al. (2012)          |
| NDRI                                     | LS    | $(B_{red} - B_{swir2}) / (B_{red} + B_{swir2})$   | Gelder et al. (2009)           |
| NDI5                                     | LS    | $(B_{nir} - B_{swir1}) / (B_{nir} + B_{swir1})$   | Gelder et al. (2009)           |
| NDI7                                     | LS    | $(B_{nir} - B_{swir2}) / (B_{nir} + B_{swir2})$   | Gelder et al. (2009)           |
| NDSVI                                    | LS    | $(B_{swir1} - B_{red}) / (B_{swir1} + B_{red})$   | Gelder et al. (2009)           |
| PPR                                      | LS/RE | $(B_{green} - B_{blue2}) / (B_{green} + B_{blue2})$   | Ramoelo et al. (2012)          |
| NRI                                      | LS/RE | $(B_{green} - B_{red}) / (B_{green} + B_{red})$   | Ramoelo et al. (2012)          |
| SIPI                                     | LS/RE | $(B_{nir} - B_{blue2}) / (B_{nir} - B_{red})$   | Ramoelo et al. (2012)          |
| TVI                                      | RE    | $0.5 * (120 * (B_{reedge} - B_{green}) - 200 * (B_{red} - B_{green}))$  | Ramoelo et al. (2012)          |
| MCARI                                    | RE    | $((B_{reedge} - B_{red}) - 0.2 * (B_{reedge} - B_{green})) * (B_{reedge} / B_{red})$  | Ramoelo et al. (2012)          |
| MTCI                                     | RE    | $(B_{nir} - B_{reedge}) / (B_{reedge} - B_{red})$   | Ramoelo et al. (2012)          |
| TCARI                                    | RE    | $3 * ((B_{reedge} - B_{red}) - 0.2 * (B_{reedge} - B_{green})) * (B_{reedge} / B_{red})$  | Ramoelo et al. (2012)          |
| MOIST                                    | LS/RE | $(B_{nir} - B_{blue2}) / (B_{nir} + B_{blue2})$   | Homer et al. (2012)            |
| LAI                                      | LS/RE | $(B_{nir}) / (B_{red} + B_{green})$   | Homer et al. (2012)            |
| SLAI                                     | LS    | $(B_{nir}) / (B_{red} + B_{green})$   | Homer et al. (2012)            |
| NDVI53                                   | LS/RE | $(B_{nir} - B_{green}) / (B_{nir} + B_{green})$   | Rouse et al. (1974)            |
| NDRE/NDVI                                | RE    | NDRE/NDVI   | Eitel et al. (2009)            |
| <i>Soil adjusted vegetation indices</i>  |       |   |                                |
| SAVI1                                    | LS/RE | $((B_{nir} - B_{red}) / (B_{nir} + B_{red} + 1.5)) * (1 + 0.5)$   | Huete (1988)                   |
| SAVI2                                    | LS/RE | $((B_{nir} - B_{red}) / (B_{nir} + B_{red} + 0.5)) * (1 + 0.5)$   | Huete (1988)                   |
| MSAVI1                                   | LS/RE | $(2 * B_{nir} + 1 - \text{SQRT}(2 * B_{nir} + 1)^2 - 8 * (B_{nir} - B_{red})) / 2$  | Qi et al. (1994)               |
| OSAVI                                    | RE    | $(1 + 0.16) * (B_{nir} - B_{reedge}) / (B_{nir} + B_{reedge} + 0.16)$   | Rondeaux et al. (1996)         |
| OSAVI2                                   | LS/RE | $(1 + 0.16) * (B_{nir} - B_{red}) / (B_{nir} + B_{red} + 0.16)$   | Rondeaux et al. (1996)         |
| MNDVI                                    | LS/RE | $(\text{NDVI} / (1 + ((0.55 * B_{red} - B_{blue2} + 0.12)) / (B_{nir}^2 - B_{red}^2)))) * (1 + 0.001 * (1 / (0.55 * B_{red} - B_{blue2} + 0.12)))$                                | Liu and Huete (1994)           |
| MNDVI2                                   | RE    | $(\text{NDVI} / (1 + ((0.55 * B_{reedge} - B_{blue2} + 0.12)) / (B_{nir}^2 - B_{reedge}^2)))) * (1 + 0.001 * (1 / (0.55 * B_{reedge} - B_{blue2} + 0.12)))$                       | Liu and Huete (1994)           |
| EVI                                      | LS/RE | $2.5 * (B_{nir} - B_{red}) / B_{nir} + (6 * B_{red}) - (7.5 * B_{blue2}) + 1$   | Ramoelo et al. (2012)          |
| SARVI                                    | LS/RE | $(1 + 0.5) * (B_{nir} - B_{red} - B_{blue2} - B_{red}) / (B_{nir} - B_{red} - B_{blue2} - B_{red} + 0.5)$   | Haboudane et al. (2004)        |
| MTVI2                                    | LS/RE | $(1.5 * 1.2 * (B_{nir} - B_{green}) - 2.5 * (B_{red} - B_{green})) / \text{SQRT}((2 * B_{nir} + 1; 2)^2) - (6 * B_{nir} - \text{SQRT}(5 * B_{red})) - 0.5$                        | Haboudane et al. (2004)        |
| TCARI/OSAVI                              | RE    | TCARI/OSAVI   | Eitel et al. (2009)            |
| MCARI/OSAVI                              | RE    | MCARI/OSAVI   | Eitel et al. (2009)            |
| MCARI/MTVI2                              | RE    | MCARI/MTVI2   | Eitel et al. (2009)            |
| WDVI                                     | LS/RE | $B_{nir} - (a * B_{red})$   | Qi et al. (1994)               |
| WDVI REDEEDGE                            | RE    | $B_{nir} - (a * B_{reedge})$  | acc.to Qi et al. (1994)        |
| PVI                                      | LS/RE | $(B_{nir} - (a * B_{red}) - b) / \text{SQRT}(1 + a^2)$  | Elvidge and Chen (1995)        |
| PVI REDEEDGE                             | RE    | $(B_{nir} - (a * B_{reedge}) - b) / \text{SQRT}(1 + a^2)$   | acc.to Elvidge and Chen (1995) |
| MSAVI ORIG                               | LS/RE | $((B_{nir} - B_{red}) / (B_{nir} + B_{red} + 1 - (2 * a * \text{NDVI} * \text{WDVI}))) * (1 + 1 - (2 * a * \text{NDVI} * \text{WDVI}))$   | Qi et al. (1994)               |
| MSAVI ORIG REDEEDGE                      | RE    | $((B_{nir} - B_{reedge}) / (B_{nir} + B_{reedge} + 1 - (2 * a * \text{NDVI}_{reedge} * \text{WDVI}_{reedge}))) * (1 + 1 - (2 * a * \text{NDVI}_{reedge} * \text{WDVI}_{reedge}))$ | acc.to Qi et al. (1994)        |
| TSAVI                                    | LS/RE | $(a * (B_{nir} - a * B_{red} - b)) / (a * B_{nir} + B_{red} - a * b + (0.08 * (1 + a^2)))$  | Qi et al. (1994)               |
| TSAVI REDEEDGE                           | RE    | $(a * (B_{nir} - a * B_{reedge} - b)) / (a * B_{nir} + B_{reedge} - a * b + (0.08 * (1 + a^2)))$  | acc.to Qi et al. (1994)        |
| SACRI                                    | LS    | $a * (B_{red} - B_{swir1} - b) / (a * B_{red} + B_{swir1} - a * b)$   | Ren et al. (2012)              |
| MSACRI                                   | LS    | $5 * (a * (B_{swir1} - a * B_{swir2} - b)) / (a * B_{swir1} + B_{swir2} + a * b)$   | Ren et al. (2012)              |
| <i>Color adjusted vegetation indices</i> |       |   |                                |
| RI (color adjustment index)              | LS/RE | $(B_{red} - B_{green}) / (B_{red} + B_{green})$   | Escadafal and Huete (1991)     |
| REI (color adjustment index)             | RE    | $(B_{reedge} - B_{green}) / (B_{reedge} + B_{green})$   | Escadafal and Huete (1991)     |

(continued on next page)

Table A1 (continued)

| Variable   | S     | Formula   | Reference                         |
|--|-------|---|-----------------------------------|
| RBI (color adjustment index)                             | LS/RE | $(B_{red} - B_{blue2}) / (B_{red} + B_{blue2})$ | acc.to Escadafal and Huete (1991) |
| SWI1 (color adjustment index)                            | LS    | $(B_{swir1} - B_{red}) / (B_{swir1} + B_{red})$ | acc.to Escadafal and Huete (1991) |
| SWI2 (color adjustment index)                            | LS    | $(B_{swir1} - B_{red}) / (B_{swir1} + B_{red})$ | acc.to Escadafal and Huete (1991) |
| NDVI SA  | LS/RE | $NDVI - (k * RI)$                               | Escadafal and Huete (1991)        |
| SAVI1 SA   | LS/RE | $SAVI1 - (k * RI)$                              | Escadafal & Huete, 1991           |
| SAVI2 SA   | LS/RE | $SAVI2 - (k * RI)$                              | Escadafal and Huete (1991)        |
| TSAVI SA   | LS/RE | $TSAVI - (k * RI)$                              | acc.to Escadafal and Huete (1991) |
| TSAVI REDEDGE SA   | RE    | $TSAVI REDEDGE - (k * RI)$                      | acc.to Escadafal and Huete (1991) |
| WDVI SA  | LS/RE | $WDVI - (k * RI)$                               | acc.to Escadafal and Huete (1991) |
| WDVI REDEDGE SA  | RE    | $WDVI REDEDGE - (k * RI)$                       | acc.to Escadafal and Huete (1991) |
| NDVI RBI   | LS/RE | $NDVI - (k * RBI)$                              | acc.to Escadafal and Huete (1991) |
| SAVI1 RBI  | LS/RE | $SAVI1 - (k * RBI)$                             | acc.to Escadafal and Huete (1991) |
| SAVI2 RBI  | LS/RE | $SAVI2 - (k * RBI)$                             | acc.to Escadafal and Huete (1991) |
| TSAVI RBI  | LS/RE | $TSAVI - (k * RBI)$                             | acc.to Escadafal and Huete (1991) |
| TSAVI REDEDGE RBI  | RE    | $TSAVI REDEDGE - (k * RBI)$                     | acc.to Escadafal and Huete (1991) |
| WDVI RBI   | LS/RE | $WDVI - (k * RBI)$                              | acc.to Escadafal and Huete (1991) |
| WDVI REDEDGE RBI   | RE    | $WDVI REDEDGE - (k * RBI)$                      | acc.to Escadafal and Huete (1991) |
| NDVI SWI1  | LS    | $NDVI - (k * SWI1)$                             | acc.to Escadafal and Huete (1991) |
| SAVI 1 SWI1  | LS    | $SAVI1 - (k * SWI1)$                            | acc.to Escadafal and Huete (1991) |
| SAVI 2 SWI1  | LS    | $SAVI2 - (k * SWI1)$                            | acc.to Escadafal and Huete (1991) |
| TSAVI SWI1   | LS    | $TSAVI - (k * SWI1)$                            | acc.to Escadafal and Huete (1991) |
| WDVI SWI1  | LS    | $WDVI - (k * SWI1)$                             | acc.to Escadafal and Huete (1991) |
| NDVI SWI2  | LS    | $NDVI - (k * SWI2)$                             | acc.to Escadafal and Huete (1991) |
| SAVI 1 SWI2  | LS    | $SAVI1 - (k * SWI2)$                            | acc.to Escadafal and Huete (1991) |
| SAVI 2 SWI2  | LS    | $SAVI2 - (k * SWI2)$                            | acc.to Escadafal and Huete (1991) |
| TSAVI SWI2   | LS    | $TSAVI - (k * SWI2)$                            | acc.to Escadafal and Huete (1991) |
| WDVI SWI2  | LS    | $WDVI - (k * SWI2)$                             | acc.to Escadafal and Huete (1991) |
| NDRE SA  | RE    | $NDRE - (k * RI)$                               | acc.to Escadafal and Huete (1991) |
| NDRE RBI   | RE    | $NDRE - (k * RBI)$                              | acc.to Escadafal and Huete (1991) |
| NDVI REI   | RE    | $NDVI - (k * REI)$                              | Escadafal and Huete (1991)        |
| NDRE REI   | RE    | $NDRE - (k * REI)$                              | acc.to Escadafal and Huete (1991) |
| SAVI1 REI  | RE    | $SAVI1 - (k * REI)$                             | Escadafal and Huete (1991)        |
| SAVI2 REI  | RE    | $SAVI2 - (k * REI)$                             | Escadafal and Huete (1991)        |
| TSAVI REI  | RE    | $TSAVI - (k * REI)$                             | acc.to Escadafal and Huete (1991) |
| TSAVI REDEDGE REI  | RE    | $TSAVI REDEDGE - (k * REI)$                     | acc.to Escadafal and Huete (1991) |
| WDVI REI   | RE    | $WDVI - (k * REI)$                              | acc.to Escadafal and Huete (1991) |
| WDVI REDEDGE REI   | RE    | $WDVI REDEDGE - (k * REI)$                      | acc.to Escadafal and Huete (1991) |
| <i>First derivatives of reflectance (FDR) and ratios</i> |       |   |                                   |
| FDR LS = 6, RE = 4                                       | LS/RE | First derivative of reflectance                 | Entcheva-Campbell et al. (2004)   |
| FDR Band ratios, all FDR                                 | LS/RE | e.g. FDR Bandratio 54/32 = FDR54/FDR32, etc.    |                                   |
| <i>Principal components (PC) and ratios</i>              |       |   |                                   |
| PC #1-7/1-5  | LS/RE | Derived principal components                    |                                   |
| PC Band ratios, all PC                                   | LS/RE | e.g. PC Bandratio 7/6 = PC#7/PC#6, etc.         |                                   |

Table A2

Overview of constructed SAV values, derived ratios and texture attributes used in this study.

| Variable   | Sensor | Description   |
|--|--------|---|
| <i>Texture parameters</i>  |        |   |
| B04 TEXTURE CONTRAST   | RE     | Texture of Band 4 calculated by ENVI contrast equation  |
| B04 TEXTURE CORRELATION  | RE     | Texture of Band 4 calculated by ENVI correlation equation   |
| B04 TEXTURE SM   | RE     | Texture of Band 4 calculated by ENVI angular second moment equation   |
| B04 TEXTURE VARIANCE   | RE     | Texture of Band 4 calculated by ENVI variance equation  |
| B05 TEXTURE CONTRAST   | RE     | Texture of Band 5 calculated by ENVI contrast equation  |
| B05 TEXTURE CORRELATION  | RE     | Texture of Band 5 calculated by ENVI correlation equation   |
| B05 TEXTURE SM   | RE     | Texture of Band 5 calculated by ENVI angular second moment equation   |
| B05 TEXTURE VARIANCE   | RE     | Texture of Band 5 calculated by ENVI variance equation  |
| NDRE TEXTURE RANGE   | RE     | Texture of NDRE calculated by TNTmips range filter  |
| NDVI TEXTURE RANGE   | RE     | Texture of NDVI calculated by TNTmips range filter  |
| <i>SAV based variables</i>   |        |   |
| SAV 0.44–2.2 µm Shrub1 (RE = 0.475–0.805 µm)                         | LS/RE  | Calculated using field site with highest TB   |
| SAV 0.44–2.2 µm Shrub >10% (RE = 0.475–0.805 µm)                     | LS/RE  | Calculated using field sites with cover > 10%   |
| SAV 0.44–2.2 µm GD (RE = 0.475–0.805 µm)                             | LS/RE  | Calculated using meadow field sites   |
| SAV 0.44–2.2 µm Shrub2 (RE = 0.475–0.805 µm)                         | LS/RE  | Calculated using field site with 2nd highest TB   |
| SAV 0.44–2.2 µm Soil1 (RE = 0.475–0.805 µm)                          | LS/RE  | Calculated using no vegetation field site 1   |
| SAV 0.44–2.2 µm Soil2 (RE = 0.475–0.805 µm)                          | LS/RE  | Calculated using no vegetation field site 2   |
| SAV 0.44–2.2 µm Soil (RE = 0.475–0.805 µm)                           | LS/RE  | Calculated using all non-vegetated field site   |
| SAV 0.655–0.865 µm Shrub1 (RE = 0.657–0.805 µm)                      | LS/RE  | Calculated using field site with highest TB   |
| SAV 0.655–0.865 µm Shrub >10% (RE = 0.657–0.805 µm)                  | LS/RE  | Calculated using field site with cover > 10%  |
| SAV 0.655–0.865 µm GD (RE = 0.657–0.805 µm)                          | LS/RE  | Calculated using meadow field site  |
| SAV 0.655–0.865 µm Shrub2 (RE = 0.657–0.805 µm)                      | LS/RE  | Calculated using field site with 2nd highest TB   |
| SAV 0.655–0.865 µm Soil1 (RE = 0.657–0.805 µm)                       | LS/RE  | Calculated using no vegetation field site 1   |
| SAV 0.655–0.865 µm Soil2 (RE = 0.657–0.805 µm)                       | LS/RE  | Calculated using no vegetation field site 2   |
| SAV 0.655–0.865 µm Soil (RE = 0.657–0.805 µm)                        | LS/RE  | Calculated using all non-vegetated field sites  |
| SAV 0.655–2.2 µm Shrub1  | LS     | Calculated using field site with highest TB   |
| SAV 0.655–2.2 µm GD  | LS     | Calculated using meadow field sites   |
| SAV 0.655–2.2 µm Shrub2  | LS     | Calculated using field site with 2nd highest TB   |
| SAV 0.655–2.2 µm Soil1   | LS     | Calculated using no vegetation field site 1   |
| SAV 0.655–2.2 µm Soil2   | LS     | Calculated using no vegetation field site 2   |
| SAV 0.71–0.805 µm Shrub1   | RE     | Calculated using field site with highest TB   |
| SAV 0.71–0.805 µm Shrub >10%   | RE     | Calculated using field site with cover > 10%  |
| SAV 0.71–0.805 µm GD   | RE     | Calculated using meadow field sites   |
| SAV 0.71–0.805 µm Shrub2   | RE     | Calculated using field site with 2nd highest TB   |
| SAV 0.71–0.805 µm Soil1  | RE     | Calculated using no vegetation field site 1   |
| SAV 0.71–0.805 µm Soil2  | RE     | Calculated using no vegetation field site 2   |
| SAV 0.71–0.805 µm Soil   | RE     | Calculated using all non-vegetated field sites  |
| SAV 0.475–0.805 µm Shrub   | RE     | Calculated using non soil field sites   |
| SAV-Ratio 0.44–2.2 (0.475–0.805) µm Soil/ Shrub >10%                 | LS/RE  | SAV 0.44–2.2 µm Soil/ SAV 0.44–2.2 µm Dense   |
| SAV-Ratio 0.44–2.2 (0.475–0.805) µm Soil/GD                          | LS/RE  | SAV 0.44–2.2 µm Soil/ SAV 0.44–2.2 µm GD  |
| SAV-Ratio 0.655–0.865 (0.657–0.805) µm Soil/ Shrub >10%              | LS/RE  | SAV 0.655–0.865 µm Soil/ SAV 0.655–0.865 µm Shrub >10%  |
| SAV-Ratio 0.655–0.865 (0.657–0.805) µm Soil/GD                       | LS/RE  | SAV 0.655–0.865 µm Soil/ SAV 0.655–0.865 µm GD  |
| SAV-Ratio 0.71–0.805 µm Soil/ Shrub >10%                             | RE     | SAV 0.71–0.805 µm Soil/ SAV 0.71–0.805 µm Shrub >10%  |
| SAV-Ratio 0.71–0.805 µm Soil/GD                                      | RE     | SAV 0.71–0.805 µm Soil/ SAV 0.71–0.805 µm GD  |
| SAV-Ratio 0.475–0.805 µm Soil/Shrub                                  | RE     | SAV 0.475–0.805 µm Soil/ SAV 0.475–0.805 µm Shrub   |
| SA-Index 0.44–2.2 (RE = 0.475–0.805) µm (Soil 1 + 2)/(Shrub1 + 2)    | LS/RE  | (SAV 0.44–2.2 µm Soil1 + SAV 0.44–2.2 µm Soil2) / (SAV 0.44–2.2 µm Shrub1 + SAV 0.44–2.2 µm Shrub2)             |
| SA-Index 0.655–0.865 (RE = 0.657–0.805) µm (Soil 1 + 2)/(Shrub1 + 2) | LS/RE  | (SAV 0.655–0.865 µm Soil1 + SAV 0.655–0.865 µm Soil2) / (SAV 0.655–0.865 µm Shrub1 + SAV 0.655–0.865 µm Shrub2) |
| SA-Index 0.655–2.2 µm (Soil 1 + 2)/(Shrub1 + 2)                      | LS     | (SAV 0.655–2.2 µm Soil1 + SAV 0.655–2.2 µm Soil2) / (SAV 0.655–2.2 µm Shrub1 + SAV 0.655–2.2 µm Shrub2)         |

## References

- AIRS Science Team, & Teixeira, J. (2013). *Aqua AIRS Level 3 Daily Standard Physical Retrieval (AIRS + AMSU), version 006*. Greenbelt, MD, USA: NASA Goddard Earth Science Data and Information Services Center (GES DISC), <http://dx.doi.org/10.5067/AQUA/AIRS/DATA301> (Accessed October 2013 at).
- Asner, G.P., & Heidebrecht, K.B. (2002). Spectral unmixing of vegetation, soil and dry carbon cover in arid regions: comparing multispectral and hyperspectral observations. *International Journal of Remote Sensing*, 23, 3939–3958.
- Asner, G.P., Wessman, C.A., Bateson, C., & Privette, J.L. (2000). Impact of tissue, canopy, and landscape factors on the hyperspectral reflectance variability of arid ecosystems. *Remote Sensing of Environment*, 74(1), 69–84.
- Bannari, A., Morin, D., Bonn, F., & Huete, A.R. (1995). A review of vegetation indices. *Remote Sensing Reviews*, 13, 95–120.
- Baskerville, G.L. (1972). Use of logarithmic regression in the estimation of plant biomass. *Canadian Journal of Forest Research*, 2, 49–53.
- Blanco, P.D., Metternicht, G.I., & Del Valle, H.F. (2009). Improving the discrimination of vegetation and landform patterns in sandy rangelands: a synergistic approach. *International Journal of Remote Sensing*, 30(10), 2579–2605.
- Breckle, S., & Wucherer, W. (2006). Vegetation of the Pamir (Tajikistan): Land Use and Desertification Problems. In E. Spehn, M. Liberman, & C. Körner (Eds.), *Land Use change and mountain biodiversity* (pp. 225–237). Boca Raton: Gustav Fischer Verlag Stuttgart.
- Breiman, L. (2001). Random forests. *Machine Learning*, 45(1), 5–32, <http://dx.doi.org/10.1023/A:1010933404324>.
- Brenning, A. (2008). Statistical geocomputing combining R and SAGA: The example of landslide susceptibility analysis with generalized additive models. In J. Böhrner, T. Blaschke, & L. Montanarella (Eds.), *SAGA – seconds out. Hamburger Beiträge zur Physischen Geographie und Landschaftsökologie*, Vol. 19. (pp. 23–32).
- Brenning, A. (2009). Benchmarking classifiers to optimally integrate terrain analysis and multispectral remote sensing in automatic rock glacier detection. *Remote Sensing of Environment*, 113, 239–247, <http://dx.doi.org/10.1016/j.rse.2008.09.005>.
- Brenning, A. (2012). Spatial cross-validation and bootstrap for the assessment of prediction rules in remote sensing: the R package 'sperores'. *Geoscience and Remote Sensing Symposium (IGARSS), 2012 IEEE International, 23–27 July 2012* (pp. 5372–5375), <http://dx.doi.org/10.1109/IGARSS.2012.6352393>.
- Brenning, A., Long, S., & Fieguth, P. (2012). Detecting rock glacier flow structures using Gabor filters and IKONOS imagery. *Remote Sensing of Environment*, 125, 227–237.
- Calvão, T., & Palmeirim, J.M. (2004). Mapping Mediterranean scrub with satellite imagery: biomass estimation and spectral behaviour. *International Journal of Remote Sensing*, 25(16), 3113–3126.
- Calvão, T., & Palmeirim, J.M. (2011). A comparative evaluation of spectral vegetation indices for the estimation of biophysical characteristics of Mediterranean semi-deciduous shrub communities. *International Journal of Remote Sensing*, 32(8), 2275–2296.



- Díaz-Uriarte, R., & Alvarez de Andrés, S. (2006). Gene selection and classification of microarray data using random forest. *BMC Bioinformatics*, 2006(7), 3, <http://dx.doi.org/10.1186/1471-2105-7-3>.
- Dobrowski, S.Z., Safford, H.D., Cheng, Y.B., & Ustin, S.L. (2008). Mapping mountain vegetation using species distribution modeling, image-based texture analysis, and object-based classification. *Applied Vegetation Science*, 11(4), 499–508.
- Duncan, J., Stow, D., Franklin, J., & Hope, A. (1993). Assessing the relationship between spectral vegetation indices and shrub cover in the Jornada Basin, New Mexico. *International Journal of Remote Sensing*, 14(18), 3395–3416.
- Eisfelder, C., Kuenzer, C., & Dech, S. (2012). Derivation of biomass information for semi-arid areas using remote-sensing data. *International Journal of Remote Sensing*, 33, 2937–2984.
- Eitel, J.U.H., Long, D.S., Gessler, P.E., Hunt, E.R., & Brown, D.J. (2009). Sensitivity of ground-based remote sensing estimates of wheat chlorophyll content to variation in soil reflectance. *Soil Science Society of America Journal*, 73, 1715.
- Elvidge, C.D., & Chen, Z. (1995). Comparison of broad-band and narrow-band Red and near-infrared vegetation indices. *Remote Sensing of Environment*, 54, 38–48.
- Elzein, T.M., Blarquez, O., Gauthier, O., & Carcaillet, C. (2011). Allometric equations for biomass assessment of subalpine dwarf shrubs. *Alpine Botany*, 121(2), 129–134.
- Entcheva-Campbell, P.K., Rock, B.N., Martin, M.E., Neefus, C.D., Irons, J.R., Middleton, E.M., et al. (2004). Detection of initial damage in Norway spruce canopies using hyperspectral airborne data. *International Journal of Remote Sensing*, 25(24), 5557–5584.
- Escadafal, R., & Chehbouni, A.G. (2008). Monitoring arid land surfaces with earth observation techniques: examples of intense and extensive land uses. In J. Qi, & K.T. Evered (Eds.), *Environmental problems of central Asia and their economic, social and security impacts* (pp. 59–72). Dordrecht, Netherlands: Springer.
- Escadafal, R., & Huete, A. (1991). Étude des propriétés spectrales des sols arides appliquée à l'amélioration des indices de végétation obtenus par télédétection. *Comptes Rendus de l'Académie des Sciences Paris*, 312, 1385–1391.
- FAO (2004). *Carbon sequestration in dryland soils*. Rome, Italy: Food And Agriculture Organization Of The United Nations.
- Frank, T.D., & Tweddale, S.A. (2006). The effect of spatial resolution on measurement of vegetation cover in three Mojave Desert shrub communities. *Journal of Arid Environments*, 67, 88–99.
- Friedman, J., Hastie, T., & Tibshirani, R. (2010). Regularization paths for generalized linear models via coordinate descent. *Journal of Statistical Software*, 33(1), 1–22.
- Fuchs, H., Magdon, P., Kleinn, C., & Flessa, H. (2009). Estimating aboveground carbon in a catchment of the Siberian forest tundra: Combining satellite imagery and field inventory. *Remote Sensing of Environment*, 113(3), 518–531.
- Gaughan, A.E., Holdo, R.M., & Anderson, T.M. (2013). Using short-term MODIS time-series to quantify tree cover in a highly heterogeneous African savanna. *International Journal of Remote Sensing*, 34(19), 6865–6882.
- Gelder, B.K., Kalleita, A.L., & Cruse, R.M. (2009). Estimating mean field residue cover on midwestern soils using satellite imagery. *Agronomy Journal*, 101(3), 635–643.
- Guanter, L., Richter, R., & Kaufmann, H. (2009). On the application of the MODTRAN4 atmospheric radiative transfer code to optical remote sensing. *International Journal of Remote Sensing*, 30, 1407–1424.
- Haboudane, D., Miller, J.R., Pattey, E., Zarco-Tejada, P.J., & Strachan, I.B. (2004). Hyperspectral vegetation indices and novel algorithms for predicting green LAI of crop canopies: Modeling and validation in the context of precision agriculture. *Remote Sensing of Environment*, 90(3), 337–352.
- Hastie, T.J., & Pregibon, D. (1992). Generalized linear models. In J.M. Chambers, & T.J. Hastie (Eds.), *Statistical models in S*. Wadsworth & Brooks/Cole.
- Hekklau, H., & Röser, M. (2008). Delineation, taxonomy and phylogenetic relationships of the genus *Krascheninnikovia* (Amaranthaceae subtribe Axyridinae). *Taxon*, 57(2), 563–576.
- Hekklau, H., & von Wehrden, H. (2011). Wood anatomy reflects the distribution of *Krascheninnikovia ceratoides* (Chenopodiaceae). *Flora – Morphology, Distribution, Functional Ecology of Plants*, 206(4), 300–309.
- Holm, A.M., Cridland, S.W., & Roderick, M.L. (2003). The use of time-integrated NOAA NDVI data and rainfall to assess landscape degradation in the arid shrubland of Western Australia. *Remote Sensing of Environment*, 85(2), 145–158.
- Homer, C.G., Aldridge, C.L., Meyer, D.K., & Schell, S.J. (2012). Multi-scale remote sensing sagebrush characterization with regression trees over Wyoming, USA: Laying a foundation for monitoring. *International Journal of Applied Earth Observation and Geoinformation*, 14, 233–244.
- Huete, A.R. (1988). A soil-adjusted vegetation index (SAVI). *Remote Sensing of Environment*, 25, 295–309.
- James, G., Witten, D., Hastie, T., & Tibshirani, R. (2013). *An introduction to statistical learning with applications in R*. New York: Springer.
- Jiménez-Muñoz, J.C., Sobrino, J.A., Mattar, C., & Franch, B. (2010). Atmospheric correction of optical imagery from MODIS and Reanalysis atmospheric products. *Remote Sensing of Environment*, 114, 2195–2210.
- Justice, C.O., & Townshend, J.G. (1981). Integrating ground data with remote sensing. In J.G. Townshend (Ed.), *Terrain analysis and remote sensing* (pp. 38–58). London: Allen and Unwin.
- Kraudzun, T., Vanselow, K.A., & Samimi, C. (2014). Realities and myths of the Teresken Syndrome – an evaluation of the exploitation of dwarf shrub resources in the Eastern Pamirs of Tajikistan. *Journal of Environmental Management*, 132, 49–59.
- Kruse, F.A., Lefkoff, A.B., Boardman, J.W., Heidebrecht, K.B., Shapiro, A.T., Barloon, P.J., et al. (1993). The spectral image processing system (SIPS) – interactive visualization and analysis of imaging spectrometer data. *Remote Sensing of Environment*, 44, 145–163.
- Lal, R. (2004). Carbon sequestration in dryland ecosystems. *Environmental Management*, 33, 528–544.
- Lazaridis, D.C., Verbesselt, J., & Robinson, A.P. (2011). Penalized regression techniques for prediction: a case study for predicting tree mortality using remotely sensed vegetation indices. This article is one of a selection of papers from Extending Forest Inventory and Monitoring over Space and Time. *Canadian Journal of Forest Research*, 41, 24–34.
- Li, X., Gao, Z., Bai, L., & Huang, Y. (2012). Potential of high resolution RapidEye data for sparse vegetation fraction mapping in arid regions. *International Geoscience and Remote Sensing Symposium (IGARSS)* (pp. 420–423) (art.no. 6351548).
- Liaw, A., & Wiener, M. (2002). Classification and regression by randomForest. *R News*, 2, 18–22.
- Liu, H.Q., & Huete, A. (1994). A systems based modification of the NDVI to minimize soil and atmospheric noise. *Geoscience and Remote Sensing Symposium, 1994. IGARSS'94. Surface and Atmospheric Remote Sensing: Technologies, Data Analysis and Interpretation., International, Vol. 1.* (pp. 128–130). IEEE.
- Luedeling, E., & Buerkert, A. (2008). Typology of oases in northern Oman based on Landsat and SRTM imagery and geological survey data. *Remote Sensing of Environment*, 112(3), 1181–1195.
- Maiersperger, T.K., Scaramuzza, P.L., Leigh, L., Shrestha, S., Gallo, K.P., Jenkerson, C.B., et al. (2013). Characterizing LEDAPS surface reflectance products by comparisons with AERONET, field spectrometer, and MODIS data. *Remote Sensing of Environment*, 136, 1–13.
- Maselli, F., Gilabert, M.A., & Conese, C. (1998). Integration of high and low resolution NDVI data for monitoring vegetation in Mediterranean environments. *Remote Sensing of Environment*, 63(3), 208–218.
- McArthur, E. D., & Stevens, R. (2004). Composite shrubs. In: Monsen SB, Stevens R, Shaw NL, compilers. Restoring western ranges and wildlands. General Technical Report. RMRS-GTR-136. p 493–537.
- METI, & NASA (2009). *Aster Global Digital Elevation Model V002*. (Sioux Falls, South Dakota).
- Mevik, B., -H., Wehrens, R., & Liland, K.H. (2013). pls: Partial least squares and principal component regression. R package version 2.4–3. <http://CRAN.R-project.org/package=pls>
- Mitchell, J.J., Glenn, N.F., Sankey, T.T., Derryberry, D.R., & Germino, M.J. (2012). Remote sensing of sagebrush canopy nitrogen. *Remote Sensing of Environment*, 124, 217–223.
- Montandon, L.M., & Small, E.E. (2008). The impact of soil reflectance on the quantification of the green vegetation fraction from NDVI. *Remote Sensing of Environment*, 112, 1835–1845.
- Mueller-Dombois, D., & Ellenberg, H. (1974). *Aims and methods of vegetation ecology*. New York: Wiley.
- Okin, G.S., Roberts, D.A., Murray, B., & Okin, W.J. (2001). Practical limits on hyperspectral vegetation discrimination in arid and semiarid environments. *Remote Sensing of Environment*, 77, 212–225.
- Pal, M. (2005). Random forest classifier for remote sensing classification. *International Journal of Remote Sensing*, 26(1), 217–222.
- Peña, M.A., Brenning, A., & Sagredo, A. (2012). Constructing satellite-derived hyperspectral indices sensitive to canopy structure variables of a Cordilleran Cypress (*Austrocedrus chilensis*) forest. *ISPRS Journal of Photogrammetry and Remote Sensing*, 74, 1–10.
- Perez-Quezada, J.F., Delpiano, C.A., Snyder, K.A., Johnson, D.A., & Franck, N. (2011). Carbon pools in an arid shrubland in Chile under natural and afforested conditions. *Journal of Arid Environments*, 75, 29–37.
- Powell, S.L., Healey, S.P., Kennedy, R.E., Moisen, G.G., Pierce, K.B., & Ohmann, J.L. (2010). Quantification of live aboveground forest biomass dynamics with Landsat time-series and field inventory data: A comparison of empirical modeling approaches. *Remote Sensing of Environment*, 114, 1053–1068.
- Qi, J., Chehbouni, A., Huete, A.R., Kerr, Y.H., & Sorooshian, S. (1994). A modified soil adjusted vegetation index. *Remote Sensing of Environment*, 48, 119–126.
- R Core Team (2013). *R: A language and environment for statistical computing*. Vienna, Austria: R Foundation for Statistical Computing (<http://www.R-project.org/>).
- Ramoelo, A., Skidmore, A.K., Cho, M.A., Schlerf, M., Mathieu, R., & Heitkönig, I.M.A. (2012). Regional estimation of savanna grass nitrogen using the red-edge band of the spaceborne RapidEye sensor. *International Journal of Applied Earth Observation and Geoinformation*, 19, 151–162.
- RapidEye AG (2009). *RapidEye standard image product specifications*. (Brandenburg an der Havel).
- Ren, H., Zhou, G., & Zhang, X. (2011). Estimation of green aboveground biomass of desert steppe in Inner Mongolia based on red-edge reflectance curve area method. *Biosystems Engineering*, 109(4), 385–395.
- Ren, H., Zhou, G., Zhang, F., & Zhang, X. (2012). Evaluating cellulose absorption index (CAI) for non-photosynthetic biomass estimation in the desert steppe of Inner Mongolia. *Chinese Science Bulletin*, 57(14), 1716–1722.
- Roderick, M.L., Noble, I.R., & Cridland, S.W. (1999). Estimating woody and herbaceous vegetation cover from time series satellite observations. *Global Ecology and Biogeography*, 8(6), 501–508.
- Roleček, J., Chytrý, M., Hájek, M., Lvončík, S., & Tichý, L. (2007). Sampling design in large-scale vegetation studies: Do not sacrifice ecological thinking to statistical purism! *Folia Geobotanica*, 42, 199–208.
- Rondeaux, G., Steven, M., & Baret, F. (1996). Optimization of soil-adjusted vegetation indices. *Remote Sensing of Environment*, 55, 95–107.
- Rouse, J.W., Haas, R.W., Schell, J.A., Deering, D.W., & Harlan, J.C. (1974). *Monitoring the vernal advancement and retrogradation (Greenwave effect) of natural vegetation*. NASA/GSFC, Type III Final Report, Greenbelt, MD, USA.
- Rudnick, J.A., & Gaspari, G.D. (2004). *Elements of the random walk an introduction for advanced students and researchers*. Cambridge; New York: Cambridge University Press (Retrieved from <http://site.ebrary.com/id/10124710>).
- Safriel, U., & Adee, Z. (2005). Dryland systems. In R. Hassan, R. Scholes, & N. Ash (Eds.), *Ecosystems and human well-being: current state and trends, Vol. 1.* (pp. 623–662). Washington, DC: Island Press.

- Sarker, L.R., & Nichol, J.E. (2011). Improved forest biomass estimates using ALOS AVNIR-2 texture indices. *Remote Sensing of Environment*, 115(4), 968–977.
- Shoshany, M. (2000). Satellite remote sensing of natural Mediterranean vegetation: a review within an ecological context. *Progress in Physical Geography*, 24(2), 153–178.
- Shoshany, M. (2012). The rational model of shrubland biomass, pattern and precipitation relationships along semi-arid climatic gradients. *Journal of Arid Environments*, 78, 179–182.
- Shoshany, M., & Karnibad, L. (2011). Mapping shrubland biomass along Mediterranean climatic gradients: The synergy of rainfall-based and NDVI-based models. *International Journal of Remote Sensing*, 32(24), 9497–9508.
- Shoshany, M., & Svoray, T. (2002). Multidate adaptive unmixing and its application to analysis of ecosystem transitions along a climatic gradient. *Remote Sensing of Environment*, 82(1), 5–20.
- Spiekermann, R., Brandt, M., & Samimi, C. (2015). Woody vegetation and land cover changes in the Sahel of Mali (1967–2011). *International Journal of Applied Earth Observation and Geoinformation*, 34, 113–121. <http://dx.doi.org/10.1016/j.jag.2014.08.007>.
- Sternberg, M., & Shoshany, M. (2001). Influence of slope aspect on Mediterranean woody formations: comparison of a semiarid and an arid site in Israel. *Ecological Research*, 16(2), 335–345.
- Strobl, C., Boulesteix, A.-L., Zeileis, A., & Hothorn, T. (2007). Bias in random forest variable importance measures: Illustrations, sources and a solution. *BMC Bioinformatics*, 8, 25. <http://dx.doi.org/10.1186/1471-2105-8-25>.
- Tajik Met Service (2013). *Climatic data for the Pamir Region*.
- Trumper, K., Ravilious, C., & Dickson, B. (2008). Carbon in drylands: desertification, climate change and carbon finance. *A UNEP-UNDP-UNCCD Technical Note for Discussions at CRIS 7, Istanbul, Turkey 03–14 November 2008*.
- UNEP (2012). *Global Environment Outlook 5*. Retrieved from. [http://www.unep.org/geo/pdfs/geo5/GE05\\_report\\_full\\_en.pdf](http://www.unep.org/geo/pdfs/geo5/GE05_report_full_en.pdf)
- USGS (2013). *Landsat 8, Fact Sheet 2013–3060*. Retrieved from. <http://pubs.usgs.gov/fs/2013/3060/pdf/fs2013-3060.pdf>
- Van Der Meer, F., Bakker, W., Scholte, K., Skidmore, A., De Jong, S., Clevers, J., et al. (2001). Spatial scale variations in vegetation indices and above-ground biomass estimates: implications for MERIS. *International Journal of Remote Sensing*, 22(17), 3381–3396.
- Vanselow, K.A. (2011). *The high-mountain pastures of the Eastern Pamirs (Tajikistan): an evaluation of the ecological basis and the pasture potential*. (Erlangen, Nürnberg, Univ., Diss., 2011. Retrieved from <http://d-nb.info/1010705040/>).
- Vanselow, K., & Samimi, C. (2014). Predictive mapping of dwarf shrub vegetation in an arid high mountain ecosystem using remote sensing and random forests. *Remote Sensing*, 6(7), 6709–6726.
- Veraverbeke, S., Gitas, I., Katagis, T., Polychronaki, A., Somers, B., & Goossens, R. (2012). Assessing post-fire vegetation recovery using red–near infrared vegetation indices: Accounting for background and vegetation variability. *ISPRS Journal of Photogrammetry and Remote Sensing*, 68, 28–39.
- Walter, H., & Breckle, S.W. (1986). *Spezielle Ökologie der Gemäßigten und Arktischen Zonen Euro-Nordasiens, Zonobiom VI – IX, volume 3 of Ökologie der Erde*. Stuttgart: Gustav Fischer Verlag.
- Wang, L., Qu, J.J., Hao, X., & Hunt, E.R. (2011). Estimating dry matter content from spectral reflectance for green leaves of different species. *International Journal of Remote Sensing*, 32(22), 7097–7109.
- Xu, L., Li, J., & Brenning, A. (2014). A comparative study of different classification techniques for marine oil spill identification using RADARSAT-1 imagery. *Remote Sensing of Environment*, 141, 14–23.
- Yang, J., Weisberg, P.J., & Bristow, N.A. (2012). Landsat remote sensing approaches for monitoring long-term tree cover dynamics in semi-arid woodlands: Comparison of vegetation indices and spectral mixture analysis. *Remote Sensing of Environment*, 119, 62–71.



# 5 Potential of space-borne hyperspectral data for biomass quantification in an arid environment: advantages and limitations

---

Harald Zandler, Alexander Brenning & Cyrus Samimi

*Remote Sensing* 2015, 7(4), pages 4565-4580



This publication extends the remote sensing approach by testing an experimental hyperspectral sensor for its ability to improve space-borne biomass predictions in the research area. Thereby, it gives an outlook on upcoming earth observation solutions in drylands and contributes to **hypothesis 2**. The layout of the published original is maintained.



## Article

## Potential of Space-Borne Hyperspectral Data for Biomass Quantification in an Arid Environment: Advantages and Limitations

Harald Zandler <sup>1,\*</sup>, Alexander Brenning <sup>2,3</sup> and Cyrus Samimi <sup>1,4</sup>

<sup>1</sup> Department of Geography, University of Bayreuth, Bayreuth 95440, Germany;  
E-Mail: cyrus.samimi@uni-bayreuth.de

<sup>2</sup> Department of Geography, Friedrich Schiller University, Löbdergraben 32, Jena 07743, Germany;  
E-Mail: alexander.brenning@uni-jena.de

<sup>3</sup> Department of Geography and Environmental Management, University of Waterloo, 200 University Avenue West, Waterloo, ON N2L 3G1, Canada

<sup>4</sup> Bayreuth Center of Ecology and Environmental Research, BayCEER, Bayreuth 95440, Germany

\* Author to whom correspondence should be addressed; E-Mail: harald.zandler@uni-bayreuth.de ;  
Tel.: +49-921-554-636.

Academic Editors: George Petropoulos and Prasad S. Thenkabail

*Received: 24 February 2015 / Accepted: 8 April 2015 / Published: 15 April 2015*

---

**Abstract:** In spite of considerable efforts to monitor global vegetation, biomass quantification in drylands is still a major challenge due to low spectral resolution and considerable background effects. Hence, this study examines the potential of the space-borne hyperspectral Hyperion sensor compared to the multispectral Landsat OLI sensor in predicting dwarf shrub biomass in an arid region characterized by challenging conditions for satellite-based analysis: The Eastern Pamirs of Tajikistan. We calculated vegetation indices for all available wavelengths of both sensors, correlated these indices with field-mapped biomass while considering the multiple comparison problem, and assessed the predictive performance of single-variable linear models constructed with data from each of the sensors. Results showed an increased performance of the hyperspectral sensor and the particular suitability of indices capturing the short-wave infrared spectral region in dwarf shrub biomass prediction. Performance was considerably poorer in the area with less vegetation cover. Furthermore, spatial transferability of vegetation indices was not feasible in this region, underlining the importance of repeated model building. This study indicates that upcoming space-borne hyperspectral sensors increase the performance of biomass prediction in the world's arid environments.

**Keywords:** arid environment; hyperspectral vegetation indices; hyperspectral bands; Hyperion; Landsat OLI; biomass; drylands; spatial transferability

---

## 1. Introduction

Remote sensing is an essential tool to study degradation of vegetation and biomass in arid environments [1,2]. However, low vegetation cover and significant background effects make optical satellite analysis challenging in these regions [3,4]. The majority of dryland studies apply multispectral sensors for biomass quantification [3] but more recently, hyperspectral techniques, using hundreds of bands, are considered as a more promising approach [2,5–8]. In arid regions, an important advantage of hyperspectral data is that narrowband and derivative indices of hyperspectral sensors are less susceptible to soil and illumination impacts [5]. Additionally, the high spectral resolution enables the analysis of the vegetation-related red-edge transition which is especially useful for quantification of green vegetation at low cover values [9]. Besides spectral properties of green vegetation, hyperspectral sensors are also able to capture reflective features of other plant tissue, like lignin or cellulose [7,8,10–12], which may be important in detecting vegetation in drylands where significant parts of plants consist of structural non-photosynthetic tissue [8,11]. In contrast to these encouraging factors, other sources conclude that areas with low vegetation cover cannot be reliably analyzed using hyperspectral data [10,13]. Therefore, it is still uncertain if space-borne hyperspectral sensors are able to significantly improve vegetation detection in extremely arid regions, and so assessments of their practical viability in comparison to broadband sensors are required [7].

The application of hyperspectral data with its numerous bands is mostly based on prior knowledge of the optimal spectral regions for a specific research question [7]. In contrast to that, particular wavelengths or indices related to a given variable may not have been tested for vegetation mapping [14], or may vary from one study to another as the spectral signal is dependent on a number of external factors [15]. Consequently, the biggest challenge for remote sensing based studies, especially in arid environments with increased background noise, is the transferability of methods or appropriate spectral indices in time and space [3].

To address these essential issues of applied hyperspectral research against a background of the forthcoming launches of new hyperspectral sensors (e.g., EnMAP), we test the utilization of NASA's Hyperion sensor for dwarf shrub biomass analysis in the Eastern Pamirs of Tajikistan. This area is especially suitable for testing the limits of optical remote sensing satellites as vegetation cover is sparse (dwarf shrub cover < 20%), large parts of local plants consist of non-photosynthetic structural materials and substrate colors are highly variable [4,16]. As multispectral methods proved to be unsuccessful or associated with large uncertainties in the research area [4,17], our main goal is to assess if novel narrowband indices of the hyperspectral Hyperion sensor improve the performance of dwarf shrub biomass detection in this arid environment compared to the commonly used multispectral sensor Landsat OLI. Thereby, spectral regions and indices that are sensitive to dwarf shrub amounts should be identified, taking the issue of false positive tests in multiple comparison studies into account. Furthermore,

transferability of vegetation indices is assessed by comparison of the most important spectral regions for dwarf shrub analysis from scenes of different regions in the study area.

## 2. Materials and Methods

### 2.1. Research Area

The Eastern Pamirs of Tajikistan are a high mountain desert plateau with mean altitudes between 3500 and 5500 meters above sea level (Figure 1). The climate is characterized by low temperatures and scarce amounts of precipitation (Murghab annual mean 1998–2012:  $-1\text{ }^{\circ}\text{C}$ , 94 mm, [18]). These natural conditions allow the development of dense, green grass vegetation only in areas with sufficient water supply (e.g., riparian vegetation in riverbeds, alpine meadows at very high altitudes). All other areas are sparsely covered and dominated by dwarf shrub vegetation adapted to water scarcity (Figure 2, [19]). These dwarf shrubs play a vital role in a region where the main economic activity is animal husbandry, as they serve both as a source of forage and fuel. The energy importance of shrubs is caused by the fact that they are the only local plants that develop woody parts, mainly in the root zone. Extensive harvesting, whereby the whole plant is dug up, has raised concerns regarding sustainable development of the region [19]. Therefore, a comprehensive assessment of the availability of this resource is needed as existing remote sensing approaches are still erroneous [4].

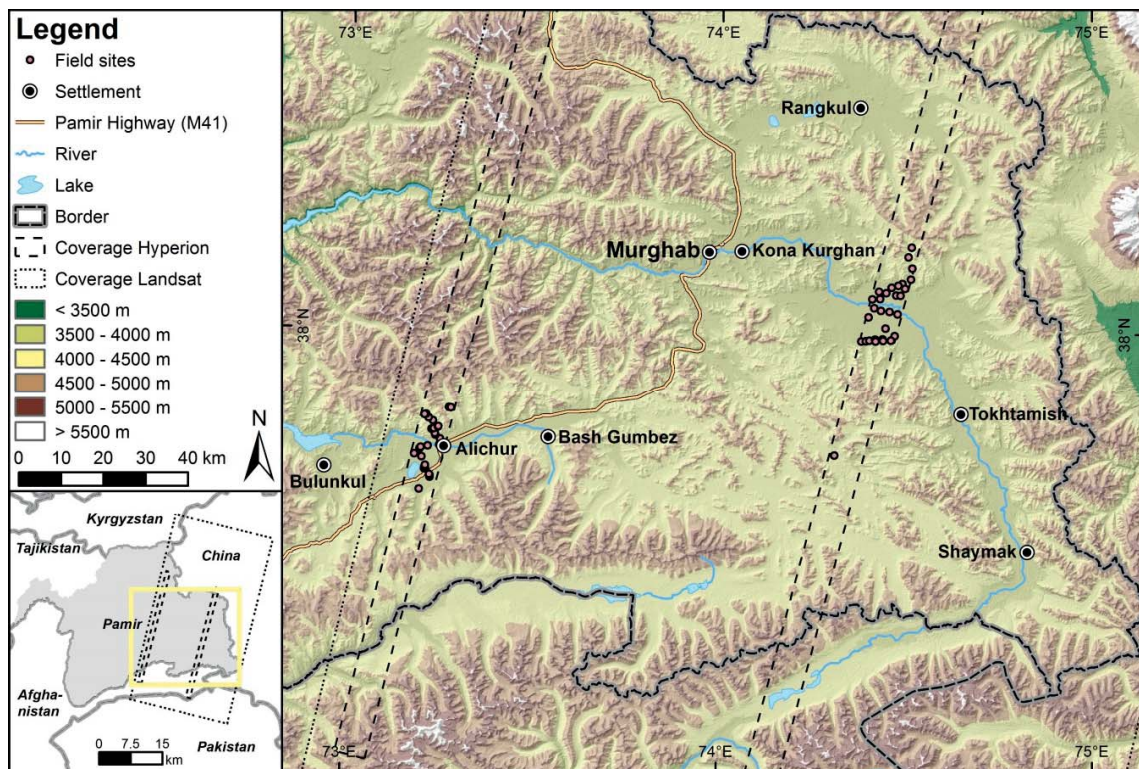


**Figure 1.** Overview of the research area, analyzed satellite images and field sites. The two Hyperion scenes were acquired on 3 August 2012 (western scene) and on 29 July 2013 (eastern scene), the Landsat OLI scene on 28 July 2013 respectively. DEM source: METI & NASA [20].



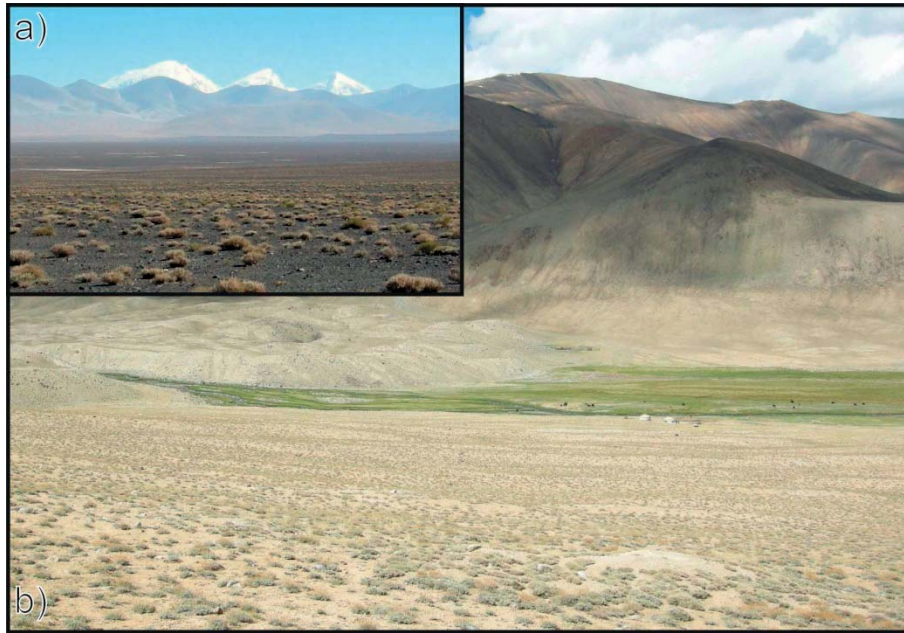


**Figure 2.** Photographs of (a) dwarf shrub stand located within the eastern Hyperion scene taken in fall 2014, and (b) dwarf shrub stand located within the western Hyperion scene with azonal grass vegetation in the background taken in summer 2013.

## 2.2. Data

Selection of satellite images was based on an acquisition date during the peak of the vegetation period to maximize the vegetation related reflectance signal in this arid environment [4].

### 2.2.1. Landsat OLI Data

A multispectral, terrain corrected image (L1T) with  $30\text{ m} \times 30\text{ m}$  spatial resolution was acquired on 28 July 2013 by the operational land imager (OLI) sensor of NASA's Landsat 8 satellite. Visual inspection and comparison to GPS measurements showed that geo-referencing of the image was accurate and no further adjustment was needed. All eight multispectral bands were included in the analysis.

### 2.2.2. Hyperion Data

Two hyperspectral, terrain corrected images (Level 1T) with  $30\text{ m} \times 30\text{ m}$  spatial resolution were acquired on 3 August 2012 (western scene) and 29 July 2013 (eastern scene) by the Hyperion sensor of NASA's Earth Observing 1 Satellite (Figure 1). The sensor spans the spectral range from 356–2577 nm with a bandwidth of  $\sim 10\text{ nm}$  leading to a total of 242 bands. Exclusion of bad bands (not calibrated, redundant, noise from atmospheric water vapor, low signal to noise ratio) left 158 bands for the analysis (*cf.* [21]). These are bands 8–57 (427–925 nm), 79–119 (933–1336 nm), 133–164 (1477–1790 nm), 183–184 (1982–1992 nm) and 188–220 (2032–2355 nm). Despite automatic terrain correction of Hyperion images, a spatial error was present in the data. This error was corrected by matching the image pixels with a nearest neighbor resampling algorithm to respective Landsat pixels using a second-order polynomial model with 19 control points (3 August 2012  $\text{RMSE}_{XY}$ : 3.37 m, 29 July 2013  $\text{RMSE}_{XY}$ : 5.02 m). The images were

not corrected for other effects such as spectral smile or striping as no generally accepted procedure exists as well as to preserve the original spectral characteristics [22].

### 2.2.3. Atmospheric Correction

All images were recalculated to at-sensor radiance with subsequent atmospheric correction using ENVI's state-of-the-art MODTRAN®-based FLAASH® approach. Aqua AIRS Level 3 Daily Standard Physical Retrieval product [23] provided information of daily atmospheric water vapor amounts for each scene to select the appropriate FLAASH® atmosphere.

### 2.2.4. Field Data

Sixty dwarf shrub stands (30 field sites in each Hyperion image) with homogenous vegetation cover and a minimum area of 60 m × 60 m were mapped in summer 2013 and fall 2014 with a handheld GPS device (horizontal RMSE ~5 m) using a study design similar to Zandler *et al.* [4]. Areas were selected preferentially to achieve the following objectives: (i) minimum size requirements [24]; (ii) mapping of a broad range of dwarf shrub densities; (iii) homogenous spectral properties and to take accessibility of field sites into account (*cf.* [4]). Furthermore, field sites were placed so that steep terrain is avoided to prevent potential spatial errors due to inaccurate terrain correction in Hyperion data. Within the stands, two subplots with 4 m side length were placed randomly and circumferences of all dwarf shrub individuals were measured inside the subplots. These measurements were used to calculate dwarf shrub total biomass using an allometric model developed specifically for the research area and the analyzed dwarf shrub species [4]. Results were averaged to represent the mean dwarf shrub biomass in kg·ha<sup>-1</sup> of the stands. The midpoint between the subplots was taken as reference pixel to extract spectral information for each stand. A descriptive comparison of site biomass amounts shows that the western Hyperion scene is characterized by higher biomass amounts compared to the eastern scene (Figure 3).

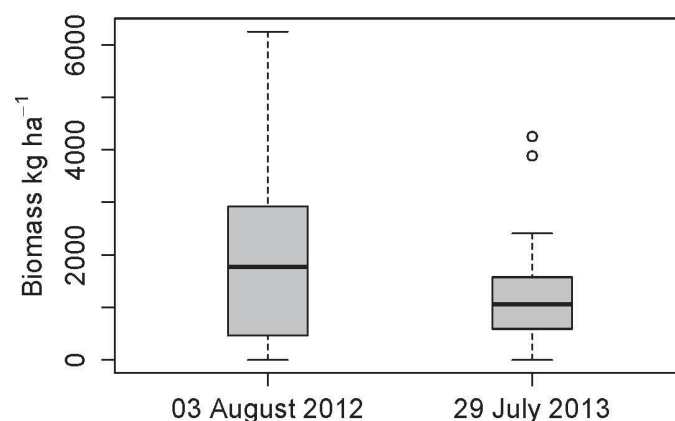


**Figure 3.** Boxplots showing dwarf shrub biomass amounts of sites located in Hyperion scenes of August 2012 and July 2013, respectively. Each scene contains 30 field sites.

### 2.3. Spectral Index Computation and Statistical Analysis

Previous studies show that several spectral regions may be important in detecting different plant materials [7,25]. The most prominent is the red-infrared transition to analyze green vegetation [26] but many other spectral regions related to non-green, structural plant parts are mentioned as well [9,10,13,14,25,27–30]. For multispectral data, a very large number of vegetation indices potentially useful in detecting various plant tissues are available, but in the research area, most commonly used indices were shown to be unsuitable for biomass prediction [4]. Furthermore, existing hyperspectral indices designed to detect features of non-photosynthetic vegetation, may be inapplicable at low cover values on various soils [29]. Therefore, since there is no prior knowledge of hyperspectral indices that may be particularly suitable for biomass detection in the research area and to fully exploit the potential of the numerous Hyperion bands, all possible unique normalized difference indices (NDIs) were computed according to the formula:

$$NDI_{a,b,c} = \frac{Ra_c - Rb_c}{Ra_c + Rb_c} \quad (1)$$

where  $R$  is reflectance, arranged in a descending order (2355–427 nm);  $a$  is the first wavelength and  $b$  is the reference wavelengths for field site  $c$ . This resulted in a total of 12,403 NDIs using Hyperion bands and 28 NDIs using Landsat OLI bands, respectively. These NDIs were grouped in four feature sets according to appearance of field sites in the two Hyperion scenes and based on the applied sensor: Western field sites ( $n = 30$ ) within the Hyperion scene from 3 August 2012 (H2012), same field sites with Landsat data (LS2013a), eastern field sites ( $n = 30$ ) within Hyperion scene from 29 July 2013 (H2013) and same field sites with Landsat data (LS2013b).

The features were paired in the correlation analysis with mean biomass of field sites as the response variable. Pearson's correlation coefficient  $R$  was preferred based on preliminary studies showing a linear relationship of biomass and vegetation indices in the research area as well as visual inspection of a part of the present data [4]. Hypothesis testing to reject the null hypothesis of zero correlation results in a multiple testing problem. For instance, performing 10,000 independent hypothesis tests at the 5% level of significance would be expected to yield 500 false rejections if all null hypotheses are true. To address this problem, the Benjamini-Hochberg procedure [31], successfully applied by Peña *et al.* [21] in a comparable study, was used to control the false discovery rate (FDR) at a level of <5% and to compute adjusted  $p$ -value thresholds for each feature set.

Graphical displays were created for visual identification and comparison of spectral regions that are sensitive to dwarf shrub biomass amounts. Denomination of spectral regions follows Thenkabail *et al.* [12].

Similar to the multiple testing problem, the highest correlation coefficients obtained in a large family of correlations is not indicative of the predictive performance achieved in a situation where optimal indices are not known in advance and optimal index selection is therefore part of the data analysis process. To assess the performance of different sensors and feature sets in this situation and account for the high dimensionality of the data, we therefore used linear regression models built with a single stepwise forward variable selection step using Pearson's correlation as the selection criterion. Larger models were not considered due to the small sample size. Predictive performances obtained for different feature sets and study areas were estimated using 100-repeated, 10-fold cross-validation. In this



estimation method, the data set is randomly subdivided into 10 disjointed subsets or partitions. One partition at a time is used as the test set and the other 90% of the data as the training set in building a linear regression using the stepwise method. This procedure is repeated for each of the partitions and for 100 independent partitionings in total.

To evaluate feature sets, absolute root mean square error (RMSE), relative RMSE (RMSE<sub>rel</sub>) and BIAS were calculated as:

$$\text{RMSE} = \sqrt{\frac{\sum_{i=1}^n (Y_i - \widehat{Y}_i)^2}{n}} \quad (2)$$

$$\text{RMSE}_{\text{rel}} = \frac{\text{RMSE}}{\bar{Y}} \times 100\% \quad (3)$$

$$\text{BIAS} = \frac{1}{n} \sum_{i=1}^n \widehat{Y}_i - Y_i \quad (4)$$

where  $Y_i$  is the measured and  $\widehat{Y}_i$  the predicted value of case  $i$ ,  $\bar{Y}$  is the observed mean value and  $n$  is the number of observations. Mean and standard deviation of these error measures over 100 cross-validation repetitions are reported.

### 3. Results

#### 3.1. Visual Comparison of Biomass-Index Correlations

A broad range of spectral indices were significantly correlated with dwarf shrub biomass in both hyperspectral images (Figure 4). Comparison of feature sets showed substantial differences in correlation for indices calculated from green to far near infrared (FNIR) regions (500–1350 nm), where indices of H2012 resulted in a number of significant correlations in contrast to H2013 with almost no significant correlations in this spectral region. Indices derived from spectral bands in the early short-wave infrared (ESWIR, 1450–1800 nm) regions were more consistent as both H2012 and H2013 showed numerous strongly significant correlations in this domain. The closest match of results of the two feature sets was in the far short-wave infrared region (FSWIR), whereby strongest correlations of dwarf shrub biomass exist with indices of wavelengths 1950–2300 nm and associated reference wavelengths from 700 to 1800 nm.

A comparison of hyperspectral feature sets with multispectral feature sets and the same field sites showed similar correlations at related wavelengths. However, correlation coefficients of the hyperspectral feature sets were higher in most cases. Large differences were visible between the eastern multispectral feature set (LS2013b) with higher correlations in the ESWIR and FSWIR in contrast to the western multispectral feature set (LS2013a) with higher correlations in the green to near infrared (NIR) spectral regions.

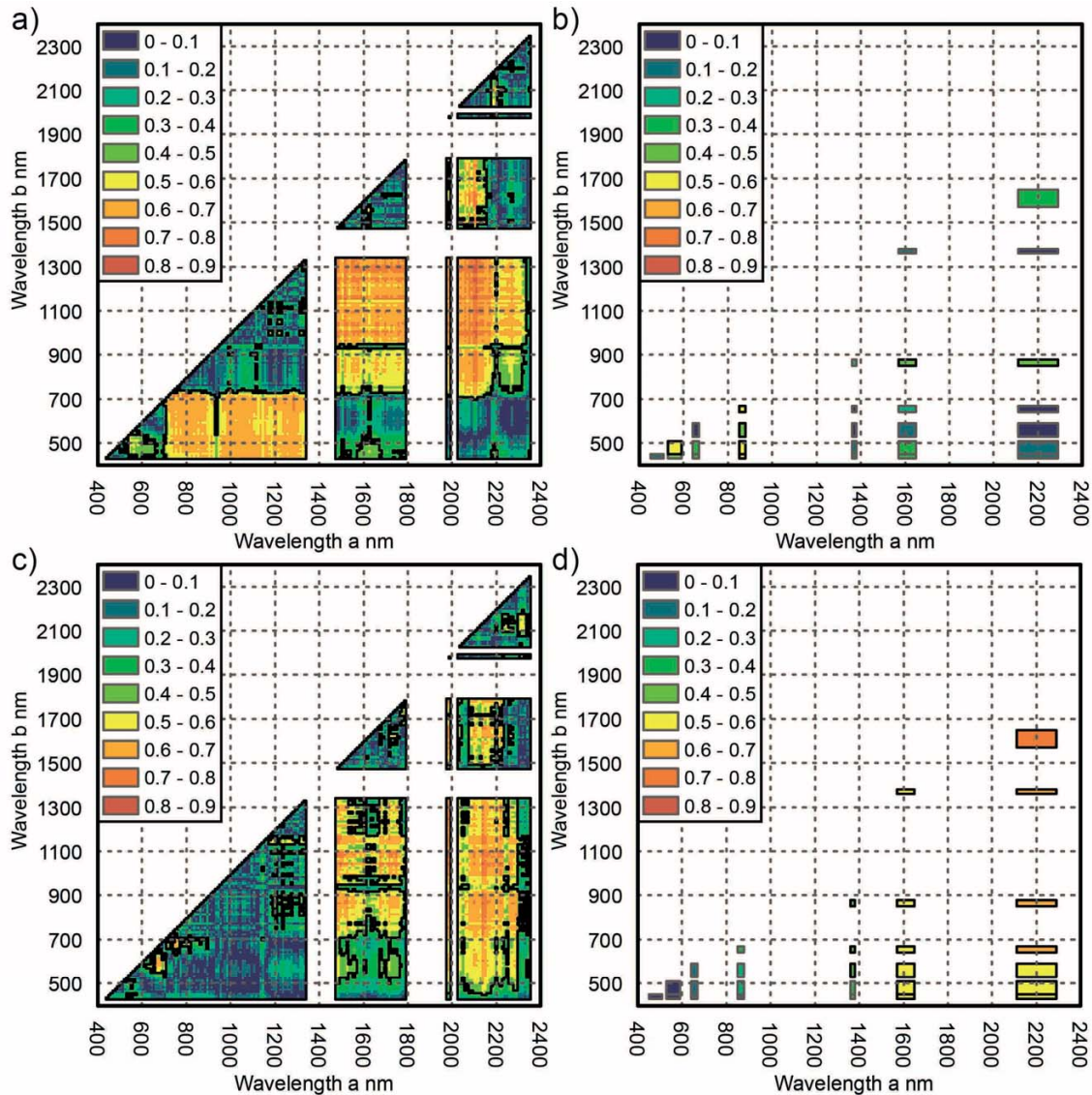


**Figure 4.** Absolute values of Pearson's correlation coefficients  $R$  of biomass with indices from field sites of feature sets (a) H2012, (b) LS2013a, (c) H2013, and (d) LS2013b. Black lines mark significant values controlled at a FDR < 5%.

### 3.2. Modeling Performance of Feature Sets

The western hyperspectral feature set (H2012) performed best in predicting dwarf shrub biomass according to the cross-validated modeling results with an RMSE of  $1121 \text{ kg}\cdot\text{ha}^{-1}$ , a RMSE<sub>rel</sub> of 58% and an  $R^2$  of 0.54 averaged over all repetitions (Table 1). The associated multispectral feature set (LS2013a) showed a higher RMSE of  $1528 \text{ kg}\cdot\text{ha}^{-1}$  (RMSE<sub>rel</sub> 78%) and lower  $R^2$  of 0.15. Both models showed a relatively small bias. Eastern feature sets generally showed poor modeling performance ranging from RMSE values of  $937\text{--}973 \text{ kg}\cdot\text{ha}^{-1}$  (77%–80% RMSE<sub>rel</sub>) whereby the hyperspectral feature set (H2013) produced slightly lower values and higher  $R^2$ . Furthermore, model bias was higher for the eastern feature sets.

**Table 1.** Cross validated modeling performance of the different feature sets averaged over all repetitions.

|                                     | Modeled Mean RMSE<br>(kg·ha <sup>-1</sup> ) | Modeled Mean R <sup>2</sup> | Modeled Mean Bias (kg·ha <sup>-1</sup> ) | Modeled Mean RMSErel (%) |
|-------------------------------------|---|-----------------------------|--|--------------------------|
| Hyperion western sites (H2012)      | 1121  | 0.54                        | -23                                      | 58                       |
| Hyperion eastern sites (H2013)      | 937   | 0.29                        | 69                                       | 77                       |
| Landsat OLI western sites (LS2013a) | 1528  | 0.15                        | 11                                       | 78                       |
| Landsat OLI eastern sites (LS2013b) | 973   | 0.16                        | 53                                       | 80                       |

3.3. Variable Selection Frequency of Indices

Stepwise variable selection averaged over all folds and repetitions showed a considerably increased occurrence of the best performing NDI compared to other relevant indices over all feature sets (Figure 5). The best NDIs of the hyperspectral feature sets showed a strong concentration of FSWIR bands with reference wavelengths mostly from the FNIR to the ESWIR. Red–infrared and red edge indices were chosen rarely. The three most commonly selected NDIs of the western hyperspectral feature set H2012 all consisted of bands around 2100 nm with reference bands in the FNIR, whereas the eastern feature set H2013 showed higher diversification with bands from 1980–2140 nm and reference bands in the NIR. Little conformity was visible between hyperspectral and multispectral feature sets. A comparison of the multispectral feature sets showed large differences with an emphasis of the western feature set (LS2013a) on the red to infrared region, specifically the index calculated from wavelengths centered at 865 nm and 655 nm which is identical to the commonly known Normalized Difference Vegetation index (NDVI), in contrast to the most frequently selected NDI of the eastern feature set (LS2013b), which is composed of FSWIR and FNIR bands.

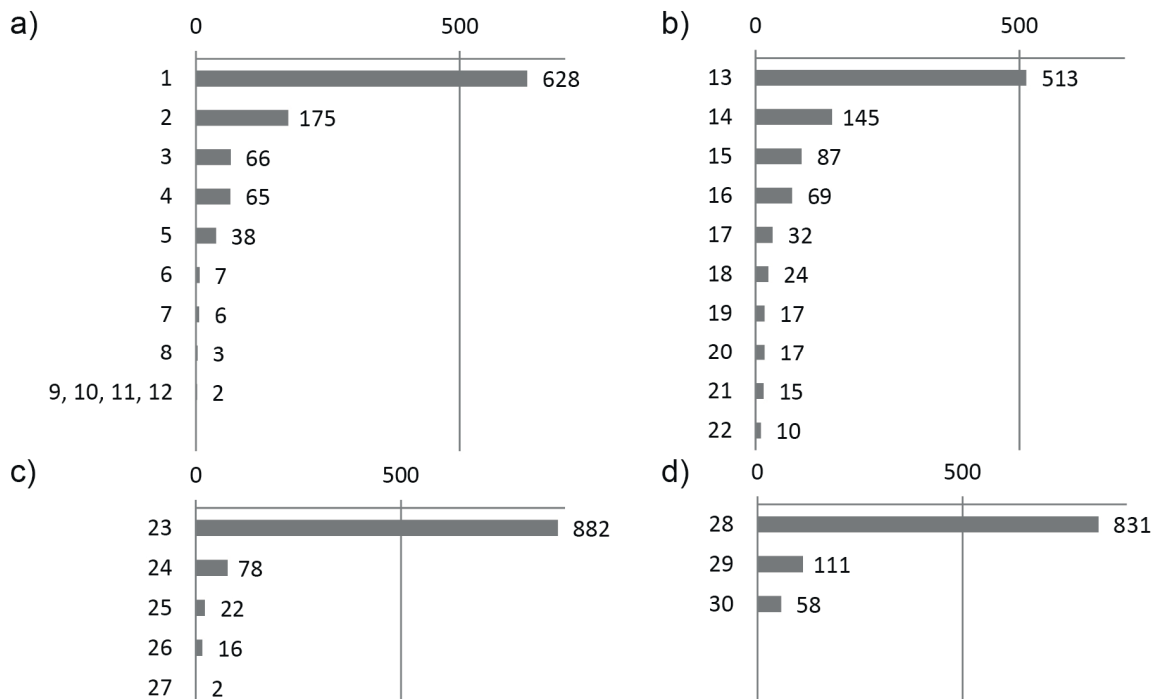


Figure 5. Cont.

| Number | Index composition       | Feature set | Number | Index composition       | Feature set |
|--------|-------------------------|-------------|--------|-------------------------|-------------|
| 1      | (2113-1003)/(2113+1003) | H2012       | 16     | (2224-1043)/(2224+1043) | H2013       |
| 2      | (2113-1295)/(2113+1295) | H2012       | 17     | (1497-1083)/(1497+1083) | H2013       |
| 3      | (2102-1336)/(2102+1336) | H2012       | 18     | (1981-1780)/(1981+1780) | H2013       |
| 4      | (2113-1336)/(2113+1336) | H2012       | 19     | (2143-874)/(2143+874)   | H2013       |
| 5      | (2113-1154)/(2113+1154) | H2012       | 20     | (681-599)/(681+599)     | H2013       |
| 6      | (2102-1285)/(2102+1285) | H2012       | 21     | (1981-1659)/(1981+1659) | H2013       |
| 7      | (2082-1507)/(2082+1507) | H2012       | 22     | (2143-1659)/(2143+1659) | H2013       |
| 8      | (2102-1305)/(2102+1305) | H2012       | 23     | (865-655)/(865+655)     | LS2013a     |
| 9      | (1689-1154)/(1689+1154) | H2012       | 24     | (561-483)/(561+483)     | LS2013a     |
| 10     | (1578-1295)/(1578+1295) | H2012       | 25     | (2201-865)/(2201+865)   | LS2013a     |
| 11     | (782-721)/(782-721)     | H2012       | 26     | (865-483)/(865+483)     | LS2013a     |
| 12     | (762-711)/(762-711)     | H2012       | 27     | (2201-1609)/(2201+1609) | LS2013a     |
| 13     | (1981-1043)/(1981+1043) | H2013       | 28     | (2201-1373)/(2201+1373) | LS2013b     |
| 14     | (2143-1043)/(2143+1043) | H2013       | 29     | (2201-865)/(2201-865)   | LS2013b     |
| 15     | (1497-1043)/(1497+1043) | H2013       | 30     | (655-561)/(655+561)     | LS2013b     |

**Figure 5.** Occurrence of the 10 most frequently chosen NDIs according to stepwise variable selection from all folds and repetitions (1000 selections) with feature sets (a) H2012, (b) H2012, (c) LS2013a and (d) LS2013b.

## 4. Discussion

### 4.1. Hyperspectral Indices for Dwarf Shrub Biomass Detection

This is the first study that addresses the sensitivity of hyperspectral narrow bands in the 400–2400 nm domain to dwarf shrub biomass in the research area, and to our knowledge, the first to analyze space-borne hyperspectral biomass detection in regions with cover values well below 20%. We showed that, even under these arid conditions, a great number of hyperspectral indices significantly correlate with dwarf shrub biomass quantities. Thereby, the green to NIR regions, which are commonly used for quantification of green cover, biomass, chlorophyll or leaf area index [7–9,12], were only partly correlated with biomass and did not constitute the indices with strongest correlations with the hyperspectral feature sets. Although the approximate red edge (700–780 nm), which is stressed as an important spectral region at low cover values in other studies [3,9,32], did show significant correlations with biomass amounts, it was not among the highest correlating hyperspectral indices.

However, high correlations commonly occurred in the ESWIR and FSWIR regions with both hyperspectral feature sets. These spectral domains are frequently mentioned as indicative of cellulose, lignin, wood or shrub material [7,8,10,13,25,27–30,33–37] and are therefore important for the detection of structural tissue. Especially the bands around 2020–2220 nm are considered as important for cellulose or lignin detection using remote sensing data [13,29,30,36,37] as they are distinctive from soil minerals and less affected by atmospheric gasses [37]. These results agree with the observed index selection frequencies where the three most important NDIs of H2012 consisted of bands with wavelength centers at 2113 nm or 2102 nm, and the second most important NDI of H2013 consisted of the band centered at 2143 nm. In previous studies, these bands were used for index computation to map crop residues with different reference wavelengths in the FSWIR [29,34,37]. The best performing NDI of H2013 utilized the wavelength centered at 1981 nm, a wavelength which may be sensitive to lignin, nitrogen [10,25] or plant residues [38]. Similarly, Oldeland *et al.* [11] state an importance of the SWIR spectral region for



dry-matter analysis in an African savanna. Therefore, hyperspectral narrow-band NDIs, capturing spectral features of plant residues, lignin and cellulose, may also be instrumental in predicting dwarf shrub biomass in arid environments, as major parts of these plants consist of dry, non-green plant materials [4].

These results indicate that indices especially designed to separately capture the reflectance signal of cellulose in senescent vegetation, are suitable for biomass modeling in arid environments as well. However, correlation analysis of established indices for mapping senescent vegetation, like the Cellulose Absorption Index (CAI) or the Shortwave Infrared Normalized Difference Residue Index (SINDRI) as given in Serbin *et al.* [34], result only in weak significant correlations with CAI (Pearson's correlation coefficients  $R$  0.49 with H2012 and 0.47 with H2013) and no significant correlation of SINDRI with total biomass in our study. Similarly, the Normalized Difference Tillage Index (NDTI), whose equivalent showed a higher correlation only partly in our study (LS2013b), was not among the most important vegetation indices in modeling dwarf shrub biomass in previous research [4]. The reason for the higher correlations at the stated wavelengths may therefore not be a result of cellulose and lignin exclusively. Besides influence of aforementioned tissue, another reason for the importance of the ESWIR and FSWIR may be that green and woody parts of shrubs result in a strong contrast to the soil and so may have a strong influence in this spectral domain [13]. Additional research, incorporating field measured spectra of different plant materials, soils and various matter combined [13], could enhance knowledge on the nature of biomass reflectance properties and main influencing factors. However, regardless of the exact mechanisms and relative contributions of photosynthetic and non-photosynthetic tissue that may be the subject of additional research, the ESWIR and FSWIR spectral regions are more suitable for biomass detection compared to traditional red-infrared NDIs in our study and may supply important additional information in remote sensing based vegetation modeling in drylands.

#### 4.2. Transferability of Spectral Indices Sensitive to Dwarf Shrub Biomass

An important objective of this study was the validity of spectral regions and indices to predict dwarf shrub biomass throughout different areas of the research area. While there was some agreement between the hyperspectral feature sets in the FSWIR, spectral regions of many NDIs that correlated strongly with dwarf shrub biomass and frequency of index selection differed noticeably between the feature sets. Therefore, a spatial generalization of specific narrow-band NDIs is difficult in this environment and individual model development is necessary. This is different to Thenkabail *et al.* [7], who report good agreement in optimal hyperspectral wavebands compared to other studies, but is in agreement with results obtained by Entcheva-Campbell *et al.* [22], who state that best performing hyperspectral NDIs for predicting ecosystem properties varied across sites. One reason for this lack in transferability of specific wavelengths may be the influence of non-constant factors that cannot fully be accounted for in correction algorithms [21]. Another reason may be a low signal-to-noise ratio characteristic of many Hyperion bands (*cf.* [27,32]) and apparent striping in the images. However, the broader 2100 nm region seems approximately transferable across hyperspectral sensors in this study, which is encouraging for future studies and indicates that an avoidance of indices based on too narrow bands may improve regional vegetation analysis [7].

The comparison of correlations and index selection frequencies of multispectral feature sets revealed a poor agreement in NDIs even though all field sites were situated in the same scene. An important reason may be the sensitivity of common broadband vegetation indices to background effects [39], like soil color, which emphasizes the importance of correction algorithms to account for these issues [4]. For example, NDVI values are especially sensitive to external interference at low vegetation cover values [40]. This may explain the importance of NDVI in the western data set with denser vegetation compared to its insignificance in the eastern data set with lower dwarf shrub cover. Another reason may be the diverse soil color prevalent in both feature sets, which is increasingly black in the eastern scene compared to a bright, brown-beige background in the western scene (Figure 2). In summary, the spatial transferability of spectral NDIs is challenging in the research area and this issue has to be considered in hyperspectral biomass modeling in drylands. These findings show that repeated variable assessment and model building is necessary in different regions and reveal the importance of knowledge discovery algorithms for advanced analysis procedures to handle huge hyperspectral datasets. However, the conformity of significant correlations comparing hyperspectral to multispectral feature sets with the same field sites suggests a high agreement at similar wavelengths between both sensors (*cf.* [41]).

#### 4.3. Modeling Performance of Sensors

The hyperspectral Hyperion sensor showed increased performance in dwarf shrub biomass modeling compared to the Landsat OLI sensor. This has been previously shown by results obtained in different regions and from varying plant species [7,12,33,42] and suggests a large potential of hyperspectral sensors for vegetation analysis in arid environments as well. Furthermore, these results indicate that biomass quantification is possible even under the challenging conditions (noisy data, spectral variability) of applied, space-borne hyperspectral remote sensing in drylands within certain limits. This study supports the findings of Okin *et al.* [15], who showed that hyperspectral vegetation cover quantification in an arid region is possible under a best case scenario with a minimization of disturbing factors. However, in the eastern scene, which is characterized by lower biomass values, the performance of the hyperspectral sensor was only slightly better than the multispectral sensor. This demonstrates the limitations of hyperspectral-based vegetation analysis when cover values fall below a certain threshold. This is similar to results of Asner and Heidebrecht [32], who assert that accurate Hyperion-based vegetation quantification is only possible with denser vegetation. Finally, although the hyperspectral sensor outperformed the multispectral sensor in this study, results of biomass prediction are connected to major uncertainties and errors as well, which can be ascribed to the natural conditions of arid environments [15]. Nevertheless, extended modeling approaches, incorporating additional variables like topography [43], texture [44], soil and color-adjusted vegetation indices [40] as shown by Zandler *et al.* [4], using operational, widely available, space-borne hyperspectral data, can significantly reduce such errors in future applications. Furthermore, future research approaches may include variables particularly sensitive to photosynthetic vegetation, non-photosynthetic vegetation or both, in a multi variable-model after analyzing their relative contribution to the mixed biomass signal. Therefore, as is also expected by Asner and Green [2], this study suggests great potential for the upcoming products of new sensors like EnMAP or HypsIRI for future remote sensing based research of the world's drylands.

## 5. Conclusions

This study showed that hyperspectral Hyperion data provides increased performance in predicting biomass in an arid environment compared to the multispectral sensor Landsat OLI. The reason is based on the higher spectral resolution, especially in the FSWIR, as highest correlations and best performing indices are situated in this region with the hyperspectral feature sets, whereby spectral regions intersecting with multispectral bands show similar correlations. The results indicate that sensors capturing spectral features of both green and woody material, which may be most distinctive in the FSWIR, are more suitable for biomass quantification in drylands that are characterized by plants consisting of non-photosynthetic parts to a large extent. Our research also revealed that spatial transferability of specific spectral indices is limited or not feasible, owing to the strong influence of background effects, underlining the importance of repeated model building and variable exploration in areas with different environmental conditions. Finally, substantial modeling errors were still present in all hyperspectral feature sets, which demonstrates the limitations of remote sensing based approaches and emphasizes the need for additional variables, such as texture or topography, for vegetation quantification in arid environments. However, the partly considerable modeling improvement with the hyperspectral sensor compared to the modern multispectral sensor in this arid setting indicates that upcoming, space-borne, operational hyperspectral sensors may enhance satellite-based vegetation analysis in drylands in the near future.

## Acknowledgments

This research was enabled by the Volkswagen Foundation funding the research project Pamir II (awarded to Cyrus Samimi) which is highly appreciated. We would also like to thank NASA and USGS for providing satellite images free of charge. Finally, the authors thank three anonymous reviewers for their constructive comments to improve the article. This publication was funded by the University of Bayreuth in the funding programme Open Access Publishing.

## Author Contributions

Harald Zandler and Alexander Brenning derived the applied methods presented in the paper and wrote the manuscript. Alexander Brenning performed statistical scripting. Harald Zandler was responsible for data collection, data processing and method application. Alexander Brenning and Cyrus Samimi revised the methods, analysis and manuscript.

## Conflicts of Interest

The authors declare no conflict of interest.

## References

1. Sommer, S.; Zucca, C.; Grainger, A.; Cherlet, M.; Zougmore, R.; Sokona, Y.; Hill, J.; Della Peruta, R.; Roehrig, J.; Wang, G. Application of indicator systems for monitoring and assessment of desertification from national to global scales. *Land Degrad. Dev.* **2011**, *22*, 184–197.

2. Asner, G.P.; Green, R. Imaging spectroscopy measures desertification in United States and Argentina. *Eos Trans. AGU* **2001**, *82*, 601–606.
3. Eisfelder, C.; Kuenzer, C.; Dech, S. Derivation of biomass information for semi-arid areas using remote-sensing data. *Int. J. Remote Sens.* **2012**, *33*, 2937–2984.
4. Zandler, H.; Brenning, A.; Samimi, C. Quantifying dwarf shrub biomass in an arid environment: Comparing empirical methods in a high dimensional setting. *Remote Sens. Environ.* **2015**, *158*, 140–155.
5. Swatantran, A.; Dubayah, R.; Roberts, D.; Hofton, M.; Blair, J.B. Mapping biomass and stress in the Sierra Nevada using lidar and hyperspectral data fusion. *Remote Sens. Environ.* **2011**, *115*, 2917–2930.
6. Schwieder, M.; Leitão, P.; Suess, S.; Senf, C.; Hostert, P. Estimating fractional shrub cover using simulated EnMAP data: A comparison of three machine learning regression techniques. *Remote Sens.* **2014**, *6*, 3427–3445.
7. Thenkabail, P.S.; Enclona, E.A.; Ashton, M.S.; van der Meer, B. Accuracy assessments of hyperspectral waveband performance for vegetation analysis applications. *Remote Sens. Environ.* **2004**, *91*, 354–376.
8. Lewis, M.; Jooste, V.; de Gasparis, A.A. Discrimination of arid vegetation with airborne multispectral scanner hyperspectral imagery. *IEEE Trans. Geosci. Remote Sens.* **2001**, *39*, 1471–1479.
9. Elvidge, C.D.; Chen, Z.; Groeneveld, D.P. Detection of trace quantities of green vegetation in 1990 AVIRIS data. *Remote Sens. Environ.* **1993**, *44*, 271–279.
10. Serrano, L.; Penuelas, J.; Ustin, S.L. Remote sensing of nitrogen and lignin in Mediterranean vegetation from AVIRIS data: Decomposing biochemical from structural signals. *Remote Sens. Environ.* **2002**, *81*, 355–364.
11. Oldeland, J.; Dorigo, W.; Wesuls, D.; Jürgens, N. Mapping bush encroaching species by seasonal differences in hyperspectral imagery. *Remote Sens.* **2010**, *2*, 1416–1438.
12. Thenkabail, P.S.; Mariotto, I.; Gumma, M.K.; Middleton, E.M.; Landis, D.R.; Huemmerich, K.F. Selection of hyperspectral narrowbands (HNBS) and composition of hyperspectral twoband vegetation indices (HVIs) for biophysical characterization and discrimination of crop types using field reflectance and Hyperion/EO-1 data. *IEEE J. Sel. Top. Appl. Earth Obs. Remote Sens.* **2013**, *6*, 427–439.
13. Asner, G.P.; Wessman, C.A.; Bateson, C.; Privette, J.L. Impact of tissue, canopy, and landscape factors on the hyperspectral reflectance variability of arid ecosystems. *Remote Sens. Environ.* **2000**, *74*, 69–84.
14. Oldeland, J.; Dorigo, W.; Lieckfeld, L.; Lucieer, A.; Jürgens, N. Combining vegetation indices, constrained ordination and fuzzy classification for mapping semi-natural vegetation units from hyperspectral imagery. *Remote Sens. Environ.* **2010**, *114*, 1155–1166.
15. Okin, G.S.; Roberts, D.A.; Murray, B.; Okin, W.J. Practical limits on hyperspectral vegetation discrimination in arid and semiarid environments. *Remote Sens. Environ.* **2001**, *77*, 212–225.
16. Vanselow, K.A. The High-Mountain Pastures of the Eastern Pamirs (Tajikistan): An Evaluation of the Ecological Basis and the Pasture Potential. Ph.D. Thesis, Friedrich Alexander University, Erlangen-Nuremberg, Germany, 2011.



17. Vanselow, K.; Samimi, C. Predictive mapping of dwarf shrub vegetation in an arid high mountain ecosystem using remote sensing and random forests. *Remote Sens.* **2014**, *6*, 6709–6726.
18. Tajik Met Service, Dushanbe, Tajikistan. Climatic data for the Pamir Region, 2013.
19. Kraudzun, T.; Vanselow, K.A.; Samimi, C. Realities and myths of the Teresken Syndrome—An evaluation of the exploitation of dwarf shrub resources in the Eastern Pamirs of Tajikistan. *J. Environ. Manage.* **2014**, *132*, 49–59.
20. *Aster Global Digital Elevation Model*, version V002; NASA LP DAAC/U.S. Geological Survey: Sioux Falls, SD, USA, 2009.
21. Peña, M.A.; Brenning, A.; Sagredo, A. Constructing satellite-derived hyperspectral indices sensitive to canopy structure variables of a *Cordilleran Cypress* (*Austrocedrus chilensis*) forest. *ISPRS J. Photogramm. Remote Sens.* **2012**, *74*, 1–10.
22. Campbell, P.K.E.; Middleton, E.M.; Thome, K.J.; Kokaly, R.F.; Huemmrich, K.F.; Lagomasino, D.; Novick, K.A.; Brunsell, N.A. EO-1 Hyperion reflectance time series at calibration and validation sites: Stability and sensitivity to seasonal dynamics. *IEEE J. Sel. Top. Appl. Earth Obs. Remote Sens.* **2013**, *6*, 276–290.
23. *Aqua AIRS Level 3 Daily Standard Physical Retrieval (AIRS+AMSU)*, version 006; NASA Goddard Earth Science Data and Information Services Center (GES DISC): Greenbelt, MD, USA, 2013.
24. Justice, C.O.; Townshend, J.G. Integrating ground data with remote sensing. In *Terrain Analysis and Remote Sensing*; Townshend, J.G., Ed.; Allen and Unwin: London, UK, 1981; pp. 38–58.
25. Fourty, T.; Baret, F.; Jacquemoud, S.; Schmuck, G.; Verdebout, J. Leaf optical properties with explicit description of its biochemical composition: Direct and inverse problems. *Remote Sens. Environ.* **1996**, *56*, 104–117.
26. Chen, Z.; Elvidge, C.D.; Groeneveld, D.P. Monitoring seasonal dynamics of arid land vegetation using AVIRIS data. *Remote Sens. Environ.* **1998**, *65*, 255–266.
27. Martin, M.E.; Aber, J.D. High spectral resolution remote sensing of forest canopy lignin, nitrogen, and ecosystem processes. *Ecol. Appl.* **1997**, *7*, 431–443.
28. Takahashi, T.; Yasuoka, Y.; Fujii, T. Hyperspectral remote sensing of riparian vegetation and leaf chemistry contents. In Proceedings of 23rd Asian Conference on Remote Sensing, Kathmandu, Nepal, 25–29 November 2002.
29. Nagler, P.L.; Inoue, Y.; Glenn, E.; Russ, A.; Daughtry, C.S. Cellulose absorption index (CAI) to quantify mixed soil–plant litter scenes. *Remote Sens. Environ.* **2003**, *87*, 310–325.
30. Daughtry, C.S. Discriminating crop residues from soil by shortwave infrared reflectance. *Agron. J.* **2001**, *93*, 125–131.
31. Benjamini, Y.; Hochberg, Y. Controlling the false discovery rate: A practical and powerful approach to multiple testing. *J. R. Stat. Soc. Ser. B Methodol.* **1995**, *57*, 289–300.
32. Asner, G.P.; Heidebrecht, K.B. Imaging spectroscopy for desertification studies: Comparing AVIRIS and EO-1 Hyperion in Argentina drylands. *IEEE Trans. Geosci. Remote Sens.* **2003**, *41*, 1283–1296.
33. Thenkabail, P.S.; Enclona, E.A.; Ashton, M.S.; Legg, C.; De Dieu, M.J. Hyperion, IKONOS, ALI, and ETM+ sensors in the study of African rainforests. *Remote Sens. Environ.* **2004**, *90*, 23–43.
34. Serbin, G.; Hunt E.R., Jr.; Daughtry, C.S.T.; McCarty, G.W.; Doraiswamy, P.C. An improved ASTER index for remote sensing of crop residue. *Remote Sens.* **2009**, *1*, 971–991.

35. Elvidge, C.D. Visible and near infrared reflectance characteristics of dry plant materials. *Int. J. Remote Sens.* **1990**, *11*, 1775–1795.
36. Elvidge, C.D. Examination of the spectral features of vegetation in 1987 AVIRIS data. In Proceedings of the First AVIRIS Performance Evaluation Workshop, Pasadena, CA, USA, 6–8 June 1988; Jet Propulsion Laboratory: Pasadena, CA, USA 1988; pp. 97–101.
37. Serbin, G.; Daughtry, C.S.T.; Hunt, E.R.; Reeves, J.B.; Brown, D.J. Effects of soil composition and mineralogy on remote sensing of crop residue cover. *Remote Sens. Environ.* **2009**, *113*, 224–238.
38. Singh, R.B.; Ray, S.S.; Bal, S.K.; Sekhon, B.S.; Gill, G.S.; Panigrahy, S. Crop residue discrimination using ground-based hyperspectral data. *J. Indian Soc. Remote Sens.* **2013**, *41*, 301–308.
39. Schmidt, H.; Karnieli, A. Sensitivity of vegetation indices to substrate brightness in hyper-arid environment: The Makhtesh Ramon Crater (Israel) case study. *Int. J. Remote Sens.* **2001**, *22*, 3503–3520.
40. Bannari, A.; Morin, D.; Bonn, F.; Huete, A.R. A review of vegetation indices. *Remote Sens. Rev.* **1995**, *13*, 95–120.
41. Thome, K.J.; Biggar, S.F.; Wisniewski, W. Cross comparison of EO-1 sensors and other earth resources sensors to Landsat-7 ETM+ using Railroad Valley Playa. *IEEE Trans. Geosci. Remote Sens.* **2003**, *41*, 1180–1188.
42. Mariotto, I.; Thenkabail, P.S.; Huete, A.; Slonecker, E.T.; Platonov, A. Hyperspectral versus multispectral crop-productivity modeling and type discrimination for the HypSIRI mission. *Remote Sens. Environ.* **2013**, *139*, 291–305.
43. Sternberg, M.; Shoshany, M. Influence of slope aspect on Mediterranean woody formations: Comparison of a semiarid and an arid site in Israel. *Ecol. Res.* **2001**, *16*, 335–345.
44. Sarker, L.R.; Nichol, J.E. Improved forest biomass estimates using ALOS AVNIR-2 texture indices. *Remote Sens. Environ.* **2011**, *115*, 968–977.

© 2015 by the authors; licensee MDPI, Basel, Switzerland. This article is an open access article distributed under the terms and conditions of the Creative Commons Attribution license (<http://creativecommons.org/licenses/by/3.0/>).

# 6 High mountain societies and limited local resources - livelihoods and energy utilization in the Eastern Pamirs, Tajikistan

---

Georg Hohberg, Fanny Kreczi & Harald Zandler

*Accepted on 04 September 2015 in Erdkunde*

## ERDKUNDE

This publication combines remote sensing approaches with interdisciplinary survey data to provide empirically based contributions to the regional degradation debate. In so doing, **hypothesis 3** is addressed. Additionally, topics of energy poverty are analyzed, but this research field is not the subject of the presented dissertation. The layout of the accepted proofread version is adopted and the content may be subject to small changes in the final form.



## HIGH MOUNTAIN SOCIETIES AND LIMITED LOCAL RESOURCES - LIVELIHOODS AND ENERGY UTILIZATION IN THE EASTERN PAMIRS, TAJIKISTAN

GEORG HOHBERG, FANNY KRECZI and HARALD ZANDLER

With 5 figures and 3 tables

Received 02 April 2015 · Accepted 04 September 2015

**Summary:** Energy supply is a key issue in isolated high mountain regions like the Eastern Pamirs of Tajikistan. This study uses an interdisciplinary approach to analyze the energy system of Alichur, an exemplary settlement in the region. Thereby, the local energy mix is evaluated, as well as the current and possible future supply of the two main resources used: Dwarf shrubs and animal manure. Finally, based on the energy system analysis, a locally adapted energy poverty index is developed. In contrast to assumptions made in literature on the topic, we found that currently only 15% of Alichur's inhabitants are energy poor, 25% are endangered by energy poverty and 60% are energy secure. However, with decreasing access to dwarf shrubs in the future, the share of energy poor households and those endangered by energy poverty may increase to more than 70%, leaving less than 30% of Alichur's households energy secure. In contrast to existing energy poverty indices, the adapted energy poverty index presented here considers social and environmental interrelationships of the case study region. It is therefore well suited for describing the energy situation of Alichur's population.

**Zusammenfassung:** Die Energieversorgung spielt eine bedeutende Rolle in isolierten Hochgebirgsregionen wie dem Ostpamir Tadschikistans. Die vorgestellte Studie nutzt einen interdisziplinären Ansatz, um das Energiesystem der Ortschaft Alichur stellvertretend für die Energieversorgung im Ostpamir zu untersuchen. Dabei werden sowohl der lokale Energiemix, als auch die gegenwärtige and zukünftige Verfügbarkeit von Zwergsträuchern und Dung als meistgenutzte Energieträger abgeschätzt. Schließlich wird auf Basis der Energiesystemanalyse ein an die lokalen Bedingungen angepasster Energiearmut-sindex entwickelt. Im Gegensatz zu gängigen Meinungen in der Literatur, wurde mit Hilfe des Energiearmut-sindex ermittelt, dass gegenwärtig nur 15% der Einwohner von Alichur als energiearm, 25% als von Energiearmut gefährdet und 60% als energiesicher gelten. Mit einer zukünftig verringerten Verfügbarkeit von Zwergsträuchern würde der Anteil an energiearmen und von Energiearmut gefährdeten Haushalten jedoch auf über 70% ansteigen, wobei weniger als 30% der Haushalte in Alichur als energiesicher gelten würden. Im Gegensatz zu bestehenden Energiearmut-sindices berücksichtigt der vorgestellte Ansatz soziale und naturräumliche Zusammenhänge in der Fallstudienregion. Er ist daher geeignet, die Energiesituation in Alichur adäquat zu beschreiben.

**Keywords:** Human-nature interaction, Central Asia, mountainous regions, energy poverty, biomass fuels, rural development, degradation

### 1 Introduction

Within the debate on global development, priority topics such as climate change and sustainable energy use have played a crucial role on the international agenda (cf. SPALDING-FECHER et al. 2005). The relevance of the current debate was highlighted by the United Nations (UN) pronouncing 2012 as the year of “Sustainable Energy for All”. Poverty alleviation, the improvement of environmental conditions through reliable access to energy and an increase of renewable energies are important pillars of the UN-resolution, which addresses more than 1.4 billion people who are lacking modern energy supply (UNITED NATIONS 2011). In this context, available research has been focusing on the topics of energy

poverty and energy access. However, the analysis of energy poverty remains a complex issue and no generally accepted approach exists. NUSSBAUMER et al. (2011) differentiate between single indicators that show one dimension of a phenomenon or a combination of single indicators assessed within a framework (such as the Millennium Development Goals programme) and composite indicators that aim to investigate more complex, multidimensional issues. One example of a single indicator is the share of household investments for energy, e.g. if more than 10% of the income is spent on energy, the household is considered energy poor (BARNES et al. 2011). SRIVASTAVA et al. (2012) make use of the energy requirements for cooking as an energy poverty benchmark. Another frequently found indicator for ener-

gy poverty is the access to modern energy carriers like electricity or gas (PACHAURI and SPRENG 2011). Although these may be important factors for energy poverty, they may not be solely decisive (PEREIRA et al. 2010; SRIVASTAVA et al. 2012). The international energy agency uses a set of indicators, such as the share of modern fuels in the energy mix and per capita commercial energy/electricity consumption (IEA 2010). MIRZA and SZIRMAI (2010) use a more complex index that connects energy inconveniences to the shortfall in meeting predefined basic energy amounts. The Multidimensional Energy Poverty Index (MEPI) – a composite indicator showing the deprivation of energy – is presented in NUSSBAUMER et al. (2011). Thereby, the authors use a set of six indicators to quantify energy poverty: modern cooking fuel, indoor pollution, electricity access, ownership of electric household appliances, ownership of electric entertainment appliances and telecommunication means. GROH (2014) links energy poverty to dependency on biomass, access to credits, energy security, energy quality and degree of remoteness. Obviously, these different approaches result in very diverse outcomes regarding the energy poverty situation. This indicates that, even though these energy poverty indices might produce valuable results for the regions assessed, they cannot be employed universally for other regions with varying living conditions (cf. BARNES et al. 2011; KATSOULAKOS 2011; PEREIRA et al. 2010; SRIVASTAVA et al. 2012).

As combating energy poverty in mountain regions is of paramount importance (KATSOULAKOS 2011), the associated analysis and identification of central elements involved is not trivial. The Eastern Pamirs of Tajikistan are a prime example of a mountain region in which energy poverty issues are crucial for sustainable development. DROUX and HOECK (2004) mention a “severe energy crisis” in the region due to a lack of energy access. Furthermore, FÖRSTER et al. (2011) highlight that energy supply plays a major role for the reduction of vegetation degradation and poverty in the Pamir-Alai Mountains. More recently, KRAUDZUN et al. (2014) investigated the status of dwarf shrubs (*Krascheninnikovia ceratoides*, *Artemisia spec.*), which are strongly linked to energy access as a central thermal energy source in the area, and concluded that thermal energy use and supply are highly diversified. KRAUDZUN (2014) emphasizes the role and increasing importance of animal manure as another locally available energy carrier and provides an overview of the dynamic energy transformation in the region. All these studies analyze aspects of energy poverty based either on a limited

database or offer only confined insights into the energy system of the Eastern Pamirs. Reliable energy consumption and provision figures are still missing, despite their relevance for improving understanding of the current and future energy situation in the region. Additionally, a comprehensive, in-depth methodology that contrasts energy demand and supply based on the background of local socio-economic conditions is also lacking. However, the energy situation of the Eastern Pamirs varies with diverse local conditions in the region’s villages and cannot be assessed with the described existing measures of energy poverty on a larger scale. Therefore, an adapted energy poverty index based on an interdisciplinary survey may be more suitable.

In order to meet this objective, we analyze the energy system of the medium sized Eastern Pamir village of Alichur. Based on a profound dataset, we develop a methodology to specify the local energy situation in the case study village. The approach intends to bridge the gap between generalized quantitative energy poverty indices on the one hand, and specific qualitative surveys on the other hand. Although all or nearly all households of Alichur are expected to be classified as energy poor using existing single indicator energy poverty indices, there is strong evidence that a more detailed consideration of the local energy consumption patterns yields a more diversified picture (KRAUDZUN 2014). Furthermore, despite very pessimistic projections regarding available energy ten years ago (DROUX and HOECK 2004), the present energy situation in the Eastern Pamirs appears relatively stable. Therefore, a locally adapted energy poverty index is considered to be more suitable than existing methods to clarify specific questions regarding the current and possible future energy security in the case study region and is used to evaluate the following two hypotheses:

1. The greatest share of households in the village can supply themselves with enough energy to satisfy their current energy demand and even possess sufficient resources to cope with shocks to the social or energy system.

Especially dwarf shrubs and animal manure currently provide relevant shares of the local energy mix at low costs (cf. KRAUDZUN 2014) and a considerable number of publications (i.e. ACHMADOV et al.; 2006; BRECKLE and WUCHERER 2006; HOECK et al. 2007) highlight the importance of dwarf shrubs for the current energy supply of the Eastern Pamirs and at the same time report alarming figures about their degradation. This leads to the second hypothesis of this study:



2. If local dwarf shrub stands are being depleted, the energy security of the local inhabitants is likely to worsen significantly in the future.

By analyzing an energy system exemplary for the Eastern Pamirs, this study aims at clarifying whether or not the energy crisis described in literature is based on scientific local evidence.

## 2 Study area

This paper analyses the energy system of Alichur, a village located in the autonomous province Gorno-Badachschanskaja Avtonomnaja Oblast (GBAO) of the Central Asian Republic of Tajikistan. GBAO covers the whole Tajik part of the Pamir Mountains. It consists of seven administrative districts (*rajons*) and one urban region. Alichur is located in the *rajon* Murghab whose administrative center is the city of Murghab. The *rajon* of Murghab is further subdivided into six departments (*jamoats*). The village of Alichur is the center of the *jamoat* Alichur, which also includes the villages of Bash Gumböz and Bulunkul and their surroundings (Fig. 1). Alichur has 1,295 inhabitants (January 2013), consisting of 314 families that are dis-

tributed between 210 separate households in the village and some further households (i.e. pasture camps and road maintenance stations) in the near surroundings. Seventy-six percent of the population are ethnic Kyrgyz and 24% are Pamiri (Shia Ismaili Mountain Tajiks, STATDAT. JAMOAT ALICHUR 2013).

According to our household survey data, the average income of people in Alichur is 155 USD per month, including official salaries, pensions, formal seasonal work and self-employed businesses. The state is the main source of monetary income: 44% of formal incomes are official salaries of which 47% are pensions. Apart from monetary income, livestock as transformable financial capital plays a great role for sustaining livelihoods in the Eastern Pamirs (cf. KRECZI 2011). The average livestock per household in Alichur is 23.1 units of small livestock (goat and sheep) and 5.5 units of big livestock (yak and cow) according to the 2013 household interviews. The Pamir Highway (M41) which passes through the village has played a crucial role in the development of the village. This main road, connecting the centers and markets of Khorog in the Western Pamirs and Osh in Kyrgyzstan, is still an important feature for livelihoods in Alichur and influences utilization patterns

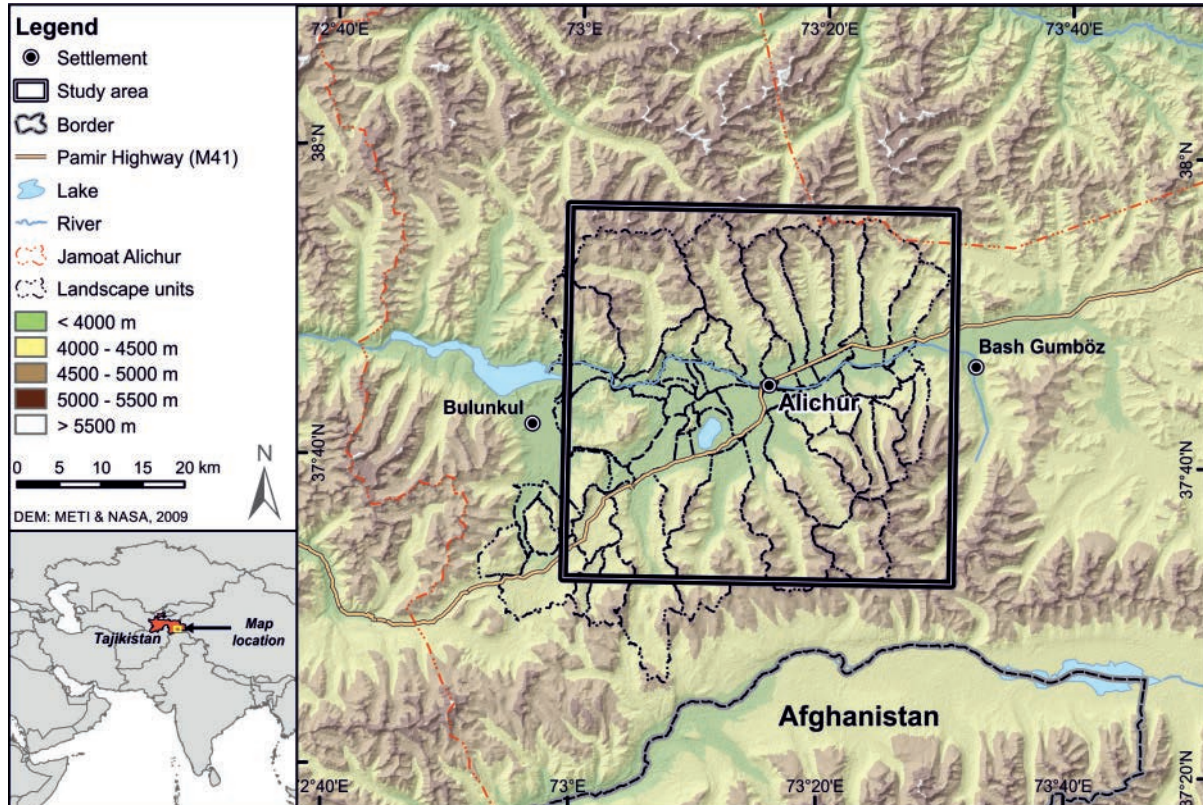


Fig. 1: Location of the study area. Area is delimited according to the availability of satellite data used for the biomass model

of local resources, which have to be transported from the periphery to the settlement.

The climate of this high mountain plateau can be characterized as cold and dry (Bulunkul annual means 1999–2012: -6.1 °C, 95 mm, TAJIK MET SERVICE 2013). Scarce dwarf shrub dominated vegetation adapted to this harsh environment is characteristic for all areas except azonal vegetation sites in riverbeds and high altitudes with good water provision. Due to the absence of trees, dwarf shrubs (*Krascheninnikovia ceratoides*, *Artemisia spec.*) are the only locally available woody biomass. Thereby, the largest share of the plant's biomass is located underground in the root zone. We will refer to these dwarf shrubs as *teresken* (*Krascheninnikovia ceratoides*) and *shyvak* (*Artemisia spec.*) in this study, as these are their locally known Kyrgyz names.

### 3 Methods

This study uses an interdisciplinary approach, incorporating qualitative and quantitative, geo-ecological and social data, to investigate the com-

plex phenomenon and the various forms of energy poverty and follows two main methodological approaches: The analysis of the local energy system of Alichur and the development of a locally adapted energy poverty index. On the energy consumption side, household interviews combined with a thermal analysis of commonly utilized energy carriers yield quantitative data on the current energy-mix. On the supply side, the capacity of the local energy carriers – *animal manure* and *dwarf shrub biomass* – are investigated in order to identify possible future developments of the energy system. A map of all available harvesting areas allows a spatial assessment of the current and anticipated future biomass supply. Following the analysis of the local energy system, a regionally adapted energy poverty index is derived (Fig. 2). For the development of this localized energy poverty index, qualitative and quantitative social data was used in different steps. Environmental data and its interpretation are incorporated again when projecting future scenarios. The index will be used to assess the present energy poverty situation at the local level and to identify possible future trends.

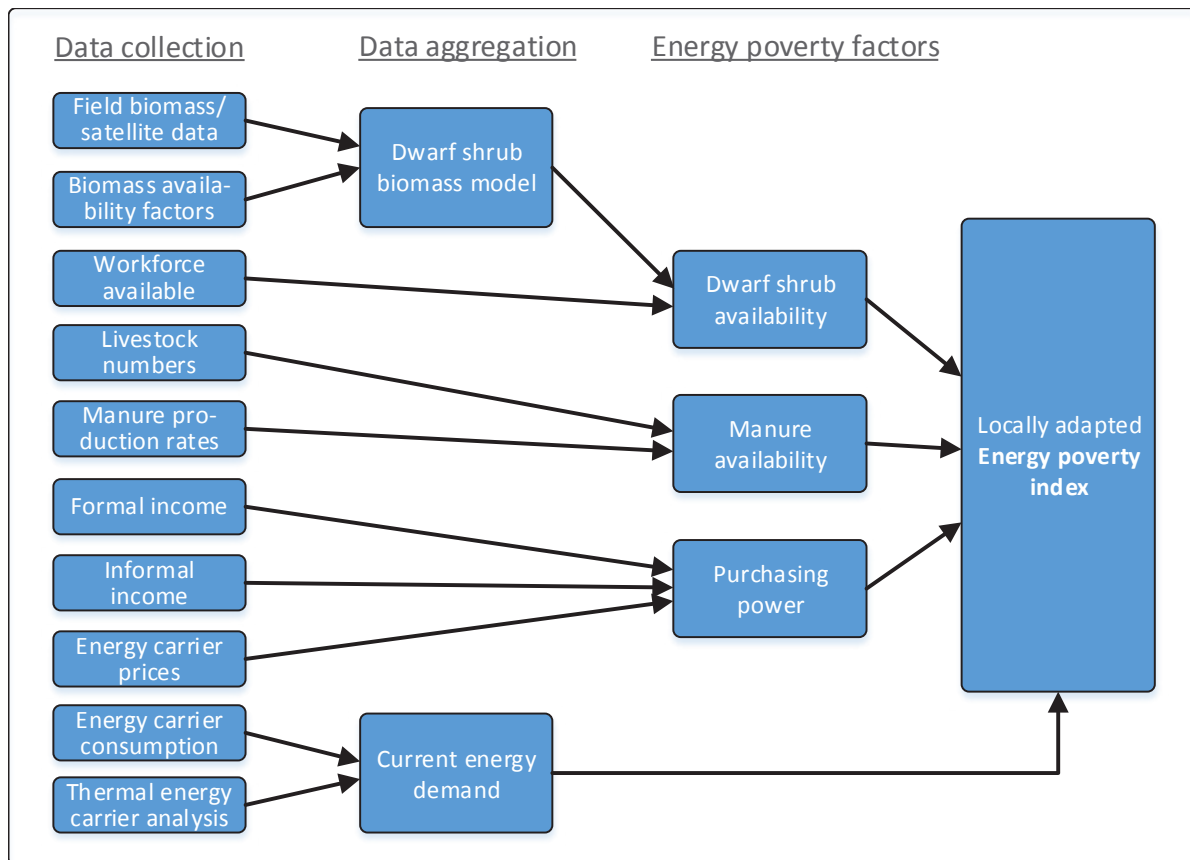


Fig. 2: Steps to a locally adapted energy poverty index for Alichur

### 3.1 Analysis of the local energy system

#### 3.1.1 Household interviews and spatial allocation

In March 2013, a comprehensive survey on the 2012 energy utilization was conducted among private households of Alichur. On the one hand, data related to demand, acquisition and consumption of local energy and, on the other hand, information about the demographic structure, living conditions and livelihood strategies of households was collected. Additionally, the spatial characteristics of local dwarf shrub biomass harvesting were analyzed. In total, 210 households were counted and visited in the village. 119 households were available for the interview. Following a test phase, which aimed to improve the questionnaire regarding structure and formulation of questions, six local assistants conducted the interviews in pairs. The interview partners represented both Kirghiz and Pamirian ethnic groups respectively. In doing so, the willingness to share information among the interviewees was increased and translation errors were minimized. Asked for amounts of energy carriers used, interviewees typically answered in units of purchase or acquisition. Specifications for masses of coal were, without exception, made in metric units such as tons or kilogram. Yet, locally generated energy carriers were mainly specified in regional units such as bundles of dwarf shrubs or different types of lorry loads of animal manure and dwarf shrubs (cf. MISLIMSHOEVA et al. 2014). In order to convert these regional units to metric units, 57 samples of dwarf shrub bundles were measured. The lorries' cargo capacity was determined by measuring the bed area as well as the bed height or the height of additional installations. In addition, two cargo density samples were each recorded for *kuik* and for dwarf shrubs. Derived conversion factors are valid for the case study of Alichur and cannot directly be transferred to other villages of the Eastern Pamirs as harvesting habits vary significantly in the region. More details on the derivation of the conversion factors are presented in HOHBERG (submitted). To improve the comparability between different types of energy carriers, thermic analysis of one representative sample of *teresken*, *shyvak*, *kuik* and *tezek* was carried out at the Institute of Combustion and Power Plant Technology, University of Stuttgart (IFK 2013). In addition to the quantitative data set, qualitative household interviews were conducted in 2013. Information concerning social aspects influencing utilization patterns, organization and acquisition

of local fuels, as well as the demand for resources was collected in semi-structured, biographical and guided expert interviews. Qualitative data served not only to complement and triangulate quantitative data, but to gain an in-depth understanding of the local energy system and living conditions, which evoke complex coping mechanisms of households. Furthermore, qualitative data played a crucial role for the deduction of the different categories that the energy poverty index is based on. The values for classification within the different categories, as well as class limits, are based on quantitative data.

To allocate biomass amounts mentioned in the interviews, a classification of the territory into landscape units was necessary. Borders used for this classification process were pasture areas and landmarks such as ridges, rivers or roads. An iterative process was employed using a digital elevation model (DEM, METI and NASA 2009), information of the local community with subsequent validation and a geographic information system (GIS) (Fig. 1).

#### 3.1.2 Manure production and dwarf shrub biomass availability and access

Based on data from the 2013 household interviews and the local veterinary (ISMANOV 2013), livestock numbers assigned to the village of Alichur were estimated. Daily manure production figures of relevant livestock species were estimated through the field survey and expert interviews and validated by literature data (BREU 2006; CHAMBERS 2001; KADIAN 2002). Finally, *kuik* production figures were estimated by multiplying the total manure production of a livestock species by the share of time it spends in a shed. *Tezek* production numbers equal the total manure production of big livestock subtracted by its *kuik* production.

The methodology to assess dwarf shrub biomass availability incorporates the application of a spatial biomass model and the definition of scenarios considering realistic limiting factors for calculation of available biomass. The development of the spatial biomass model was performed using RapidEye (RAPID EYE AG 2009), Landsat OLI (USGS 2013) and ASTER DEM (METI and NASA 2009) satellite images. The methods, data and the best performing model of ZANDLER et al. (2015) were applied, but modeling was restricted to the 20 highest ranking remote sensing variables according to the importance assessment therein. As empirical models are



always connected to modeling errors, respective restrictions were introduced to avoid overly optimistic biomass predictions. ZANDLER et al. (2015) state that better performing biomass models showed an RMSE of approximately 1,000 kg/ha under the given research conditions. Therefore, this value was subtracted from all predicted biomass values in this study to provide a conservative assessment of biomass availability. Resulting negative values were set to zero. To take aforementioned realistic limiting factors related to dwarf shrub harvest into account, field observations and interviews were used to develop different scenarios. Generally, two different dwarf shrub harvesting practices can be distinguished: harvesting on foot or donkey, referred to as *individual harvest* herein, or *motorized harvest* in pairs or groups using available vehicles. Furthermore, harvesters only excavate dwarf shrubs in regions where a certain minimum biomass amount is available. Areas with biomass densities below certain thresholds are usually not harvested even though they are easily accessible and frequently found near villages. Therefore, in Scenario 1, harvest takes place only in areas with more than 500 kg/ha and the biomass was set to zero in all areas below this level. In Scenario 2, the harvesting threshold was raised to 1,000 kg/ha to allow for a natural variability of worthwhile harvesting area selection. These thresholds are especially important when it comes to modeling *individual harvest* by foot or donkey. *Individual harvest* is restricted to a walking distance of 90 minutes around the village of Alichur, a value above which travel times do not allow for a daily return to Alichur from the harvest area. Due to the comparably high transportation effort and cost and a generally larger number of involved harvesters, *motorized harvest* is only conducted in areas with higher quantities of biomass available. Therefore, two additional scenarios with higher thresholds, one with a 1,500 kg/ha (Scenario 3) and another with a 2,000 kg/ha (Scenario 4), were calculated.

Besides availability, accessibility to dwarf shrub biomass is instrumental for its utilization. To access more remote dwarf shrub areas for harvesting, former Soviet lorries, remnants of Soviet times, are used in Alichur. The model GAZ-66, which is an all-terrain Soviet military lorry that can drive on inclinations of up to 30° when unloaded (NTIS 1973), is the lorry most frequently utilized for these purposes. However, when used for harvesting, these lorries are loaded up to two meters high with dwarf shrubs and the maximum passable inclination is lower so that a maximum drivable inclination of 20° is as-

sumed. A DEM (METI and NASA 2009) was employed to identify areas with inclinations lower than or equal to 20° in the study region. Additionally, a shapefile of the local road network in Alichur district and one of all water bodies in the region were used for evaluation of dwarf shrub accessibility. All areas that are not covered by a water body and connected to the village of Alichur by road or are accessible from Alichur by passing only areas with inclinations lower than or equal to 20° are evaluated as accessible by motorized vehicle. In total, 85,700 ha are accessible by motorized vehicle in the project region.

### 3.2 Local energy poverty index

Animal manure and dwarf shrub biomass are identified as crucial for the energy supply of households in the case study village of Alichur. Therefore, a household's livestock ownership (access to manure) and available workforce (harvest of dwarf shrubs) are key factors determining energy security. As a matter of course, monetary income can compensate both of these two factors. In order to assess the energy situation of the households, the availability of the aforementioned factors of workforce, livestock possession and monetary income is quantified on the household level into the three categories of *sufficient quantity*, *medium quantity* and *low quantity*. In this context, *sufficient quantity* corresponds to a factor's capability to provide 100% or more, *medium quantity* to provide 50% to less than 100% and *low quantity* to provide less than 50% of the annual average energy demand. Livestock ownership, being a substantial part of a household's tied up financial capital in the Eastern Pamirs (KRECZI 2011), is not taken into account within the calculation of monetary income. In order to consider a household's situation as energy secure, at least one of the described key factors must be available at a *sufficient quantity* and a second factor at a *medium quantity*. An energy secure household is able to satisfy its total energy demand and can cope with shocks, trends and seasonal changes. Households that have one of the factors at *sufficient quantity* or two factors at *medium quantities* are considered to be endangered by energy poverty. Though these households are currently able to satisfy their energy demand, they are vulnerable to changes in the livelihood system. Finally, energy poor households cannot supply themselves with sufficient energy carriers, are relying on external help and/or complex bundles of survival strategies.

## 4 Results and discussion

### 4. The local energy system of Alichur

With five out of the 119 interviewed households giving contradictory statements about their energy consumption, 114 valid datasets resulted from the survey (54% of all households). The masses of resource consumption resulting from these household interviews are depicted in table 1 together with heat of combustion figures resulting from thermic analysis (IFK 2013).

We found that households in Alichur consumed on average 161.7 gigajoules (GJ) of energy in 2012 (Fig. 3). Ninety point six percent of this consumption is provided by the local resources of manure, dwarf shrubs and – to a very small extent – by decentralized solar power (households having little solar panels on their roofs). The energy utilized from manure amounts to 84.7 GJ per year and makes up around 52.4% of the total energy consumed per household. Both *kuik* and *tezek* were used by the inhabitants of Alichur. Yet, *kuik* was reported to be responsible for energy generation of 78.7 GJ per household (48.7% of the total energy mix), while *tezek* only provided 6.0 GJ (3.7% of the total energy mix). On average 6,047 kg *kuik* and 396 kg *tezek* were used per household. Sixty-one point one Gigajoule per household was generated by burning dwarf shrubs, which translates into 37.9% of the energy mix and is equivalent to 3,367 kg dwarf shrubs. People reported that they generally had no preferences for *teresken* or *shyvak* and used either one depending on which was more easily accessible. Solar panels deliver no more than 0.6 GJ per household and year, about 0.4% of the total energy used. In 2012, 9.3% of the total energy mix (15.1 GJ or 655 kg) was provided by coal, the only external energy carrier imported to Alichur for room heating.

These findings show some similarities to HOECK et al. (2007) and MISLIMSHOEVA et al. (2014) who studied energy consumption in settlements of the Western Pamirs. They indicate that the largest share of energy consumed was met by local biomass. Yet, energy demand from biomass was mainly satisfied by dwarf shrubs according to HOECK et al. (2007) and by animal manure according to MISLIMSHOEVA et al. (2014). This is different to our work where the energy carriers of animal manure and dwarf shrubs account for approximately equal shares of the energy mix, underlining strong regional differences in energy utilization (cf. KRAUDZUN 2014). Our study is the first to analyze dwarf shrub consumption on a more extensive database in this region. With a total consumption of 3.4 t of dwarf shrubs per household and year, our findings range between the 1.2 t given by WIEDEMANN et al. (2012) and 7.9 t given by DROUX and HOECK (2004). These studies derived their figures from a much smaller sample. The resulting total energy consumption of 161.7 GJ per household and year with an average of 5.06 persons per household is rather high as compared to the Tajik average, which is 18.1 GJ per person (91.6 GJ per 5.06 persons) (BREU and HURNI 2003). Regional references state figures between 69 GJ and 140 GJ in the Western Pamirs (HOECK et al. 2007; MISLIMSHOEVA et al. 2014). As energy demand may increase due to bad energy infrastructure (HOECK et al. 2007), increasing elevation (MISLIMSHOEVA et al. 2014) and lacking access to energy grids, our results are within a plausible range.

Keeping the overall energy mix of Alichur in mind, the focus of this research is on the most important local energy carriers of manure and dwarf shrubs. We estimated the total livestock numbers of Alichur at 1,500 yaks, 200 cows, 2,000 goats and 2,900 sheep. Milk-yaks, young yaks and few bulls are kept in the shed during night time (VANSELOW 2011).

Tab. 1: Average resource consumption figures of Alichur and heat of combustion of selected energy carriers used in Alichur (Source: IFK 2013)

| Energy Carrier  | <i>Teresken</i> | <i>Shyvak</i> | <i>Kuik</i> | <i>Tezek</i> | Coal              |
|---|-----------------|---------------|-------------|--------------|-------------------|
| Average amount consumed per year and HH                   | 1,343 kg        | 2,024 kg      | 6,047 kg    | 396 kg       | 655 kg            |
| Standard deviation of the amount consumed per year and HH | 1,798 kg        | 1,532 kg      | 2,786 kg    | 817 kg       | 615 kg            |
| Heat of combustion [MJ/kg]                                | 17.8            | 18.5          | 13.0        | 15.2         | 23.0 <sup>a</sup> |

<sup>a</sup> estimated based on a calorific value of 6.40 kWh/kg (REA 2012)

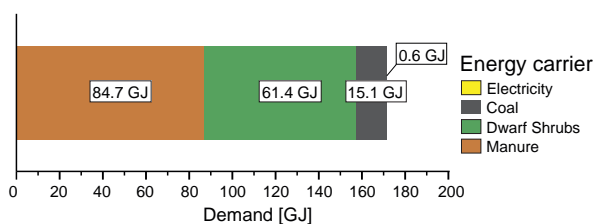


Fig. 3: Average primary energy consumption of Alichur households in 2012

The remaining yaks, approximately 50%, are left to graze day and night. Small livestock as well as cows are kept in sheds during the night in summer and winter. Therefore, it is assumed that 25% of the yak droppings and 50% of sheep, goat and cow droppings accumulate in sheds and are the source of *kuik*. Due to the droppings' consistency, only yak and cow manure can be collected from the pastures for use as *tezek*. Assuming all can be collected, these account for 75% of the produced yak manure and 50% of the cow manure. Estimated figures consider a moisture content of 7% for *kuik* and *tezek*. This value was evaluated for air dried *kuik* and *tezek* from Alichur by IFK (2013). Table 2 gives *tezek* and *kuik* production figures per head and year. Multiplying the livestock figures derived with the manure production figures we calculated a potential *kuik* production capacity of 889 t per year and a potential *tezek* production capacity of 1,558 t per year in the vicinity of Alichur.

With a calculated *kuik* production capacity of only 889 t and an estimated total *kuik* consumption of 1,260 t, clearly all available *kuik* was utilized in 2012 in Alichur and additional imports from neighboring areas were required. In contrast, only around 80 t of *tezek* were used by the households of Alichur, where the production of *tezek* during this year was around 1,558 t. This amounts to only 5% of the theoretically available *tezek*.

In total, 789 t of dwarf shrubs were harvested in the vicinity of Alichur in 2012. Out of these, 82 t were exported from the region, 707 t were used by the inhabitants of Alichur themselves. Dwarf shrub harvesting activities in 27 *landscape units* were conducted (Fig. 4). This includes 76% of all *landscape units* bordering the Pamir Highway (19 out of 25) and 44% of all identified *landscape units* (27 out of 61). Depending on the selection of the harvesting sites, different means of transport are required: *Individual harvest* is practiced within walking distance from the village center. HOHBERG (submitted) derives a cost distance raster for individual harvest around Alichur, which is based on empirical field data. He considers a walking distance of 90 minutes around Alichur as

a maximum range for individual harvest. The resulting area for individual harvest is used in this work (red outline in Fig. 4). *Motorized harvest* takes place preferably along the Pamir Highway at medium distances of around 25 km away from Alichur and to a smaller extent also in areas not accessible from the Pamir Highway.

Regarding biomass availability, cross validated error measures of the spatial biomass model resulted in a bias of 47 kg/ha, a RMSE of 910 kg/ha and a relative RMSE of 54%, showing a similar performance compared to remote sensing based biomass quantification studies in other regions (ZANDLER et al. 2015). Predicted areal mean biomass of the conservative model including the whole area (Fig. 4) was 921 kg/ha. Spatially, lowest amounts were predicted at summit areas, in the Alichur Valley at lower elevations, in the vicinity of Alichur and near main roads. Highest amounts were predicted for slopes of northerly and southerly reaching side valleys with the maxima at valley ends at higher altitudes. Total predicted dwarf shrub biomass for all *landscape units* ranged from 153,522 t (Scenario 2) to 164,503 t (Scenario 1). Reachable biomass for *individual harvest* by foot or donkey varied from 8,343 t (Scenario 2) to 10,080 t (Scenario 1). Regarding accessible biomass by vehicle (*motorized harvest*), the amount of dwarf shrub ranged from 63,821 t (Scenario 4) to 75,479 t (Scenario 3). These results indicate that, although accessibility is an important issue, biomass availability is still high in the surroundings of Alichur, which contradicts the findings of DROUX and HOECK (2004), who provide evidence of an alarming energy situation due to the rapid decline of dwarf shrub vegetation in the region based on biomass estimates. However, this is the first study to analyze biomass availability in this region based on empirical data, in contrast to existing rough estimates. Furthermore, our findings are supported by the more recent work of KRAUDZUN et al. (2014), KRAUDZUN (2014) and VANSELOW and SAMIMI (2014), who state that the situation is more complex and that intact dwarf shrub vegetation may commonly exist side by side with degraded areas. In accordance with this, our spatial distribution of modeled biomass (Fig. 4) shows no or low biomass amounts near the Pamir Highway in comparably easily accessible regions, but high biomass quantities at a certain distance from these main routes, but still in the vicinity of Alichur. All these figures only depict the present day available biomass amounts that could be exploited under the given assumptions, without considering sustainable



Tab. 2: *Tezek* and *kuik* production figures of relevant livestock species

|              | Sheep   | Goat    | Cow      | Yak      |
|--------------|---------|---------|----------|----------|
| <i>Tezek</i> | --      | --      | 970 kg/a | 909 kg/a |
| <i>Kuik</i>  | 49 kg/a | 49 kg/a | 970 kg/a | 303 kg/a |

development or other mechanisms that may influence dwarf shrub utilization. To assess long-term impacts of harvesting on biomass and therefore energy availability, figures on regeneration of dwarf shrubs are very important. As these plants are extremely slow growing (WALTER and BRECKLE 1986), comprehensive studies on this issue were not possible during our work, although observations of a few disturbed areas (n=5) indicate that regeneration takes place at a rate of about 14–39 kg/ha\*a. With dwarf shrubs growth figures of 20–30 kg/ha\*a (WALTER and BRECKLE 1986), 70 kg/ha\*a (CLEMENS 2001), 30–70 kg/ha\*a (max. 150 kg/ha\*a) (BRECKLE and WUCHERER 2006) in the literature, our measurements appear rather conservative.

A comparison of the harvested and modeled biomass on the subject of accessibility shows a general agreement in their distribution, as in most cases highest amounts were harvested in regions where high amounts of biomass are accessible. However, there are some discrepancies especially in the southwestern *landscape units* along the Pamir Highway, where harvesting amounts were high but available biomass was low according to the model. This may be partly explained by errors in the model, but may also result from clouds in the satellite images in those regions, which led to zero modeled biomass. Finally, results of the regional biomass model have to be interpreted carefully, as remote sensing based methods are limited in this environment and errors are relatively large (ZANDLER et al. 2015).

#### 4.2 An energy poverty index adapted to the local situation of Alichur

Through the energy-system analysis performed, it becomes clear that none of the existing energy poverty indices initially mentioned adequately reflect the energetic situation of Alichur. Setting an energy poverty threshold based on the share of monetary income households spent on energy carriers (i.e. 10% as mentioned in BARNES et al. 2011) neglects the importance of local biomass like dwarf shrubs and *kuik* in the energy system investigated. Similarly, as no household in Alichur is connect-

ed to the electricity or the gas grid simply because these do not exist, access to modern energy carriers as suggested by IEA (2010) cannot serve as an energy poverty index in Alichur. Furthermore, the composite index presented in NUSSBAUMER et al. (2011) is not able to differentiate between households in Alichur, as either all or none of the indicators apply to every household. This situation is comparable when considering other energy poverty indices as well (e.g. GROH 2014) and thereby supports the necessity of a locally adapted energy poverty index.

During the energy system analysis, we identified access to the three energy carriers of *kuik*, dwarf shrubs and coal as being critical for satisfying people's demand for heating and cooking (Fig. 3). For the energy index developed, we focus on people's ability to purchase energy carriers and to supply themselves with dwarf shrubs at minimum cost (or nearly free of charge). Due to the fact that *kuik*, in contrast to coal, is available all year round and can be purchased at considerably lower costs in comparison to coal, it serves as a measure for the amount of energy that people are able to purchase in our energy index. When considering coal consumption besides donations by the Red Cross, commercial coal is currently consumed by wealthier households in Alichur only. These households use coal regardless of its higher price because of its convenience in comparison to *kuik* and dwarf shrubs. Coal therefore does not influence energy poverty and is not directly included in the energy poverty index.

We observed that, in regard to its calorific value, *kuik* was the cheapest energy carrier available in Alichur. On average the price of one ton of *kuik* was 41 USD in 2012. In order to cover an energy demand of 161.7 GJ, 12.3 t of *kuik* are needed. At the given price this requires 504 USD (252 USD to cover 50% of the energy demand). In 2012, the interviewed households on average spend 17% of their monetary income on energy, though the standard deviation was 19% and thus rather high. It is assumed that no more than 36% (the average plus one standard deviation) of a household's income can be spent on energy carriers.

In section 3.1.2 we derived *kuik* production figures of the animals kept in the Eastern Pamirs.

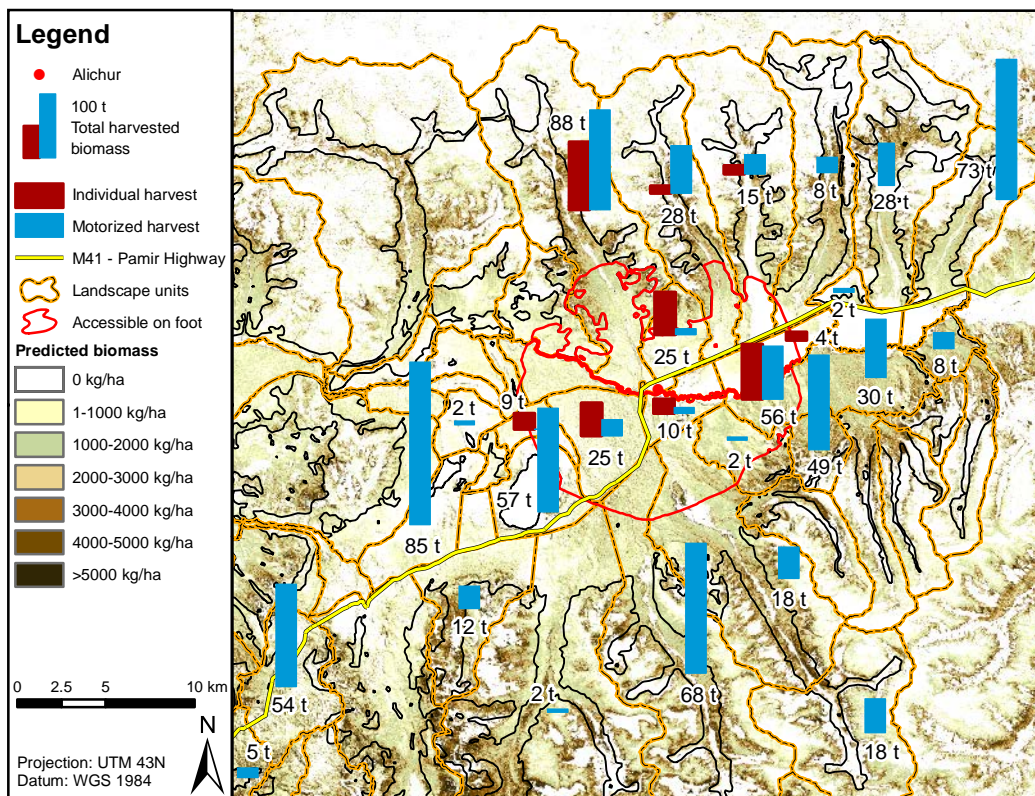


Fig. 4: Harvesting pattern and predicted biomass according to the empirical biomass model

Using the livestock numbers given in the household interviews, calculation of each household's *knik*-self-supply rate is possible. *Livestock ownership* is therefore an essential category regarding a household's energy situation.

Harvesting dwarf shrubs is a labor-intensive activity. With up to 93% of the dwarf shrubs' biomass located below the ground (YUSUFBEKOV and KASACH 1972), the act of digging out the dwarf shrubs and carrying dwarf shrub bundles (*teng*) entails substantial physical labor. Therefore, *workforce* is a crucial category for biomass acquisition. HOECK et al. (2007) state that in the Western Pamirs, harvesting biomass is mostly performed by women and children. However, our findings suggest that mainly men between the ages of 15 to 45 are employed in this activity. We found that at least one man in this age group is needed to collect enough dwarf shrubs to satisfy 50% of a household's average annual energy consumption. If a household's total annual energy consumption should be satisfied by dwarf shrubs, at least two men at the specified age are needed. This positive influence to energy security due to increased participation of household members in energy resource supply is different to the concept presented in

MIRZA and SZIRMAI (2010), where increased involvement of household members contributes to energy poverty. Again, this shows that energy poverty indices have to be adapted to the regional objective.

Households possessing at least one of the three factors of *monetary income*, *livestock ownership* or *workforce* in *sufficient quantity* and one factor in *medium quantity*, or who possess all three factors in *medium quantity* are considered energy secure (Tab. 3). These households dispose of enough resources to supply themselves with energy carriers to satisfy no less than 150% of their current energy demand. Through diversification in these households' energy consumption, energy secure households are not vulnerable and can resist smaller shocks to the energy system. Households with only one factor at a *sufficient quantity* and all other factors at *low quantities* or with only two factors at a *medium quantity* are classified as *endangered by energy poverty*. Even though these households can currently satisfy 100% of their entire energy demand and potentially even more, they are vulnerable to shocks. A shortage in one of the factors, caused for instance by a sick household member, unemployment or high losses of livestock during winter, cannot be compensated. Finally, households, which can currently only

satisfy less than 100% of their energy demand by themselves and are relying on external help, are classified as *energy poor*.

94 of the household interviews contained complete and consistent information on the described factors. The situation of 56 of these households (60%) was classified as *energy secure*. While 24 households (25%) can currently supply themselves with energy but are *endangered by energy poverty*, 14 households (15%) are *energy poor* at present, according to this classification. With an annual demand of 205 t of dwarf shrubs harvested by individual harvest and 502 t harvested by motorized harvest and 8,343 t to 10,080 t of dwarf shrubs accessible for *individual harvest*, resp. 63,821 t to 75,479 t accessible for *motorized harvest*, the current harvesting practices can be continued for a considerable period of time even without considering regrowth. We therefore conclude that biomass availability is sufficient in the medium-term and dwarf shrub supply will not cease within the near future. However, the spatial distribution of biomass and related harvesting patterns show that the largest quantities are located in areas at considerable distance to the village center or in regions that are difficult to access (e.g. valley slopes). The present harvesting situation suggests that considerable resources are needed to harvest dwarf shrubs even to-

day. However, considering that the regrowth rates of dwarf shrubs are potentially below the current rate of usage, future access to dwarf shrubs may be even more costly in terms of workforce needed (and capital when *motorized harvest* is considered). According to our method of estimating energy poverty, increasing the workforce needed to gather dwarf shrubs negatively affects the local household's energy security situation. For instance, if the workforce required to supply a household with sufficient dwarf shrub biomass would double in the future, only 27 households (29%) could consider themselves energy secure, while 35 households (37%) would be endangered by energy poverty and 32 households (34%) could not supply themselves with the energy they require (Fig. 5).

Our results demonstrate that energy poverty is a complex phenomenon, which depends on a number of regionally varying social, economic and natural factors. This finding is similar to the results of SRIVASTAVA et al. (2012), who revealed that energy poverty strongly varies according to local conditions. As PEREIRA et al. (2010) point out, analysis of energy poverty always depends on the definition of a poverty line, which in turn depends on a profound understanding of the utilization of energy resources. Our in-depth analysis of Alichur's local

Tab. 3: Categorization of the local energy situation

|                            | Sufficient quantity   | Medium quantity   | Low quantity   |
|----------------------------|---|---|--|
| <b>Monetary income</b>     | At least 100 % of the average annual energy consumption can be purchased by the annual monetary income<br><br>36 % of the annual income<br>>= 504 USD   | At least 50 % of the average annual energy consumption can be purchased by the annual monetary income<br><br>36 % of the annual income<br>>= 252 USD  | Less than 50 % of the average annual energy consumption can be purchased by the annual monetary income<br><br>36 % of the annual income<br>< 252 USD             |
| <b>Livestock ownership</b> | The livestock owned produces enough <i>kuik</i> to cover at least 100% of the average annual energy consumption<br><br><i>kuik</i> production >= 12.3 t | The livestock owned produces enough <i>kuik</i> to cover at least 50% of the average annual energy consumption<br><br><i>kuik</i> production >= 6.2 t | The livestock owned produces less <i>kuik</i> than required to cover at least 50% of the average annual energy consumption<br><br><i>Kuik</i> production < 6.2 t |
| <b>Workforce</b>           | The household's workforce can harvest enough dwarf shrubs to cover at least 100% of the average annual energy consumption<br><br>Workforce >= 2 persons | The household's workforce can harvest enough dwarf shrubs to cover at least 50% of the average annual energy consumption<br><br>Workforce = 1 person  | The household's workforce cannot harvest enough dwarf shrubs to cover at least 50% of the average annual energy consumption<br><br>No workforce                  |



energy system suggests that, in the Eastern Pamirs of Tajikistan, besides monetary income and livestock ownership, the ability of a household to access local energetic resources is the main factor determining regional energy poverty. Other factors, which are only partly addressed by our energy poverty index, are the social structure of households and social networks within the community, which might also affect a household's energy supply, demand and coping strategies in bottleneck situations, but are difficult to quantify (e.g. JOHNSON and BRYDON 2012; SAN et al. 2012; MISLIMSHOEVA et al. 2014). Finally, regional disparities are significant within the Eastern Pamirs of Tajikistan and different energy carriers may be decisive for the regional energy situation in other villages, as examples given in KRAUDZUN (2014) show.

**5 Conclusion**

This study is the first interdisciplinary analysis of an energy system located in the Eastern Pamirs based on extensive quantitative and qualitative surveys. The study shows that existing energy poverty indices are not adequately capable of distinguishing between different energetic circumstances of households in the Eastern Pamirs. The energy system analysis performed in this study demonstrates that *monetary income, livestock ownership* and *workforce* of households are fundamental to ensure energy supply in this peripheral mountain setting and are important indicators for regional energy poverty. The derived energy poverty index for Alichur includes these aspects and results in a highly diversified energy situation of local households. This confirms BARNES et al. (2011) and SRIVASTAVA et al. (2012), who state that energy poverty indices have to be adapted on a regional scale. Furthermore, as energy access and therefore energy poverty is determined by a number of factors, our

results emphasize the complexity of this field and the importance of interdisciplinary research strategies. Finally, we showed that a profound characterization of the local energy situation in peripheral mountain regions is only possible with a combination of social and environmental data.

We suggest that presently only a small share of Alichur's population is affected by severe energy poverty. According to our index, the majority of the local households may be considered energy secure or at least able to satisfy their current energy demand without external help. These new, empirically-based findings confirm our initial hypothesis and contradict earlier studies that depict a widespread and severe energy crisis in the Eastern Pamirs. However, our results also support the second hypothesis stating that the energetic dependency on regionally available dwarf shrubs in combination with increasingly difficult accessibility may significantly reduce energy security in the future. As energy poverty is not only based on regional resource availability but also depends on demography, future access to markets (e.g. China) and the price of coal, a comprehensive outlook on future developments is beyond the scope of this study and requires additional data, models and research. Further studies, focusing on livelihood strategies, local particularities of energy poverty and dwarf shrub regeneration could improve the picture of dynamic ecological aspects, as well as of social and economic features of households influencing consumption patterns and therefore, energy poverty at the micro-level.

**Acknowledgements**

The authors would like to express their thanks to the Volkswagen Foundation for enabling the research through funding the research project "Pamir

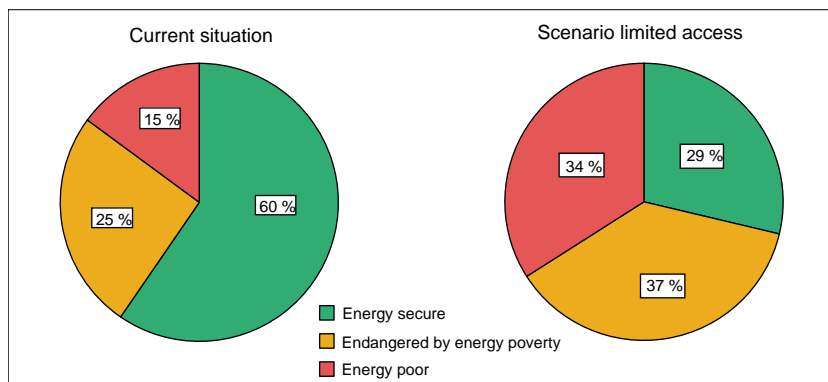


Fig. 5: Energy poverty in Alichur: a) Current situation and b) Situation with limited access to dwarf shrubs

II<sup>?</sup>. Furthermore, we would like to thank the DLR for the data provision from RESA and the USGS for providing remote sensing products.

At the regional level we are grateful for having been in the privileged situation of being supported by GIZ, especially concerning the recruitment of local assistants, without whose great contribution this study would not have been possible.

We would like to thank the inhabitants of Alichur for their support of this study with their hospitality, patience and openness. Particularly to those who provided us with comments, and constructive criticism, we would like to express our gratitude. Furthermore, we thank two anonymous reviewers for their constructive remarks to improve the manuscript.

## References

- ACHMADOV, K.; BRECKLE S. and BRECKLE U. (2006): Effects of grazing on biodiversity, productivity, and soil erosion of alpine pastures in Tajik mountains. In: SPEHN, E.; KÖRNER, C. and LIBERMANN, M. (eds.): Land-use change and mountain biodiversity. Boca Raton, 241–249.
- BARNES, D. F.; KHANDKER, S. R. and SAMAD, H. A. (2011): Energy poverty in rural Bangladesh. In: Energy Policy 39, 894–904. DOI: 10.1016/j.enpol.2010.11.014
- BRECKLE, S. and WUCHERER, W. (2006): Vegetation of the Pamir (Tajikistan): land use and desertification problems. In: SPEHN, E.; KÖRNER, C. and LIBERMANN, M. (eds.): Land-use change and mountain biodiversity. Boca Raton, 225–237.
- BREU, T. (2006): Sustainable development in the Tajik Pamirs: the role of knowledge for sustainable land management. Centre for Development and Environment (CDE). Berne.
- BREU, T. and HURNI, H. (2003): The Tajik Pamirs: challenges of sustainable development in an isolated mountain region. Centre for Development and Environment (CDE). Berne. [http://www.cde.unibe.ch/CDE/pdf/The\\_Tajik\\_Pamirs.pdf](http://www.cde.unibe.ch/CDE/pdf/The_Tajik_Pamirs.pdf) (Date: 12.01.2015)
- CHAMBERS, B. (2001): Making better use of livestock manures on arable land. ADAS Gleadthorpe Research Centre. Mansfield.
- CLEMENS, J. (2001): Ländliche Energieversorgung in Astor. Aspekte des nachhaltigen Ressourcenmanagements im nordpakistanischen Hochgebirge. Sankt Augustin.
- DROUX, R. and HOECK, T. (2004): Energy for Gorno Badakhshan! Hydropower and Firewood Cultivation. Analysis of the Energy Situation in the Tajik Pamirs and Its Consequences for Land Use and Resource Management. Centre for Development and Environment (CDE). Berne.
- FÖRSTER, H.; PACHOVA, N. I. and RENAUD, F. G. (2011): Energy and land use in the Pamir-Alai Mountains: examples from five social-ecological regions. In: Mountain Research and Development 31, 305–314. DOI: 10.1659/MRD-JOURNAL-D-11-00041.1
- GROH, S. (2014): The role of energy in development processes. The energy poverty penalty: case study of Arequipa (Peru). In: Energy for Sustainable Development 18, 83–99. DOI: 10.1016/j.esd.2013.12.002
- HOECK, T.; DROUX, R.; BREU, T.; HURNI, H. and MASELLI, D. (2007): Rural energy consumption and land degradation in a post-Soviet setting – an example from the west Pamir Mountains in Tajikistan. In: Energy for Sustainable Development 11, 48–57.
- HOBBERG, G. (Submitted): Modellierung biomassedominierter Energiesysteme. Methodenentwicklung anhand eines Fallbeispiels im Ost-Pamir, Tadschikistan. PhD Thesis. Stuttgart.
- IEA (2010): Energy Poverty – How to make modern energy access universal? Special early excerpt of the World Energy Outlook 2010 for the UN General Assembly on the Millennium Development Goals. Paris.
- IFK (INSTITUT FÜR FEUERUNGS- UND KRAFTWERKSTECHNIK) (2013): Analysenbefund Nr. 2013/173/1631. Stuttgart.
- ISMANOV, A (2013): Viehzahlen Alichur. Persönliche Mitteilung an Georg Hohberg, Alichur.?
- JOHNSON, N. and BRYDON, K. M. (2012): Factors affecting fuelwood consumption in household cookstoves in an isolated rural West African village. In: Energy 46 (1), 310–321.
- KADIAN, P. and KAUSALIK, S. (2002): Rural energy for sustainable development: participatory assessment of energy resources. New Delhi.
- KATSOUKAKOS, N. (2011): Combating energy poverty in mountainous areas through energy-saving interventions: insights from Metsovo, Greece. In: Mountain Research and Development 31, 284–292. DOI: 10.1659/MRD-JOURNAL-D-11-00049.1
- KRAUDZUN, T. (2014): Bottom-up and top-down dynamics of the energy transformation in the Eastern Pamirs of Tajikistan’s Gorno Badakhshan region. In: Central Asian Survey 33 (4), 550–565.
- KRAUDZUN, T.; VANSELOW, K. A. and SAMIMI, C. (2014): Realities and myths of the Teresken Syndrome – An evaluation of the exploitation of dwarf shrub resources in the Eastern Pamirs of Tajikistan. In: Journal of Environmental Management 132, 49–59. DOI: 10.1016/j.jenvman.2013.10.019
- KRECCI, F. (2011): Vulnerabilities in the Eastern Pamirs. Berlin Geographical Papers 39. Berlin.
- MALLA, S. (2013): Household energy consumption patterns and its environmental implications: assessment of energy access and poverty in Nepal. In: Energy Policy 61,

- 990–1002. DOI: 10.1016/j.enpol.2013.06.023
- METI and NASA (2009): Aster Global Digital Elevation Model V002. Sioux Falls. <https://lpdaac.usgs.gov/> (Date: 22.06.2015)
- MIRZA, B. and SZIRMAI, A. (2010): Towards a new measurement of energy poverty: a cross-community analysis of rural Pakistan. UNU-MERIT Working Papers ISSN 1871-987. Maastricht.
- MISLIMSHOEVA, B.; HABLE, R.; FEZAKOV, M.; SAMIMI, C.; ABDULNAZAROV, A. and KOELLNER, T. (2014): Factors influencing households' firewood consumption in the Western Pamirs, Tajikistan. In: *Mountain Research and Development* 34, 147–156. DOI: 10.1659/MRD-JOURNAL-D-13-00113.1
- NUSSBAUMER, P.; BAZILIAN, M. and MODI, V. (2011): Measuring energy poverty: focusing on what matters. Oxford Poverty & Human Development Initiative. Oxford. [http://www.ophi.org.uk/wp-content/uploads/OPHI\\_WP\\_42\\_Measuring\\_Energy\\_Poverty1.pdf](http://www.ophi.org.uk/wp-content/uploads/OPHI_WP_42_Measuring_Energy_Poverty1.pdf) (Date: 12.01.2015)
- NTIS (1973): The GAZ-66 truck, its design and technical servicing. Springfield. [http://www.russianmilitarytrucks.com/docs/Gaz66\\_Tech\\_Man%28en%29.pdf](http://www.russianmilitarytrucks.com/docs/Gaz66_Tech_Man%28en%29.pdf) (Date: 12.01.2015)
- PACHAURI, S. and SPRENG, D. (2011): Measuring and monitoring energy poverty. In: *Energy Policy* 39, 7497–7504. DOI: 10.1016/j.enpol.2011.07.008
- PEREIRA, M. G.; FREITAS, M. A. V. and DA SILVA, N. F. (2010): Rural electrification and energy poverty: empirical evidences from Brazil. In: *Renewable and Sustainable Energy Reviews* 14, 1229–1240. DOI: 10.1016/j.rser.2009.12.013
- RAPIDEYE AG (2009): RapidEye Standard Image Product Specifications. Brandenburg.
- REA, S. (2012): Coking and thermal coal projects. **Presentation. Celsius Coal Limited. Ort?**
- SAN, V.; SPOANN, V.; LY, D.; CHHENG, N. V. (2012): Fuelwood consumption patterns in Chumriey Mountain, Kampong Chnang Province, Cambodia. In: *Energy* 44 (1), 335–346.
- SPALDING-FECHER, R.; WINKLER, H. and MWAKASONDA, S. (2005): Energy and the world summit on sustainable development: what next? In: *Energy Policy* 33, 99–112. DOI: 10.1016/S0301-4215(03)00203-9
- STATDAT.JAMOAT ALICHUR (2013): Statistical data collected from the Jamoat Alichur.
- SRIVASTAVA, L.; GOSWAMI, A.; DILJUN, G. M. and CHAUDHURY, S. (2012): Energy access: revelations from energy consumption patterns in rural India. In: *Energy Policy* 47, 11–20. DOI: 10.1016/j.enpol.2012.03.030
- TAJIK MET SERVICE (2013): Climatic dataset for the Pamir Region acquired from the Tajik hydrometeorological service. Dushanbe.
- UNITED NATIONS (2011): 2012 International Year of sustainable energy for all. <http://www.un.org/en/events/sustainableenergyforall/> (Date:12.01.2015)
- USGS (2013): Landsat 8, Fact Sheet 2013–3060. Sioux Falls. <http://pubs.usgs.gov/fs/2013/3060/pdf/fs2013-3060.pdf> (Date: 12.01.2015)
- VANSELOW, K. (2011): The high mountain pastures of the Eastern Pamirs (Tajikistan). An evaluation of the ecological basis and the pasture potential. Erlangen.
- VANSELOW, K. and SAMIMI, C. (2014): Predictive mapping of dwarf shrub vegetation in an arid high mountain ecosystem Using remote sensing and random forests. In: *Remote Sensing* 6, 6709–6726. DOI: 10.3390/rs6076709
- WALTER, H. and BRECKLE, S. W. (1986): *Ökologie der Erde* (Vol. 3): Spezielle Ökologie der Gemäßigten und Arktischen Zonen Euro-Nordasiens, Zonobiom VI – IX. Stuttgart.
- WIEDEMANN, C.; SALZMANN, S.; MIRSHAKAROV, I. and VOLKMER, H. (2012): Thermal insulation in high mountainous regions: a case study of ecological and socioeconomic impacts in the Eastern Pamirs, Tajikistan. In: *Mountain Research and Development* 32, 294–303. DOI: 10.1659/MRD-JOURNAL-D-11-00093.1
- YUSUFBEKOV, K. and KASACH, A. (1972): *Teresken na Pamire*. Dushanbe.
- ZANDLER, H.; BRENNING, A. and SAMIMI, C. (2015): Quantifying dwarf shrub biomass in an arid environment: comparing empirical methods in a high dimensional setting. In: *Remote Sensing of Environment* 158, 140–155. DOI: 10.1016/j.rse.2014.11.007



**Authors**

Georg Hohberg  
 University of Stuttgart  
 Department of Landscape Planning and Ecology  
 Keplerstr. 11  
 70174 Stuttgart  
 Germany  
 e-mail: georg.hohberg@ilpoe.uni-stuttgart.de

Fanny Kreczi  
 Freie Universität Berlin  
 Institute of Geographical Sciences  
 Centre for Development Studies (ZELF)  
 Malteserstr. 74-100  
 12249 Berlin  
 Germany  
 e-mail: f.kreczi@fu-berlin.de

Harald Zandler  
 University of Bayreuth  
 Department of Geography  
 Nuernbergerstr. 38  
 95440 Bayreuth  
 Germany  
 Email: Harald.Zandler@uni-bayreuth.de



# 7 Scenarios of solar energy utilization on the ‘Roof of the World’: potentials and environmental benefits

---

Harald Zandler, Bunafsha Mislímshoeva & Cyrus Samimi

*Submitted on 05 August 2015 to Mountain Research and Development*

**Mountain Research  
and Development**

This publication provides an assessment of the solar photovoltaic energy potential, evaluating this resource as a woody biomass substitute. By combining a GIS based radiation model and field and literature data into an integrative approach, **hypothesis 4** is addressed. The costs and potential environmental effects of regional solar energy implementation are calculated. As this article was not published before the submission date of this thesis, the format of the manuscript is adapted to this synopsis and the content may be altered in the final form.



## Scenarios of solar energy utilization on the ‘Roof of the World’: potentials and environmental benefits

Harald Zandler<sup>1\*</sup>, Bunafsha Mislimgshoeva<sup>2</sup> & Cyrus Samimi<sup>1,3</sup>

\*Corresponding author: [harald.zandler@uni-bayreuth.de](mailto:harald.zandler@uni-bayreuth.de)

<sup>1</sup> Professorship of Climatology, Faculty of Biology, Chemistry and Earth Sciences, University of Bayreuth, Universitätsstrasse 30, 95447 Bayreuth, Germany

<sup>2</sup> Professorship of Ecological Services, Faculty of Biology, Chemistry and Earth Sciences, University of Bayreuth, Universitätsstrasse 30, 95447 Bayreuth, Germany

<sup>3</sup> Bayreuth Center of Ecology and Environmental Research, BayCEER, Dr. Hans-Frisch-Straße 1-3, 95448 Bayreuth, Germany

### Abstract

Peripheral mountain areas in developing countries are often characterized by energy poverty and simultaneously a high natural potential of solar energy. The Eastern Pamirs of Tajikistan are a prime example of this situation with lacking energetic infrastructure, remoteness, pressure on local natural resources and high incident radiation amounts. However, an integrative assessment of the feasible potential of solar photovoltaic power utilization is lacking in this region as well as in many other mountainous environments. Therefore, we conducted an evaluation of the natural potential, the feasibility and the effects of increased solar photovoltaic electricity generation. Methodologically, we used climatic measurements, a spatial radiation model, field and literature based scenarios of energy requirements, financial frame conditions and biomass data for respective assessments. Results showed that a high natural potential of solar radiation for photovoltaic applications, comparable to some of the most favorable regions, exists. Calculations based on the derived scenarios indicate that the generation of basic thermal energy amounts for hot water boiling with a photovoltaic power plant is feasible within reasonable cost limits in the district capital. A realization of the designed photovoltaic power plant can significantly alter the energetic situation of the region by alleviating energy poverty, increase carbon sequestration by up to 1,500 t/year and reduce uprooting of dwarf shrub stands by up to 2,000 ha/year. We illustrate that the presented integrative approach can be applied straightforwardly when some climatic measurements and field observations are available and that solar photovoltaic energy is an important alternative to other renewable energy resources for the sustainable development of peripheral high mountain communities.

**Keywords:** Eastern Pamirs; Tajikistan; solar energy potential; photovoltaics; high mountain regions; radiation model; alternative energy resources; reduction of vegetation degradation, carbon emission savings

## Introduction

Remote mountain areas serve as illustrative examples of renewable energy potentials in environments characterized by abundant energy scarcity (Förster et al. 2011). Thereby, the Eastern Pamirs of Tajikistan, often referred to as the ‘Roof of the World’, constitute a region with natural and socio-economic conditions that are of special interest to assess the feasibility and possible effects of alternative energy sources. The population is highly dependent on locally available fuel, such as biomass from dwarf shrubs or animal manure, to meet their daily energy demand in a cold and harsh climate. This is mainly caused by a lack of energy infrastructure (as the remote location prevents the connection to the national energy grid), the scarcity or high costs of imported energy (e.g. coal) and poverty (Wiedemann et al. 2012; Kraudzun 2014; Kraudzun et al. 2014). The associated harvesting of dwarf shrub biomass has raised alarming concerns of environmental degradation (Breu et al. 2005; Breckle and Wucherer 2006; Hoeck et al. 2007; Wiedemann et al. 2012), whereas more recent studies indicate that the situation is not that severe (Kraudzun 2014; Kraudzun et al. 2014; Vanselow and Samimi 2014). However, all studies conclude that increased development of renewable energy resources is necessary for a sustainable development (Hoeck et al. 2007; Förster et al. 2011; Wiedemann et al. 2012; Kraudzun 2014; Kraudzun et al. 2014). This situation is of special interest against the background of a large anticipated natural potential of regenerative energy resources: high altitude, pronounced aridity and prevailing clear sky conditions lead to high solar irradiation with up to 90 % of extraterrestrial radiation reaching the surface under ideal conditions. The given circumstances related to lacking infrastructure, peripheral locality, thermal biomass utilization and pressure on the environment with simultaneously high natural potential of renewable energy resources are typical for many mountain areas worldwide, as examples from Nepal (Bhandari and Stadler 2011; Poudyal et al. 2012), Tibet (Wang and Qiu 2009; Limao et al. 2012), Bhutan (Gilman et al. 2009), Chile (Fthenakis et al. 2014) and Greece (Katsoulakos 2011) illustrate. However, in the Eastern Pamirs and many other peripheral mountain regions, neither an assessment of the natural potential of solar energy resources nor an evaluation of feasible photovoltaic power utilization has been carried out. Furthermore, the environmental effects of enforced photovoltaic energy development in the future, e.g. a reduction in dwarf shrub clearance or an increased carbon sequestration (cf. Limao et al. 2012), remain unknown. Generally, existing research on renewable energy resources in developing regions is mostly focused on different methods to derive available solar radiation amounts (Huld et al. 2012), or on the economic comparison of different techniques for rural electrification (Mainali and Silveira 2013), or is based on the environmental and social effects of installed renewable energy infrastructure (Limao et al. 2012). This study aims to integrate different parts of research fields regarding renewable solar energy - from resource assessment to the possible implementation of solar energy supply - by an evaluation of the potential effects of a solar energy utilization scenario in a high mountain environment.

In order to close present regional research gaps and to serve as a general methodological example in assessing the feasible potential of renewable energy resources in peripheral mountain areas, options of utilizing solar energy for electricity generation based on measured natural conditions and socio-economic factors should be examined. Therefore, the main objectives of this study are: (1) to map spatial amounts of monthly solar radiation and derive inclinations resulting in maximum annual incident radiation with a simple method applicable to other economically disadvantaged mountain regions; (2) develop realistic scenarios of solar energy



requirements and financial frame conditions to design a photovoltaic power plant in the region's largest settlement based on available radiation amounts; and (3) examine the expected environmental benefits caused by the anticipated substitution of biomass with solar energy.

## Methodology

### Research area

The Eastern Pamirs of Tajikistan are a high mountain plateau with altitudes mostly between 3,500 m and 5,500 m, covering more than 38,000 km<sup>2</sup> with an area approximately identical to the extent of the *rajon* (district) Murghab (Figure 1). Murghab is also the name of the district's capital and we will refer to the town with this geographic designation throughout this article. The climate is cold and arid with mean temperatures of -1 °C and an average precipitation below 100 mm in the valleys (Murghab annual means 1998-2012, Tajik Hydrometeorological Service 2013). Due to these environmental conditions, forests and trees are absent and dwarf shrubs (*Krascheninnikovia ceratoides*, *Artemisia spec.*) constitute the only locally available woody vegetation. Since energy requirements for cooking and heating are high and the local hydro power plant is unable to deliver sufficient energy, these dwarf shrubs are a major fuel source besides animal manure and imported coal (Kraudzun 2014). Therefore, intensive harvesting of dwarf shrubs takes place whereby the whole plant is extracted as the largest share of biomass is located within the root zone (Zandler et al. 2015). Economically, the region is dominated by animal husbandry, and so besides its importance as a thermal energy carrier, dwarf shrubs are also an essential winter forage source for livestock (Kraudzun 2014). This concurrent utilization and the slow regeneration of dwarf shrubs have led to raising concerns regarding sustainable development and increased the demand for renewable alternatives (Kraudzun et al. 2014). To assess the potential of solar energy, the town of Murghab was selected as the main study site as more than half of the Eastern Pamir's population lives here (about 7000 people in 1515 households (Kreczi 2011)). The existence of a soviet-era hydropower plant which is intended to be modernized in the near future serves as a reference to compare anticipated solar energy amounts. Additionally, a local electricity grid exists which allows for the distribution of energy without additional costs (Kraudzun 2014).

### Assessment of solar radiation amounts

Four automatic weather stations, erected at various locations (Figure 1) to cover main villages and different climatological conditions simultaneously (different altitudes, valley expositions, compass directions), serve as a basis for the assessment of the natural potential of solar energy. At these stations, the parameters global radiation, wind speed, wind direction, relative humidity and temperature are measured at a half hourly interval. The time period available for this study ranges from November 2012 until October 2013 for the Pik Pionerka station (12 months) and from January 2013 until December 2014 for the three other stations (24 months). It was necessary to use own measurements as official climate stations do not measure global radiation. A preliminary observation of the data revealed that - although there is prevailing wind activity in the research area, the potential of this renewable energy resource is considerably below solar energy even at favorable locations and positive synergy effects are negligible. Therefore, wind energy was abandoned as an energy carrier for this study.

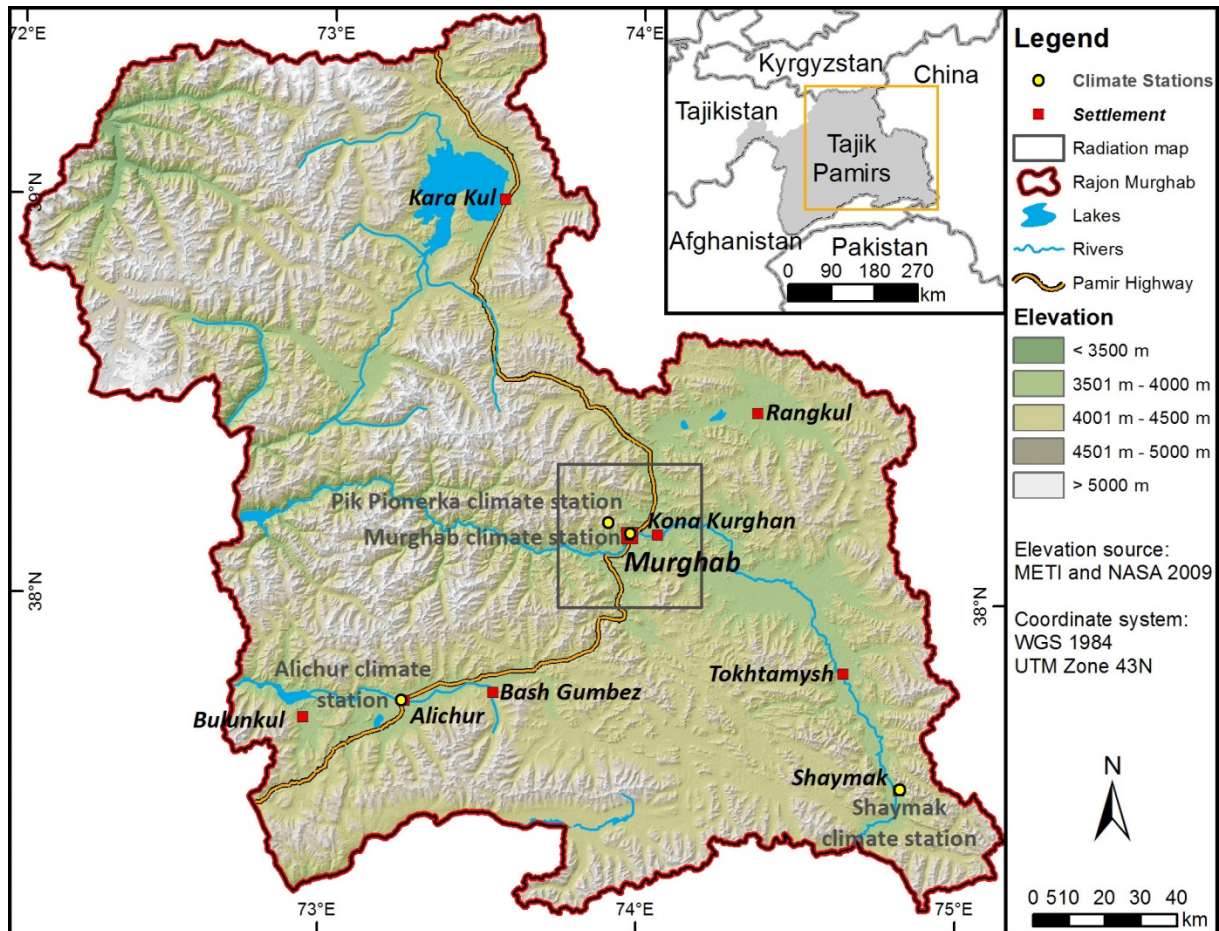


**Figure 1** Map of the study region, climate stations and outline of implementation area for the radiation model.

To spatially map available monthly solar radiation amounts for the Murghab area, measured global radiation data and an ASTER global digital elevation model (GDEM, METI and NASA 2009) were used to calibrate and validate a geographic information system (GIS) based solar radiation model from ArcGIS software (Fu and Rich 1999). This approach was chosen as existing studies showed good performance of comparable GIS based radiation models (Hofierka and Kaňuk 2009; Kumar 2012), and it is considered as an appropriate method in regions with strongly undulating relief (Tovar-Pescador et al. 2006; Pons and Ninyerola 2008). Other methods, e.g. satellite based derivation of radiation amounts, were not considered as there is reason to believe that they are connected to large uncertainties in mountainous terrain (Huld et al. 2012; Amillo et al. 2014). Furthermore, this relatively simple method was selected as it may be a feasible approach in other peripheral mountain regions as well, as extensive and costly measurement campaigns are unlikely to be conducted such regions. To assess performance of the model, the station with the shorter available period and minimal angle of horizon (Pik Pionerka) served as a reference to derive atmospheric input parameters for the model (transmissivity), whereby all other weather stations (Alichur, Murghab, Shaymak) were used for validation and error calculation. Global radiation measurements and the spatial model refer to incident radiation on a horizontal surface. However, to maximize the solar radiation amount that falls on a photovoltaic (PV) cell, solar panels have to be tilted towards the sun and so a conversion from horizontal to inclined radiation is necessary (Evseev and Kudish 2009). To model ideal panel inclinations, yearly radiation sums were modelled iteratively for different tilt angles (southern orientation)

using 5000 points randomly located within Murghab district and with slopes below 20 degrees (Figure 2) to limit the analysis to areas more suitable for potential PV plants (cf. Arán Carrión et al. 2008). The ideal panel inclination was determined as the angle resulting in a maximum annual global radiation sum. This inclination and respective 5000 random points were then used to construct a conversion model based on linear regression between monthly inclined radiation (dependent variable) and monthly horizontal radiation (independent variable). The regression equation was applied to calculate monthly raster maps of incoming global radiation on an ideally tilted surface from the validated horizontal radiation raster. The maps may be generated for the entire Eastern Pamirs to assess spatially resolved solar energy amounts but were restricted to the vicinity of Murghab (i.e. a rectangle with 20 km in each direction from the city center, Figure 1) in this study. They represent the natural potential of solar energy and serve as a basis for site selection and derivation of mean global radiation amounts.

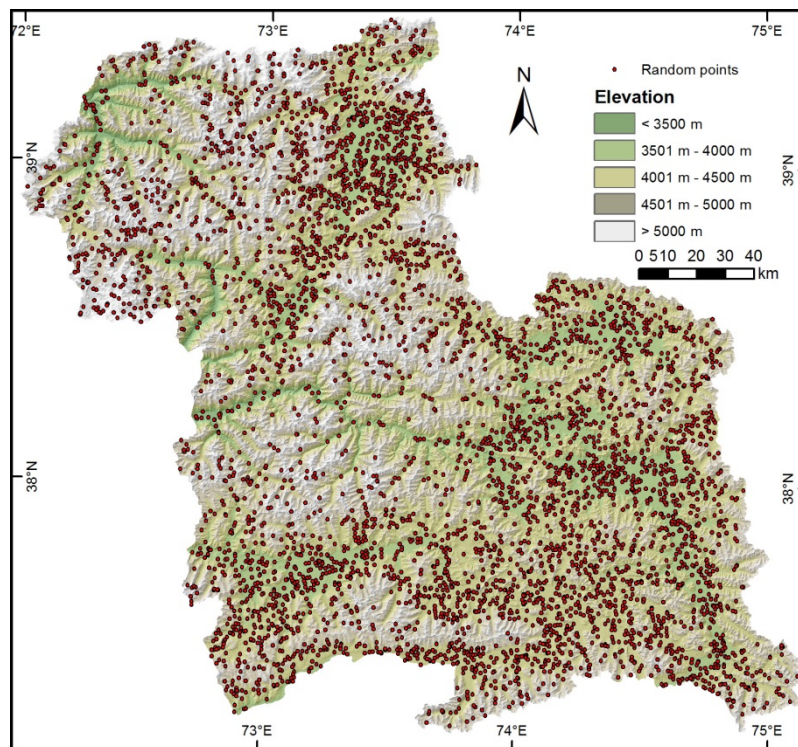


**Figure 2** Locations of 5000 random points used for modeling ideal panel inclination.

### Scenarios of potential solar energy utilization

In the research area, small scale use of solar PV systems for lighting or radio applications is popular (Kraudzun 2014), but larger implementations, which are able to replace thermal energy sources, are absent. Therefore, descriptive utilization scenarios are necessary to assess the feasible potential of solar energy in the research area. Descriptive scenarios are not predictions but tools for the scientific evaluation of possible situations and should represent plausible future developments (Nakićenović and Intergovernmental Panel on Climate Change 2000). Scenarios are frequently applied for studying the potential or perspectives of renewable energy resources (Lund 2007; Shrestha et al. 2007). The scenarios used in this study are based on following assumptions:



a. The financial frame condition scenario is derived from the financial plan of the KfW development bank planning to modernize the local hydropower plant in Murghab for five million Euros (AHK 2013). This budget is hypothesized as a reasonable investment in the regional energy infrastructure. Thus, the maximum amount of investments for this study was assumed as 6,646,500 US\$ (5,000,000 €). The foreign currency translation is set to the annual average of the year 2014 (Oanda 2015).

b. The average annual energy requirement scenario is estimated based on the observation of household energy consumption habits. In the context of this study, household energy consumption is estimated for water boiling, lighting and television, as existing literature shows that electric energy is used for the mentioned appliances when available in the Pamirs (Kraudzun 2014; Mislimeshova et al. 2014). Water boiling is assessed to be a minimum of 10 l/day/household. It is assumed that a household boils water five times a day for tea (1.5 l each time) and 2.5 l for washing dishes. Water for household use is usually brought inside and so kept roughly at room temperature. For water boiling, we selected a 2,400 W electric kettle. The mean measured time for bringing one liter of 17 °C warm water to boil with the selected device is around three minutes (n=10). Considering natural variability of water temperatures and allowing for potentially increased hot water demand, we set the daily operation time to 45 min/day. As for lighting, it is assumed that each household has four lamps, each 9 W (for one room, corridor, outside in front of the house, one additional room or toilet) and the total length of lighting is 7 h/day. Watching television (a 14.2 W for the selected device) is assessed as 6 h/day/household. Cooking/heating is an important component of the total energy consumption. However, as cooking and heating based on PV energy seems to be unrealistic in the research area (due to extraordinarily large energy requirements in this cold climate), it is not included in this study. To assess the costs that would be required to generate energy for heating and cooking applications as well, some preliminary rough estimations are carried out and included in the discussion section.

### Photovoltaic power plant design and cost assessment

Calculation of required infrastructure and total cost is based on the annual energy requirement scenario and a modified approach following Chandel et al. (2014). Therefore, all formulas given in this section are deduced from Chandel et al. (2014) if not stated otherwise:

The panel generation factor (PGF) is based on available radiation amounts and is a central variable to calculate the number of PV panels necessary to generate a desired energy amount. As the required energy has to be minimally provided throughout the year, the month with the lowest incident radiation is taken as a reference for the PV design. Five percent losses (e.g. by dust) are also included.

$$PGF = solar\ irradiance \frac{kWh}{day} * (1 - 0.05) \quad (1)$$

Required energy amounts from the PV modules (PVreq) is calculated by multiplying the energy needs of the scenario times 1.3 to consider 30 % energy losses in the PV system (Chandel et al. 2014). Total watt peak (Wp) rating for PV modules is then derived as:

$$Wp \text{ rating } kW = \frac{PVreq}{PGF} \quad (2)$$

Further calculations are based on PV module specifications. We selected the Solarworld Sunmodule Plus SW 275 mono (SolarWorld AG 2015, Table 1) for the theoretical PV power plant. The cost of the respective module is 331 US\$ (Europe Solarshop 2015a). The number of required PV modules is then calculated as:

$$\text{Number of required PV modules} = \frac{Wp \text{ rating } W}{\text{Module maximum Power } W(Pmax)} \quad (3)$$

Inverters are necessary to convert the generated energy from direct current (DC) to alternating current (AC). The size of inverters should be approximately 30 % larger than the total wattage of modules (Chandel et al. 2014). Satcon Power Gate Plus 100 kW PVS-0100-240 with integrated maximum power point tracking was selected as the inverter model with a total cost of 28,197.89 US\$ (KingSolarman 2015). The number of required inverters is then calculated as:

$$\text{Number of required PV modules} = \frac{Wp \text{ rating } W}{\text{Module maximum Power } W(Pmax)} \quad (4)$$

As solar energy amounts are not equally available throughout the day, battery based energy storage is necessary to allow for a constant electrical power supply. Hoppecke 26 OPzS solar.power 4700 / 48V batteries (Hoppecke Battery GmbH 2015) were selected as storage devices with a unit cost of 35,029.71 US\$ (Europe Solarshop 2015b). Maximum discharge of batteries is set to 40 % and a battery loss of 15 % was assumed (Chandel et al. 2014). Battery autonomy was set to one day and a discharge over 10 hours was expected. Required number of batteries is then calculated from:

$$\text{Required battery capacity Ah} = \frac{\text{total energy requirements } W}{\text{Battery voltage} * \text{depth of discharge} * (1 - \text{losses})} \quad (5)$$

$$\text{Number of required batteries} = \frac{\text{Required battery capacity Ah}}{\text{Battery capacity at Discharge over 10 hours Ah}} \quad (6)$$

To control for energy charging and unloading, additional inverters are necessary. We selected bidirectional Eaton Power Xpert Storage 2250 kW inverters with a unit price of approximately 330,000 US\$ as storage control devices (Eaton 2014). Number of required battery inverters is then derived as:

$$\text{Number of required battery inverters} = \frac{PVreq}{2250 \text{ kW (inverter wattage)}} \quad (7)$$

Finally, all costs for the theoretical PV plant construction are summarized. In addition to the material costs, installation costs of 15 % were assumed (cf. SMA 2015).

## Assessment of maximum biomass and carbon savings

Observations by [Kreczi \(2013\)](#) showed that on average 3.3 medium sized dwarf shrubs are needed for bringing one liter of water to boil. The mean weight of local dwarf shrubs, 234 g, is taken from measurements (n=243) for the local allometric model presented in [Zandler et al. \(2015\)](#). Carbon content of 18 oven-dried dwarf shrub samples was determined with Thermo Quest Flash EA 1112 CHN elemental analyzer at the BayCEER laboratory of the University of Bayreuth. These values were used to calculate maximum biomass and carbon savings by assuming a total substitution of potential dwarf shrub biomass usage for water heating by PV energy. Furthermore, for the assessment it is hypothesized that no other energy carriers for hot water generation are utilized. To assess maximal reduction of cleared dwarf shrub areas, a mean value of 2,087 kg dwarf shrub biomass per ha dwarf shrub stand was assumed according to predictions of the best biomass model presented in [Zandler et al. \(2015\)](#).

**Table 1:** Technical data of the Solarworld Sunmodule Plus SW 275 mono PV panel ([SolarWorld AG 2015](#)).

| Variable                        | Unit | Value |
|---------------------------------|------|-------|
| Maximum power (Pmax)            | W    | 275   |
| Max.power voltage (Vpm)         | V    | 31    |
| Max.power current (Ipm)         | A    | 8.94  |
| Open circuit voltage (VOC)      | V    | 39.4  |
| Short circuit current (ISC)     | A    | 9.58  |
| Maximum system voltage          | Vdc  | 1,000 |
| Temperature coefficient of Pmax | %/°C | -0.45 |
| Temperature coefficient of VOC  | %/°C | -0.3  |
| Temperature coefficient of ISC  | %/°C | 0.04  |

## Results

### Modeled solar radiation amounts and potential energy requirements

Mean measured sum of horizontal solar radiation amounts of the validation stations was 1,751 kWh/m<sup>2</sup>/year in the reference period (2013-2014). The monthly radiation model showed a coefficient of determination (R<sup>2</sup>) of 0.96, a root mean squared error (RMSE) of 11.76 kWh/m<sup>2</sup>/month (relative RMSE of 8.06 %) and a bias of -5,31 kWh/m<sup>2</sup>/month. Monthly variation of modeling errors showed higher errors in winter than in summer with an error of 7.25 % averaged over the whole year ([Table 2](#)). Modeling of ideal panel inclinations showed good performances (R<sup>2</sup> of 0.94 to 0.99) and led to an optimum tilt angle of 26° degrees south to maximize annual solar radiation amounts. Solar incident radiation on ideally inclined surfaces showed an average increase of 11.1 % compared to horizontal solar radiation amounts on the whole raster. Suitable areas for potential PV plants, characterized by flat terrain and minimum inclined radiation values of above 3 kWh/m<sup>2</sup>/day (December), are mainly located to the East of Murghab ([Figure 3a](#)). The selected site for this study shows a linear distance to the nearest grid connected houses of approximately 1,660 m and a mean slope of 3.8 degrees ([Figure 3b](#)). At the study site, the averaged minimum radiation on an ideally inclined surface reached 3.04 kWh/m<sup>2</sup>/day in December and a maximum of 7.33 kWh/m<sup>2</sup>/day in July ([Table 3](#)). The



constructed scenario on energy demand resulted in a required daily energy amount of 2.14 kWh/day per household which implies a total energy demand of 3,237.86 kWh/day for Murghab.

**Table 2:** Modeling errors of the spatial solar radiation model.

| Month          | Error %     | Absolute error Wh/m <sup>2</sup> /day |
|----------------|-------------|---------------------------------------|
| January        | 11.44       | 325                                   |
| February       | 6.39        | 220                                   |
| March          | 3.32        | 146                                   |
| April          | 5.01        | 278                                   |
| May            | 3.06        | 181                                   |
| June           | 2.16        | 152                                   |
| July           | 2.57        | 185                                   |
| August         | 13.40       | 814                                   |
| September      | 5.71        | 325                                   |
| October        | 5.53        | 219                                   |
| November       | 12.61       | 397                                   |
| December       | 15.77       | 411                                   |
| Yearly average | <b>7.25</b> | <b>304</b>                            |

**Table 3:** Mean horizontal and inclined solar radiation amounts within the area of the potential PV plant.

| Month          | Horizontal solar radiation kWh/m <sup>2</sup> /day | Inclined (26° S) solar radiation kWh/m <sup>2</sup> /day |
|----------------|--|--|
| January        | 2.54   | 3.64   |
| February       | 3.12   | 4.11   |
| March          | 4.46   | 5.28   |
| April          | 5.08   | 5.43   |
| May            | 5.90   | 5.82   |
| June           | 7.07   | 6.71   |
| July           | 7.61   | 7.33   |
| August         | 5.27   | 5.45   |
| September      | 5.37   | 6.11   |
| October        | 4.24   | 5.39   |
| November       | 2.86   | 4.02   |
| December       | 2.10   | 3.04   |
| Yearly average | <b>4.63</b>  | <b>5.19</b>  |

### Photovoltaic power plant specifications and cost

The minimum panel generation factor of 2.88 resulted in 5,309 required PV modules to meet the necessary W<sub>p</sub> rating of 1,459.98 kWh . DC/AC transformation required 19 inverters. Furthermore, 57 batteries and two battery inverters were needed to provide continuous energy. This design led to a material cost of 4,949,709 US\$ and a total cost of 5,692,166 US\$ including labor expenses of 15 %. The annual variation of solar radiation resulted in 2.25 kWh/day/household of available energy in December (minimum) and 5.44 kWh/day/household of available energy in July (maximum, Table 4). The general layout of the PV plant led to an arrangement of 13 PV modules in an array, resulting in 409 arrays in 20 rows. Considering a pitch

distance of two meters plus the module length, this resulted in a total PV plant area of 274 x 74 m (Figure 3c).

**Table 4:** Annual variation of anticipated energy availability of designed PV plant per household and day considering losses.

| Month          | kWh/day/household | Panel generation factor |
|----------------|-------------------|-------------------------|
| January        | 2.70              | 3.46                    |
| February       | 3.05              | 3.90                    |
| March          | 3.91              | 5.02                    |
| April          | 4.03              | 5.16                    |
| May            | 4.32              | 5.53                    |
| June           | 4.97              | 6.38                    |
| July           | 5.44              | 6.97                    |
| August         | 4.04              | 5.18                    |
| September      | 4.53              | 5.81                    |
| October        | 4.00              | 5.12                    |
| November       | 2.98              | 3.82                    |
| December       | 2.25              | 2.88                    |
| Yearly average | <b>3.85</b>       | <b>4.93</b>             |

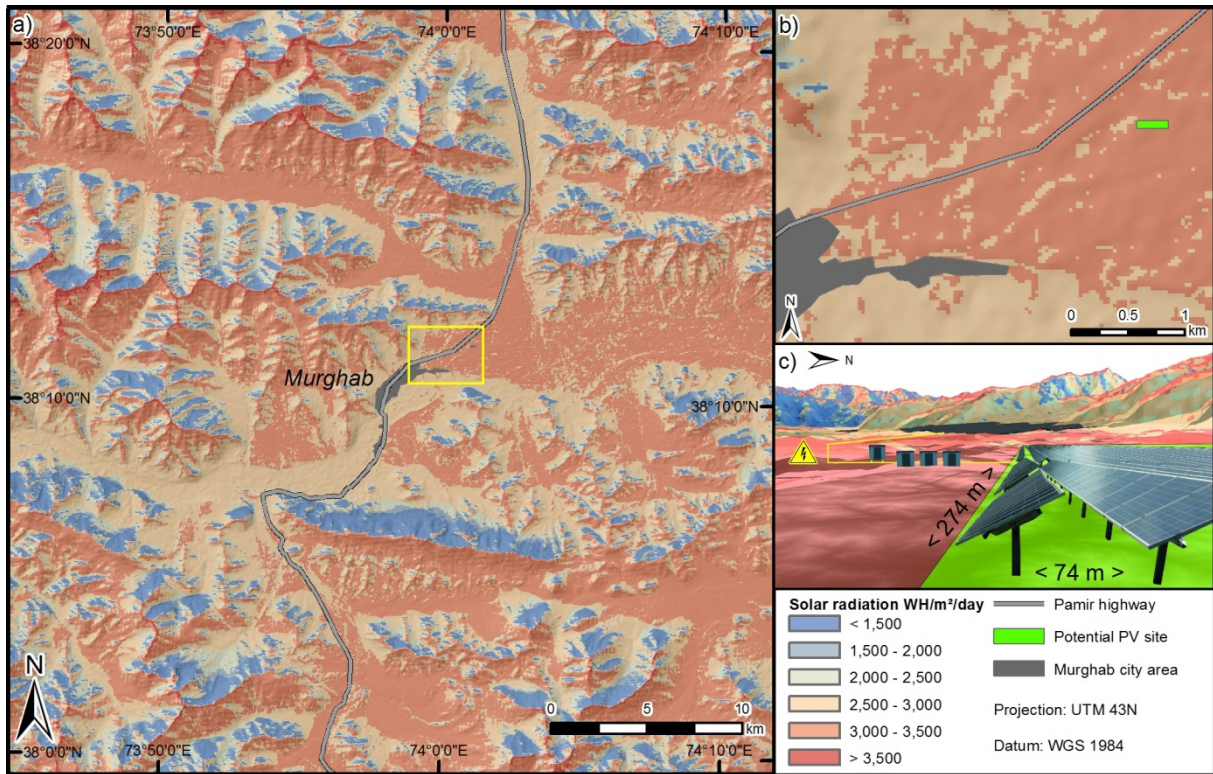


**Figure 3** Modeled minimum solar radiation amounts (December) on a 26° inclined surface for a) the Murghab area, b) the selected region for the potential PV plant and c) a 3D illustration of the potential PV plant.

## Potential biomass and carbon savings

Calculation of potential savings resulted in a maximum reduction of 4,270 t of fresh dwarf shrub biomass per year in Murghab which corresponds to 2,046 ha dwarf shrub area when considering average biomass stocks. With a carbon content of 45.44%, these values result in a maximum decrease of carbon extraction of 1,533 t per year (219 kg per capita) due to potential dwarf shrub harvest in Murghab.

## Discussion

### Performance of solar radiation model

This is the first study that assesses solar energy resources in the research area and may serve as a methodological example for other peripheral mountain areas. The measured solar radiation amounts are comparable to some of the world's most favorable areas for PV development such as Oman (Gastli and Charabi 2010), Spain (Arán Carrión et al. 2008; Pons and Ninyerola 2008), Nepal (Poudyal et al. 2012) or Tibet (Limao et al. 2012). The performance measures (coefficient of determination, RMSE, percentage error rate) of the spatial solar radiation model resulted in equal or better performance in relation to similar approaches (Tovar-Pescador et al. 2006; Pons and Ninyerola 2008; Kumar 2012) and analogous temporal error variations with higher relative errors in winter than in summer months (Pons and Ninyerola 2008). Huld et al. (2012) reported very good performances of satellite based methods to derive solar radiation amounts at lower altitudes, and this approach may be an important alternative when no ground based measurements are available; but the authors state higher errors in mountainous terrain in their study compared to our results. Therefore, the presented method is seen as a reliable and simple approach to derive spatial solar radiation amounts in mountainous regions. However, the negative bias of our model showed that solar radiation is slightly underestimated and derived energy amounts may therefore be regarded as a conservative estimate. The modeled increase of solar radiation from a horizontal to an ideally inclined surface is in the same range as the reported value of 10-12% in other studies (Hartley et al. 1999; Arán Carrión et al. 2008). Hence, calculated solar radiation values available to the solar PV panels constitute a stable foundation to derive potentially generated energy amounts.

### Feasibility of solar PV energy generation

The estimated cost of approximately 5.7 million US\$ for the potential PV plant is slightly lower than the budget of a comparable project in Murghab (AHK 2013). When transferred to investment cost per installed kWp, the PV plant price of 3,900 US\$ per kWp is located at the upper range of figures compiled in Ondraczek (2014). As these costs are related to grid connected PV plants without energy storage, resulting costs of presented PV plant are regarded as financially reasonable. However, the study does not represent an economic assessment of different energy supply systems but shows that thermal energy can be generated from solar PV energy within certain limits and considering realistic cost limits. This would differ substantially if additional thermal energy amounts besides hot water preparation should be met with solar PV energy: if two hours of cooking with a 1,500 W electric stove would be included in the cost assessment, the necessary budget to fulfill the energy requirements would more than double to

nearly 14 million US\$. If heating with a 2,000 W electric heating device and a daily usage of six hours would be included additionally, the total cost of a potential PV plant with energy storage would amount to a total cost of more than 45 Million US\$, which would correspond to an eightfold budget increase compared to the presented scenario. These sums indicate that an implementation of energy generation for heating and cooking using PV energy is not feasible considering the current situation.

The running energy project of the KfW development bank provides an opportunity to compare potential energy amounts generated with solar energy to potential hydro energy amounts. The planned hydropower plant will have an installed maximum capacity of 800 kW (AHK 2013). Without any losses, this would result in a daily maximum production of 19,200 kWh, which corresponds to a budget of 6,646,500 US\$. Solar PV energy, when losses and expenses for energy storage are not considered, would result in approximately 1.4 times higher generated daily energy amounts in the most favorable month (July) with the same budget. Furthermore, a number of limitations may have to be considered regarding hydro energy. A modernization of the hydro power plant may not lead to significantly increased energy amounts as the intake channel will not be substantially enlarged (Kraudzun 2014) and water is a limited resource in this arid environment. Especially in winter, when temperatures of down to -30°C to -40°C occur, a large amount the water in the catchment of the hydro power plant is frozen and does not contribute to the river discharge and energy generation. Similar to comparable Asian high mountain regions (Wang and Qiu 2009), this shows that energy generation with solar PV energy is an important alternative to hydro energy in the Eastern Pamirs.

### **Anticipated effects of PV energy utilization**

The access to modern energy through the presented fictitious PV plant would most likely alter the energy situation in the Eastern Pamirs. On the one hand, characteristics of energy poverty like the inconveniences related to energy supply (Mirza and Szirmai 2010), indoor pollution (Nussbaumer et al. 2011) or dependency on biomass (Groh 2014) may be significantly reduced. Especially the use of dwarf shrubs, presently the most popular fuel for instant water boiling (Wiedemann et al. 2012; Kraudzun et al. 2014), would be expected to decrease as electric kettles would replace current practices. With a maximum reduction in dwarf shrub clearance of 20.5 km<sup>2</sup> per year, the potential PV plant would not only lower the pressure on vegetation resources, but may also have positive effects on livestock breeding as dwarf shrubs play an important part for the regional pasture potential (Vanselow 2011). This would in turn result in increased availability of animal manure, the second important regional thermal energy carrier (Kraudzun 2014), and thus lead to an indirect improvement of the local energy situation. With a carbon savings potential of 219 kg per capita and year, greenhouse gas emissions could be lowered significantly. Although a comparison of this value to other regions is problematic due to different scales and environments, our results are relatively high in relation to findings by Limao et al. (2012), who state that 432,900 t of yearly carbon savings can be gained from a decrease in woody biomass clearings through solar energy implementation in Tibet, which converts to a per capita value of 158 kg using regional population figures provided by the National bureau of statistics of China (2005).



## Methodological limitations

Only two years of climatic measurements were available to calibrate and validate the presented radiation model. Therefore, it is challenging to ascertain that the available data is representative of average climatic conditions. However, our measurements show large conformity with available climatic parameters from the official climate stations averaged over 15 years (Tajik Hydrometeorological Service 2013). Furthermore, precipitation data from the Tropical Rainfall Measuring Mission (TRMM 2014) which may be a proxy for cloudiness and therefore solar radiation, indicates that the relevant time period may be regarded as representative of the long term average. Therefore, we expect that measurements used for this study are largely representative of the long term average solar radiation. Similarly, field observations that form the basis of scenarios on energy requirements do not allow a comprehensive insight into energy consumption habits of local households. An extensive survey on the potential use of electric energy would be needed to enable more accurate scenario specifications. Economically, our feasibility assessment is based on the comparison to a regional investment project. Hence, an increased evaluation of economic feasibility would improve the comparability to other peripheral mountain regions. However, as commonly used economic indicators are also based on a number of assumptions and highly variable input factors (Branker et al. 2011), additional research and a sensitivity analysis would have been necessary, which was beyond the scope of this study. Besides, research on the temporal variation of discharge volumes in conjunction with the specifications of the planned local hydropower plant would be required to calculate monthly generated electricity amounts and thus allow an objective comparison of PV and hydro energy potentials. Finally, as both the scenarios and derived figures of dwarf shrub biomass use and savings are based on assumptions and subject to temporal variations, it is important to consider the associated uncertainties of the study.

## Conclusion

The presented approach integrates different areas of renewable energy research to assess the natural potential, the feasibility and the effects of increased solar photovoltaic electricity generation in a peripheral mountain region. Thereby, we derived the first atlas of solar resources in the Eastern Pamirs of Tajikistan from field measurements. Results showed a high natural potential of solar energy. A good modeling performance indicates the suitability of the method in other mountain areas when some climatic data is available. The modeled radiation amounts combined with realistic scenarios based on own observations, a running energy project and existing research suggest that basic thermal energy can be generated with photovoltaic applications within reasonable cost limits. The presented calculations emphasize that the realization of the fictitious photovoltaic power plant would considerably change the region's energy situation by increasing the sustainability of local energy resource use, alleviating energy poverty and fostering carbon sequestration. More generally, this study showed that solar photovoltaic energy has great potential to improve sustainable development and livelihoods of remote mountain communities as similar conditions persist worldwide. Therefore, solar energy constitutes a suitable alternative to other regenerative energy resources in mountainous environments. We recommend that future studies concentrate on the assessment of the local potential and effects of hydro energy systems based on field measurements and on changes in household's energy consumption if electric energy is increasingly available.

## References

- AHK. 2013. Delegation of the German economy for Central Asia News. KfW financing modernization of hydro-power plant in the Pamirs with 5 million euros. [in German]. <http://zentralasien.ahk.de/news/einzelansicht-nachrichten/artikel/kfw-finanziert-modernisierung-von-wasserkraftwerk-im-pamir-fuer-5-mio-euro/?cHash=da9bf6df826d7cc83d89fd24ca34d009>; accessed on 03 March 2015.
- Amillo A, Huld T, Müller R. 2014. A New Database of Global and Direct Solar Radiation Using the Eastern Meteosat Satellite, Models and Validation. *Remote Sensing* 6:8165–8189.
- Arán Carrión J, Espín Estrella A, Aznar Dols F, Zamorano Toro M, Rodríguez M, Ramos Ridao A. 2008. Environmental decision-support systems for evaluating the carrying capacity of land areas: Optimal site selection for grid-connected photovoltaic power plants. *Renewable and Sustainable Energy Reviews* 12:2358–2380.
- Bhandari R, Stadler I. 2011. Electrification using solar photovoltaic systems in Nepal. *Applied Energy* 88:458–465.
- Branker K, Pathak MJM, Pearce JM. 2011. A review of solar photovoltaic levelized cost of electricity. *Renewable and Sustainable Energy Reviews* 15:4470–4482.
- Breckle S-W, Wucherer W. 2006. Vegetation of the Pamir (Tajikistan): Land Use and Desertification Problems. In E. Spehn, M. Liberman, and C. Körner (eds.), *Land Use Change and Mountain Biodiversity*. Boca Raton, FL.
- Breu T, Maselli D, Hurni H. 2005. Knowledge for sustainable development in the Tajik Pamir Mountains. *Mountain Research and Development* 25:139–146.
- Chandel M, Agrawal GD, Mathur S, Mathur A. 2014. Techno-economic analysis of solar photovoltaic power plant for garment zone of Jaipur city. *Case Studies in Thermal Engineering* 2:1–7.
- Eaton. 2014. Eaton Power Xpert Storage 2250 kW bidirectional inverter data sheet. <http://www.eaton.com/ecm/groups/public/@pub/@electrical/documents/content/pa08303002e.pdf>; accessed on 12 June 2015.
- Europe Solarshop. 2015a. SolarWorld 275 Mono price quote. <http://www.europe-solarshop.com/solar-panels/solarworld-275.html>; accessed on 10 June 2015.
- Europe Solarshop. 2015b. Battery Hoppecke 26 OPzS solar.power 4700 / 48V price quote. <http://www.europe-solarshop.com/batteries/battery-hoppecke-26-opzs-solar-power-4700-48v.html>; accessed on 11 June 2015.
- Evseev EG, Kudish AI. 2009. The assessment of different models to predict the global solar radiation on a surface tilted to the south. *Solar Energy* 83:377–388.
- Förster H, Pachova NI, Renaud FG. 2011. Energy and Land Use in the Pamir-Alai Mountains: Examples From Five Social-ecological Regions. *Mountain Research and Development* 31:305–314.



- Fthenakis V, Atia AA, Perez M, Florenzano A, Grageda M, Lofat M, Ushak S, Palma R. 2014. Prospects for photovoltaics in sunny and arid regions: A solar grand plan for Chile-Part I- investigation of PV and wind penetration. In: Photovoltaic Specialist Conference (PVSC), 2014 IEEE 40th. IEEE. p. 1424–1429.
- Fu P, Rich PM. 1999. Design and implementation of the Solar Analyst: an ArcView extension for modeling solar radiation at landscape scales. In: Proceedings of the 19th annual ESRI user conference. San Diego, USA. p. 1–33.
- Gastli A, Charabi Y. 2010. Solar electricity prospects in Oman using GIS-based solar radiation maps. *Renewable and Sustainable Energy Reviews* 14:790–797.
- Gilman P, Heimiller D, Cowlin SC. 2009. Potential for Development of Solar and Wind Resource in Bhutan. National Renewable Energy Laboratory.
- Groh S. 2014. The role of energy in development processes—The energy poverty penalty: Case study of Arequipa (Peru). *Energy for Sustainable Development* 18:83–99.
- Hartley LE, Martínez-Lozano JA, Utrillas MP, Tena F, Pedrós R. 1999. The optimisation of the angle of inclination of a solar collector to maximise the incident solar radiation. *Renewable Energy* 17:291–309.
- Hoeck T, Droux R, Breu T, Hurni H, Maselli D. 2007. Rural energy consumption and land degradation in a post-Soviet setting—an example from the west Pamir mountains in Tajikistan. *Energy for Sustainable Development* 11:48–57.
- Hofierka J, Kaňuk J. 2009. Assessment of photovoltaic potential in urban areas using open-source solar radiation tools. *Renewable Energy* 34:2206–2214.
- Hoppecke Battery GmbH. 2015. Battery Hoppecke 26 OPzS solar.power 4700 / 48V datasheet. [http://www.europe-solarshop.com/downloadfiles/hoppecke-batteries/OPzS\\_solar.power\\_en0213.pdf](http://www.europe-solarshop.com/downloadfiles/hoppecke-batteries/OPzS_solar.power_en0213.pdf); accessed on 11 June 2015.
- Huld T, Müller R, Gambardella A. 2012. A new solar radiation database for estimating PV performance in Europe and Africa. *Solar Energy* 86:1803–1815.
- Katsoulakos N. 2011. Combating Energy Poverty in Mountainous Areas Through Energy-saving Interventions: Insights From Metsovo, Greece. *Mountain Research and Development* 31:284–292.
- KingSolarman. 2015. Satcon 100 kw inverter details and price quote. <http://king-solarman.com/satcon-powergate-plus-pvs-100-100kw-240vac-inverter.html>; accessed on 11 June 2015.
- Kraudzun T. 2014. Bottom-up and top-down dynamics of the energy transformation in the Eastern Pamirs of Tajikistan’s Gorno Badakhshan region. *Central Asian Survey* 33:550–565.
- Kraudzun T, Vanselow KA, Samimi C. 2014. Realities and myths of the Teresken Syndrome – An evaluation of the exploitation of dwarf shrub resources in the Eastern Pamirs of Tajikistan. *Journal of Environmental Management* 132:49–59.

- Kreczi F. 2011. Vulnerabilities in the Eastern Pamirs. Berlin Geographical Papers 39.
- Kreczi F. 2013. Preliminary data of 2013 energy consumption survey in the Eastern Pamirs of Tajikistan. Berlin, Germany: Freie Universität Berlin.
- Kumar L. 2012. Reliability of GIS-based solar radiation models and their utilisation in agro-meteorological research. Citeseer.
- Limao W, Hongqiang L, Shengkui C. 2012. A Study of the Ecological Effects of Solar Energy Development in Tibet. *Mountain Research and Development* 32:83–91.
- Lund H. 2007. Renewable energy strategies for sustainable development. *Energy* 32:912–919.
- Mainali B, Silveira S. 2013. Alternative pathways for providing access to electricity in developing countries. *Renewable Energy* 57:299–310.
- METI, NASA. 2009. ASTER Global Digital Elevation Model V002. Sioux Falls, South Dakota.
- Mirza B, Szirmai A. 2010. Towards a new measurement of energy poverty: A cross-community analysis of rural Pakistan. UNU-MERIT, Maastricht Economic and Social Research and Training Centre on Innovation and Technology.
- Mislimshoeva B, Hable R, Fezakov M, Samimi C, Abdunazarov A, Koellner T. 2014. Factors Influencing Households' Firewood Consumption in the Western Pamirs, Tajikistan. *Mountain Research and Development* 34:147–156.
- Nakićenović N, Intergovernmental Panel on Climate Change eds. 2000. Special report on emissions scenarios: a special report of Working Group III of the Intergovernmental Panel on Climate Change. Cambridge ; New York: Cambridge University Press.
- National bureau of statistics of China. 2005. China statistical yearbook 2005. <http://www.stats.gov.cn/tjsj/ndsj/2005/indexeh.htm>; accessed on 29 June 2015.
- Nussbaumer P, Bazilian M, Modi V. 2011. Measuring energy poverty: focusing on what matters. Oxford: Oxford Poverty & Human Development Initiative.
- Oanda. 2015. Historical currency exchange rates. <http://www.oanda.com/lang/de/currency/historical-rates/>; accessed on 10 June 2015.
- Ondraczek J. 2014. Are we there yet? Improving solar PV economics and power planning in developing countries: The case of Kenya. *Renewable and Sustainable Energy Reviews* 30:604–615.
- Pons X, Ninyerola M. 2008. Mapping a topographic global solar radiation model implemented in a GIS and refined with ground data. *International Journal of Climatology* 28:1821–1834.
- Poudyal KN, Binod BK, Sapkota B, Kjeldstad B. 2012. Estimation of Global Solar Radiation Using Clearness Index and Cloud Transmittance Factor at Trans-Himalayan Region in Nepal. *Energy and Power Engineering* 04:415–421.

- Shrestha RM, Malla S, Liyanage MH. 2007. Scenario-based analyses of energy system development and its environmental implications in Thailand. *Energy Policy* 35:3179–3193.
- SMA. 2015. Technology Compendium 2 - Solar Stand-Alone Power and Backup Power Supply. <http://files.sma.de/dl/10040/INSELVERSOR-AEN101410.pdf>; accessed on 12 June 2015.
- SolarWorld AG. 2015. Sunmodule Plus SW 265 – 280 mono. [http://www.europe-solarshop.com/downloadfiles/sw/mono\\_265-280\\_en.pdf](http://www.europe-solarshop.com/downloadfiles/sw/mono_265-280_en.pdf); accessed on 6 June 2015.
- Tajik Hydrometeorological Service. 2013. Climatic dataset for the Pamir Region acquired from the Tajik hydrometeorological service. Dushanbe, Tajikistan.
- Tovar-Pescador J, Pozo-Vázquez D, Ruiz-Arias JA, Batlles J, López G, Bosch JL. 2006. On the use of the digital elevation model to estimate the solar radiation in areas of complex topography. *Meteorological Applications* 13:279.
- TRMM. 2014. Tropical Rainfall Measuring Mission Project and Other Sources Monthly Rainfall Product (TRMM Product 3B43 v7), :Goddard Space Flight Center Distributed Active Archive Center (GSFC DAAC). [http://disc.gsfc.nasa.gov/datacollection/TRMM\\_3B43\\_V7.shtml](http://disc.gsfc.nasa.gov/datacollection/TRMM_3B43_V7.shtml); accessed on 06 July 2015.
- Vanselow KA. 2011. The high-mountain pastures of the Eastern Pamirs (Tajikistan): an evaluation of the ecological basis and the pasture potential. Erlangen, Nürnberg, Univ., Diss.
- Vanselow K, Samimi C. 2014. Predictive Mapping of Dwarf Shrub Vegetation in an Arid High Mountain Ecosystem Using Remote Sensing and Random Forests. *Remote Sensing* 6:6709–6726.
- Wang Q, Qiu H-N. 2009. Situation and outlook of solar energy utilization in Tibet, China. *Renewable and Sustainable Energy Reviews* 13:2181–2186.
- Wiedemann C, Salzmann S, Mirshakarov I, Volkmer H. 2012. Thermal Insulation in High Mountainous Regions: A Case Study of Ecological and Socioeconomic Impacts in the Eastern Pamirs, Tajikistan. *Mountain Research and Development* 32:294–303.
- Zandler H, Brenning A, Samimi C. 2015. Quantifying dwarf shrub biomass in an arid environment: comparing empirical methods in a high dimensional setting. *Remote Sensing of Environment* 158:140–155.



## PART III

# SYNTHESIS AND OUTLOOK





## 8 Synthesis

---

This chapter provides an integrative discussion of findings from the individual manuscripts in relation to the research questions and hypotheses of the dissertation. Each hypothesis is repeated and respective conclusions and answers summarized. Remote sensing based quantification of woody biomass represents the central objective of this dissertation which reintroduces the first hypothesis:

**Hypothesis 1:** A combination of a large set of specifically adapted satellite based variables together with adequate selection and modeling techniques enables spatial biomass prediction even under difficult arid conditions.

The submitted thesis successfully performed woody biomass quantification in an arid environment using space-borne optical data (**Manuscript 1**). In so doing, it is the first study that derives spatially resolved dwarf shrub quantities in the research area and, to the knowledge of the author, it is also the first approach that addresses this task in a region with such a low rate of areal vegetation cover using satellite images. However, relatively high prediction errors were apparent in the presented models (RMSE  $\sim 1000$  kg/ha). Therefore, the first research question cannot with certainty be answered in the affirmative. The stated uncertainties necessarily have to be considered when interpreting respective results. Furthermore, the findings are strictly limited to the analyzed area of interest. Yet, these uncertainties and errors are comparable to existing space-borne earth observation studies deriving plant biomass in other regions and are a common phenomenon in remote sensing based analysis, as various error sources exist. Among them, the low intensity of the spectral plant signal constitutes the greatest challenge in the analyzed area.

Considering the first hypothesis in more detail, the presented results verify that a large set of predictor variables is necessary for the analysis and that specific adaptations to arid conditions are of central importance. Most common remote sensing variables and indices were not applicable for biomass prediction; nor were variables that adjust for soil brightness among the essential variables, which implies a result differing from prior expectations. Experimental indices, such as color adjusted VIs and SAV or PC derivatives, represented the most important predictors, and these variables were complemented by measures of vegetation pattern (texture) and topography. This shows that the integration of soil information and a complex, regionally adapted variable set are required for woody biomass prediction under conditions of scarce areal vegetation cover. As transferability of spectral variables is a crucial issue and *a priori* information on optimal predictors is frequently unavailable, the selection of such suitable variable sets and associated variable weighting or selection procedures are key remote sensing topics; which leads to the second part of the hypothesis. Results confirmed that an adequate model enabling high dimensional data handling is necessary. Models that either penalize variables or include variable shrinking resulted in smaller errors and lower overfitting. Most widely used methods, such as multiple linear regression, performed poorly or were not successful in biomass prediction. The

## SYNOPSIS

performance of statistical models showed some overlap compared with existing research, especially regarding the better models, but differing results were reported for the algorithms with lower predictive capability in this study. An important reason for this may be that the application of a statistical model cannot be universally determined as it is dependent on the number of the predictors, the relationship of the predictors to the dependent variable, and the interrelation between the predictors in a given context. In summary, biomass quantification in the most arid regions simultaneously requires sophisticated models that are able to handle several variables and a large number of predictors, including various spectral bands. The latter result is directly related to the discussion of the second hypothesis:

**Hypothesis 2:** The coverage of a broad spectral range and a high spectral resolution increase modeling performance. Hence, hyperspectral data is especially suitable for detecting woody vegetation in drylands.

The results of this thesis provide clear indications that a broad spectral range is important for woody biomass prediction in drylands. Variables or indices utilizing the whole or a large part of the sensors' available spectral range ranked high in the performance assessment, and variables that cover different spectral regions were jointly integrated in the best performing models (**Manuscript 1**). However, the results do not unequivocally indicate certain optimal spectral regions in the multispectral study and both showed similar performances. Important spectral variables comprised bands from the red to NIR regions indicative of photosynthetic parts, red-edge bands sensitive to chlorophyll content or vegetation state, SWIR bands potentially capturing senescent or woody materials, and the blue to red/red-edge domain that may adjust for soil color effects according to literature on the subject. Hence, both sensors comprise bands potentially important in detecting woody vegetation, although some spectral bands may be too broad to precisely reflect features of respective tissue. The absence of the higher spectral resolution in the SWIR may have been compensated for by the additional red-edge band and texture measures of the RapidEye sensor. A synergetic usage of both sensors slightly increased modeling performance. In addition to existing research, these findings strongly suggest a great potential of hyperspectral data for woody biomass analysis; which leads to the second part of this hypothesis (**Manuscript 2**).

In this thesis, with a multitude of available spectral bands, hyperspectral data was shown to improve the modeling of woody biomass and decreased the relative RMSE by up to 20 percentage points compared to multispectral sensors. Thereby, a very large number of spectral indices significantly correlated with dwarf shrub biomass. Though, commonly used band combinations that are indicative of photosynthetic materials did not show the highest correlations with biomass and were not among the most important variables. However, indices from the early SWIR or far SWIR spectral regions highly correlated with dwarf shrub biomass and were among the most important hyperspectral variables. Hence, this spectral domain may be especially suitable for woody biomass quantification in arid environments, since it detects green as well as non-photosynthetic materials, containing cellulose and lignin, and respective tissue is most distinguishable from the background using these wavelengths. Furthermore, the relatively narrow bands may be required to capture small absorption and reflection features of perennial vegetation or reference wavelengths unaffected by

## SYNOPSIS

background variations. The presented findings showed that space-borne hyperspectral sensors enable and improve the modeling of woody plant spectral properties in the world's drylands.

In spite of the mentioned encouraging factors regarding hyperspectral remote sensing of scarce woody vegetation, this thesis also clearly demonstrated the limits of hyperspectral data. First, space-borne hyperspectral imagery is currently in an experimental stage and respective research is restricted to small test regions, which also applied in this study. The presented results also underline the boundaries in the transferability of specific hyperspectral VIs. This may be owing to regional differences in soil color that may diversely influence VI-values, and color correction may also be required for hyperspectral data analysis. Similarly to the first manuscript, this limited transferability emphasizes the relevance of techniques that are able to handle large data sets for repeated model fitting and automatically select or weigh variables. This becomes particularly obvious in light of the more than 12,000 unique VIs that are available using hyperspectral bands. Finally, although hyperspectral data considerably improved modeling in one region, notable errors were still present, and very low vegetation cover resulted in an only slightly higher performance of the hyperspectral sensor compared to multispectral images in parts of the research area. This indicates that below a certain vegetation threshold, the plant signal is increasingly affected by background effects or noise, and space-borne detection is very constrained regardless of the sensor. In summary, this thesis outlined a number of solutions and methods for the derivation of woody vegetation quantities in arid environments. Taking the connected uncertainties into account, the results of the remote sensing approach provide data on the spatial distribution of dwarf shrub amounts over a region covering more than 20,000 km<sup>2</sup>. These outcomes enable the analysis of regional research issues; which leads to findings regarding the third hypothesis:

**Hypothesis 3:** Despite some rather pessimistic assessments regarding dwarf shrub resources in existing research, there are still regions with large stocks of dwarf shrub biomass to meet local thermal energy demands.

Biomass maps confirm the findings of more recent research studies on the degradation of dwarf shrub formations and extend the regional picture by providing empirically based biomass quantities. Results clearly showed a diversification in the biomass availability of different regions (**Manuscript 1**). The highest dwarf shrub amounts are present in side valleys and on higher elevations, the least amounts in the main valleys, at lower altitudes and in the north-central region. A qualitative comparison suggests depletion in areas of increased human utilization, with a distribution of scarcer dwarf shrub amounts near main roads (e.g. Pamir highway) and larger villages, especially near Murghab, in contrast to high dwarf shrub amounts in more remote areas and around smaller villages (e.g. Shaymak). A more sophisticated assessment of the regional situation was provided through an integrative evaluation with interdisciplinary methods in a case study village (**Manuscript 3**). In this evaluation, dwarf shrub biomass accessible to harvesters was calculated and then compared to actual demand. The consideration of modeling uncertainties led to the conception of a conservative model which subtracts the average error from the prediction to calculate expected minimum quantities. This resulted in relatively large dwarf shrub amounts that are

## SYNOPSIS

available to the local population with the current harvesting practices and possibilities of transport. Considering local figures on yearly dwarf shrub use, the model showed that woody biomass resources are sufficient to meet fuel demands on the medium term. Most households of the case study village are therefore able to meet their basic energy demands, and the presented results contradict studies suggesting a severe energy crisis. According to these empirically based results, the third hypothesis can be verified on the medium term and on a local scale.

However, considering the time scale as a central factor influences this perspective substantially. Soviet literature and additional findings indicate a regeneration rate that is too slow for the recovery of dwarf shrub stocks near settlements, given the contemporary harvesting quantities. Cleared areas are also visible in the vicinity of the case study village. Hence, a depletion of dwarf shrub resources is not unlikely in the long run. Additionally, the distances to lucrative harvesting areas increase and accessibility is lessened. For some households, this may hamper or prevent the provision of a basic energy supply. At present, many areas with high dwarf shrub biomass amounts are only accessible by vehicle with reasonable effort, and the availability of affordable motor fuel is a key issue for the regional thermal energy supply. Finally, the presented results are restricted to the case study village which may not be representative of the whole region as the energy situation is highly diversified in general and energy demand is much higher in Murghab as it is the largest settlement. However, these findings provide a first assessment of the energy situation based on extensive empirical data, and substantially improve the state of geographical research in the Eastern Pamirs. Yet, the presented thesis was not only aimed at the assessment of current woody biomass resources, but intended to evaluate the feasibility of solar energy as a possible alternative with the associated fourth hypothesis:

**Hypothesis 4:** An integrative approach, combining climatic measurements, GIS based radiation modeling, and additional survey data, enables an assessment of the feasibility and effects of increased solar photovoltaic energy utilization.

This dissertation represents the first study providing field based information on regional solar energy resources in the Eastern Pamirs (**Manuscript 4**). The underlying GIS based radiation model achieved good results in spatially determining the natural solar energy potential. It thereby enabled the derivation of ideal panel inclinations and created a sound basis for the calculation of potentially generated energy amounts. Errors resulted in slightly underestimated radiation quantities, but were similar to existing studies in complex mountain terrain. The main uncertainties of the model originate from the restrictions of a relatively short time period of climatic measurements, but comparisons to other data indicate sufficient representativeness of the long term conditions. The calculation of financial requirements for the construction of a solar photovoltaic power plant in the district capital Murghab using various scenarios of energy demand enabled addressing to the third research question. The generation and storage of thermal energy for cooking and heating purposes using photovoltaic systems demands excessive costs and is not considered to be feasible in regard to the present situation. However, restricting the energy requirements to the generation of basic electric energy supply for lighting, entertainment devices and, more importantly, the

## SYNOPSIS

generation of hot water, resulted in a different conclusion. With a total cost of less than five million Euros, such a potential realization proved to lie within reasonable cost limits as this is the budget of a comparable, ongoing regional hydro-energy project. Field observations and existing social surveys indicate that the aforementioned forms of electric energy utilization are most likely viable. The generation of thermal energy with photovoltaic systems may constitute a feasible alternative to dwarf shrub use to a certain degree. In agreement with high mountain research results of comparable areas, this shows that solar resources are an important renewable energy option besides other regional energy carriers.

The development of a photovoltaic power plant for basic electric energy supply would substantially alter the energy system of the region. The presented thesis performed an assessment of the anticipated environmental effects through the hypothesized substitution of dwarf shrub biomass with electric energy for hot water boiling. The potential decrease of cleared annual dwarf shrub stands would result in a significant increase of carbon fixation in the ecosystems and simultaneously, enhance pasture quality. A reduction of negative effects related to energy poverty, such as indoor pollution or excessive physical labor in supplying energy, would considerably improve the living conditions of the local population. The locally adapted assessment of the solar energy potential based on the integration of different fields of renewable energy research showed that photovoltaic systems have the realistic possibility to substantially contribute to sustainable development in the Eastern Pamirs of Tajikistan.

## 9 Outlook

---

Pursuing a research objective inevitably leads to the emergence of new research questions, the recognition of limitations, and the formation of new ideas to overcome related problems. Several approaches were not tested in this dissertation. In addition to the image based analysis of woody vegetation, a sampling of field based spectra would generate further information on unique spectral features of shrub biomass as compared to soil or other plants. Respective data may enable a target oriented search on ideal spectral regions or the testing of alternative modeling concepts based on fractional analysis of soil, green, and nonphotosynthetic vegetation (Meyer and Okin 2015). Other SMA methods, presently problematic due to the lack of pure endmember sites in arid regions, may become more suitable in the near future due to new algorithms, such as endmember purification procedures (Ma et al. 2015). These techniques would constitute fundamentally different approaches and provide important references on the performance of various methods in a region that sets the limits of remote sensing. In addition to these concepts, the analyzed time period of a research approach is central to addressing certain objectives. Due to the complexity and limitations of arid regions, this thesis focused on the derivation of present biomass in a first step, and hence represents a static approach. However, temporal vegetation dynamics in relation to human activities are another central issue in the Eastern Pamirs. Future research may therefore primarily aim at the development of appropriate change detection algorithms based on the findings of existing remote sensing studies. In this context, different potential techniques are available (Lu et al. 2004; Hecheltjen et al. 2014). Since the Landsat sensor showed to be of use in biomass detection, within certain limits, and the Landsat legacy project provides decades of satellite imagery, an approach with Landsat time series using specifically adapted change thresholds (cf. Zhu and Woodcock 2014) may enable important insights on vegetation degradation and the inference of related causes.

The presented results clearly showed that a number of variables spanning the spectrum from the blue to the SWIR domain are important for the derivation of woody biomass in arid regions. Data from recently launched and upcoming sensors, complementing these spectral domains with more bands, are hypothesized to significantly increase performance of biomass modeling in drylands. The multispectral Sentinel 2a sensor, launched on 23<sup>rd</sup> of June 2015, will provide freely available images with a medium spatial resolution (10 m to 60 m) and a spectral configuration that includes several red-edge and two SWIR bands (ESA 2015a). This sensor incorporates the advantages of the RapidEye and Landsat sensors and may be especially suitable for regional vegetation modeling which will be tested in the research area when respective data becomes available. Such an analysis may be supplemented by texture attributes derived from SPOT-5 imagery with up to 2.5 m spatial resolution (ESA 2015b) which is accessible free of charge since 2014 after an application process. Besides multispectral images, the thesis indicates a large potential of operational hyperspectral data. Data from the upcoming Hyperspectral Infrared Imager (HyspIRI, California Institute of Technology 2015) or the Environmental Mapping and Analysis Program (EnMAP, EnMAP Science Advisory Group 2015) will allow for extensive and profound analysis in this regard.



## SYNOPSIS

Especially the coupling of hyperspectral bands with topographic predictors or other techniques successfully applied in the presented dissertation, such as color adjustments and SAV variables, are considered a promising approach for increasing modeling performance. Therefore, research on the suitability of sensors using models that enable high dimensional data handling will continue to improve remote sensing applications in these challenging ecosystems.

This study focused on a broad range of remote sensing techniques and variables, but some amplification may increase the accuracy of the approach. First, future work may concentrate on the main variables that proved to contribute to biomass modeling and on the respective correction algorithms. Increased sampling of bare soil spectral properties with various background colors in relation to woody biomass features would enable the development of new adjustment indices that are considered very advantageous in this thesis. Further, due to the multitude of different soil colors that may diversely affect vegetation indices, a preceding classification that differentiates between soil color classes and subsequent partitioned biomass models may enhance dwarf shrub mapping with additional ground truth data. Similarly, the presented approach could be connected to sophisticated classification results, as presented in [Vanselow \(2011\)](#). If such a classification is extended to the whole research area with additional satellite images, this might improve the preclassification applied in this thesis. A further option for increasing modeling performance is the inclusion of more accurate topographic variables, as they proved to be a central factor for biomass modeling. Products of the TerraSAR-X add-on for Digital Elevation Measurement (TanDEM-X) mission may provide topographic data with a higher spatial resolution (12 m) and outstanding accuracy and may be globally available at the end of 2016 ([Bräutigam et al. 2015](#)). Apart from applied topographic variables, a direct integration of modeled annual solar radiation may be a better indicator of biomass quantities because it is a main driver of evapotranspiration, and hence of water availability, which represents a key limiting factor for vegetation growth in arid regions.

The evaluation of the energy situation, by linking dwarf shrub amounts to accessibility and demand, was restricted to a rather local scale as regional survey data was not completely analyzed during the finalization of this thesis. Therefore, the assessment will be extended to the whole region in a next step to provide a comprehensive image of the energy conditions in the Eastern Pamirs. The district capital Murghab is of main interest in this context. Another important regional research issue is the empirical appraisal of sustainable dwarf shrub harvesting amounts. To address this subject, comprehensive figures on the regeneration of shrubs would be required. However, these plants are characterized by an extremely slow growth rate in this environment and sophisticated dendrochronological dating attempts, tested in collaboration with experts from the University of Erlangen-Nuremberg (Dr. Jussi Griebinger), have not yet been successful. Future research may therefore focus on long-term observations of meticulously maintained field plots and enclosures (cf. [Su et al. 2015](#)) to shed light on the regrowth of dwarf shrubs under different conditions.

## SYNOPSIS

Finally, the integrative feasibility study of solar photovoltaics as an alternative thermal energy source may be complemented in various ways. A longer time period of climatic measurements will enhance the reliability of the model. Although the performance of the GIS based radiation model showed adequate results, comparative testing using other and more complex models may increase modeling accuracy (Ruiz-Arias et al. 2009). Shifting the focus to a more financial perspective with calculations of economic indicators may allow for a better comparison with other developing mountain regions. Measurements on river discharge together with technical specifications of hydro-power systems may provide data to directly compare different locally available energy resources. In addition, the actual as well as the potential electric energy demand and usage should be increasingly analyzed using a social scientific approach for a better adaption of basic assessment scenarios. Therefore, the presented study provides insights into the state of local energy resources and analyzing methods, but also points out various ways of adapting and improving related future research.

# Literature

---

- AIRS science team, Teixeira J. 2013. Aqua AIRS Level 3 Daily Standard Physical Retrieval (AIRS+AMSU), version 006, Greenbelt, MD, USA: NASA Goddard Earth Science Data and Information Services Center (GES DISC),.
- Amillo A, Huld T, Müller R. 2014. A New Database of Global and Direct Solar Radiation Using the Eastern Meteosat Satellite, Models and Validation. *Remote Sensing* 6:8165–8189.
- Arán Carrión J, Espín Estrella A, Aznar Dols F, Zamorano Toro M, Rodríguez M, Ramos Rídao A. 2008. Environmental decision-support systems for evaluating the carrying capacity of land areas: Optimal site selection for grid-connected photovoltaic power plants. *Renewable and Sustainable Energy Reviews* 12:2358–2380.
- Asner GP, Green R. 2001. Imaging spectroscopy measures desertification in United States and Argentina. *Eos, Transactions American Geophysical Union* 82:601–606.
- Asner GP, Heidebrecht KB. 2002. Spectral unmixing of vegetation, soil and dry carbon cover in arid regions: Comparing multispectral and hyperspectral observations. *International Journal of Remote Sensing* 23:3939–3958.
- Asner GP, Wessman CA, Bateson C, Privette JL. 2000. Impact of tissue, canopy, and landscape factors on the hyperspectral reflectance variability of arid ecosystems. *Remote Sensing of Environment* 74:69–84.
- Bannari A, Morin D, Bonn F, Huete AR. 1995. A review of vegetation indices. *Remote Sensing Reviews* 13:95–120.
- Baskerville GL. 1972. Use of logarithmic regression in the estimation of plant biomass. *Canadian Journal of Forest Research* 2:49–53.
- Beck R. 2003. EO-1 User Guide v. 2.3. Sioux Falls, SD. <http://eo1.usgs.gov/documents/EO1userguidev2pt320030715UC.pdf>; accessed on 07 August 2015.
- Benjamini Y, Hochberg Y. 1995. Controlling the False Discovery Rate: A Practical and Powerful Approach to Multiple Testing. *J. R. Statist. Soc. B* 57:289–300.
- Bhandari R, Stadler I. 2011. Electrification using solar photovoltaic systems in Nepal. *Applied Energy* 88:458–465.
- Bradley AP. 1997. The use of the area under the {ROC} curve in the evaluation of machine learning algorithms. *Pattern Recognition* 30:1145 – 1159.
- Branker K, Pathak MJM, Pearce JM. 2011. A review of solar photovoltaic levelized cost of electricity. *Renewable and Sustainable Energy Reviews* 15:4470–4482.

## SYNOPSIS

- Bräutigam B, Martone M, Rizzoli P, Gonzalez C, Wecklich C, Borla Tridon D, Bachmann M, Schulze D, Zink M. 2015. Quality assessment for the first part of the TANDEM-X global digital elevation model. *International Archives of the Photogrammetry, Remote Sensing & Spatial Information Sciences* XL-7/W3.
- Breckle S-W, Wucherer W. 2006. Vegetation of the Pamir (Tajikistan): Land Use and Desertification Problems. In E. Spehn, M. Liberman, and C. Körner (eds.), *Land Use Change and Mountain Biodiversity*. Boca Raton, FL.
- Breiman L. 2001. Random forests. *Machine learning* 45:5–32.
- Brenning A. 2009. Benchmarking classifiers to optimally integrate terrain analysis and multispectral remote sensing in automatic rock glacier detection. *Remote Sensing of Environment* 113:239–247.
- Brenning A. 2012. Spatial cross-validation and bootstrap for the assessment of prediction rules in remote sensing: the R package *sperrrest*. In: *Geoscience and Remote Sensing Symposium (IGARSS), 2012 IEEE International*. IEEE. p. 5372–5375.
- Brenning A, Long S, Fieguth P. 2012. Detecting rock glacier flow structures using Gabor filters and IKONOS imagery. *Remote Sensing of Environment* 125:227–237.
- Breu T. 2006. *Sustainable Land Management in the Tajik Pamirs: The Role of Knowledge for Sustainable Development*. Berne: NCCR North-South / Centre for Development and Environment (CDE).
- Breu T, Maselli D, Hurni H. 2005. Knowledge for Sustainable Development in the Tajik Pamir Mountains. *Mountain Research and Development* 25:139–146.
- Budka H. 2003. *Methoden der fernerkundungsgestützten Landnutzungskartierung und ihre Anwendung auf das Weidepotential des Ost-Pamir (Tadschikistan)*. University of Erlangen-Nuremberg. Diploma thesis. University of Erlangen-Nuremberg, Germany.
- Buyantuyev A, Wu J, Gries C. 2007. Estimating vegetation cover in an urban environment based on Landsat ETM+ imagery: A case study in Phoenix, USA. *International Journal of Remote Sensing* 28:269–291.
- California Institute of Technology. 2015. *HyspIRI Mission Study*. <https://hyspiri.jpl.nasa.gov/>; accessed on 24 August 2015.
- Calvão T, Palmeirim JM. 2004. Mapping Mediterranean scrub with satellite imagery: biomass estimation and spectral behaviour. *International Journal of Remote Sensing* 25:3113–3126.
- Calvão T, Palmeirim JM. 2011. A comparative evaluation of spectral vegetation indices for the estimation of biophysical characteristics of Mediterranean semi-deciduous shrub communities. *International Journal of Remote Sensing* 32:2275–2296.

## SYNOPSIS

- Chandel M, Agrawal GD, Mathur S, Mathur A. 2014. Techno-economic analysis of solar photovoltaic power plant for garment zone of Jaipur city. *Case Studies in Thermal Engineering* 2:1–7.
- Droux R, Hoeck T. 2004. Energy for Gorno Badakhshan! Hydropower and Firewood Cultivation. Analysis of the Energy Situation in the Tajik Pamirs and Its Consequences for Land Use and Resource Management. Joint Diploma Thesis. Centre for Development and Environment (CDE), University of Berne, Switzerland.
- Dürr B, Zelenka A. 2009. Deriving surface global irradiance over the Alpine region from METEOSAT Second Generation data by supplementing the HELIOSAT method. *International Journal of Remote Sensing* 30:5821–5841.
- Eisfelder C, Kuenzer C, Dech S. 2012. Derivation of biomass information for semi-arid areas using remote-sensing data. *International Journal of Remote Sensing* 33:2937–2984.
- Elvidge CD, Chen Z. 1995. Comparison of broad-band and narrow-band red and near-infrared vegetation indices. *Remote Sensing of Environment* 54:38 – 48.
- EnMAP Science Advisory Group. 2015. Environmental Mapping and Analysis Program - Preparing to Exploit the Science Potentials. [http://www.enmap.org/sites/default/files/pdf/pub/EnMAP\\_komplett\\_web\\_eng.pdf](http://www.enmap.org/sites/default/files/pdf/pub/EnMAP_komplett_web_eng.pdf); accessed on 24 August 2015.
- ERDAS. 1999. ERDAS Field Guide. Fifth Edition, Revised and Expanded. Atlanta, GA: ERDAS Inc.
- Erdélyi R, Wang Y, Guo W, Hanna E, Colantuono G. 2014. Three-dimensional Solar Radiation Model (SORAM) and its application to 3-D urban planning. *Solar Energy* 101:63–73.
- ESA. 2015a. SPOT HRG/HRS. <https://earth.esa.int/web/guest/data-access/browse-data-products/-/article/spot-5-hrg-archive>; accessed on 24 August 2015.
- ESA. 2015b. Sentinel 2. <https://earth.esa.int/web/guest/missions/esa-future-missions/sentinel-2>; accessed on 24 August 2015.
- Escadafal R, Huete A. 1991. Étude des propriétés spectrales des sols arides appliquée à l'amélioration des indices de végétation obtenus par télédétection. *C. R. Acad. Sci. Paris* 312:1385–1391.
- ESRI. 2015. Independent Report Highlights Esri as Leader in Global GIS Market. <http://www.esri.com/esri-news/releases/15-1qtr/independent-report-highlights-esri-as-leader-in-global-gis-market>; accessed on 14 August 2015.
- Förster H, Pachova NI, Renaud FG. 2011. Energy and Land Use in the Pamir-Alai Mountains: Examples From Five Social-ecological Regions. *Mountain Research and Development* 31:305–314.

## SYNOPSIS

- Fuchs H, Magdon P, Kleinn C, Flessa H. 2009. Estimating aboveground carbon in a catchment of the Siberian forest tundra: Combining satellite imagery and field inventory. *Remote Sensing of Environment* 113:518–531.
- Fu P, Rich PM. 1999. Design and implementation of the Solar Analyst: an ArcView extension for modeling solar radiation at landscape scales. In: *Proceedings of the 19th annual ESRI user conference*. San Diego, USA. p. 1–33.
- Gaughan AE, Holdo RM, Anderson TM. 2013. Using short-term MODIS time-series to quantify tree cover in a highly heterogeneous African savanna. *International Journal of Remote Sensing* 34:6865–6882.
- Gelder BK, Kaleita AL, Cruse RM. 2009. Estimating Mean Field Residue Cover on Midwestern Soils Using Satellite Imagery. *Agronomy Journal* 101:635.
- Gilman P, Heimiller D, Cowlin SC. 2009. Potential for Development of Solar and Wind Resource in Bhutan. National Renewable Energy Laboratory.
- Guanter L, Richter R, Kaufmann H. 2009. On the application of the MODTRAN4 atmospheric radiative transfer code to optical remote sensing. *International Journal of Remote Sensing* 30:1407–1424.
- Hand DJ, Till RJ. 2001. A simple generalisation of the area under the ROC curve for multiple class classification problems. *Machine learning* 45:171–186.
- Hassan RM, Scholes RJ, Ash N eds. 2005. *Ecosystems and human well-being: current state and trends: findings of the Condition and Trends Working Group of the Millennium Ecosystem Assessment*. Washington, DC: Island Press.
- Hecheltjen A, Thonfeld F, Menz G. 2014. Recent Advances in Remote Sensing Change Detection – A Review. In: Manakos I, Braun M, editors. *Land Use and Land Cover Mapping in Europe*. Vol. 18. Dordrecht: Springer Netherlands. p. 145–178.
- Heklau H, von Wehrden H. 2011. Wood anatomy reflects the distribution of *Krascheninnikovia ceratoides* (Chenopodiaceae). *Flora - Morphology, Distribution, Functional Ecology of Plants* 206:300–309.
- Hergarten C. 2004. Investigations on land cover and land use of Gorno Badakhshan (GBAO) by means of land cover classifications derived from LANDSAT 7 data making use of remote sensing and GIS techniques. Diploma thesis. Centre for Development and Environment (CDE), University of Berne, Switzerland.
- Hoeck T, Droux R, Breu T, Hurni H, Maselli D. 2007. Rural energy consumption and land degradation in a post-Soviet setting—an example from the west Pamir mountains in Tajikistan. *Energy for Sustainable Development* 11:48–57.
- Hofierka J, Kaňuk J. 2009. Assessment of photovoltaic potential in urban areas using open-source solar radiation tools. *Renewable Energy* 34:2206–2214.



## SYNOPSIS

- Hohberg G. submitted. Modeling of biomass dominated energy systems. Case study based methodology development in the Eastern Pamirs, Tajikistan [in German]. Unpublished dissertation. Stuttgart, Germany: University of Stuttgart.
- Hohberg G, Kreczi F. 2013. Unpublished preliminary data of 2013 energy consumption survey in the Eastern Pamirs of Tajikistan. Berlin, Germany: Freie Universität Berlin.
- Holm AM, Cridland SW, Roderick ML. 2003. The use of time-integrated NOAA NDVI data and rainfall to assess landscape degradation in the arid shrubland of Western Australia. *Remote Sensing of Environment* 85:145–158.
- Huete A. 2014. Vegetation Indices. In: *Encyclopedia of Remote Sensing*. New York, NY: Springer. p. 883–886.
- Huete AR. 1988. A soil-adjusted vegetation index (SAVI). *Remote Sensing of Environment* 25:295 – 309.
- Huld T, Müller R, Gambardella A. 2012. A new solar radiation database for estimating PV performance in Europe and Africa. *Solar Energy* 86:1803–1815.
- Irons JR, Petersen GW. 1981. Texture transforms of remote sensing data. *Remote Sensing of Environment* 11:359 – 370.
- Jackson R, Pinter P, Reginato R. 1980. Hand held radiometry: a set of notes developed for use at the workshop of hand held radiometry. Phoenix, AZ: NTIS.
- James G, Witten D, Hastie T, Tibshirani R. 2013. *An Introduction to Statistical Learning*. New York, NY: Springer New York.
- Jiménez-Muñoz JC, Sobrino JA, Mattar C, Franch B. 2010. Atmospheric correction of optical imagery from MODIS and Reanalysis atmospheric products. *Remote Sensing of Environment* 114:2195–2210.
- Justice CO, Townshend JG. 1981. Integrating ground data with remote sensing. In: *Terrain analysis and remote sensing*. London: Townshend, J.G., Ed.; Allen and Unwin. p. 38–58.
- Khorram S, Nelson SAC, Koch FH, van der Wiele CF. 2012. *Remote Sensing*. Boston, MA: Springer US.
- Kraudzun T. 2014. Bottom-up and top-down dynamics of the energy transformation in the Eastern Pamirs of Tajikistan's Gorno Badakhshan region. *Central Asian Survey* 33:550–565.
- Kraudzun T, Vanselow KA, Samimi C. 2014. Realities and myths of the Teresken Syndrome – An evaluation of the exploitation of dwarf shrub resources in the Eastern Pamirs of Tajikistan. *Journal of Environmental Management* 132:49–59.
- Kreutzmann H. 2002. Gorno-Badakhshan: Experimente mit der Autonomie: sowjetisches Erbe und Transformation im Pamir. In: *Internationales Asienforum*. 33. p. 31–46.

## SYNOPSIS

- Kruse FA, Lefkoff AB, Boardman JW, Heidebrecht KB, Shapiro AT, Barloon PJ, Goetz AFH. 1993. The spectral image processing system (SIPS)—interactive visualization and analysis of imaging spectrometer data. *Remote sensing of environment* 44:145–163.
- Kumar L. 2012. Reliability of GIS-based solar radiation models and their utilisation in agro-meteorological research. Citeseer.
- Laliberte AS, Rango A. 2011. Image Processing and Classification Procedures for Analysis of Sub-decimeter Imagery Acquired with an Unmanned Aircraft over Arid Rangelands. *GIScience & Remote Sensing* 48:4–23.
- Lazaridis DC, Verbesselt J, Robinson AP. 2011. Penalized regression techniques for prediction: a case study for predicting tree mortality using remotely sensed vegetation indices. This article is one of a selection of papers from Extending Forest Inventory and Monitoring over Space and Time. *Canadian Journal of Forest Research* 41:24–34.
- Limao W, Hongqiang L, Shengkui C. 2012. A Study of the Ecological Effects of Solar Energy Development in Tibet. *Mountain Research and Development* 32:83–91.
- Li X, Gao Z, Bai L, Huang Y. 2012. Potential of high resolution RapidEye data for sparse vegetation fraction mapping in arid regions. In: *Geoscience and Remote Sensing Symposium (IGARSS), 2012 IEEE International*. IEEE. p. 420–423.
- Lu D, Mausel P, Brondízio E, Moran E. 2004. Change detection techniques. *International Journal of Remote Sensing* 25:2365–2401.
- Luedeling E, Buerkert A. 2008. Typology of oases in northern Oman based on Landsat and SRTM imagery and geological survey data. *Remote Sensing of Environment* 112:1181–1195.
- Lund H. 2007. Renewable energy strategies for sustainable development. *Energy* 32:912–919.
- Mainali B, Silveira S. 2013. Alternative pathways for providing access to electricity in developing countries. *Renewable Energy* 57:299–310.
- Ma L, Zhou Y, Chen J, Cao X, Chen X. 2015. Estimation of Fractional Vegetation Cover in Semiarid Areas by Integrating Endmember Reflectance Purification Into Nonlinear Spectral Mixture Analysis. *IEEE Geoscience and Remote Sensing Letters* 12:1175–1179.
- Matese A, Toscano P, Di Gennaro S, Genesio L, Vaccari F, Primicerio J, Belli C, Zaldei A, Bianconi R, Gioli B. 2015. Intercomparison of UAV, Aircraft and Satellite Remote Sensing Platforms for Precision Viticulture. *Remote Sensing* 7:2971–2990.
- McArthur ED, Stevens R, others. 2004. Composite shrubs. Restoring western ranges and wildlands: 2004:493–437.
- Van Der Meer F, Bakker W, Scholte K, Skidmore A, De Jong S, Clevers J, Addink E, Epema G. 2001. Spatial scale variations in vegetation indices and above-ground biomass estimates: implications for MERIS. *International Journal of Remote Sensing* 22:3381–3396.

## SYNOPSIS

- METI, NASA. 2009. ASTER Global Digital Elevation Model V002. Sioux Falls, SD. [https://lpdaac.usgs.gov/dataset\\_discovery/aster/aster\\_products\\_table/astgtm](https://lpdaac.usgs.gov/dataset_discovery/aster/aster_products_table/astgtm); accessed on 07 August 2015.
- Mevik B-H, Wehrens R, Liland KH. 2015. Partial Least Squares and Principal Component regression. <http://cran.ms.unimelb.edu.au/web/packages/pls/pls.pdf>; accessed on 12 August 2015. Reference manual available at <http://cran.r-project.org>.
- Meyer T, Okin GS. 2015. Evaluation of spectral unmixing techniques using MODIS in a structurally complex savanna environment for retrieval of green vegetation, nonphotosynthetic vegetation, and soil fractional cover. *Remote Sensing of Environment* 161:122–130.
- Montandon L, Small E. 2008. The impact of soil reflectance on the quantification of the green vegetation fraction from NDVI. *Remote Sensing of Environment* 112:1835–1845.
- Mueller-Dombois D, Ellenberg H. 1974. *Aims and methods of vegetation ecology*. New York: Wiley.
- Mutanga O, Rugege D. 2006. Integrating remote sensing and spatial statistics to model herbaceous biomass distribution in a tropical savanna. *International Journal of Remote Sensing* 27:3499–3514.
- Nakićenović N, Intergovernmental Panel on Climate Change eds. 2000. *Special report on emissions scenarios: a special report of Working Group III of the Intergovernmental Panel on Climate Change*. Cambridge ; New York: Cambridge University Press.
- Okin GS, Roberts DA, Murray B, Okin WJ. 2001. Practical limits on hyperspectral vegetation discrimination in arid and semiarid environments. *Remote Sensing of Environment* 77:212–225.
- Oldeland J, Dorigo W, Wesuls D, Jürgens N. 2010. Mapping Bush Encroaching Species by Seasonal Differences in Hyperspectral Imagery. *Remote Sensing* 2:1416–1438.
- Painuly JP. 2001. Barriers to renewable energy penetration; a framework for analysis. *Renewable energy* 24:73–89.
- Pal M. 2005. Random forest classifier for remote sensing classification. *International Journal of Remote Sensing* 26:217–222.
- Peerbhay KY, Mutanga O, Ismail R. 2013. Commercial tree species discrimination using airborne AISA Eagle hyperspectral imagery and partial least squares discriminant analysis (PLS-DA) in KwaZulu–Natal, South Africa. *ISPRS Journal of Photogrammetry and Remote Sensing* 79:19–28.
- Peña MA, Brenning A, Sagredo A. 2012. Constructing satellite-derived hyperspectral indices sensitive to canopy structure variables of a Cordilleran Cypress (*Austrocedrus chilensis*) forest. *ISPRS Journal of Photogrammetry and Remote Sensing* 74:1–10.

## SYNOPSIS

- Perez-Quezada JF, Delpiano CA, Snyder KA, Johnson DA, Franck N. 2011. Carbon pools in an arid shrubland in Chile under natural and afforested conditions. *Journal of Arid Environments* 75:29–37.
- Pons X, Ninyerola M. 2008. Mapping a topographic global solar radiation model implemented in a GIS and refined with ground data. *International Journal of Climatology* 28:1821–1834.
- Poudyal KN, Binod BK, Sapkota B, Kjeldstad B. 2012. Estimation of Global Solar Radiation Using Clearness Index and Cloud Transmittance Factor at Trans-Himalayan Region in Nepal. *Energy and Power Engineering* 04:415–421.
- Powell SL, Cohen WB, Healey SP, Kennedy RE, Moisen GG, Pierce KB, Ohmann JL. 2010. Quantification of live aboveground forest biomass dynamics with Landsat time-series and field inventory data: A comparison of empirical modeling approaches. *Remote Sensing of Environment* 114:1053–1068.
- Qi J, Chehbouni A, Huete AR, Kerr YH, Sorooshian S. 1994. A modified soil adjusted vegetation index. *Remote sensing of environment* 48:119–126.
- Ramoelo A, Skidmore AK, Cho MA, Schlerf M, Mathieu R, Heitkönig IMA. 2012. Regional estimation of savanna grass nitrogen using the red-edge band of the spaceborne RapidEye sensor. *International Journal of Applied Earth Observation and Geoinformation* 19:151–162.
- RapidEye AG. 2011. Satellite imagery product specifications. Brandenburg an der Havel, Germany: Version.
- Ren H, Zhou G, Zhang X. 2011. Estimation of green aboveground biomass of desert steppe in Inner Mongolia based on red-edge reflectance curve area method. *Biosystems Engineering* 109:385–395.
- Roleček J, Chytrý M, Hájek M, Lvončík S, Tichý L. 2007. Sampling design in large-scale vegetation studies: Do not sacrifice ecological thinking to statistical purism! *Folia Geobotanica* 42:199–208.
- Ruiz-Arias JA, Tovar-Pescador J, Pozo-Vázquez D, Alsamamra H. 2009. A comparative analysis of DEM-based models to estimate the solar radiation in mountainous terrain. *International Journal of Geographical Information Science* 23:1049–1076.
- Ruß G, Brenning A. 2010. Spatial Variable Importance Assessment for Yield Prediction in Precision Agriculture. In: Cohen P, Adams N, Berthold M, editors. *Advances in Intelligent Data Analysis IX*. Vol. 6065. Lecture Notes in Computer Science. Springer Berlin Heidelberg. p. 184–195.
- Samimi C, Kraus T. 2004. Biomass estimation using Landsat-TM and-ETM+. Towards a regional model for Southern Africa? *GeoJournal* 59:177–187.
- Sarker LR, Nichol JE. 2011. Improved forest biomass estimates using ALOS AVNIR-2 texture indices. *Remote Sensing of Environment* 115:968–977.

## SYNOPSIS

- Schwieder M, Leitão P, Suess S, Senf C, Hostert P. 2014. Estimating Fractional Shrub Cover Using Simulated EnMAP Data: A Comparison of Three Machine Learning Regression Techniques. *Remote Sensing* 6:3427–3445.
- Serrano L, Penuelas J, Ustin SL. 2002. Remote sensing of nitrogen and lignin in Mediterranean vegetation from AVIRIS data: Decomposing biochemical from structural signals. *Remote sensing of Environment* 81:355–364.
- Shoshany M, Svoray T. 2002. Multidate adaptive unmixing and its application to analysis of ecosystem transitions along a climatic gradient. *Remote Sensing of Environment* 82:5–20.
- Shrestha RM, Malla S, Liyanage MH. 2007. Scenario-based analyses of energy system development and its environmental implications in Thailand. *Energy Policy* 35:3179–3193.
- Spiekermann R, Brandt M, Samimi C. 2015. Woody vegetation and land cover changes in the Sahel of Mali (1967–2011). *International Journal of Applied Earth Observation and Geoinformation* 34:113–121.
- Stehman SV, Czaplewski RL. 1998. Design and analysis for thematic map accuracy assessment: fundamental principles. *Remote Sensing of Environment* 64:331–344.
- Sternberg M, Shoshany M. 2001. Influence of slope aspect on Mediterranean woody formations: comparison of a semiarid and an arid site in Israel. *Ecological Research* 16:335–345.
- Strobl C, Boulesteix A-L, Zeileis A, Hothorn T. 2007. Bias in random forest variable importance measures: Illustrations, sources and a solution. *BMC bioinformatics* 8:25.
- Su H, Liu W, Xu H, Wang Z, Zhang H, Hu H, Li Y. 2015. Long-term livestock exclusion facilitates native woody plant encroachment in a sandy semiarid rangeland. *Ecology and Evolution* 5:2445–2456.
- Swatantran A, Dubayah R, Roberts D, Hofton M, Blair JB. 2011. Mapping biomass and stress in the Sierra Nevada using lidar and hyperspectral data fusion. *Remote Sensing of Environment* 115:2917–2930.
- Tajik Hydrometeorological Service. 2013. Climatic dataset for the Pamir Region acquired from the Tajik hydrometeorological service. Dushanbe, Tajikistan.
- Takayama T, Ohki T, Sekine H, Ohnishi S, Shiodera S, Evri M, Osaki M. 2013. Application of hyperspectral data for assessing peatland forest condition with spectral and texture classification. In: *Geoscience and Remote Sensing Symposium (IGARSS), 2013 IEEE International. IEEE.* p. 1007–1010.
- Tovar-Pescador J, Pozo-Vázquez D, Ruiz-Arias JA, Batlles J, López G, Bosch JL. 2006. On the use of the digital elevation model to estimate the solar radiation in areas of complex topography. *Meteorological Applications* 13:279.

## SYNOPSIS

- Tucker CJ, Vanpraet CL, Sharman MJ, Van Ittersum G. 1985. Satellite remote sensing of total herbaceous biomass production in the senegalese sahel: 1980–1984. *Remote Sensing of Environment* 17:233–249.
- Tueller PT. 1987. Remote Sensing Science Applications in Arid Environments. *Remote Sensing of Environment*:13–154.
- UNEP. 2012. Global Environment Outlook 5. [http://www.unep.org/geo/pdfs/geo5/GEO5\\_report\\_full\\_en.pdf](http://www.unep.org/geo/pdfs/geo5/GEO5_report_full_en.pdf); accessed on 16 July 2015.
- USGS. 2015. Landsat 8 (L8) Data Users Handbook. Sioux Falls, SD. <http://landsat.usgs.gov/documents/Landsat8DataUsersHandbook.pdf>; accessed on 07 August 2015.
- Vanselow KA. 2011. The high-mountain pastures of the Eastern Pamirs (Tajikistan): an evaluation of the ecological basis and the pasture potential. Erlangen, Nürnberg, Univ., Diss.
- Vanselow K, Samimi C. 2014. Predictive Mapping of Dwarf Shrub Vegetation in an Arid High Mountain Ecosystem Using Remote Sensing and Random Forests. *Remote Sensing* 6:6709–6726.
- Veraverbeke S, Gitas I, Katagis T, Polychronaki A, Somers B, Goossens R. 2012. Assessing post-fire vegetation recovery using red–near infrared vegetation indices: Accounting for background and vegetation variability. *ISPRS Journal of Photogrammetry and Remote Sensing* 68:28–39.
- de Vries BJM, van Vuuren DP, Hoogwijk MM. 2007. Renewable energy sources: Their global potential for the first-half of the 21st century at a global level: An integrated approach. *Energy Policy* 35:2590–2610.
- Walter H, Breckle SW. 1986. Spezielle Ökologie der Gemäßigten und Arktischen Zonen Euro-Nordasiens, Zonobiom VI – IX. Gustav Fischer Verlag.
- Wang L, Qu JJ, Hao X, Hunt ER. 2011. Estimating dry matter content from spectral reflectance for green leaves of different species. *International Journal of Remote Sensing* 32:7097–7109.
- Wang Q, Qiu H-N. 2009. Situation and outlook of solar energy utilization in Tibet, China. *Renewable and Sustainable Energy Reviews* 13:2181–2186.
- Wiedemann C, Salzmann S, Mirshakarov I, Volkmer H. 2012. Thermal Insulation in High Mountainous Regions: A Case Study of Ecological and Socioeconomic Impacts in the Eastern Pamirs, Tajikistan. *Mountain Research and Development* 32:294–303.
- Wilson JB. 2011. Cover plus: ways of measuring plant canopies and the terms used for them: Cover plus. *Journal of Vegetation Science* 22:197–206.



## SYNOPSIS

Wood J. 1841. *A Personal Narrative of a Journey to the Source of the River Oxus. By the Route of the Indus, Kabul, and Badakhshan, Performed Under the Sanction of the Supreme Government of India, in the Years 1836, 1837, and 1838.* London: John Murray.

Yang J, Weisberg PJ, Bristow NA. 2012. Landsat remote sensing approaches for monitoring long-term tree cover dynamics in semi-arid woodlands: Comparison of vegetation indices and spectral mixture analysis. *Remote Sensing of Environment* 119:62–71.

Zhu Z, Woodcock CE. 2014. Continuous change detection and classification of land cover using all available Landsat data. *Remote Sensing of Environment* 144:152–171.



PART IV

APPENDIX



# Publications, presentations, posters and review activity of the author

---

## Peer reviewed publications

- Hohberg G, Kreczi F, Zandler H. 2015. High mountain societies and limited local resources - livelihoods and energy utilization in the Eastern Pamirs, Tajikistan. *Erdkunde*: accepted on 04 September 2015
- Zandler H, Brenning A, Samimi C. 2015. Potential of space-borne hyperspectral data for biomass quantification in an arid environment: advantages and limitations. *Remote Sensing* 7(4):4565–4580
- Zandler H, Brenning A, Samimi C. 2015. Quantifying dwarf shrub biomass in an arid environment: comparing empirical methods in a high dimensional setting. *Remote Sensing of Environment* 158:140–155
- Mayr M, Samimi C, Röhrig J, Eisold J, Zandler H. 2012. Modellierung der oberflächennahen Grundwasserneubildung im Cuvelaibecken (Nordost Namibia). In: Borg E., Daedelow H. & Johnson R: *RapidEye Science Archive (RESA) - Vom Algorithmus zum Produkt*, 4. RESA Workshop (DLR): pp. 53-70. Neustrelitz. Germany

## Published abstracts of presentations and posters

- Zandler H, Morche T, Samimi C. 2015. Wind and solar energy resources on the 'Roof of the World'. Poster-abstract in: *EGU General Assembly Conference Abstracts* 17: p. 3427. Vienna. Austria
- Zandler H, Brenning A, Samimi C. 2015. Remote sensing in arid high mountains: biomass mapping in the Eastern Pamirs of Tajikistan. Poster-abstract in: *Interdisziplinarität in der Hochgebirgsforschung - Tagungsband der 24. Jahrestagung des AK Hochgebirge*: p. 57. Hamburg. Germany
- Zandler H, Samimi C. 2014. Potential erneuerbarer Energieressourcen im Ostpamir. Presentation-abstract in: *Ressourcen der Gebirgsräume: Nutzung, Wandel, Bewertung - Tagungsband der Jahrestagung AK Hochgebirge & ARGE*: p. 14. Berne. Switzerland
- Kraudzun T, Zandler H. 2013. Das ‚Teresken-Syndrom‘? – Zwergsträucher, Energie und Weiden im Ostpamir, Tadschikistan. Presentation-abstract in: 58. *Deutscher Geographentag 2013 - Kongress für Wissenschaft, Schule und Praxis – Programmheft*: p. 146. Passau. Germany
- Zandler H, Vanselow K, Samimi C. 2013. Hyperspectral data for dwarf shrub detection? Using hyperspectral Hyperion data for the construction of dwarf shrub related, non-green

## APPENDIX

vegetation indices in the high mountains of the Eastern Pamirs. Poster-abstract in: Tagungsband der 22. Jahrestagung des AK Hochgebirge: pp. 25-26. Bonn. Germany

### Presentations and posters without published abstracts

Zandler H, Brenning A, Samimi C. 2015. Space-borne earth observation in an arid environment – The limits of remote sensing? Poster presentation at the 6th ESA Advanced Training Course on Land Remote Sensing, 14-18 September 2015. Bucharest. Romania

Zandler H. 2015. Assessing woody biomass with remote sensing methods. Presentation at the International Conference on Energy Resources in Central Asian Mountains in the era of global change. 29–30 May 2015. Dushanbe. Tajikistan

Zandler H. 2015. Renewable energy resource on the roof of the World? Empirical contributions to high mountain research in the Eastern Pamirs. Presentation at the geographical colloquium of the Friedrich-Alexander University Erlangen-Nuremberg. 20 May 2015. Erlangen. Germany

Zandler H, Brenning A, & Samimi C. 2015. Dwarf shrub biomass mapping in an arid environment: independent and synergetic performance of RapidEye and Landsat OLI. Poster presentation at the DLR 7th annual RapidEye Science Archive (RESA) Workshop. 29-30 April 2015. Bonn. Germany

Zandler H. 2015. Dwarf shrubs in the Eastern Pamirs – distribution and regeneration. Presentation at the Regional Workshop of the joint Tajik-German research initiative “The presence and future of energy resources in the framework of sustainable development”. 19-20 July 2013. Murghab. Tajikistan

### Review activity for scientific journals

ISPRS Journal of Photogrammetry and Remote Sensing

Remote Sensing

Journal of Integrative Environmental Sciences

Land



# Declaration / eidesstattliche Erklärung

---

I hereby declare that this dissertation was written by me and that I did not use any other sources and means than specified. This thesis has not been submitted at any other university for acquiring an academic degree.

## **(Eidesstattliche) Versicherungen und Erklärungen**

(§ 5 Nr. 4 PromO)

*Hiermit erkläre ich, dass keine Tatsachen vorliegen, die mich nach den gesetzlichen Bestimmungen über die Führung akademischer Grade zur Führung eines Doktorgrades unwürdig erscheinen lassen.*

(§ 8 S. 2 Nr. 5 PromO)

*Hiermit erkläre ich mich damit einverstanden, dass die elektronische Fassung meiner Dissertation unter Wahrung meiner Urheberrechte und des Datenschutzes einer gesonderten Überprüfung hinsichtlich der eigenständigen Anfertigung der Dissertation unterzogen werden kann.*

(§ 8 S. 2 Nr. 7 PromO)

*Hiermit erkläre ich eidesstattlich, dass ich die Dissertation selbständig verfasst und keine anderen als die von mir angegebenen Quellen und Hilfsmittel benutzt habe.*

(§ 8 S. 2 Nr. 8 PromO)

*Ich habe die Dissertation nicht bereits zur Erlangung eines akademischen Grades anderweitig eingereicht und habe auch nicht bereits diese oder eine gleichartige Doktorprüfung endgültig nicht bestanden.*

(§ 8 S. 2 Nr. 9 PromO)

*Hiermit erkläre ich, dass ich keine Hilfe von gewerblichen Promotionsberatern bzw. -vermittlern in Anspruch genommen habe und auch künftig nicht nehmen werde.*

Bayreuth, 22.09.2015, .....

Ort, Datum, Unterschrift